DIURNAL ENERGETICS OF A RESERVOIR SURFACE LAYER

Department of Conservation &Environment
Perth, Western Australia
Bulletin 75 October 1980

DIURNAL ENERGETICS OF A RESERVOIR SURFACE LAYER

BY

K. N. RAYNER

DEPARTMENT OF CONSERVATION AND ENVIRONMENT
WESTERN AUSTRALIA

A Joint Report of

ENVIRONMENTAL DYNAMICS
DEPARTMENT OF CIVIL ENGINEERING
UNIVERSITY OF WESTERN AUSTRALIA
NEDLANDS 6009
WESTERN AUSTRALIA

and

DEPARTMENT OF CONSERVATION AND ENVIRONMENT
1 MOUNT STREET
PERTH 6000
WESTERN AUSTRALIA

ACKNOWLEDGEMENTS

The author would like to thank the following people:

- Professor Jorg Imberger, who supervised the Project, giving expert guidance and encouragement throughout,

- Mr. Bob Hebbert, for his assistance and valuable discussion,

- the staff of the Mechanical and Civil Engineering Workshops for their skilled construction of equipment used during the fieldwork,

- Mr. Greg Ivey, Mr. Vincent Lyne and others who assisted with the fieldwork,

- Mr. Ian Watson and Mr. Vincent Lyne for proof reading the manuscript, Ms. Pippa Davis for assisting with the drafting of diagrams and Ms. Deborah Foote for typing the manuscript.

This work was completed in the Civil Engineering Department of the University of Western Australia and was funded by the Australian Water Resources Council as part of the Research Project 74/70 entitled "Management of Water Quality in Reservoirs".

SYNOPSIS

Mixing of the surface waters of a reservoir, induced by meteorological forces, is a major factor determining the quality of the water throughout the full depth. The aim of the project described herein was to study the air-water interaction over the Wellington Reservoir and develop a theoretical description of the important observed features.

The epilimnion, or seasonal well mixed layer, was observed to undergo a diurnal cycle of heating and mixing, which in turn governed the seasonal cycle, including the formation and subsequent erosion of a seasonal thermocline. The diurnal cycle has been successfully simulated by a numerical model of integral well mixed layer energetics. The model has direct application in the study of biological production in reservoir surface waters. In addition, it is shown that the theory of well mixed layer energetics may be applied to a study of the seasonal cycle in reservoirs, and also to oceanic and atmospheric problems.

TABLE OF CONTENTS

LIST OF FIGURES

LIST OF TABLES

LIST OF PLATES

CHAPTER 1

INTRODUCTION

In July 1974, a Study funded by the Australian Water Resources Council and entitled "Management of Water Quality in Reservoirs" was commenced within the Engineering School at the University of Western Australia. The Study concentrated on the Wellington Reservoir, situated some 160 km south of Perth, where increased salinity levels had resulted from clearing of the reservoir catchment's native forest for agricultural purposes. In addition to alleviating this specific problem, the objective of the Study was to develop management procedures applicable to a variety of water quality problems occurring in medium sized reservoirs. The Study was completed in 1980 with the publication of the final report by Imberger and Hebbert (1980).

The Project described in the present report was initiated, as part of the above Study, to investigate the interaction between meteorological processes and the reservoir surface layer. In particular, it was considered necessary to understand the heating and mixing cycles which lead to the formation of the seasonal thermocline, which itself has a profound effect on internal water movements and on the vertical transport of water constituents. The aims of the Project were:

(a) to experimentally observe and measure meteorological and water properties which modify the reservoir surface density structure,

(b) to develop theoretical and numerical descriptions of those observed processes considered to be important, and so attempt to simulate the observed surface density structure,

(c) to recommend procedures applicable to simulation o the seasonal reservoir surface density structure.

Over the summer months of 1975-76, a series of intensive field investigations were conducted aboard a raft anchored near the centre of the main water body. The raft provided a platform for a permanent, continuously recording weather station and was also used during the field work to mount sensitive meteorological sensors. Profiles of temperature and salinity, measured hourly over four separate days, revealed a striking diurnal cycle of morning heating followed by afternoon and evening mixing, occurring within the epilimni which is normally considered to be well mixed. Integral descriptions of turbulent kinetic energy, heat, mass, momentum and salinity were developed and incorporated into a numerical model of the diurnal cycle. The model's description of turbulent transfers at the surface includes the effect of atmospheric stability, which is very important over a medium sized reservoir. The model has successfully simulated the diurnal cycle for the four field days, so meeting the above aims.

A brief guide to the contents of this report is as follows. Chapters 2 and 3 provide the methods for computing turbulent and radiative transfers at the reservoir surface; these are boundary conditions for the model. Chapter 4 detail

the measurement of temperature and salinity profiles which revealed the diurnal cycle. The integral formulation of well mixed layer energetics is presented in Chapter 5 and is incorporated into the framework of a numerical model in Chapter 6. Chapter 7 contains an analysis of the model results, with conclusions and recommendations for future work appearing in Chapter 8.

CHAPTER 2

THEORY OF ATMOSPHERIC SURFACE TRANSFERS

Over recent years, considerable research has focused on the physics of turbulent and radiative transfers in the atmospheric surface layer. In this chapter, a few established relationships are presented, providing a basis for experimental methods and computations described in Chapter 3.

2.1 TURBULENT TRANSFERS IN THE SURFACE LAYER

2.1.1 Surface Layer Scaling and Parameterization

The Navier-Stokes equation for meteorological considerations is conventionally written in the form

$$\frac{d\underset{\sim}{\bar{U}}}{dt} + f\,\hat{\underset{\sim}{k}} \times \underset{\sim}{\bar{U}} = -\frac{1}{\rho}\nabla p + \frac{1}{\rho}\frac{\partial \underset{\sim}{\tau}}{\partial z}, \qquad (2.1)$$

with $\underset{\sim}{\bar{U}}$ horizontal mean velocity, with x and y components,

$\hat{\underset{\sim}{k}}$ unit vertical vector,

f Coriolis parameter,

ρ density of air,

∇p horizontal pressure gradient $\frac{\partial p}{\partial x} + \frac{\partial p}{\partial y}$,

$\underset{\sim}{\tau}$ Reynolds stress vector.

In deriving eq. 2.1 and other relations, properties of the flow are split into mean and fluctuating components, as follows:

horizontal velocity	$\underset{\sim}{u} = \underset{\sim}{\bar{U}} + \underset{\sim}{u}'$, $\underset{\sim}{\bar{u}}' = 0$
vertical velocity	$w = \bar{W} + w'$, $\bar{w}' = 0$
temperature	$T = \bar{T} + \theta'$, $\bar{\theta}' = 0$
specific humidity	$q = \bar{q} + q'$, $\bar{q}' = 0$

The overbar denotes a time average (assuming stationarity of the turbulence). It will be retained in the following equations only for products of fluctuating quantities, e.g. the Reynolds stress is defined as

$$\frac{\tau}{\rho} = -\overline{u'w'} = \qquad (2.2)$$

friction velocity.

Kraus (1972) shows, by a scaling argument applied to eq. 2.1, that the Reynolds stress is effectively constant in the atmospheric surface layer up to a height of several tens of metres. In this layer, rotational effects are negligible and so the mean flow is considered in two dimensions only.

The heat equation may be written as

$$\frac{dT}{dt} \quad \frac{1}{\rho C_p}\left(\frac{\partial H}{\partial z} + \frac{\partial Q}{\partial z}\right), \qquad (2.3)$$

with Q radiation flux,

C_p specific heat of air,

H turbulent heat flux = $\rho C_p \overline{\theta'w'}$.

Finally, the equation for vertical momentum, neglecting frictional and Coriolis effects, is

$$\frac{dW}{dt} \quad -\frac{1}{\rho}\frac{\partial p'}{\partial z} + \frac{g}{T}\Delta T\ , \qquad (2.4)$$

with p' dynamic pressure

ΔT temperature difference between the parcel of air and its surroundings.

Monin-Obukhov Length

Monin and Obukhov (1954) examined the physical quantities

$$u_*,\ \frac{H}{\rho C_p} \text{ and } \frac{g}{T}$$

from the above equations and by dimensional analysis defined a length scale

$$L = - \frac{u_*^3}{k \frac{g}{T} \frac{H}{\rho C_p}} , \qquad (2.5)$$

with k von Kármán constant (defined later).

On the basis of dynamic similarity they proposed that any mean property of the turbulent flow may be described in terms of the dimensionless variable z/L. The Monin-Obukhov length, L, may be evaluated for a given set of meteorological conditions and is a measure of the height of the dynamic sublayer within which thermally induced effects are unimportant.

Moisture Correction

Air containing water vapour has a lower molecular wei than dry air and hence a higher gas contant R as it appears in the Ideal Gas Law

$$p = \rho R T. \qquad (2.6)$$

It is common meteorological practice, when dealing with mixtures of air and water vapour, to retain a constant value of R and include moisture correction in the temperature, giving virtual temperature

$$T_v = T(1 + 0.61q) \text{ in degrees Kelvin.} \qquad (2.7)$$

Eq. 2.7 is derived simply from Dalton's Law.

When investigating turbulent flow over water bodies, the buoyancy induced by water vapour excess close to the surface should be considered. Busch (1973) incorporates this effect into the Monin-Obukhov length

$$L = - \frac{u_*^3 T_v}{kg\overline{\theta_v' w'}} , \qquad (2.8)$$

where θ_v' is the fluctuating component of virtual potential temper ature. The buoyancy flux term $\overline{\theta_v' w'}$ may be expanded using eq. 2.7

$$\overline{\theta_v'w'} = \overline{\theta'w'}(1+0.61q) + 0.61T\,\overline{q'w'} + 0.61\,\overline{\theta'q'w'},$$

$$\simeq \overline{\theta'w'} + 0.61T\,\overline{q'w'}\ , \text{ (neglecting minor terms)}$$

$$= \frac{1}{\rho C_p} H + 0.61\,\frac{T}{\rho} E\ ,$$

where E is the turbulent mass flux of water vapour.

$$\text{So,}\quad L = \frac{-\rho u_*^3\, T_v}{kg\left[\frac{H}{C_p} + 0.61TE\right]}\ . \qquad (2.9)$$

2.1.2 Flux - Profile Relationships

The theory of flux - profile relationships in the surface layer has been well documented by Dyer (1974), Businger (1973) and others. Although no profile measurements were conducted during this project, the theory covering such work will be utilized and is therefore summarised below.

Similarity Hypothesis

Monin and Obukhov (1954) parameterised the non-dimensional gradients of wind, potential temperature and specific humidity in terms of the stability parameter z/L:

$$\frac{kz}{u_*}\frac{dU}{dz} = \phi_M\left(\frac{z}{L}\right), \qquad (2.10)$$

$$\frac{kz}{\theta_*}\frac{d\theta}{dz} = \phi_H\left(\frac{z}{L}\right), \qquad (2.11)$$

$$\frac{kz}{q_*}\frac{dq}{dz} = \phi_W\left(\frac{z}{L}\right), \qquad (2.12)$$

$$\text{where } u_* = \left(\frac{\tau}{\rho}\right)^{\frac{1}{2}}, \qquad (2.13)$$

$$\theta_* u_* = -\frac{H}{\rho C_p}\ , \qquad (2.14)$$

$$q_* u_* = -\frac{E}{\rho}\ . \qquad (2.15)$$

k is the von Kármán constant defined such that $\phi_{M,H,W} = 1$ for $z/L = 0$.

Over the last decade, the development of instrumentatic to directly measure turbulent fluxes of momentum, heat and moisture has permitted precise evaluation of the ϕ functions. Dyer (1974) summarises the various proposed forms and concludes that the following are most acceptable.

Unstable:

$$\phi_M = (1 - \gamma\left(\frac{z}{L}\right))^{-\frac{1}{4}}, \tag{2.16}$$

$$\phi_H = \phi_W = (1 - \gamma\left(\frac{z}{L}\right))^{-\frac{1}{2}}, \tag{2.17}$$

where $\gamma \simeq 16$.

Stable:

$$\phi_M = \phi_H = \phi_W = 1 + \alpha\left(\frac{z}{L}\right), \tag{2.18}$$

where $\alpha \simeq 5$.

Hicks (1976), in a re-analysis of the Wangara data (Clarke *et al.*(1971)), found that eq. 2.18 holds only for slightly stable conditions ($0 < z/L < 0.5$). For higher stabilities he found that velocity profiles depart from the log-linear form of eq. 2.18 toward a purely logarithmic form (ϕ_M constant), but that this state is never reached. He further observed that in very stable conditio the profile above a few metres becomes linear with height, indicating a decoupling of this air from that near the surface, i.e.:

$$\frac{dU}{dz} = \frac{cu_*}{kL}, \quad \frac{z}{L} > 10, \tag{2.19}$$

so $\phi_M = c(z/L)$ (2.20)

where c is a constant ($c \simeq 0.8$).

Carsons and Richards (1978) lend their support to Hicks' (1976) findings and provide an empirical formula for the transition between eq. 2.18 and eq. 2.20:

$$\phi_M = \left(8 - 4.25(z/L)^{-1} + (z/L)^{-2}\right), \quad \left(0.5 < (z/L) < 10\right) . \qquad (2.21)$$

While it is well established that $\phi_M = \phi_H = \phi_W$ for $(0<(z/L)<0.5)$ there is currently no information on the relationship between the ϕ's at higher stabilities. It is assumed here that they are equal.

Profile Descriptions

Following Paulson (1970) eqs. 2.10 to 2.12 may be integrated to the form:

$$U = \frac{u_*}{k}\left[\ell n\left(\frac{z}{z_o}\right) - \psi_M\right] , \qquad (2.22)$$

$$\theta-\theta_o = \frac{\theta_*}{k}\left[\ell n\left(\frac{z}{z_H}\right) - \psi_H\right], \qquad (2.23)$$

$$q-q_o = \frac{q_*}{k}\left[\ell n\left(\frac{z}{z_W}\right) - \psi_W\right], \qquad (2.24)$$

where z_o, z_H and z_W are roughness lengths. The ψ functions have the form

$$\psi = \int_{\zeta_o}^{\zeta} \frac{1-\phi(\zeta)}{\zeta}\, d\zeta, \qquad (2.25)$$

where $\zeta = z/L$.

In neutral conditions ($\phi = 1$), $\psi = 0$ and the eqs. 2.22 to 2.24 reduce to the familiar logarithmic profile.

Paulson (1970) gives analytical solutions to eq. 2.25. For the ϕ function of eq. 2.16 and eq. 2.17 integration yields

$$\psi_M = 2\ell n[(1+x)/2] + \ell n[(1+x^2)/2] - 2\mathrm{Tan}^{-1}x + \frac{\pi}{2} , \qquad (2.26)$$

$$\psi_H = \psi_W = 2\ell n[(1+x^2)/2], \tag{2.27}$$

where $x = (1 - \gamma\left(\frac{z}{L}\right))^{\frac{1}{4}}$. For ϕ given by eq. 2.18,

$$\psi_M = \psi_H = \psi_W = - \alpha\left(\frac{z}{L}\right) . \tag{2.28}$$

Carson and Richards (1978) evaluated ψ numerically for the two regimes where $(z/L) > 0.5$, given by eq. 2.20 and eq. 2.21. Alternatively, to obtain an analytical solution, ψ may be evaluated separately for each regime.

For $(0.5 < \zeta \leq 10)$

$$\psi = \int_{\zeta_o}^{0.5} \frac{1-\phi(\zeta)}{\zeta} d\zeta + \int_{0.5}^{\zeta} \frac{1-\phi(\zeta)}{\zeta} d\zeta$$

$$= 0.5\zeta^{-2} - 4.25\zeta^{-1} - 7\ell n(\zeta) - 0.852. \tag{2.29}$$

For $\zeta > 10$

$$\psi = \int_{\zeta_o}^{0.5} \frac{1-\phi(\zeta)}{\zeta} d\zeta + \int_{0.5}^{10} \frac{1-\phi(\zeta)}{\zeta} d\zeta + \int_{10}^{\zeta} \frac{1-\phi(\zeta)}{\zeta} d\zeta$$

$$= \ell n\zeta - 0.76\zeta - 12.093. \tag{2.30}$$

In obtaining the above results the lower limit of integration, ζ_o, has been taken as equal to zero. This approximation holds only for very small values of the roughness lengths z_o, z_H and z_W such as those found over water.

2.1.3 Bulk Aerodynamic Formulae

Utilising the theory presented in the previous section it is feasible to make precise estimates of turbulent fluxes from measurements of the vertical profiles of wind, temperature and humidity over water. However, conducting such a measurement programme is a major undertaking and was considered beyond the scope of this project. For this and similar projects, where

surface turbulent fluxes represent only part of the dynamics of the system under investigation, it is desirable to have a method of calculating these fluxes using only routinely available single height observations. The bulk aerodynamic formulae provide such a method.

Bulk aerodynamic formulae for stress, heat and moisture fluxes are written as follows:

$$-\frac{\tau}{\rho} = \overline{u'w'} = -u_* u_* = -C_D U^2. \tag{2.31}$$

$$\frac{H}{\rho C_p} = \overline{\theta'w'} = -u_* \theta_* = -C_H U(\theta-\theta_s). \tag{2.32}$$

$$\frac{E}{\rho} = \overline{q'w'} = -u_* q_* = -C_W U(q-q_s). \tag{2.33}$$

C_D, C_H and C_W are the respective bulk transfer coefficients. U, θ and q are measured at some reference height (usually 10 metres) and subscript s refers to surface measurement.

Considering the theory discussed in preceding sections it is obvious that the bulk transfer coefficients will not be constants, but will be strongly dependent on stability. Several authors (Deardorff (1968), Carson and Richards (1978)) have investigated this dependency. A similar analysis is presented here.

Neutral Conditions

For neutral conditions, eqs. 2.31 to 2.33 may be written in the general form

$$F_a = -u_* a_* = -C_{aN} U \Delta a \tag{2.34}$$

where the subscript N refers to neutral stability and a is one of the variables U, θ or q.

A generalised form of eqs. 2.21 to 2.24 for neutral conditions is

$$\Delta a = \frac{a_*}{k}\left[\ell n\left(\frac{z}{z_a}\right)\right] \quad , \text{ where } z_a \text{ is } z_o,\ z_H \text{ or } z_w \tag{2.35}$$

and specifically

$$U = \frac{u_*}{k}\left[\ell n\left(\frac{z}{z_o}\right)\right]. \tag{2.36}$$

Substitution of eq. 2.35 and eq. 2.36 into eq. 2.34 yields

$$C_{aN} = k^2/\left[\ell n\left(\frac{z}{z_o}\right)\ \ell n\left(\frac{z}{z_a}\right)\right] \ , \tag{2.37}$$

and specifically

$$C_{DN} = k^2/\left(\ell n\left(\frac{z}{z_o}\right)\right)^2. \tag{2.38}$$

Non-Neutral Conditions

Generalised forms of eq. 2.34 and eqs. 2.22 to 2.24 are

$$F_a = - u_* a_* = - C_a\ U\ \Delta a \ , \tag{2.39}$$

$$\Delta a = \frac{a_*}{k}\left[\ell n\left(\frac{z}{z_a}\right) - \psi_a\right]. \tag{2.40}$$

Substitution into eq. 2.39 of eqs. 2.40, 2.22, 2.37 and 2.38 leads to the expression

$$\frac{C_a}{C_{aN}} = \left(1 + \frac{C_{aN}}{k^2}\left(\psi_M\psi_a - \frac{k\psi_a}{\sqrt{C_{DN}}} - \frac{k\psi_M\sqrt{C_{DN}}}{C_{aN}}\right)\right)^{-1} \ , \tag{2.41}$$

and specifically

$$\frac{C_D}{C_{DN}} = \left(1 + \frac{C_{DN}}{k^2}\left(\psi_M{}^2 - \frac{2k\psi_M}{\sqrt{C_{DN}}}\right)\right)^{-1}. \tag{2.42}$$

Eqs. 2.41 and 2.42 give the ratio of the transfer coefficients to their neutral value as a function of stability. For a given stability (z/L), ψ_a and ψ_M may be evaluated from eqs. 2.26 to 2.30.

Roughness lengths do not appear explicitly in eqs. 2.41 and 2.42, but they are implicitly specified by the selected neutral transfer coefficients.

Bulk Richardson Number

The stability length L, as defined by eq. 2.8, is difficult to estimate directly unless actual measurements of heat and moisture fluxes are available. From the established relations of Section 2.1.2 however, it is possible to obtain an expression for L in terms of a measurable bulk stability parameter called the Bulk Richardson Number, defined as

$$Ri_B = \frac{gz}{T_v} \frac{(\Delta\theta + 0.61 T_v \Delta q)}{U^2} . \qquad (2.43)$$

The Monin-Obukhov similarity functions for temperature and moisture profiles are identical (see eq. 2.17 and eq. 2.18), indicating similar transfer mechanisms for heat and moisture. From now on the two will be considered together, assuming equality of bulk transfer coefficients and roughness lengths. Subscript HW will be used.

Substituting for $\Delta\theta$, Δq and U in eq. 2.43 from eq. 2.22, eq. 2.23 and eq. 2.24 gives

$$Ri_B = \frac{gz}{T_v} \frac{\left(\frac{\theta_*}{k} + 0.61 T_v \frac{q_*}{k}\right)\left(\ell n\left(\frac{z}{z_{HW}}\right) - \psi_{HW}\right)}{\left[\frac{u_*}{k}\left(\ell n\left(\frac{z}{z_o}\right) - \psi_M\right)\right]^2} .$$

Substituting eqs. 2.37 and 2.38 and rearranging gives

$$Ri_B = \frac{zkg(\theta_* u_* + 0.61 T_v q_* u_*)}{u_*^3 T_v} \frac{\left(\frac{k\sqrt{C_{DN}}}{C_{HWN}} - \psi_{HW}\right)}{\left(\frac{k}{\sqrt{C_{DN}}} - \psi_M\right)^2} ,$$

and the first term, by definition, is z/L, so

$$Ri_B = \frac{z}{L}\ \Phi\left(\frac{z}{L}\right) \tag{2.44}$$

where $\Phi\left(\frac{z}{L}\right) = \frac{\left(\frac{k\sqrt{C_{DN}}}{C_{HWN}} - \psi_{HW}\right)}{\left(\frac{k}{\sqrt{C_{DN}}} - \psi_M\right)^2}$.

The relationship of C_a/C_{aN} to Ri_B has not been formally derived but is presented in graphical form in Figures 2.1 and 2.2. These are composite plots for the stable and unstable cases showing the relations:

(a) C_D/C_{DN}, $C_{HW}/C_{HWN} \sim f(Ri_B)$,

(b) $\frac{z}{L} \sim f(Ri_B)$,

(c) ϕ_M, $\phi_{HW} \sim f(\frac{z}{L})$.

In view of the uncertainty of the recent formulations of Hicks (1976) for $\phi_{M,H,W}$ at higher stability (eqs. 2.20 and 2.21), the log-linear form eq. 2.18 has been plotted over the whole range of (z/L) in Figure 2.1 for reference. Also plotted is the curve for C_D/C_{DN} resulting from the use of eq. 2.18 only; it can be seen that C_D (and hence stress) vanishes for low values of Ri_B (~ 0.2). The curves for C_{HW}/C_{HWN} and ϕ_{HW} have not been plotted in Figure 2. since they are very similar to C_D/C_{DN} and ϕ_M respectively.

Neutral Transfer Coefficients at 10 m

Several authors provide estimates of the 10 m neutral transfer coefficients C_{DN}, C_{HN} and C_{WN} arising from extensive fiel measurements of profiles and eddy fluxes over water bodies. These authors invariably warn against the use of neutral coefficients in non-neutral conditions.

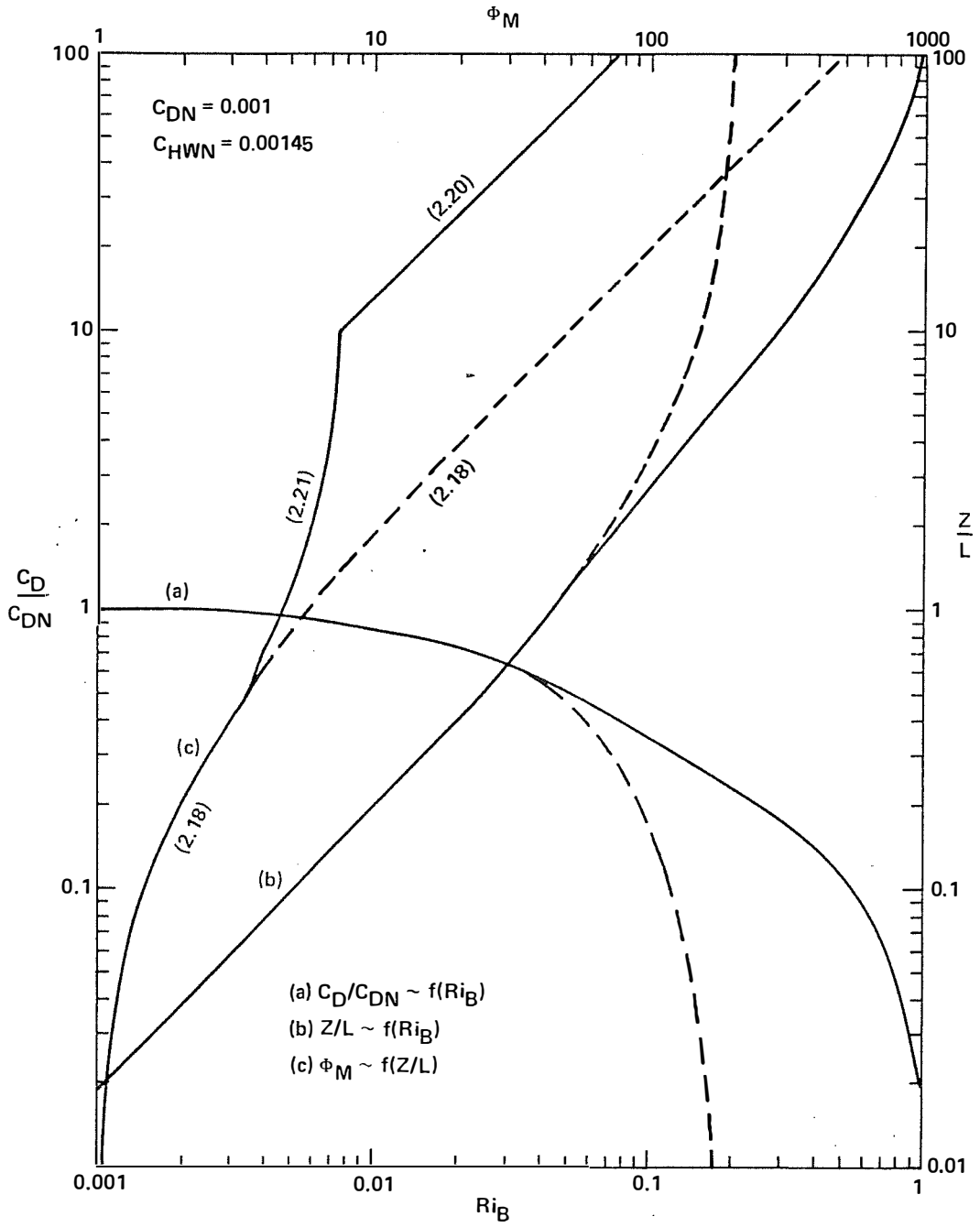

FIGURE 2.1 Stability relationships - stable case. Dashed lines indicate use of the log-linear relation eq. 2.18 only

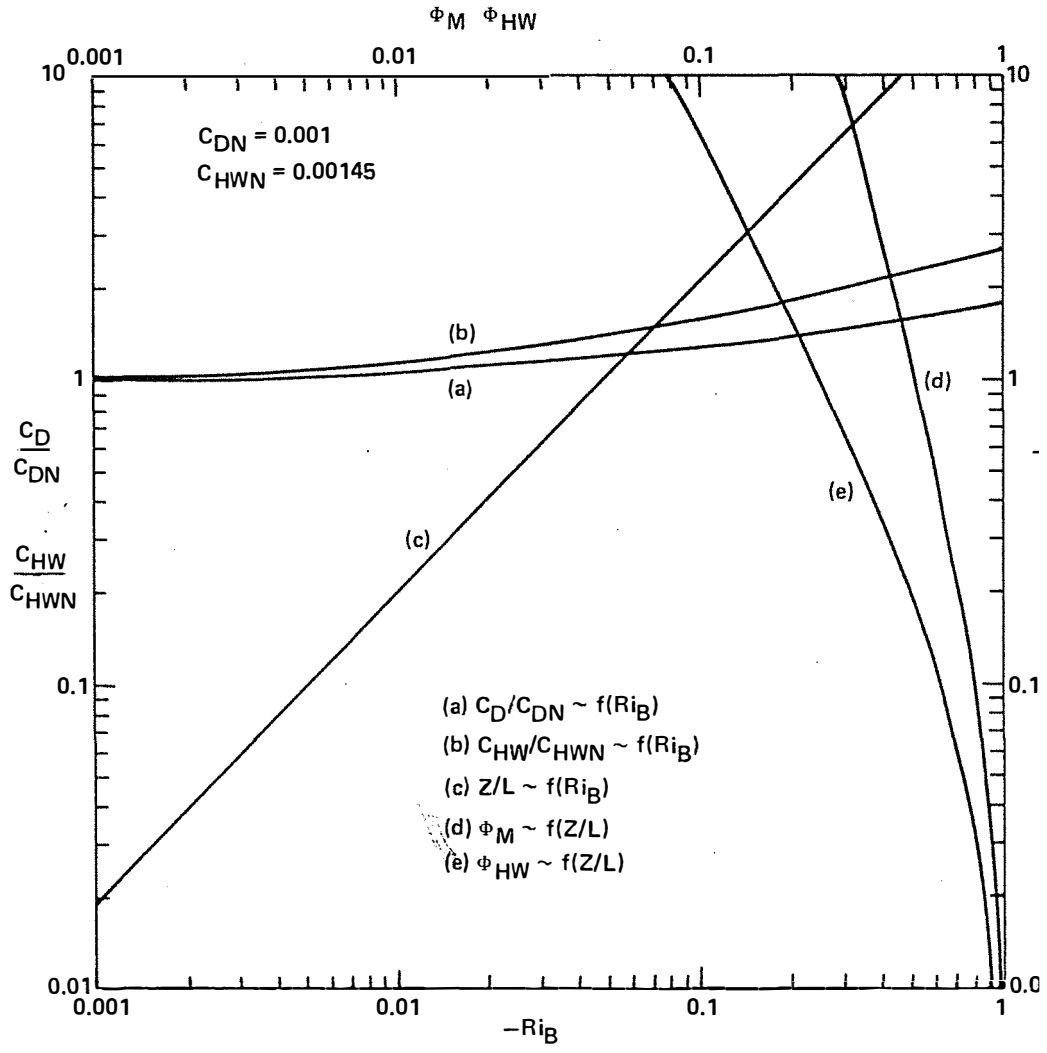

FIGURE 2.2 Stability relationships - unstable case

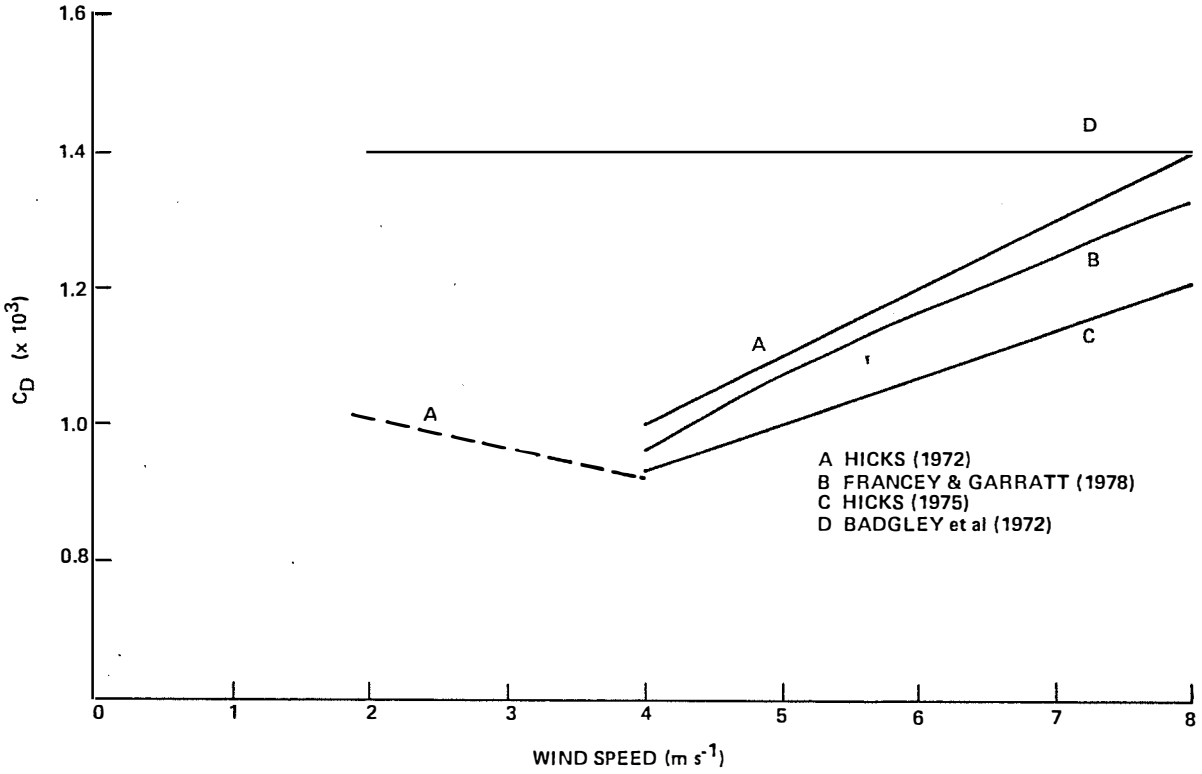

FIGURE 2.3 Neutral drag coefficient estimates from various authors

Figure 2.3 shows four differing descriptions of C_{DN}. The slight increase of C_{DN} with velocity is commonly observed. At low wind speeds the situation is unclear, however Hicks (1972) reports aerodynamically smooth behaviour with $C_{DN} \sim 1.0 \times 10^{-3}$.

Values for C_{HN} and C_{WN} between 1.3×10^{-3} and 1.5×10^{-3} appear suitable for the range of wind speeds of interest (Hicks (1975), Hicks (1972), Pond, Fissel and Paulson (1974)). Francey and Garratt (1978) found a smaller value of C_{HN} exhibiting wind speed dependence. Even if this is the case, sensible heat transfer at the reservoir surface is insignificant when compared to latent heat transfer.

2.1.4 Internal Boundary Layers

When air from the land flows over a body of water, the flow is modified due to the change in surface roughness, temperature and humidity. An internal boundary layer develops over the water surface and equilibrium conditions are set up in the lower portion of this layer. Hence, in the bottom portion of the internal boundary layer, advective effects are small and the constant flux layer relations of the previous section are applicable

A number of models of internal boundary layer development and subsequent spatial distribution of fluxes have appeared in the atmospheric sciences literature. These models employ either a mixing length hypothesis (Taylor (1970), Weisman (1975)) or a turbulent energy closure scheme (Peterson (1969)). Both methods suffer limitations. Weisman assumes the similarity functions (eq. 2.10 to eq. 2.12) hold throughout the layer, thereby forcing the solution of layer development. He finds his solution to be strongly dependent on the mixing length scale height and although

he presents some justification for the "correct choice" of scale height, the results must be considered tentatively.

No solution to boundary layer development will be attempted here. However, it is necessary to recognise the existence of this layer in the reservoir situation and to ensure that measurements are conducted in the equilibrium sublayer where the established bulk transfer equations hold. Petersen (1969) indicates that the fetch must be 100 times the observation level for equilibrium to be assured. Hicks (1975) suggests a cautious fetch/height ratio of 1000 to ensure that the effect of upwind non-uniformities are minimised. On the basis of these and other guidelines, meteorological sensors described in the next chapter were mounted so as to have a minimum fetch/height ratio of 200. Lower measurement levels were precluded due to the possibility of the raft superstructure modifying the airflow.

2.2 RADIATION TRANSFERS BETWEEN AIR AND WATER

To enable an investigation of the diurnal cycle of heating and mixing in the reservoir surface layer, information on the diurnal cycle of radiative transfers between the air and the water is required. This contrasts with long term (seasonal) reservoir models which generally require only daily integrals of radiation.

Some simple expressions for radiation calculation are set out below. These are taken directly from the T.V.A. (1972) report to which the reader is referred for further detail. While there

are more accurate formulations of radiation transfer available, the added complexity is not warranted here in view of the good results presented in the next chapter.

2.2.1 Solar Radiation

The T.V.A. (1972) report sets out in detail the formulae for computing solar radiation at the surface, incorporating atmospheric attenuation, reflection and cloud effects. A summary of these appears below, for use in subsequent chapters.

Extra-terrestrial Solar Radiation

The radiation Q_{so} impinging on a horizontal plane at the top of the atmosphere is

$$Q_{so} = \frac{I_o}{r} \sin\alpha, \tag{2.45}$$

with I_o solar constant = $1353 W/m^2$,

r radius vector, defined below,

α solar altitude (radians).

The solar altitude is determined from the expression

$$\sin\alpha = \sin\phi \sin\delta + \cos\phi \cos\delta \cosh, \tag{2.46}$$

with ϕ latitude (radians),

δ declination of sun (radians),

h local hour angle of sun (radians).

The variables r and δ may be considered constant over a day and are given by:

$$r = 1 + 0.017\cos\left[\frac{2\pi}{365}(186 - d)\right] \tag{2.47}$$

$$\delta = 23.45\left(\frac{\pi}{180}\right) \cos\left[\frac{2\pi}{365}(172 - D)\right] \tag{2.48}$$

Computation of the local hour angle, h, requires a two part formula:

(a) for the sun east of the local meridian

$$h = ST + 12 - DTSL + ET, \tag{2.49}$$

(b) for the sun west of the local meridian

$$h = ST - 12 - DTSL + ET \tag{2.50}$$

with ST standard time of time zone,

DTSL difference between local and standard time,

ET the equation of time.

ET, accounting for the apparent irregular angular motion of the sun, is given by:

$$ET = -60(0.123570\sin d - 0.004289\cos d + 0.153809\sin 2d + 0.060783\cos 2d), \tag{2.51}$$

where $d = \frac{2\pi}{365.242}(D-1)$

and D is the day number of the year. h must be converted to radians for use in eq. 2.46.

Methods to compute atmospheric absorption and scattering are also provided in the T.V.A. (1972) report. An alternative approach, detailed in the next chapter, uses the geometric relationships above together with known daily maximum global radiation figures to compute approximately the global radiation throughout a day.

2.2.2 Water Surface Radiation

A water surface emits radiation in the wavelength range 6.8 μ to 100 μ for normal temperatures around 300K. Plancks' Law may be applied to determine the total emission (integrated over all wavelengths), i.e.

$$Q_{LR} = \varepsilon \sigma T^4 \tag{2.52}$$

with ε emissivity (≃ 0.96)

σ Stephan-Boltzman constant ($\sigma = 2.0411 \times 10^{-7}$ kJ/m^2 hr K^4),

T the absolute temperature of the water surface.

Water is practically opaque for wavelengths greater than 2.65 μ, so all long-wave transfers, including emissions, must come from a very thin surface layer. In this respect, long-wave radiation transfer is similar to turbulent, sensible and latent heat transfers which must also come from a surface conductive layer. In other words, their effects on the heat distribution in the water body will be similar.

2.2.3 Atmospheric Radiation

While some of the surface emitted long-wave radiation passes through the atmosphere into space, much is absorbed by atmospheric constituents (water vapour, carbon dioxide, ozone) and re-emitted back to earth. The T.V.A. (1972) report summarises a number of empirical formulae for calculating this atmospheric radiation for clear skies, based on surface vapour pressure and air temperature measurements. Swinbank's (1963) formula is preferred:

$$Q_{LA} = 0.937 \times 10^{-5} \sigma T_2^{6} (1-R_a), \tag{2.53}$$

with T_2 air temperature at 2 m height,

R_a water surface reflectivity ($\simeq$ 0.3).

Field tests show this formula to be accurate to $\pm 12 Wm^{-2}$.

Clouds emit long-wave radiation and are accounted for by a factor in eq. 2.53:

$$Q_{LAC} = (1+0.17C^2)\, Q_{LA} \tag{2.54}$$

where C is the part of the sky covered with clouds, measured in tenths of the total sky.

The atmospheric radiation spectrum has its maxima near

14 μ, compared to the solar spectrum maxima at about 0.7 μ. The two spectra are almost completely separate, and hence solar and atmospheric radiation may be treated quite independently. Atmospheric radiation may be treated identically to water surface radiation, as described in the previous section.

2.2.4 Absorption of Solar Radiation in Water

Solar radiation penetrating the surface is absorbed within the water body, thereby heating it. Absorption of longer wavelengths occurs more rapidly so only the visible part of the solar spectrum (0.36 to 0.76 μ) penetrates below one metre. For depths greater than one metre the attentuation profile is well described by Beer's Law:

$$q(z) = Q_s e^{-bz} \tag{2.55}$$

with Q_s solar radiation at the surface,

z depth,

b bulk extinction coefficient dependent on the turbidity of the water.

To describe attenuation over the full depth of water, account must be taken of the wavelength dependency. The T.V.A. (1972) report recommends use of three extinction coefficients, i.e.:

$$q(z) = Q_s(a_1 e^{-b_1 z} + a_2 e^{-b_2 z} + a_3 e^{-b_3 z}) \tag{2.56}$$

where the a and b coefficients vary depending on water turbidity.

C H A P T E R 3

FIELD MEASUREMENTS OF METEOROLOGY

3.1 BACKGROUND

As discussed in Chapter 1, the overall aim of the Wellington Reservoir Study was to develop a numerical model incorporating all important mechanisms, including meteorological forcing. An initial task of this Project was to install a meteorological station on the reservoir to service the Study as a whole. A set of RIMCO meteorological sensors and a RIMCO Event Recorder were purchased for this purpose. These were installed with the assistance of staff from the CSIRO Division of Land Resources Management, on a raft constructed in the Civil Engineering workshop at the University of Western Australia (U.W.A.). Plate 3.1(a) shows the raft with event recorder, and Plate 3.1(b) shows a jarrah tree used as an anchor point and meteorological platform. A brief description of this system is given below.

The RIMCO Event Recorder is a data logging system designed to have very low power requirements, making it suitable for unattended operations at remote sites. Data are punched as ASCII characters onto paper tape and are readable at most computer installations. The normal mode of operation is to record events as they occur on any one of the 14 channels. The appearance of a particular channel code on the tape indicates that an event has occurred on that channel. One such event is the lapse of a time interval (5 or 6 minutes) as measured by a mechanical clock. Time

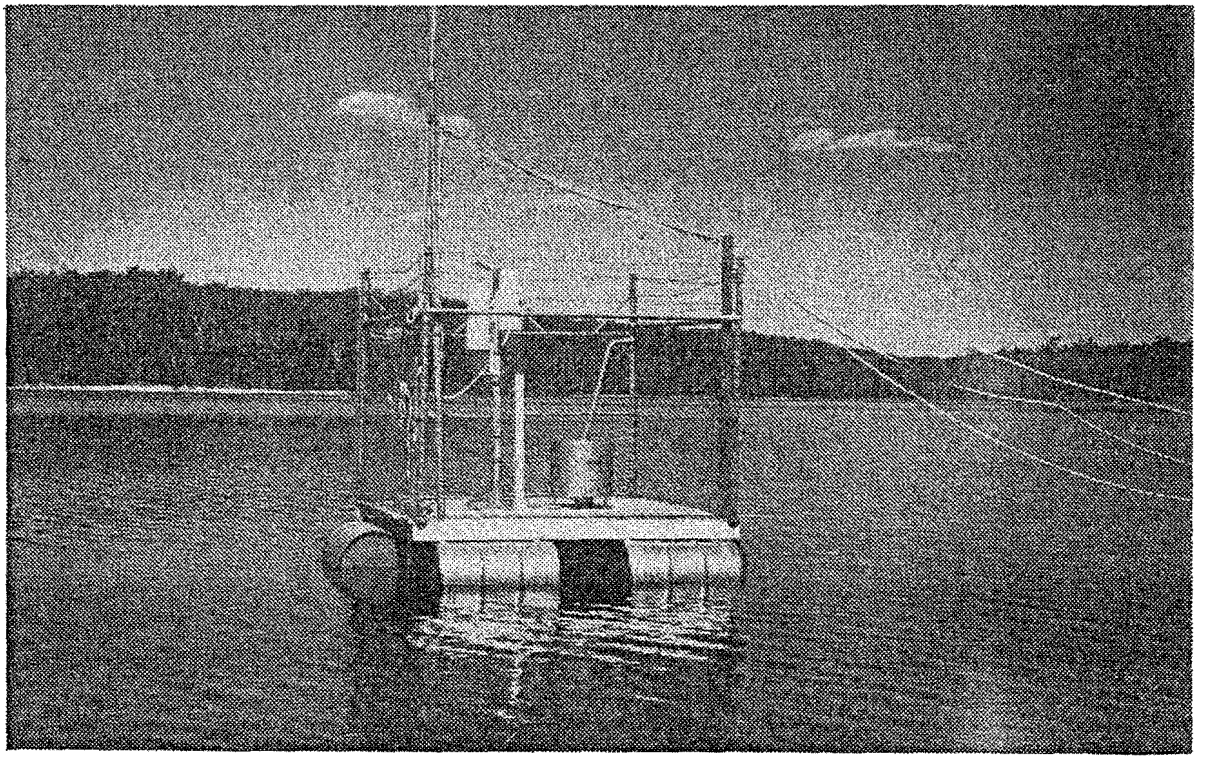

PLATE 3.1(a) Raft and RIMCO system: Event Recorder, sensors for air temperature, water temperature and relative humidity, plus a solar charger for the recorder battery

PLATE 3.1(b) Tree platform with RIMCO sensors for wind speed, wind direction and solar radiation

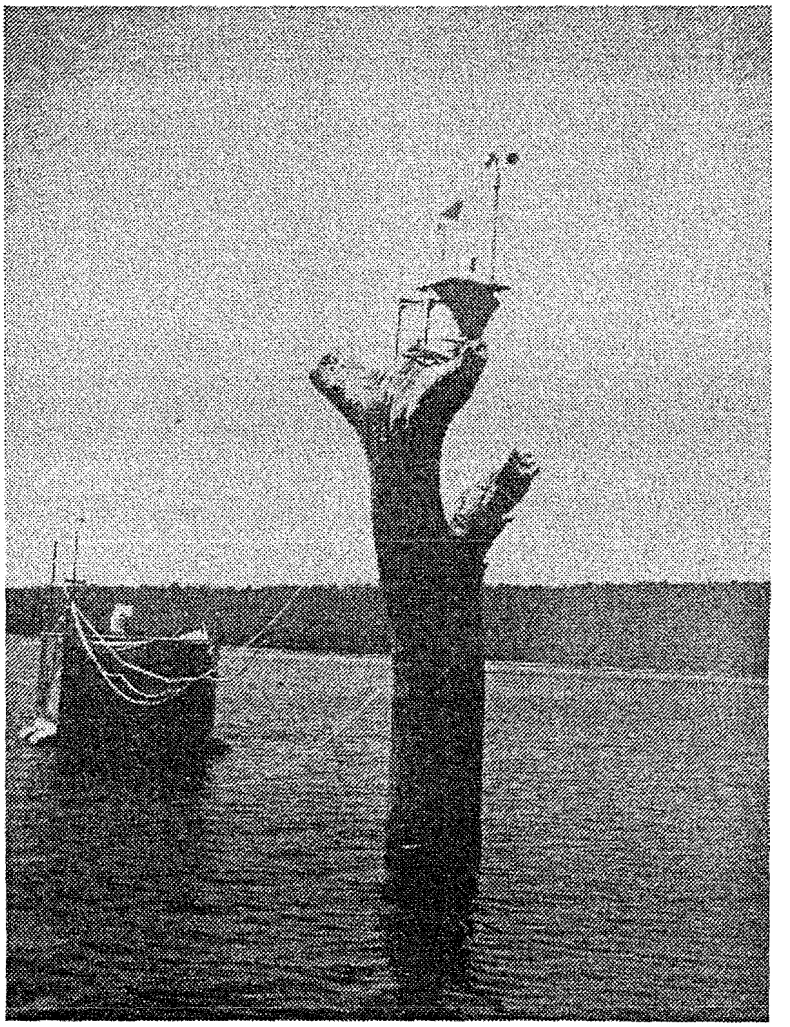

channel marks are thus interspersed with other channel marks on the tape. The Event Recorder is housed in a sealed cylinder and can be seen in the centre of the raft (Plate 3.1(a)) protected by a bullet-proof shield. A bank of solar cells, seen at the top of the 2 metre post, provides a charging current for the Recorder's Ni-Cad battery.

Whilst attractive in concept the Event Recorder system has some fundamental problems. Meteorological sensors designed to provide events for recording are generally deficient in both resolution and accuracy. Temperature and humidity sensors on the two metre post (Plate 3.1(a)) and wind speed, wind direction and solar radiation sensors (Plate 3.1(b)) all rely on mechanical movement to actuate reed relay closures. Understandably, these are not capable of achieving the accuracies attained by electronic sensors. If system failure occurs between visits, data recovery is often very difficult, since the time base must be inferred from an analysis of time marks.

Whilst the Event Recorder system was capable of providing useful data for the Study, requirements of high accuracy and resolution in this Project led to the assembling of a second complete set of instruments for use during the intensive field-work. This included construction of some of the sensors and most of the signal handling circuits. These instruments are described in detail in Sections 3.2 and 3.3. Sections 3.4 and 3.5 describe the processing of field data and subsequent computation of meteorological fluxes.

3.2 GENERAL EQUIPMENT FOR FIELDWORK

A brief description of the data recording equipment

and the power source used throughout the fieldwork is given below.

3.2.1 Data Recording

During the fieldwork phase of this Project, no sophisticated digital data acquisition system was available for recording meteorological or other data. The author was fortunate to procure on loan, from the CSIRO Division of Atmospheric Physics, a set of six Messmotors. A Messmotor is a precision DC motor which drives a six digit decade counter. The increment of the counter over a set interval (say one hour) is a measure of the integral of the input voltage. The box of Messmotors is shown in Plate 3.2 (No. 1).

A set of six high stability amplifiers was included (No. 2 in Plate 3.2) to provide buffering for meteorological sensor outputs and to amplify these outputs to the required 0-5 Volt range.

Multiple-point calibrations were conducted on each Messmotor-amplifier pair, giving operating expressions of the form:

$$\text{Input voltage} = a \times (\text{counts/minute}) + b.$$

Linearity was excellent. Subsequent calibrations and single-point checks throughout the fieldwork revealed high stability. An overall accuracy of ±1% can be assumed for the Messmotor system.

In the field, the counters were read and recorded manually once every hour. Readings were staggered by 30 seconds to ensure a precise hourly integral for each input. Errors introduced by this method of reading are negligible.

3.2.2 Power

Where possible instruments were purchased or constructed to run off batteries. Two heavy duty 12 volt lead accumulator

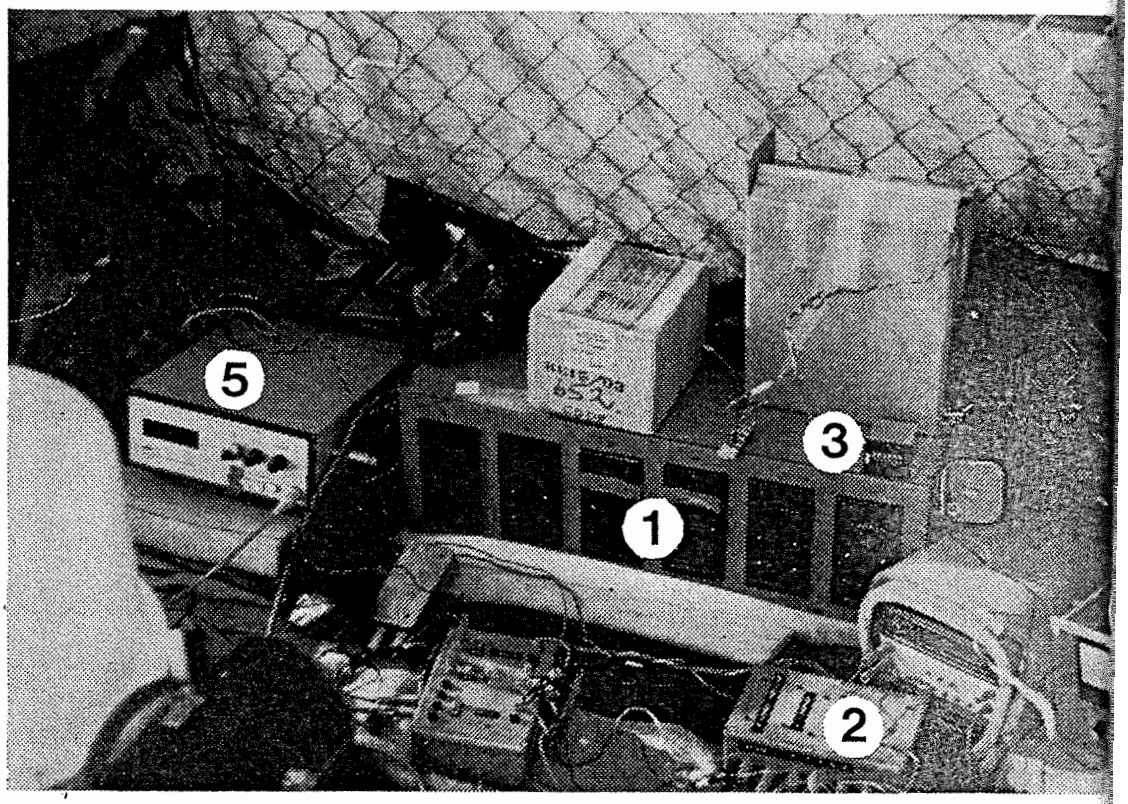

PLATE 3.2 Raft - based instruments:

1. Messmotors
2. Amplifiers
3. Anemometer pulse counter
4. VAISALA relative humidity meter
5. A.L.E. conductivity meter

batteries supplied ±12 volts to the amplifiers and also 24 volts to an inverter which, as required, supplied 240 VAC to a Digital Voltmeter (DVM) and other equipment. Other dry cells were used to power meteorological sensors, avoiding earth loops in the recording system.

3.3 METEOROLOGICAL INSTRUMENTATION FOR FIELDWORK

The meteorological instruments and associated data recording methods are described below for each of the parameters measured.

3.3.1 Wind Speed

A $3^3/_4$" RIMCO cup anemometer was installed at a height of four metres on an aluminium mast, as seen in Plate 3.3 (No. 1). This instrument operates on the light-chopper principle with the output pulse train being integrated on a decade counter supplied with the anemometer (see Plate 3.2 No. 3). The counter readings were recorded and reset hourly. Relevant instrument specifications are:

(a) starting speed - 0.1 m/sec,

(b) flow coefficient - 1.74 m/rev.

The counter readings for the RIMCO Event Recorder anemometer mounted on the tree were also recorded manually for checking. The two units were in good agreement throughout the fieldwork. No independent calibrations were performed on either instrument.

3.3.2 Air Temperature

Air temperature was measured by a nominal 5kΩ thermistor

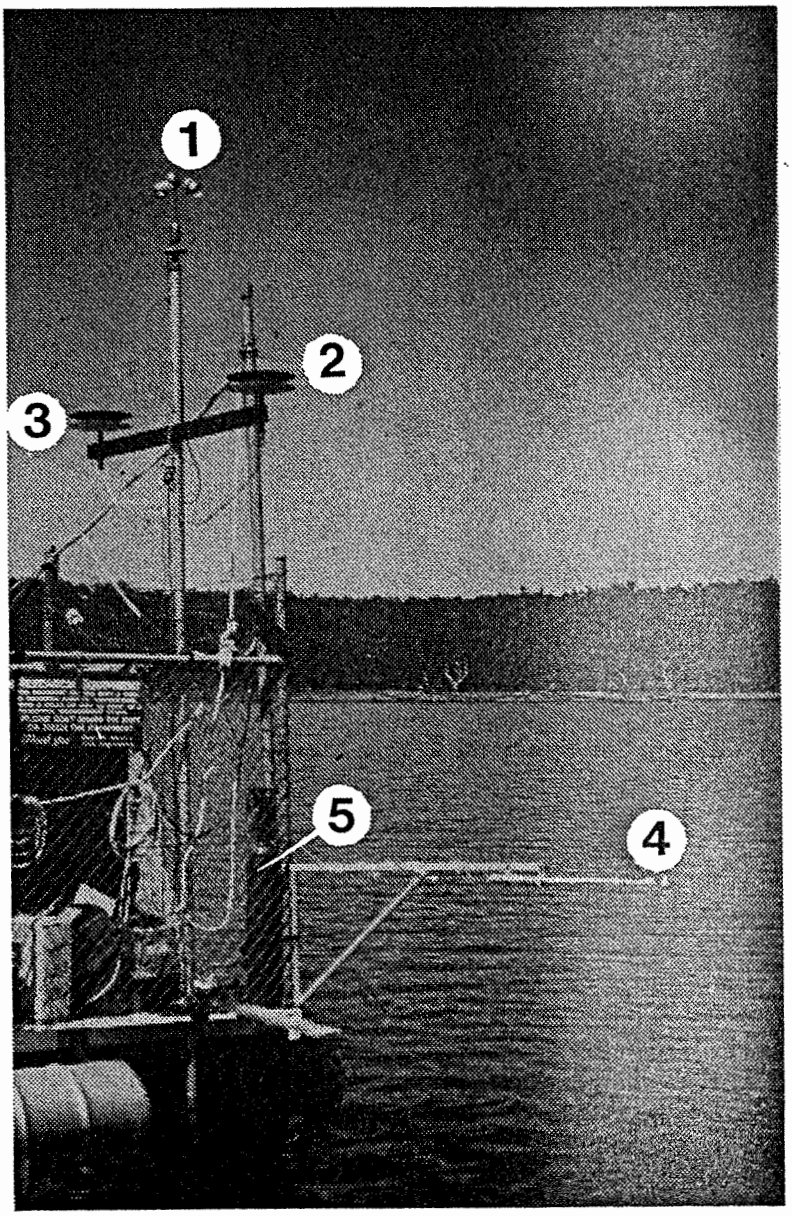

PLATE 3.3 Meteorological sensors:

1. RIMCO sensitive cup anemometer
2. Air temperature probe and shield
3. VAISALA relative humidity probe and shield
4. Net radiometer
5. Dry nitrogen supply

mounted at a height of three metres on the mast cross arm. The radiation shield seen in Plate 3.3 (No. 2) consisted of four horizontal discs separated by PVC spacers and painted black and white on inside and outside surfaces respectively. Disc size and spacing was determined in order to give radiation protection for sun angles > 5^{o}, while causing no interference to natural ventilation.

This thermistor, like all thermistors in the system, was incorporated in a Wheatstone Bridge circuit. The output voltage was linearised by placing a 5kΩ shunt resistance across the thermistor arm of the bridge and balancing the bridge at the bottom of the temperature range.

Extensive multiple-point calibrations were performed prior to field days to determine the operating expression for the thermistor circuit. Two-point (hot and cold) calibrations were also performed on the raft at the start and end of field days. Over the full period, accuracy was maintained within $\pm 0.2^{o}C$.

3.3.3 Water Surface Temperature

Water surface temperature was measured with circuitry similar to that used for air temperature.

The water temperature probe mounting seen in Plate 3.4 (No. 1) was carefully designed to ensure that the probe remained just beneath the surface. The radiation shield was connected via hinged arms to the raft, giving the shield vertical and rotational freedom. Three buoys supported the shield at its corners. These in turn were weighted by a single submerged lead sinker attached with three nylon cords. The weight ensured that the buoys (and hence the

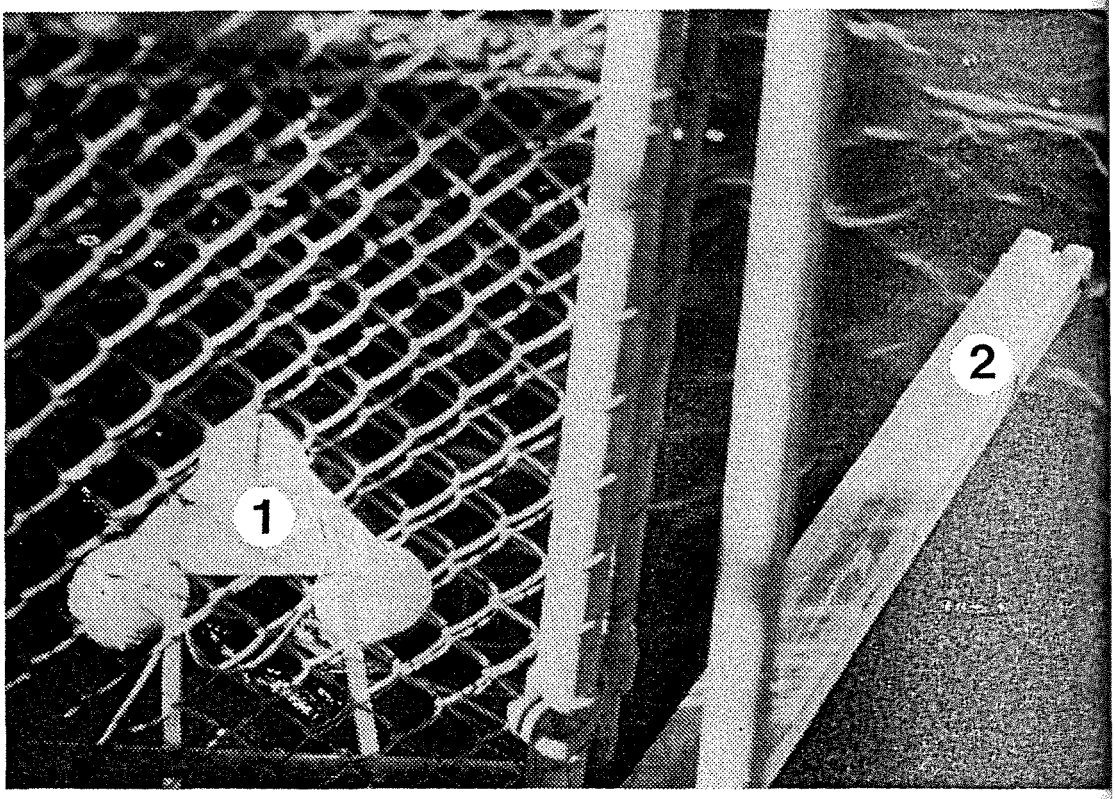

PLATE 3.4 Water temperature sensor:
1. Probe and radiation shield
2. Extension arm and pulley for conductivity/ temperature probe

probe) always followed wave troughs, but provided no upward inertia which would have caused the probe to surface.

Calibration of the water temperature probe was conducted simultaneously with that for air temperature. On only one occasion did observed errors fall outside the range $\pm 0.1^{o}C$.

3.3.4 Relative Humidity

A VAISALA HM11 humidity meter was purchased for the Project. It uses a thin film capacitive sensor which responds rapidly to relative humidity over the full 0 to 100% range. The manufacturer gives the following specifications:

(a) humidity range - 0 to 100% RH,

(b) temperature range - $-40^{o}C$ to $80^{o}C$,

(c) response time - 1 sec for 90% response,

(d) temperature coeff. - 0.05% per $1^{o}C$,

(e) overall accuracy - ±2%.

The humidity probe was mounted adjacent to the air temperature probe in an identical radiation shield (see Plate 3.3 No. 3). No signal conditioning was required prior to amplification and recording by a Messmotor.

Instrument calibration was performed prior to field-work by adjusting the meter output at known humidities over saturated salt solutions, namely Lithium Chloride and Potassium Sulphate. Overall, the instrument functioned very well and within the manufacturer's specifications, except for a tendency to drift slowly upward when humidity was high. The meter is seen in Plate 3.2 (No. 4).

3.3.5 Net Radiation

A SOLAR RADIATION INSTRUMENTS LTD. Net Radiometer (seen in Plate 3.3 No. 4) was obtained on loan from the CSIRO Division of Land Resources Management for the duration of the fieldwork. The operating principles of this type of instrument are given by Funk (1959). The CSIRO calibration certificate details are:

(a) sensitivity at $20^{o}C$ -

short-wave: 0.332 $mV/mWcm^2$

long-wave: 0.331 $mV/mWcm^2$,

(b) accuracy of calibration - ±2.5%

The thin polythene hemispheres which act as a wind-shield for the upper and lower thermopiles were inflated with dry nitrogen gas. The nitrogen bottle and gas lines are seen in Plate 3.3 (No. 5). A slow flow of gas was regulated by a needle valve, adjusted to give several bubbles of exhaust gas per minute through a jar filled with water.

The net radiometer functioned well over the experimental period. No direct calibration was carried out and the CSIRO calibration data were used. Calculations detailed in the next section show that the net radiation data agree with available formulae for both short-wave and long-wave radiation. No significant absolute errors are apparent, however, a small relative (percentage) error, in the range +0 to -4%, has been estimated from the calculations. This is quite acceptable and may be due to instrument aging or slight opacity of the polythene caused by photo-oxidation by ultra-violet light (see Funk (1959)).

3.3.6 Solar Radiation Absorption

Results from the January and February field days indicated that the form of solar radiation absorption in the reservoir was a major factor in the subsequent behaviour of the surface layer. As it was not possible to purchase or borrow an underwater solarimeter at that stage, a unit was designed and manufactured. This is shown in Plate 3.5.

The thermopile, originally from a solarimeter, was obtained from the CSIRO. It was seated on a PVC base and encased in a brass cylinder. The glass faceplate was sealed with an O ring.

The unit was held horizontally by three arms suspended from a point on the signal cable which was also used to lower the probe. To avoid noise and signal loss in the cable, an operational amplifier was incorporated in the cylinder.

A test was performed on two faceplates of different thickness to determine their transmittance characteristics and hence whether they might modify the solar spectrum being measured beneath the water. Figure 3.1 shows copies of the plots produced by a Grating Spectrophotometer. They show the transmittance or absorbance of the two faceplates over the wavelength ranges 0.8 - 2.5 μ and 2.5 to 3.4 μ. Also shown is the true 100% line of the instrument. Absolute values are of little interest but the important points are:

i) the transmittance is high and varies little over the range 0.8 to 2.7 μ. It is obviously also high in the visible range, 0.3 to 0.8 μ,

ii) the transmittance falls sharply after 2.7 μ.

Comparing these results with Table 3.1, taken from Irvin and Pollack (1968), it can be seen that the glass faceplates

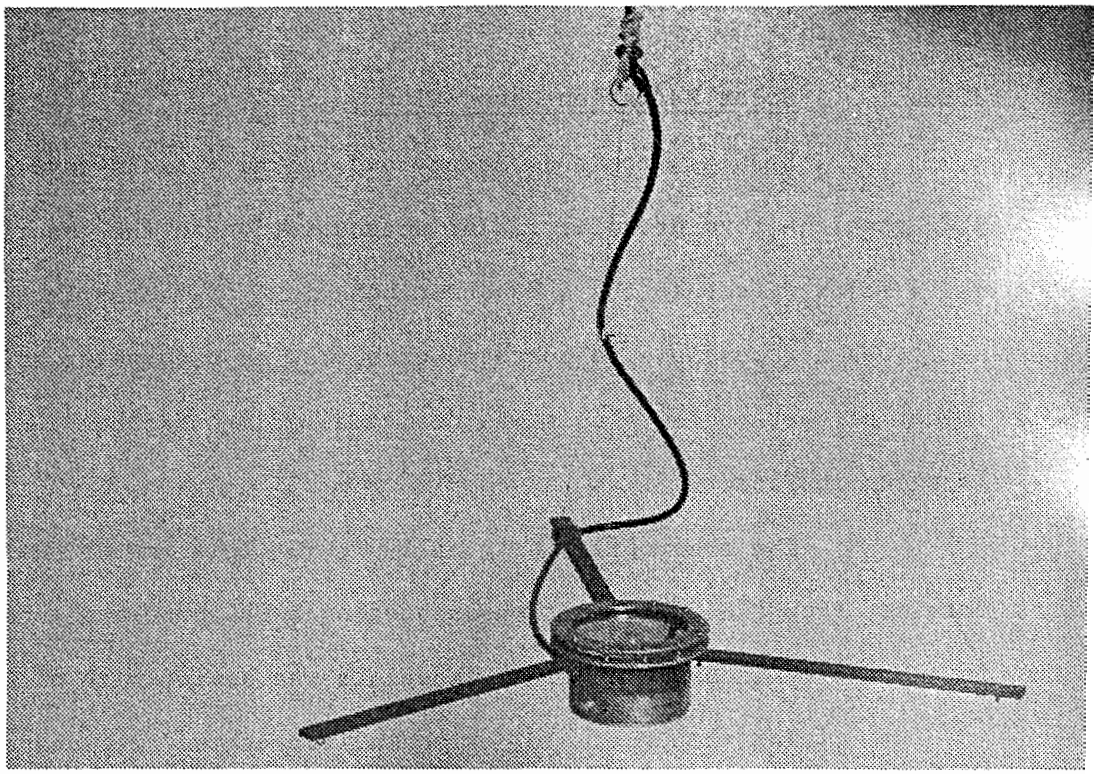

PLATE 3.5 Underwater solarimeter showing:
(a) signal cable, suspension arm and wire
(b) thermopile, amplifier circuit card

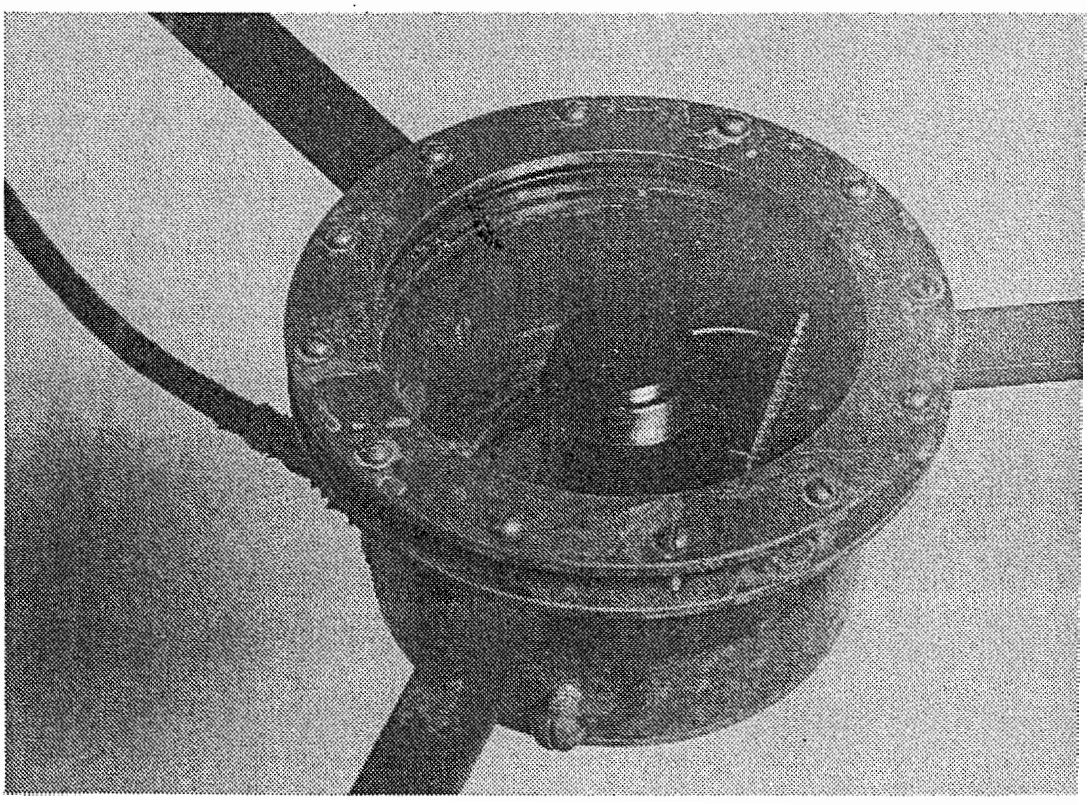

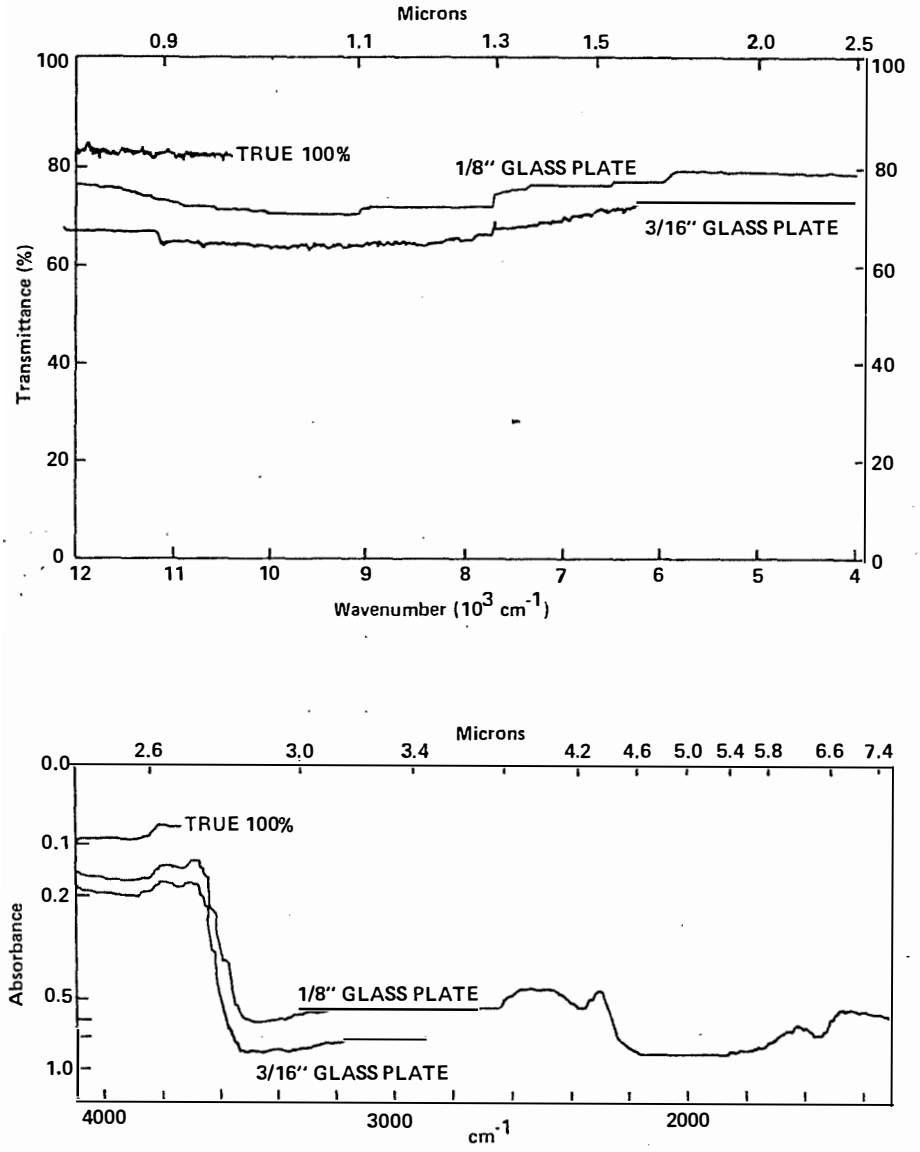

FIGURE 3.1 Spectrophotometer plots of transmittance (absorbance) for two glass faceplates for the underwater solarimeter

WATER: ABSORPTION COEFFICIENT k AND REAL (n_r) AND IMAGINARY (n_i) PARTS OF INDEX OF REFRACTION VERSUS WAVELENGTH λ

λ (μ)	n_r	k	n_i	λ (μ)	n_r	k	n_i
0.20	1.424	8×10^{-2}	1.3×10^{-7}	2.25	1.290	17	0.0003(
0.25	1.377	3×10^{-2}	6.0×10^{-8}	2.30	1.286	23	0.00042
0.30	1.359	1.5×10^{-2}	3.6×10^{-8}	2.35	1.282	30	0.00056
0.35	1.349	3×10^{-3}	8×10^{-9}	2.40	1.276	42	0.00080
0.40	1.343	1×10^{-3}	3×10^{-9}	2.45	1.270	61	0.00118
0.45	1.339	2×10^{-4}	7×10^{-10}	2.50	1.246	83	0.00165
0.50	1.336	2.5×10^{-4}	8×10^{-10}	2.55	1.213	97	0.00196
0.55	1.334	3.5×10^{-4}	1.5×10^{-9}	2.60	1.180	99	0.00204
0.60	1.332	1.5×10^{-3}	7×10^{-9}	2.625	1.160	109	0.00227
0.65	1.331	2.5×10^{-3}	1.3×10^{-8}	2.65	1.140	131	0.00276
0.70	1.330	0.006	3.3×10^{-8}	2.70	1.134	235	0.00504
0.75	1.329	0.025	1.49×10^{-7}	2.75	1.133	1 100	0.02401
0.76	1.329	0.026	1.5×10^{-7}	2.80	1.232	4 212	0.09361
0.80	1.328	0.021	1.34×10^{-7}	2.90	1.310	10 580	0.2435
0.806	1.328	0.020	1.2×10^{-7}	2.95	1.325	11 700	0.2740
0.85	1.327	0.041	2.77×10^{-7}	3.00	1.351	10 860	0.2586
0.90	1.328	0.067	4.80×10^{-7}	3.10	1.426	7 430	0.1828
0.95	1.327	0.365	2.76×10^{-6}	3.20	1.509	3 700	0.09422
0.97	1.327	0.46	3.55×10^{-6}	3.30	1.470	1 650	0.04333
1.00	1.326	0.355	2.82×10^{-6}	3.40	1.449	698	0.01888
1.05	1.325	0.131	1.10×10^{-6}	3.50	1.423	334	0.00930
1.06	1.325	0.128	1.07×10^{-6}	3.60	1.402	198	0.00567
1.10	1.324	0.190	1.66×10^{-6}	3.75	1.372	119	0.00355
1.15	1.3225	0.800	7.32×10^{-6}	3.83	1.358	111	0.00338
1.19	1.323	1.05	9.9×10^{-6}	4.00	1.349	151	0.00481
1.20	1.323	1.020	9.74×10^{-6}	4.50	1.341	411	0.01472
1.25	1.322	0.890	8.85×10^{-6}	4.66	1.338	468	6.00173
1.258	1.322	0.88	8.8×10^{-6}	4.80	1.336	431	0.01647
1.30	1.321	1.08	11.17×10^{-6}	5.0	1.331	308	0.01225
1.35	1.320	2.70	29.0×10^{-6}	5.26	1.318	229	0.00959
1.40	1.320	13	14.48×10^{-5}	5.5	1.303	276	0.01208
1.45	1.319	26.0	3.00×10^{-4}	5.8	1.266	699	0.03226
1.50	1.318	17.3	0.0002065	6.0	1.313	2 138	0.10208
1.55	1.317	9.6	0.0001184	6.05	1.324	2 328	0.11208
1.60	1.316	6.2	0.0000789	6.4	1.347	852	0.04339
1.65	1.316	5.1	0.0000670	6.5	1.338	794	0.04107
1.66	1.315	5.0	0.000066	7.0	1.323	618	0.03443
1.70	1.315	5.15	0.0000697	7.5	1.303	579	0.03456
1.75	1.314	6.4	0.0000891	8.0	1.293	566	0.03603
1.80	1.312	8.0	0.0001146	8.5	1.286	557	0.03768
1.85	1.311	9.5	0.0001399	9.0	1.269	566	0.04054
1.90	1.309	80.5	0.001217	9.5	1.245	579	0.04377
1.94	1.307	114.0	0.00176	10.0	1.214	668	0.05316
1.95	1.307	110	0.001707	10.5	1.185	826	0.0690
2.00	1.304	68	0.0010S2	11	1.151	1 165	0.1021
2.05	1.302	41	0.0006689	11.5	1.145	1 672	0.1530
2.10	1.300	26	0.0004345	12	1.160	2 191	0.2092
2.15	1.296	19	0.000325	12.5	1.19	2 451	0.2438
2.20	1.293	16	0.000280	13	1.220	2 821	0.2918
2.21	1.292	15.5	0.000272	13.5	1.245	2 980	0.3202

TABLE 3.1 Absorption coefficients for water (Irvine and Pollack (1968))

will transmit all wavelengths of interest below the water. The absorption coefficient in water increases rapidly for wavelengths > 2.6 μ, just before the corresponding increase for glass. Furthermore, almost all the power in the solar spectrum is contained at wavelengths below this level.

Unfortunately, due to failure of the thermopile, it was possible to obtain only one data set for the absorption profile and then not without complication. The thermopile was not temperature compensated and consequently, due to solar heating of the sealed cylinder prior to use, the output showed a large negative offset at a depth of three metres as seen in Figure 3.2. Nevertheless, the offset was constant over the period of investigation (checked by consistency of successive profiles) and so some useful analysis is still possible.

Because only a small amount of radiation reaches the three metre level (5% to 12% from the T.V.A. (1972) report) the overall shape of the attenuation curve is relatively insensitive to even large percentage errors at that depth. Therefore, for the purposes of analysing Figure 3.2 it can be reasonably assumed that 10% of the solar flux penetrates to three metres. This allows definition of a new origin and re-scaling of the data, taking the surface reading as 100%.

A simple procedure may now be used to determine an attenuation profile of the form given by eq. 2.56:

(a) plot the data $q(z)/Q_s$ vs. z on a log-linear graph,

(b) determine the values of a_1 and b_1 for the lowest linear portion of the plot,

(c) subtract the curve $a_1 e^{-b_1 z}$ from the original data. Replot the remaining flux values to determine a_2 and b_2 etc.

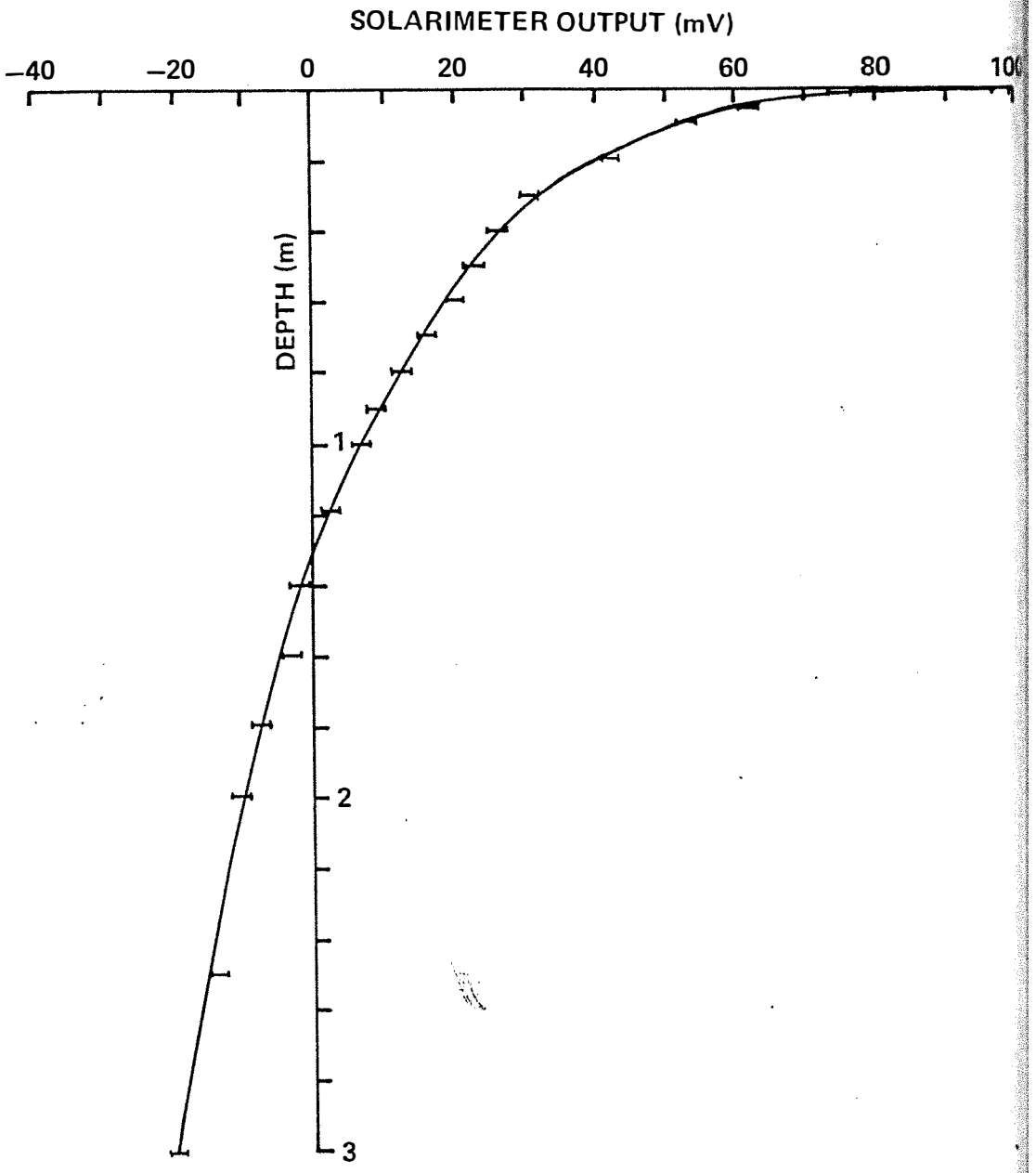

FIGURE 3.2 Solar radiation attenuation profile measured by the underwater solarimeter. Error bars indicate the reading accuracy

The resultant expression for the data collected is

$$q(z)/Q_s = 0.54e^{-0.561z} + 0.30e^{-6.89z} + 0.16e^{-69z} \quad . \quad (3.1)$$

The value of b_3 is tentative; it indicates that 16% of radiation is absorbed essentially in the first 2 cm.

Whilst the expression has been determined with reasonable confidence, this aspect of field measurement should receive close attention in any future studies.

3.4 DATA PROCESSING

The fieldwork associated with this Project was conducted in the early months of 1976. Reliable data sets were obtained for four separate days during this period, namely January 15 (15 01 76), February 3 (03 02 76), February 5 (05 02 76) and April 5 (05 04 76). The methods employed to process these data are described below.

3.4.1 Data Storage

In the field, the meteorological data in the form of hourly Messmotor counter readings were entered onto coded data sheets. Also recorded were hourly spot readings of meteorological sensor outputs to provide a check for, and supplement to, the Messmotor recordings. Periodically, observations of wave height, cloud cover and wind direction was also recorded.

Data from coded sheets were punched onto cards and then transferred to disc on a large mainframe computer, where some minor editing was performed.

3.4.2 Data Reduction

From the calibration information obtained, as described

in Section 3.3, calibration expressions were determined for each instrument for individual field days. Checks were performed where redundant calibration information was available, resulting in estimates of measurement accuracy summarised below:

Parameter	Accuracy
Wind speed	±0.2 m/sec
Air temperature	±0.2^{o}C
Water temperature	±0.15^{o}C
Relative Humidity	±3%
Net Radiation	+0, -3 mW/cm^{2}

Processed meteorological data for the four field days appear in Appendix A1. Included in the data are readings from the Event Recorder anemometer, pyranometer and a Kipp Solarimeter which was used in the April fieldwork.

To facilitate examination of the data, computer plots of individual parameters were produced. Examples of these plots for the day 050276 are displayed in Figure 3.3(a) and (b). The timebase on all plots was in hours, starting either from midnight or 0400 hours. Varying vertical scales and zeros were used to enhance the plots. Points to note when viewing them are as follows

1. The stepped plots indicate that data were averaged over the various periods (usually hourly). Crosses represent the spot readings taken. The accuracy of the spot readings varies depending on the parameter fluctuations and the instruments response. In particular, readings taken from the humidity meter may be quite unrepresentative of the mean humidity.
2. The dashed stepped line on the wind speed plots indicates data from the Event Recorder anemometer.

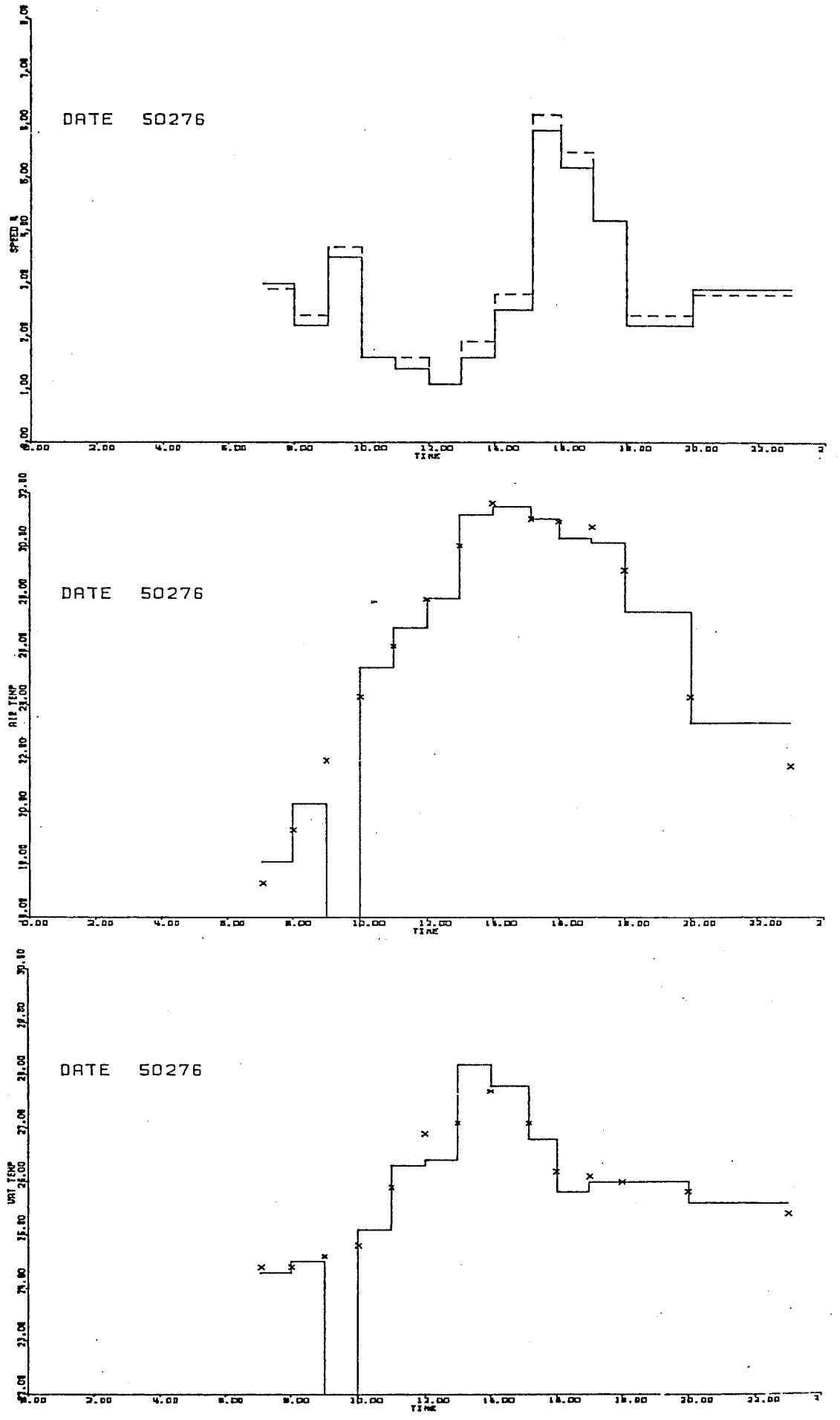

FIGURE 3.3(a) Computer plot of processed meteorological data averages for 05 02 76: wind speed, air temperature, water temperature

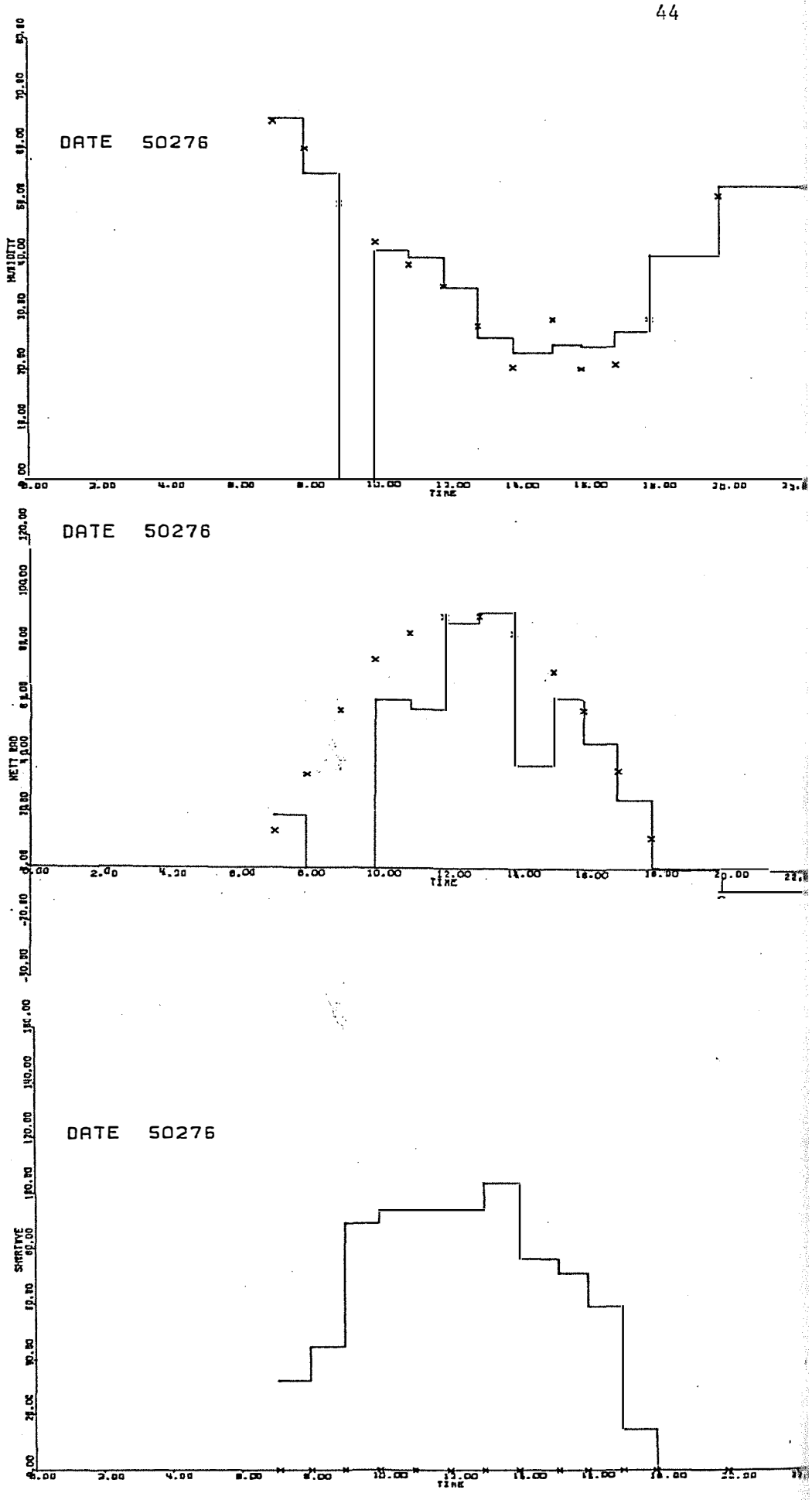

FIGURE 3.3(b) Computer plot of processed meteorological data averages for 05 02 76: humidity, net radiation, short-wave radiation

3. Errors in the data averages become obvious when viewing the plots. Identification of these errors was the fundamental reason for plotting the data. These errors may be due to instrument failure or reading error. They have been corrected as far as possible, as described in the next section.
4. Inspection of the short-wave radiation plots reveals that, as expected, the Event Recorder pyranometer resolution is too coarse for the present application.

3.4.3 Time Series Synthesis

Monin and Kolesnikova (1968) indicate that micrometeorological fluctuations tend to have a spectral gap at a period of about 10 minutes: turbulent eddies have timescales somewhat shorter than 10 minutes and large scale circulations have timescales somewhat larger than 10 minutes. On this basis it may be considered optimal to measure 10 minute averages of meteorological variables. This was unfortunately not practical during the labour-intensive field experiments of this Project.

From inspection of the data (hourly averages and spot readings) plus additional processed data from the Event Recorder system, it proved possible to synthesise time series of the meteorological variables. The latter source of data is of doubtful quality and so was used primarily to provide time base information for wind speed, the most variable parameter.

The method of time series synthesis was as follows. Large transparent copies of individual plots (as displayed in Figure 3.3) were overlaid with transparent graph paper and, where applicable, underlaid with plots of the Event Recorder data. Any

available supplementary data were marked on the overlay (e.g. profiling probe surface temperature data). Conserving the integral of verified Messmotor averages and giving appropriate attention to all the additional information, a smooth sequence of line segments was then drawn to fit the data. Points from these new representations were subsequently fed back into the computer. The resultant data set contained mostly half hourly values but in a few cases this interval was decreased to 15 minutes in order to describe changes observed on the Event Recorder plots. Copies of these data files appear in Appendix A2.

To a small degree this double handling of data may have degraded overall accuracy. However, the procedure provided a reasonably accurate representation of the daily cycle of meteorological variables, making it possible to compute the corresponding cycles of fluxes. Step changes, which may possibly cause problems in numerical simulation models, have been removed. Importantly, the resolutions of wind speed changes in the data has been improved In following chapters, terms dependent on the third power of the wind speed are computed; neglect of short term peak values would introduce large errors.

3.5 FLUX COMPUTATIONS

From the processed meteorological data the various radiative and turbulent fluxes may be computed, as described in Chapter 2. Although a numerical model of a reservoir will incorporate its own flux computation, it is instructive to calculate these here in order to examine the importance of atmospheric stability effects in the reservoir situation.

3.5.1 Radiative Fluxes

From an inspection of the data it is evident that net radiation is the only radiation measurement with sufficient resolution to describe diurnal variability. In view of this the following computations were performed in order to predict the various radiation components plotted in Figures 3.4(a) to (d).

Net radiation may be expressed in terms of its various components as defined in Section 2.2:

$$Q_N = (1-R)\ Q_s + Q_{LAC} - Q_{LR} \qquad (3.2)$$

The short-wave reflectance, R, is defined below .

$(1-R)Q_s$ is the main term in the balance; it is that part of the incoming short-wave radiation which penetrates the water surface and is absorbed below. This term was evaluated from eq. 3.2 using measured Q_N, with Q_{LAC} and Q_{LR} calculated from eq. 2.54 and eq. 2.52. It is plotted in Figures 3.4(a) to (d) as a diamond symbol. Also plotted as dotted lines are Q_{LAC} and Q_{LR}. Note that downward radiation fluxes are considered here as being positive.

As a check on the estimate of the short-wave component, a simplified independent calculation was performed. Values for the normal and diffuse components of short-wave (Q_{sN} and Q_{sD} respectively) were obtained from Spencer (1976). These were used in the formulae of eq. 2.46 to eq. 2.51 to produce a diurnal cycle of short-wave at Wellington Reservoir. After subtracting the reflected component, given in the T.V.A. (1972) report as $R\ Q_s$ where

$$R = 1.18\alpha^{-0.77} \qquad (3.3)$$

for clear skys, the results were plotted in Figures 3.4(a) to (d) as the dashed line. Agreement between this curve and the values

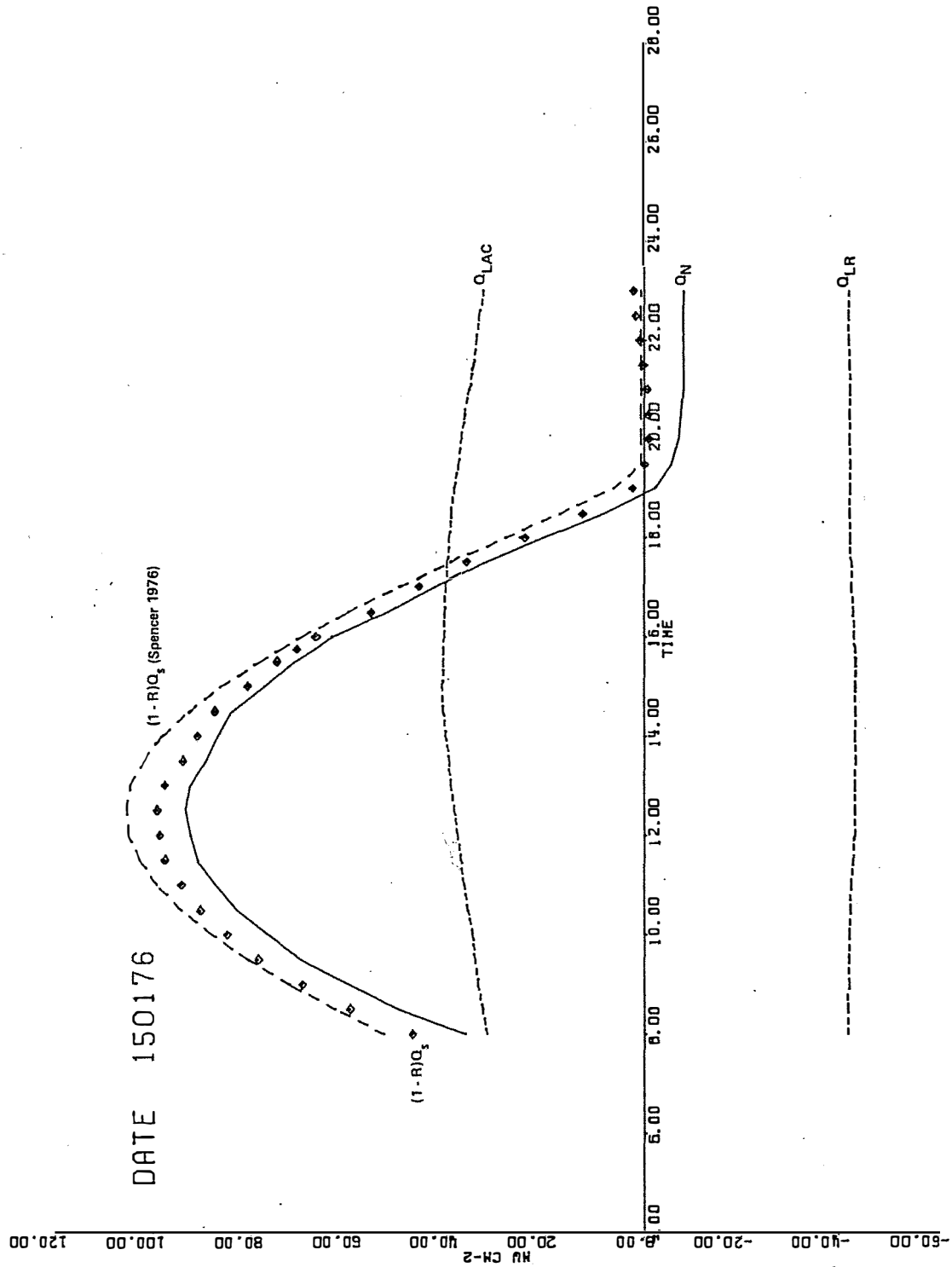
DATE 150176
(1-R)Q$_s$ (Spencer 1976)
(1-R)Q$_s$
Q$_{LAC}$
Q$_N$
Q$_{LR}$
TIME
MV CM-2
0.00
6.00
10.00
12.00
14.00
16.00
18.00
20.00
22.00
24.00
26.00
28.00
-60.00
-40.00
-20.00
0.00
20.00
40.00
60.00
80.00
100.00
120.00

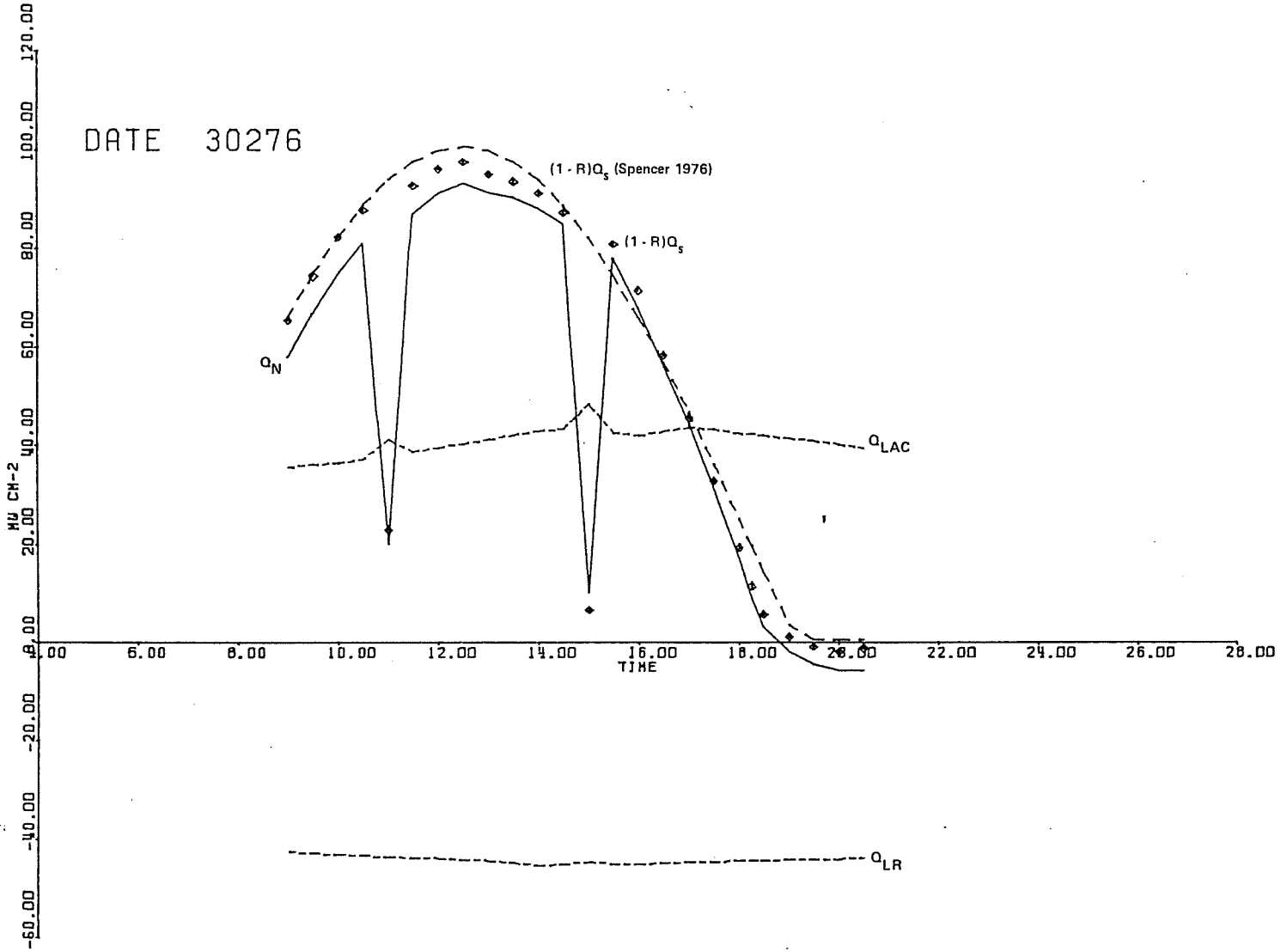

(b) Radiation fluxes for 03 02 76

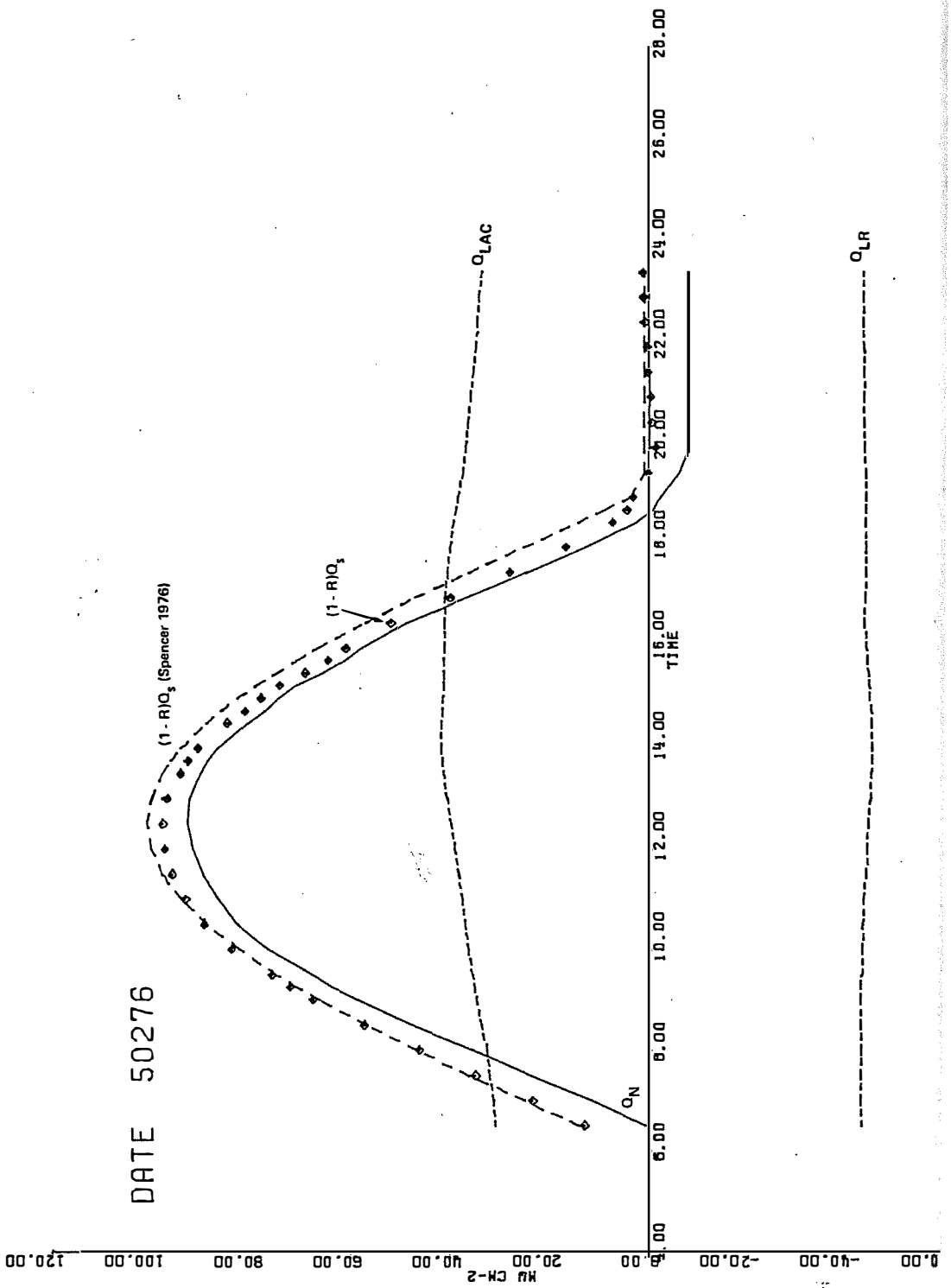
DATE 50276
$(1-R)Q_s$ (Spencer 1976)
$(1-R)Q_s$
Q_N
Q_{LAC}
Q_{LR}
TIME
MU CM-2
0.00
4.00
6.00
8.00
10.00
12.00
14.00
16.00
18.00
20.00
22.00
24.00
26.00
28.00
0.00
-40.00
-20.00
20.00
40.00
60.00
80.00
100.00
120.00

from eq. 3.2 is good for clear days (eg. 05 02 76). The curve also serves as a reference for days when cloud or smoke were present

An encouraging feature of the plots is the behaviour of the two long-wave radiation formulae. It was not necessary to force the night-time zero for short-wave; it resulted from the balance of eq. 3.2. The method slightly under predicts the short-wave during daytime hours, however for this Project the accuracy is acceptable.

The Event Recorder pyranometer was designed to give one count per 14.8 mW Hr cm^{-2}. This resolution was too coarse to provide a time representation similar to those of Figure 3.4(a) to (d). It was decided however to check the integrated values of this instrument against the integral of the calculated and predicted curves. For the day 05 02 76 between the times 0800 and 1300 the pyranometer, predicted (eq. 3.2), and calculated integrals were respectively

414 433 448 mW Hr cm^{-2}.

Other comparisons confirmed the 4% difference between values, although the pyranometer exhibited poor cosine response for low solar altitudes.

3.5.2 Turbulent Fluxes

Bulk aerodynamic formulae described in Section 2.1.3 are suitable for computing turbulent fluxes of heat, water vapour and momentum from the meteorological data. As there are a number of interesting aspects to this computation, a flow diagram of the program has been included in Appendix B1 and a copy of the program appears in Appendix C1.

Neutral Transfer Coefficients

Following the discussion in Section 2.1.3, the choice of neutral transfer coefficients applicable to a measurement height of ten metres was as follows:

$$C_{DN10} = 1.0 \times 10^{-3} \qquad U \leq 5\text{m/sec}$$

$$= (1.0 - 0.07(U-5)) \times 10^{-3} \qquad U > 5\text{m/sec}$$

$$C_{HWN10} = 1.35 \times 10^{-3}$$

The relatively low wind speeds experience on the four field days have been taken into account in the above choice

Effect of Measurement Height

The transfer coefficients must be altered if measurements are made at other than the standard ten metre height. In view of the discussion in Section 2.1.4 regarding the internal boundary layer problem, measurement heights for wind speeds and air temperature/humidity were chosen to be four and three metres respectively.

The neutral drag coefficient for four metres is given by

$$C_{DN4} = C_{DN10} \left[\left(\ell n \left(\frac{10}{z_o} \right) \right)^2 / \left(\ell n \left(\frac{4}{z_o} \right) \right)^2 \right] \tag{3.4}$$

with z_o computed from eq. 2.38. Similarly

$$C_{HWN3} = C_{HWN10} \left[\frac{\ell n \left(\frac{10}{z_o} \right) \quad \ell n \left(\frac{10}{z_{HW}} \right)}{\ell n \left(\frac{3}{z_o} \right) \quad \ell n \left(\frac{3}{z_{HW}} \right)} \right] \tag{3.5}$$

with z_{HW} from eq. 2.37.

Vapour Pressure and Specific Humidity Calculations

Wigley (1974) gives a formula for the saturation vapour pressure e_s:

$$e_s = 1013.25 \exp[13.3185t - 1.9760t^2 - 0.6445t^3 - 0.1299t^4] \quad (3.6)$$

where $t = 1 - \frac{T_s}{T}$.

T and T_s are the air temperature and steampoint temperature respectively (both in ^oK). He shows this formula to be accurate to within 0.1% over the wide range ($-50^oC < T < 140^oC$).

The vapour pressure of unsaturated air is then

$$e = \frac{\phi\, e_s}{100} \quad (3.7)$$

where ϕ is relative humidity (%). Specific humidity is given by

$$q = \frac{0.662e}{p} \quad (3.8)$$

where p is atmospheric pressure.

Stability Correction to Transfer Coefficients

Figures 2.1 and 2.2 show the correction to the drag coefficient as Ri_B varies. These graphs (corrected for measurement height) are useful for manual flux calculations; Ri_B may be calculated from field observations via eq. 2.43. The graphs are not useful for computing purposes however unless empirical expressions for the relations $C_a/C_{aN} \sim f(Ri_B)$ are obtained.

Hicks (1975) suggests an alternative method of stability correction which is attractive from a computing viewpoint. The fluxes may be calculated using an estimate of the transfer coefficients C_D and C_{HW}. A provisional estimate of z/L may then be obtained from eq. 2.9 and using this, C_D and C_{HW} may be corrected with eq. 2.41 and eq. 2.42. The process is repeated iteratively until z/L converges to a constant value.

This procedure (see Appendices B1 and C1) was found to perform very well. After starting the coefficients at their neutral

values, satisfactory convergence usually occurred within five steps. For sequential calculations, it would be more efficient to use the previously determined coefficients as commencement values for a new iteration.

Results of Calculations

Figure 3.5(a) to (d) are plots presenting the results of calculations for the four field days.

Examining first the plots of transfer coefficient and stabilities it can be seen that both of these vary markedly over any day. The horizontal lines on the plots represent (from bottom up) the level of C_{DN4}, C_{HWN3} and $Ri_B = z/L = 0$. During early and mid-morning the atmospheric layer is very unstable in some cases (see Figure 3.5(b)). This is due to the combined effect of light winds, a negative air-water temperature differential and the buoyancy of water vapour. During calm hot afternoon the stability is reversed, with a positive temperature differential dominating the vapour buoyancy. Corresponding to the stability variations, the transfer coefficients vary by a factor of three or more, leading to enhanced transfers (eg. evaporation) in the morning and suppressed transfers on hot afternoons. If the calculations are correct there are serious implications regarding the practice of using constant transfer coefficients for all calculations. Hicks (1975), discussing unstable oceanic conditions, concludes that,

> "... in winds of less than about 2 m s^{-1}, greatly enhanced transfer coefficients should be common. In such light winds, it is quite probable that the atmospheric stability exceeds the limits imposed by our present knowledge of the flux-gradient relationships. This, in itself, is sufficient reason to argue against the blind adoption of the conventional 10 m reference level for the deduction of eddy fluxes from bulk aerodynamic data; the use of lower elevations when the magnitude of L is small might be more advisable". (1975, 522)

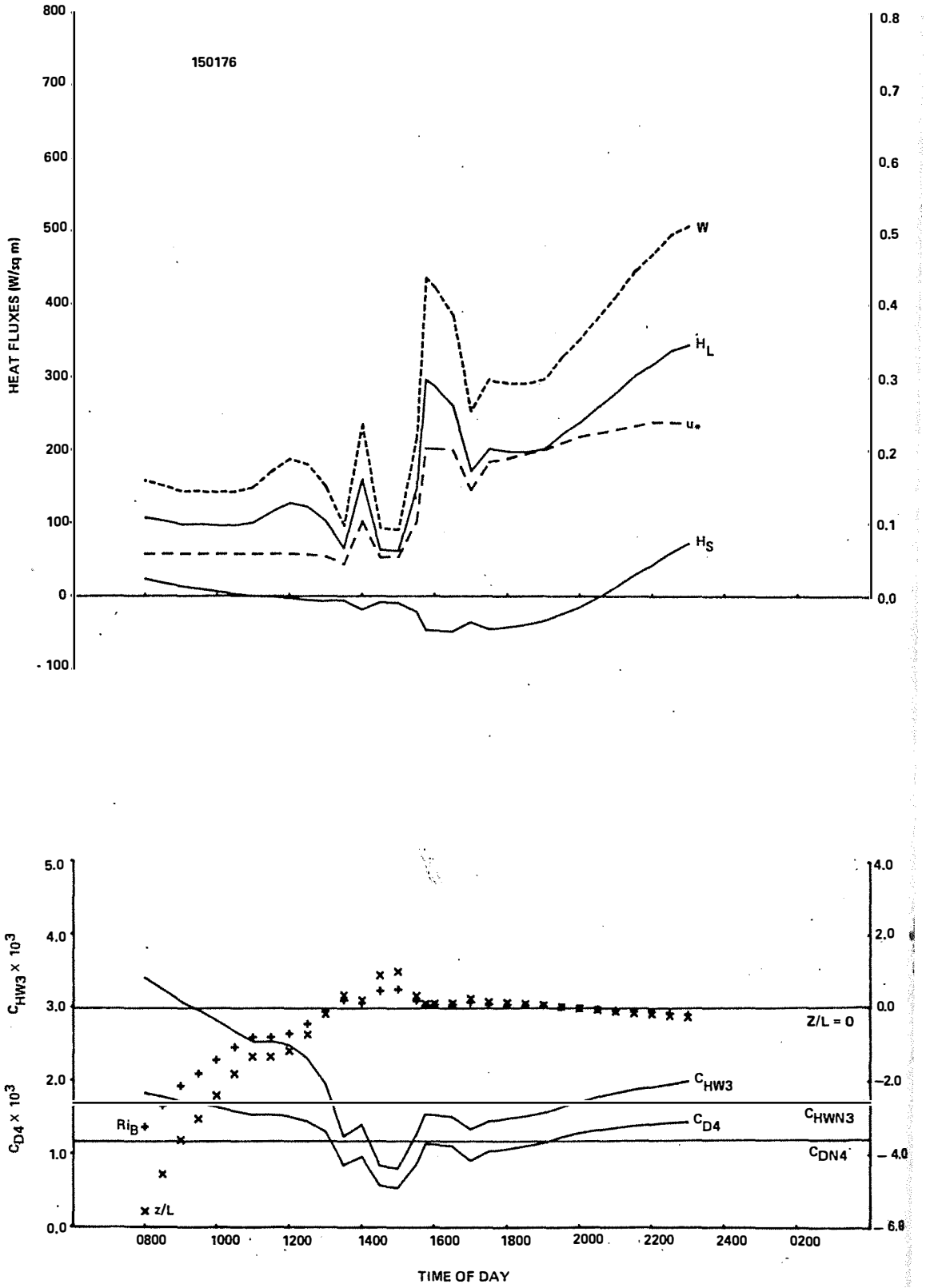

FIGURE 3.5(a) Turbulent fluxes, transfer coefficients and stability parameters for 15 01 76

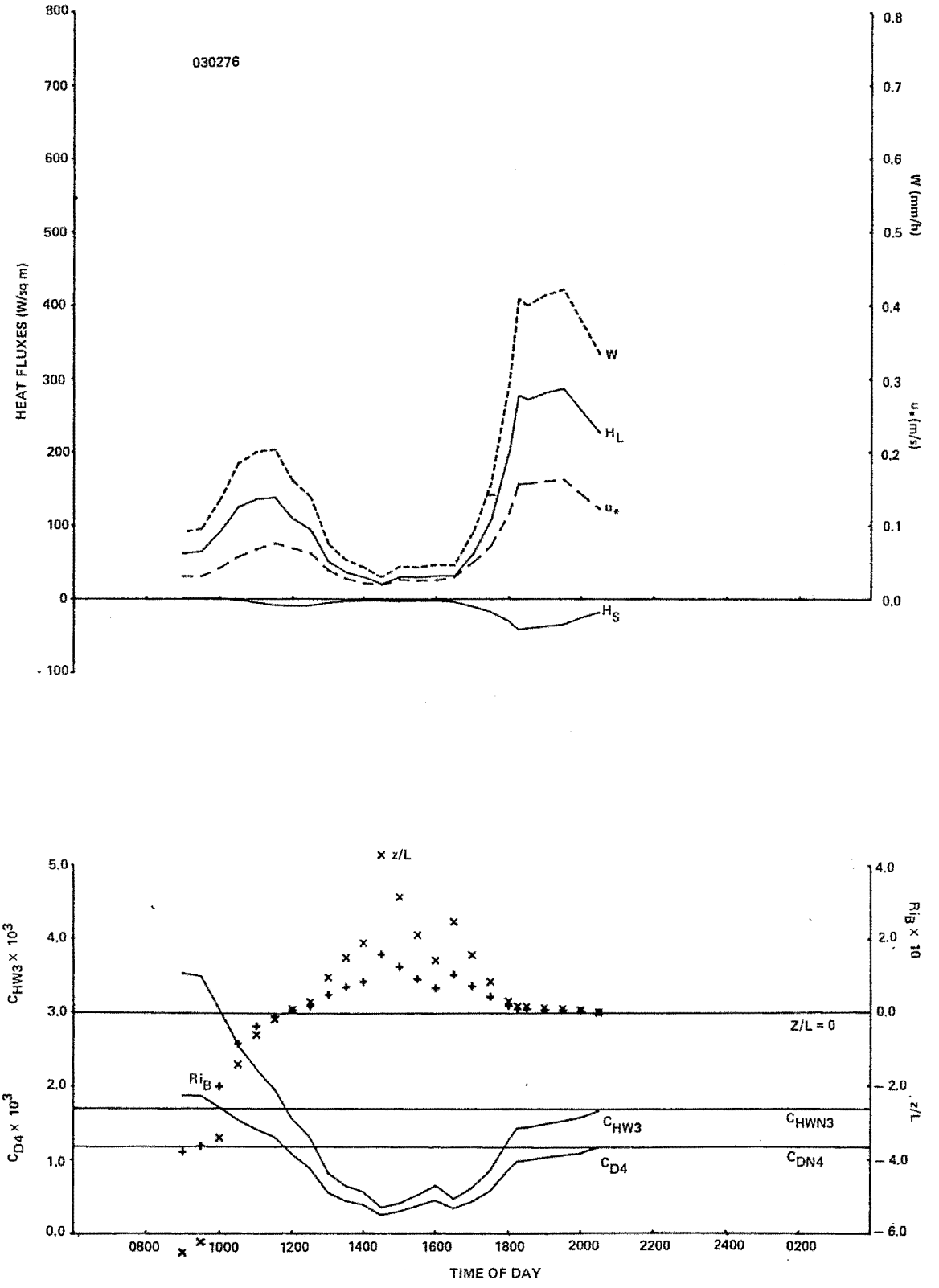

(b) Turbulent fluxes, transfer coefficients and stability parameters for 03 02 76

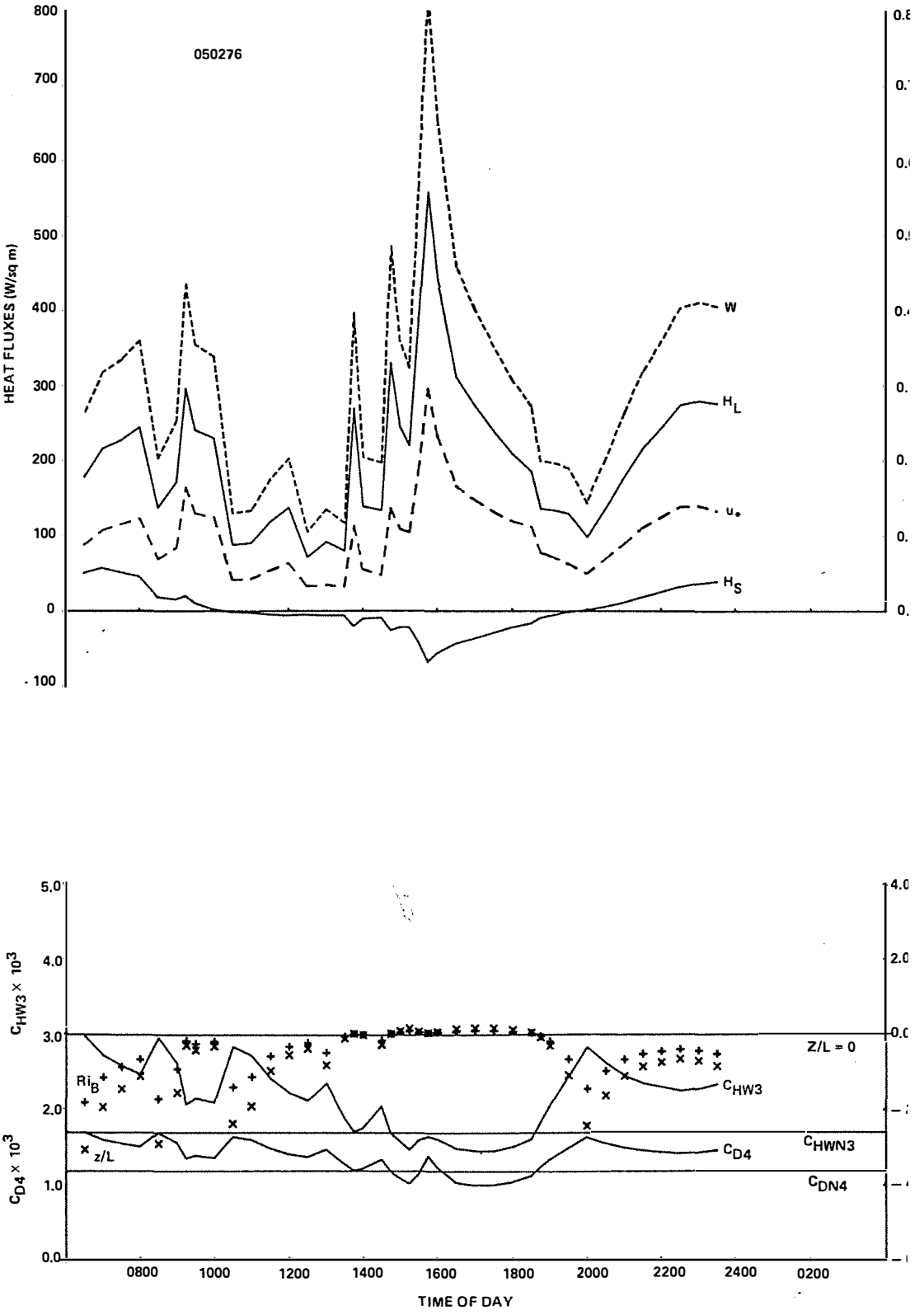

(c) Turbulent fluxes, transfer coefficients and stability parameters for 05 02 76

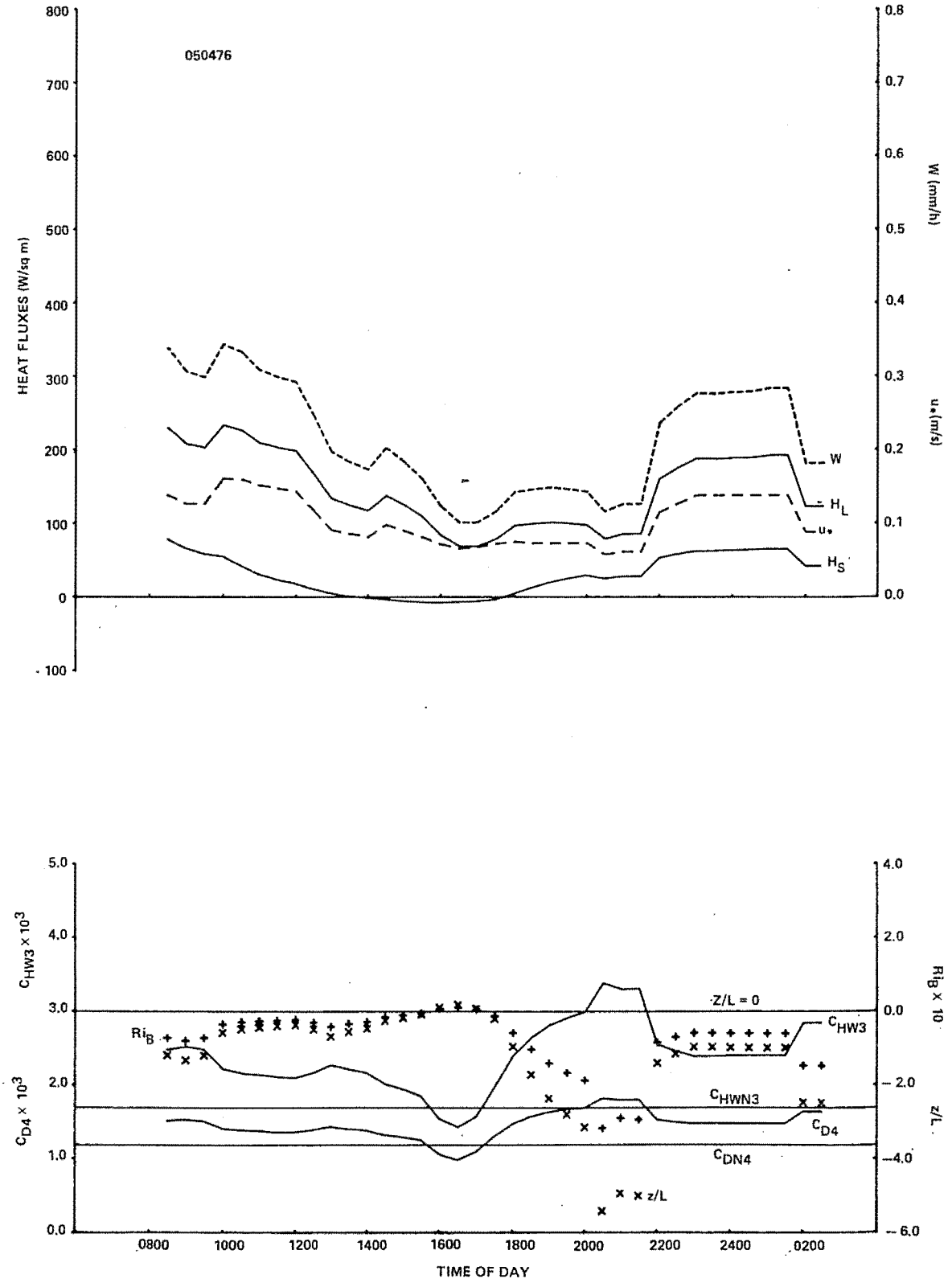

(d) Turbulent fluxes, transfer coefficients and stability parameters for 05 04 76

In considering the applicability of the foregoing method of calculation, two observations can be made. Firstly, in the reservoir case it is of paramount importance that measurements be made within the equilibrium sublayer of the internal boundary layer. In retrospect, lower measurement heights would have been preferable, although proximity to the raft may have caused problems Secondly and of importance, the water surface temperature measured and used in the stability calculation may not represent the actual 'skin temperature' of the surface in light wind conditions. This skin temperature will be closer to the air temperature for all stabilities, reducing the temperature differential and hence also th stability effect. The only tangible means of obtaining the skin temperature would be by direct measurement of the emitted long-wave radiation with a Barnes Radiometer or a similar instrument. For the purpose of this Project it must be accepted that stability effects may be over-estimated.

In view of the latter point, one modification to the flux computations was considered necessary. Little is known about the surface layer similarity functions ($\phi_{M,H,W}$ from eq. 2.16 and eq. 2.17) for instabilities beyond $z/L \sim -1$. Considering the uncertainly of stability determination beyond this point and the likelihood of obtaining unrealistically high results, fluxes were re-computed with values of the transfer coefficients held below the value appropriate to $z/L = -1$. Hence the fluxes plotted in the early mornings and some evenings have been slightly suppressed.

As a check on the iteration procedure and on all of the surface layer relations stated or derived in Section 2.1, Ri_B was calculated by two methods:

i) from the meteorological data via eq. 2.43.

ii) from the derived relation eq. 2.44.

The agreement between the two was excellent for the unstable and slightly stable regimes (within 3%) and reasonable for higher stabilities (within 10%). The high stabilities involve use of the similarity function eq. 2.21 which may be inaccurate.

CHAPTER 4

RESERVOIR SURFACE LAYER OBSERVATIONS

In this chapter, surface layer temperature and salinity profiles measured at the Wellington raft station are presented, together with a general description of the diurnal cycle apparent in these profiles. This chapter should therefore provide a qualitative understanding of reservoir surface behaviour prior to the theoretical treatment in Chapter 5.

On each of the four field days selected for analysis, the reservoir surface layer observations consisted of hourly profil of temperature and salinity. These profiles and the meteorological recordings were staggered by 30 minutes for operational reasons.

No fixed point velocity measurements within the surface layer were conducted as no instrumentation with the required resolution was available.

4.1 WATER TEMPERATURE PROFILES

Plate 4.1 is a photograph of the probe used for most of the fieldwork. The thermistor is located at the bottom of the probe stem where it is well exposed but sheltered from solar radiation. On the raft, the probe cable was threaded over the pulley on the hinged wooden arm (shown in Plate 3.4, No. 2) thus keeping the measurements free from raft interference. Depth of the probe was measured by matching cable markings to a base mark on the arm.

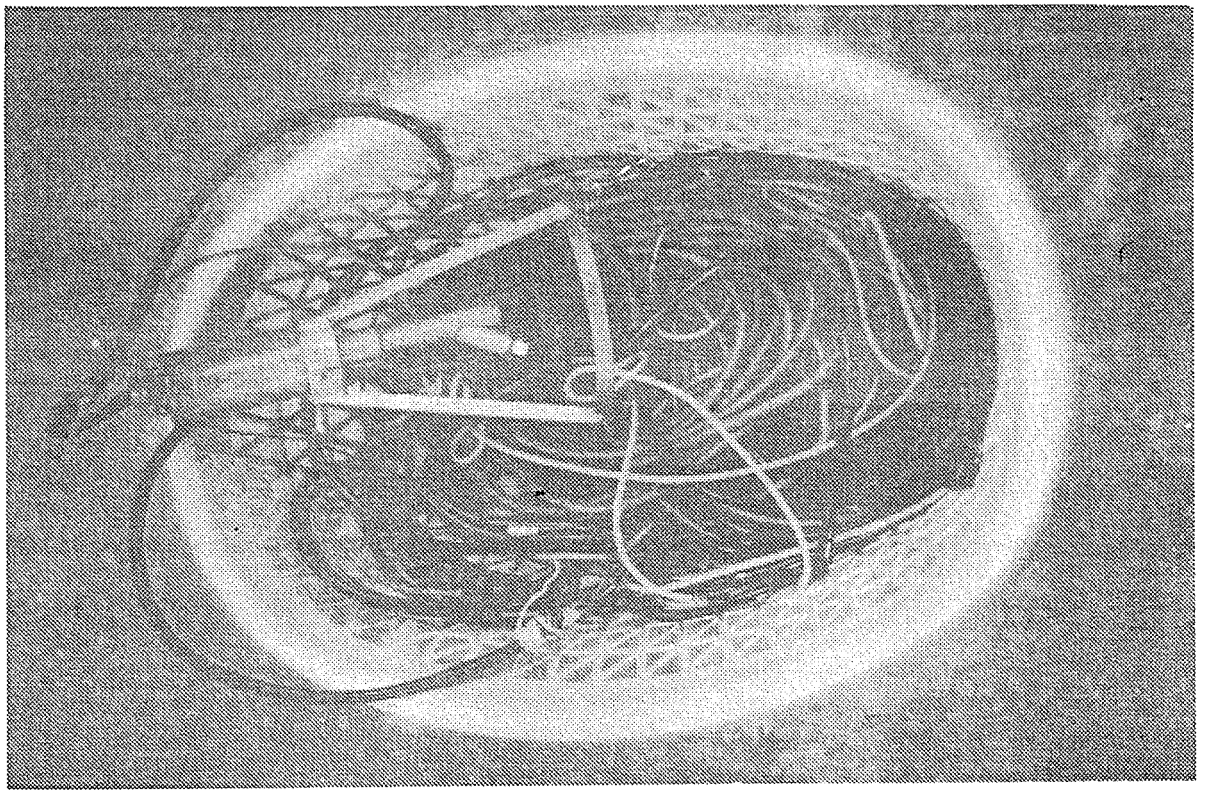

PLATE 4.1 Conductivity/temperature profiling probe

The circuitry for the thermistor was as for other thermistors; a stable linearised Wheatstone Bridge. The bridge output was fed directly to a DVM. A fast response thermistor was chosen (τ < one second) to allow rapid profiles to be taken. This introduced the problem of correctly reading the DVM when the probe was not held perfectly still in a region of marked temperature gradient (the readings became quite variable). Electrical or thermal filtering was not a satisfactory solution in view of the requirement to complete profiles rapidly. In retrospect, the ideal measurement system would be one which integrates the signal over a specified period (1-10 seconds say).

Calibration of the thermistor circuit was performed prior to field trips in a laboratory controlled temperature bath. Prior to each field day a multiple-point calibration was again performed and this provided the operating expressions for the field day. Prior to each profiling drop, the temperature of a bucket of surface water was measured by the thermistor and a thermometer. These values were recorded for subsequent analysis and can be seen in the processing output (Appendix A3).

The limit of absolute accuracy of thermistor measurements must be taken as $0.1^{o}C$, corresponding to the smallest graduation on the thermometers used. Calibration expressions were determined to this accuracy and normally appear as a combination of two linear expressions spanning the temperature range of interest. The bucket checks indicate that, apart from obvious reading errors, $0.1^{o}C$ absolute accuracy was usually obtained.

Relative accuracy of measurements within a profile would be as high as $0.01^{o}C$ if calibration drift was the only

consideration. However, the uncertainty introduced by the temperature fluctuations described above degrades this relative accuracy where strong temperature gradients exist.

The data collection procedure will be described in Section 4.3.

4.2 WATER SALINITY PROFILES

Salinity was determined from a measure of water conductivity as described below. The conductivity cell, being the core of a Philips PW 9510 cell is shown in Plate 4.1. It consists of two platinum coated plates separated by about 0.7 cm with electrical connections to each. The cell is orientated at an angle away from the probe stem to ensure adequate flushing as the probe is lowered. The probe assembly was designed to cause minimal disturbance at the point of measurement while being lowered.

Conductivity was measured by one of two meters manufactured locally by Automated Laboratory Equipment. One such meter is shown in Plate 3.2 (No. 5). It applies an AC potential across the cell and measures the resulting conductivity in μmhos/cm. To improve measurement precision during the fieldwork, the meter's analog output was also measured by the DVM.

Early experience with the meters highlighted the need for great care in order to obtain meaningful results. Measurements tended to drift over a short period and temperature compensation built into the meter circuit proved to be quite inadequate. Described below are the calibration procedures adopted in order to obtain reasonably accurate salinity data.

Standard solutions of reagent grade NaCl in distilled

and de-ionized water were prepared, covering the concentration range 200 - 700 ppm. These solutions were immersed in a controlled temperature bath which was cycled over a wide range of expected water temperatures, with solution conductivity being measured at specific stable temperatures. The results were then plotted as shown in Figure 4.1 for Meter 2. From the individual lines, the slopes were determined which in turn specified the temperature coefficients

$$\alpha = \left(\frac{\text{slope} \times 100}{C_{25}}\right) \%/^{o}C$$

C_{25} is the conductivity at 25°C, the reference temperature for conductivity measurement. Values of α so determined are printed against the plots. These values of α were then plotted as a function of salinity. Two such plots are shown in Figures 4.2. The plot for Meter 2 shows the desirable result; α is practically independent of salinity. The plot for Meter 1 shows α strongly dependent on salinity, for reasons unknown. Fortunately, Meter 2 was used for all but the January fieldwork.

With a value of α determined from Figure 4.2, conductivity may be corrected to a 25°C equivalent by

$$C_{25} = \frac{C}{(1 - \alpha \frac{T}{100})} \tag{4.1}$$

Conductivity is also a linear function of salinity. From Figure 4.1 we may obtain values of C_{25} for each solution, giving the required relation. Due to the tendency of the meters to drift however, a two point calibration (conductivity and temperature for two solutions) was performed on the raft immediately prior to each profile. This information is tabulated in the processing output (Appendix A3).

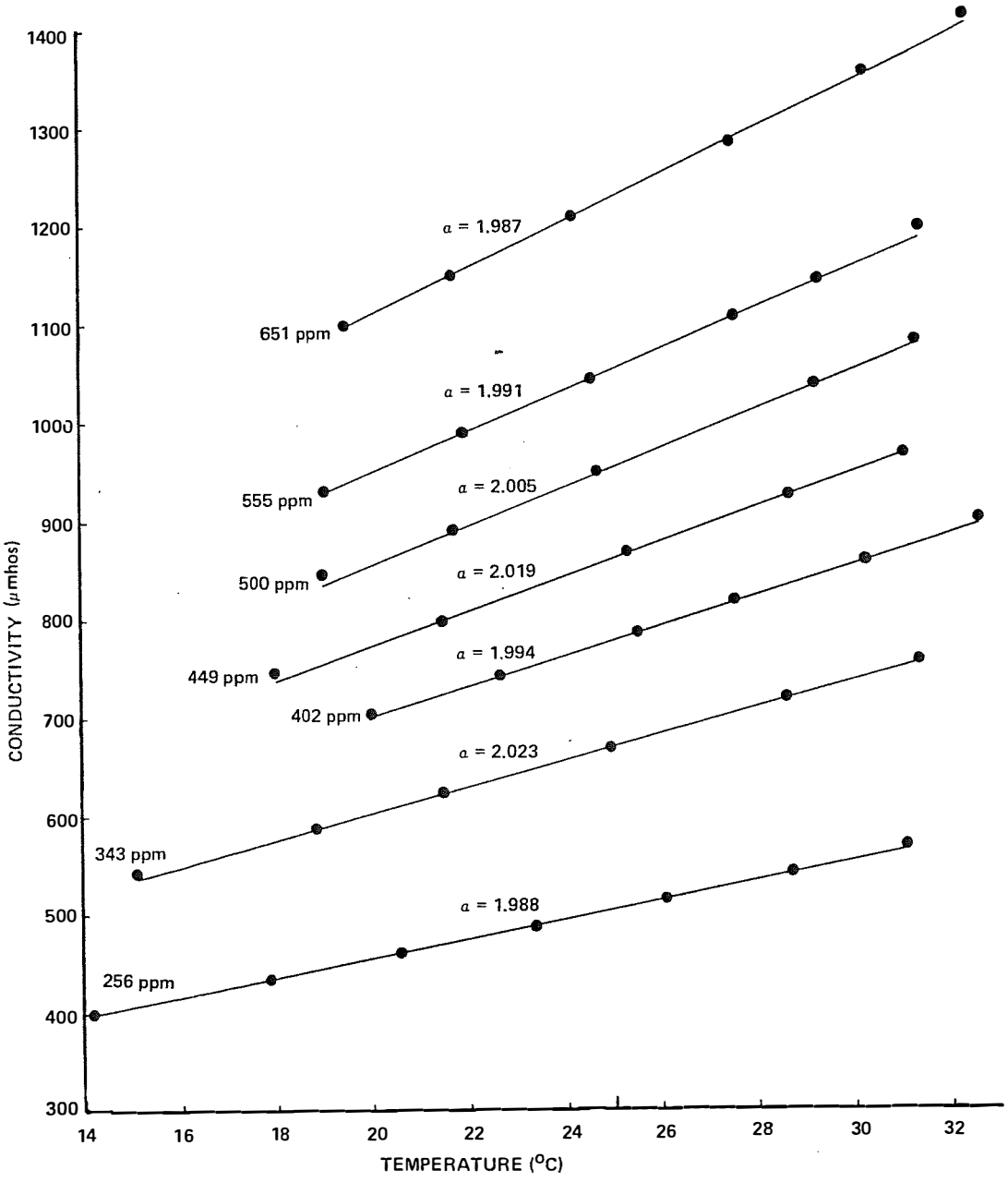

FIGURE 4.1 Conductivity vs temperature for Meter 2 for various salinities

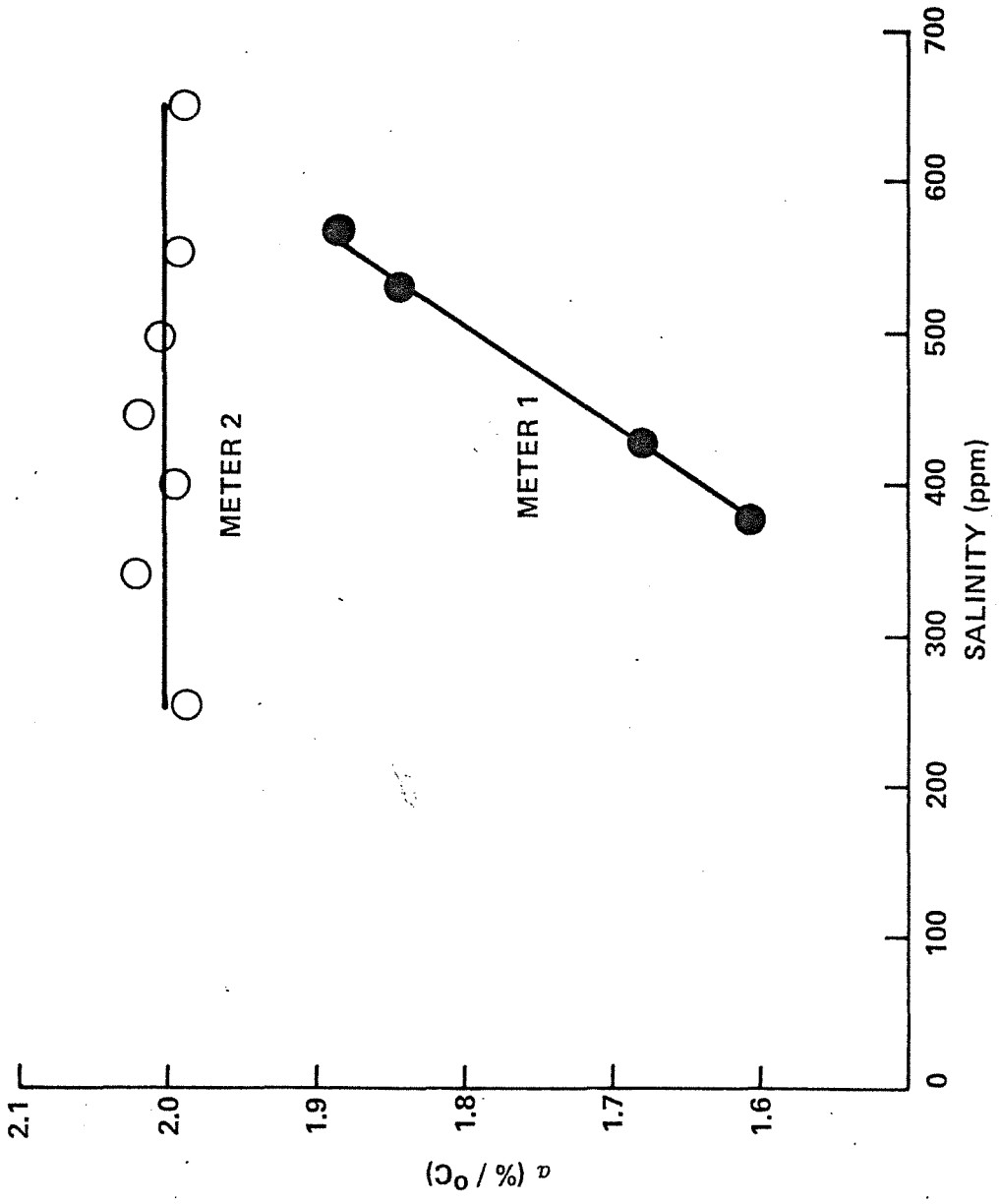
METER 2
METER 1
2.1
2.0
1.9
1.8
1.7
1.6
α (‰ / °C)
0
100
200
300
400
500
600
700
SALINITY (ppm)

4.3 DATA ACQUISITION AND PROCESSING

4.3.1 Profile Data Collection and Storage

The hourly profiling procedure consisted of lowering and holding the probe at pre-determined depths, then reading, from the DVM, the values of conductivity and thermistor output. These values were entered manually on a coded sheet and subsequently transferred to a computer together with the meteorological data.

To obtain the required resolution in regions of possible strong gradients, the depth increments were chosen as follows; 0.2 m for the first metre, 0.5 m from one to five metres and one metre increments thereafter, stopping at some depth within the seasonal thermocline.

4.3.2 Data Reduction

When processing the temperature profile data, the calibration expressions were not modified to reflect bucket calibrations, in view of the generally good agreement.

To process conductivity data, a new calibration expression was determined from the two-point salinity/conductivity calibration for each profile. These expressions appear in the processing output (Appendix A3). The temperature coefficient α was taken as 2% for Meter 2 and 1.7% for Meter 1. The latter value was chosen from Figure 4.2 for an average value of surface layer salinity (450 ppm).

The resultant processed profiles are presented as printouts in Appendix A4 and computer plots of temperature in Appendix A5. Several profiles appear in each plot to highlight the diurnal cycle. Note that the last profile on one plot appears as

the first on the next plot to aid comparison.

At the commencement of this Project, it was intended to observe the surface salinity profile carefully in order to relate residual salt measurements to evaporation. Inspection of Appendices A3 and A4 reveals however that lack of measurement accuracy and resolution precludes any meaningful analysis. The task was simply beyond the capability of the conductivity meter and calibration system. As there is no structure of interest in the surface salinity profiles they have not been plotted.

4.4 RESERVOIR SURFACE LAYER BEHAVIOUR

4.4.1 A Qualitative Examination

From a perusal of the temperature plots of Appendix A5 and of the profile listings of Appendix A4 (which contain information for depths below 12 metres) it is possible to gain an understanding of the structure of the reservoir surface during summer. The essential features of the structure have been included in the schematic in Figure 4.3. Close to the surface, the temperature structure varies on a diurnal timescale whereas the temperature and salinity structure below a depth of several metres is stable, varying only on a seasonal timescale.

A qualitative examination of the plots of Appendix A5 and the meteorological fluxes (Figure 3.5) reveals the following typical summer daily pattern. In the early morning there is a deep homogenous surface layer, sometimes as deep as the seasonal well mixed layer itself. Solar heating in light wind conditions (with small evaporative and sensible heat losses) results in the cessation of mixing throughout most of this layer by mid-morning. At this

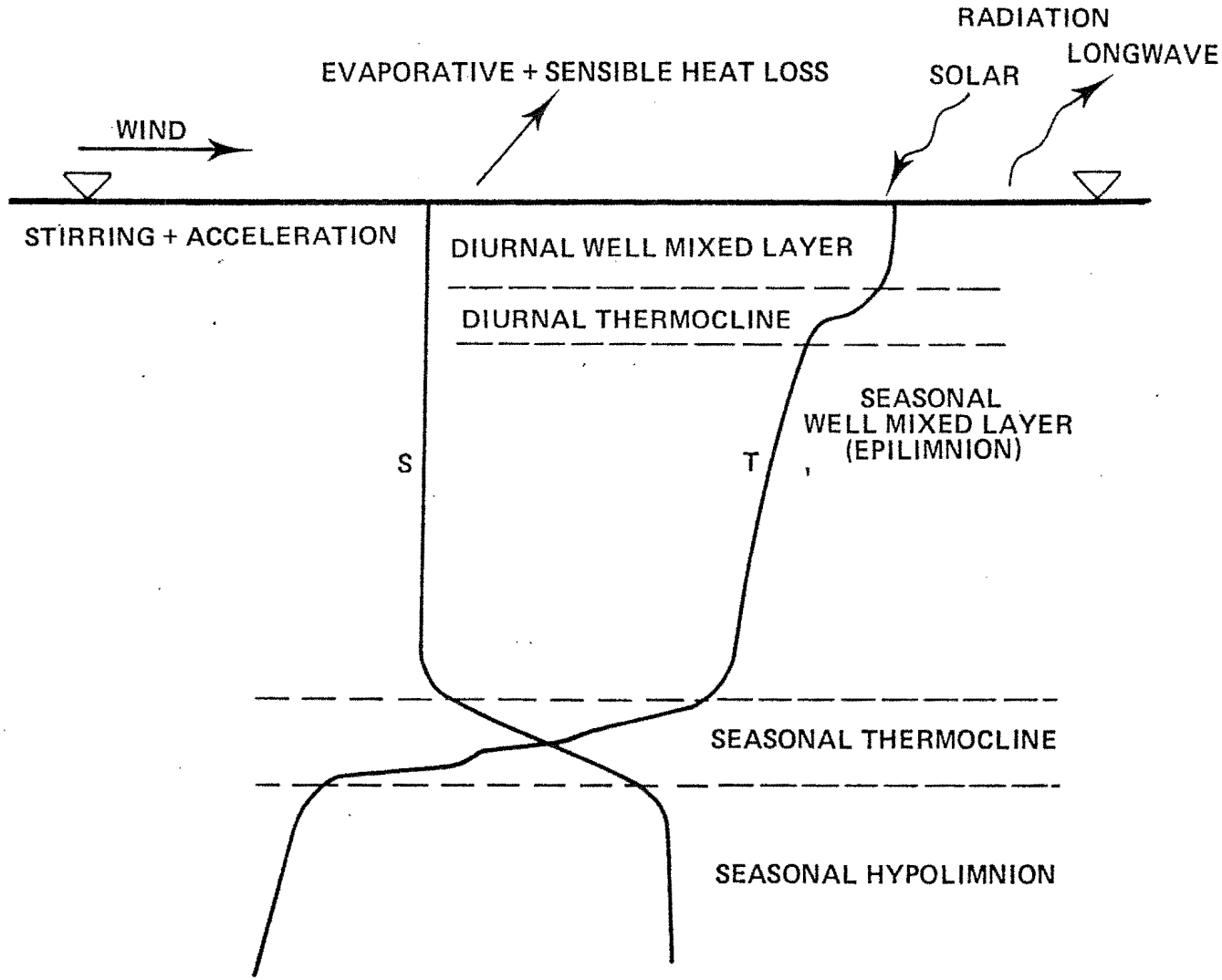

FIGURE 4.3 Essential features of reservoir surface transfers and structure to several metres depth

stage there is not enough mixing energy available from wind stirrin
or surface convection to overcome the stable buoyancy gradient induced by solar heating. Continued solar heating results in the formation of a temperature profile, the form of which is determined by the solar attenuation profile eq. 3.1. The diurnal well mixed layer may have practically disappeared. The picture changes in the afternoon if the wind strength increases (see Appendix A5.2) Wind stirring, surface convective overturn due to evaporative cooling, and internal shear instability now override the decreasing solar input and so the diurnal well mixed layer deepens for the remainder of the day. If stirring and/or cooling are strong enough (e.g. a storm or cold night) mixing may proceed to the base of the seasonal well mixed layer, following which, erosion of the seasonal thermocline will commence. This was observed in the April field day (050476) (see Appendix A5.10).

It is quite evident that the seasonal temperature structure represents the cumulative effect of the diurnal heating and mixing cycles over many successive days. In early summer, intensifying solar radiation heats the upper waters, forming a stable density structure which resists mixing. When significant mixing does occur, it penetrates only to a medium depth and serves only to sharpen the temperature gradient at that depth. Over time, this leads to the formation of the seasonal thermocline, which in mid-summer may be quite thick (e.g. three metres) and very strong (e.g. $5^{o}C$). Evening convective mixing becomes stronger in autumn, causing the diurnal well mixed layer to deepen to the full seasonal well mixed layer depth and then encroach on the seasonal thermocline which is consequently sharpened. The seasonal

structure is destroyed completely by mid-winter.

4.4.2 Significance of the Reservoir Temperature Structure

The temperature structure of a reservoir, as determined by its diurnal and seasonal cycles, is important for a number of reasons. These are discussed below.

Biological production (phytoplankton and zooplankton) is dependent on the concentration of nutrients and on light intensity. Under favourable conditions, blooms may occur over periods as short as a few hours. Such conditions occur near the surface on hot, still days where the diurnal well mixed layer is very shallow and hence downward mixing of the biological constituents is limited. An investigation of these biological processes in a reservoir necessitates a sound understanding of the diurnal cycle.

The seasonal thermocline acts as a strong barrier to mixing, impeding the movement of water and its dissolved constituents between the epilimnion and hypolimnion. Dissolved oxygen, which is replenished at the surface, may become depleted in the hypolimnion due to bacterial action, with a subsequent degeneration of water quality. In the Wellington Reservoir it is also observed that cold, high salinity inflows remain in the hypolimnion, being prevented from mixing upward by the seasonal thermocline. A similar phenomenon is found in the atmosphere where pollutants may be trapped in a neutral layer beneath a temperature inversion.

Reservoir flows which occur within a temperature stratified region are modified by the effects of buoyancy. Imberger *et al.* (1979) summarize the theory which describes selective withdrawal and inflow of water in the stratified waters within or below the seasonal thermocline.

In order to manage the quality of water in a reservoir where the above effects are present, it is necessary to be able to predict the behaviour of the temperature and salinity structure on both daily and seasonal timescales. With the data presented in Chapters 3 and 4, an analysis of the diurnal cycle is possible. During any one of the field days the seasonal thermocline may be considered to be stationary. All the mechanisms which act together to form the seasonal thermocline and well mixed layer are present and active in the diurnal cycle. It is therefore proposed to develop, in the following chapters, a model of the diurnal cycle, the predictions of which will be compared against the observed profiles. If validated for the diurnal case, the model may then be used for seasonal predictions where averaged meteorological data are used.

CHAPTER 5

THEORY OF MIXED LAYER ENERGETICS

In recent years, well mixed layers have been modelled by two distinctly different methods. Mellor and Durbin (1975) and others have obtained solutions to the fundamental equations based upon simplifications of second order closure schemes. The main body of work, however, has concentrated on the development of models in which the vertical distributions of temperature, velocity and other constituents are specified. As Niiler and Kraus (1977) point out, the simplicity and physical insight afforded by this integral approach is adequate justification for pursuing it.

In the following sections a general well mixed layer model is developed. Firstly, in Section 5.1, a set of equations describing the energetics of a well mixed layer are derived. In Section 5.2, existing models and specifically the assumptions employed by those models are surveyed. Finally, in Section 5.3, a complete description of selected parameterization schemes with an evaluation of the various coefficients is presented. This section also deals with problems specific to a medium sized reservoir.

5.1 WELL MIXED LAYER INTEGRAL RELATIONS

Figure 5.1 shows schematically a well mixed layer in a body of water. The various parameters shown are

τ surface wind stress

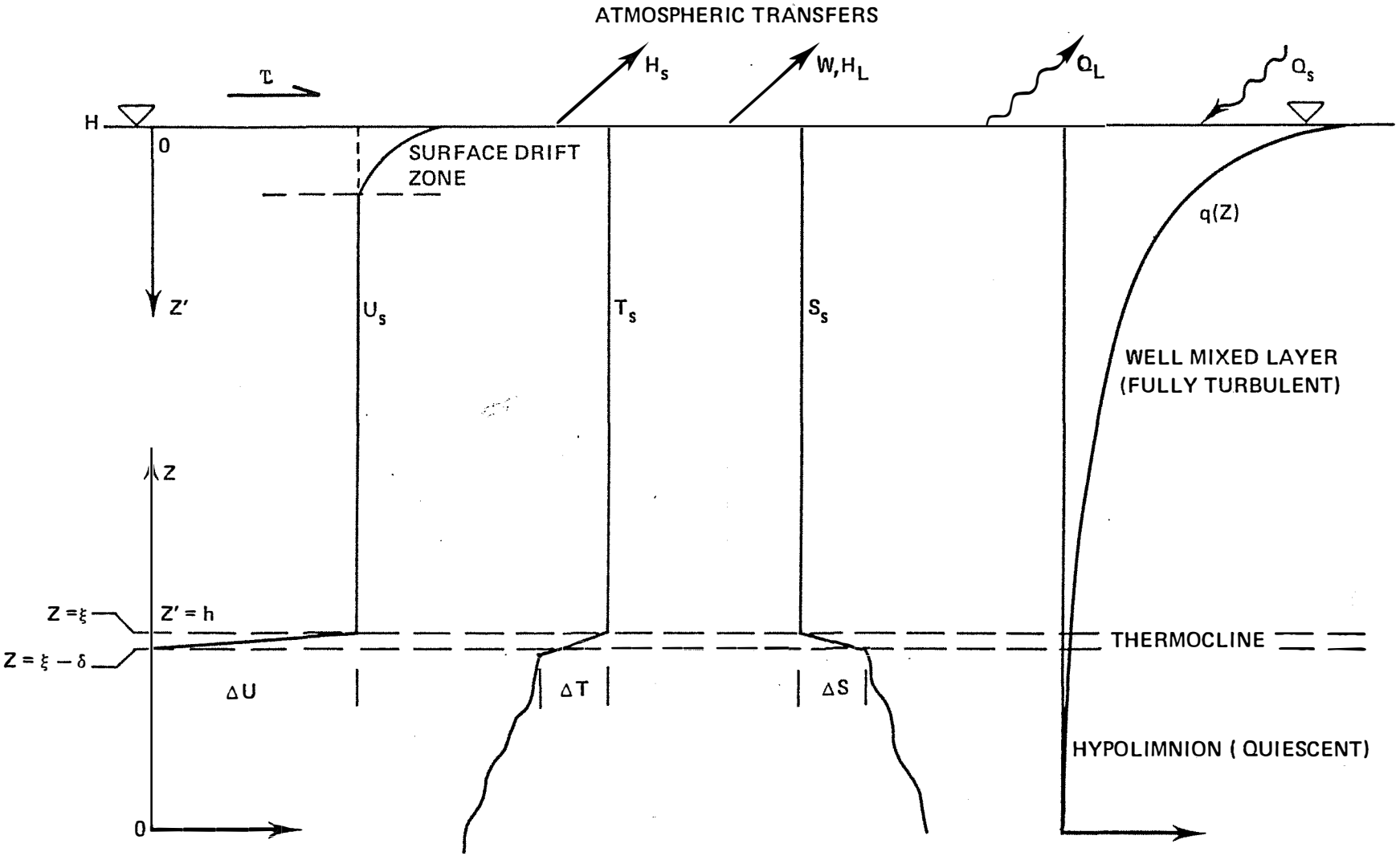

FIGURE 5.1 Features of a well mixed layer in a water

H_S surface sensible heat flux

H_L latent heat loss

W evaporation rate

Q_L net long-wave radiation

Q_S net short-wave radiation

q(z) short-wave penetration profile

T_S well mixed layer temperature

S_S well mixed layer salinity

U_S well mixed layer velocity

ΔT thermocline temperature jump

ΔS thermocline salinity jump

ΔU thermocline velocity jump

h well mixed layer depth

δ thermocline thickness

In terms of previously defined parameters,

i) $Q_L = Q_{LR} - Q_{LAC}$

ii) $Q_S = \{-(1-R)Q_s\}$ from eq. 3.2

iii) $W = \frac{E}{1000}$ (with units of m s^{-1})

In Figure 5.1, two possible co-ordinate systems are shown. All fluxes are positive upward. Hereafter, the name well mixed layer will be abbreviated to WML.

Assumptions implicit in the formulation of WML models are:

1. The WML is uniformly mixed with constituent profiles as shown in Figure 5.1, and moves as a slab.
2. Horizontal advection of temperature or salinity differences may be ignored; hence the model is one-dimensional.

It is not strictly necessary to specify uniform profiles of temperature, salinity and velocity in order to use the integral approach described below. Instead it is necessary that, at every level within the WML, the appropriate temperature, salinity and velocity scales are the layer averages of each variable, so that the integral method will correctly describe the various physical mechanisms involved in WML formation.

To obtain a solution giving the WML temperature, salinity, velocity and depth over time, the one-dimensional equations for heat, mass, salt, momentum and turbulent kinetic energy must be solved throughout the layer. With the assumed structure of Figure 5.1 it is possible to integrate these equations over the full depth ($0 \leq z \leq H$) and so include the integrated influence of all the relevant terms. The origin ($z = 0$) may be at the reservoir bed, or at some level in the water below which no surface effects penetrate.

The following procedure is employed in the evaluation of integrals. The integral of a parameter $f(z,t)$ over ($0 \leq z \leq H$) may be separately evaluated for three regions; the epilimnion ($\xi < z \leq H$), the thermocline ($\xi-\delta < z \leq \xi$) and the hypolimnion ($0 \leq z \leq \xi-\delta$), giving three integrals

$$\int_0^H f\,dz = \int_0^{\xi-\delta} f\,dz + \int_{\xi-\delta}^{\xi} f\,dz + \int_{\xi}^{H} f\,dz$$

If $f(z,t)$ is itself a time derivative and the limits of integration, ξ and $\xi-\delta$, also vary with time, then the integration must obey Leibnitz's Rule.

5.1.1 Heat

The one-dimensional equation of heat may be written as

$$\frac{\partial T}{\partial t} = -\frac{\partial}{\partial z}\overline{\theta' w'} - \frac{1}{\rho_o C_p}\frac{\partial q(z)}{\partial z} \qquad (5.1)$$

where ρ_o is a reference water density.

As an example of the integration procedure described above, the three integrals are evaluated below, term by term.

(A) Hypolimnion $(0 \rightarrow \xi-\delta)$

$$\int_o^{\xi-\delta} \frac{\partial T}{\partial t}\, dz = \frac{\partial}{\partial t} \int_o^{\xi-\delta} T\, dz - T(\xi-\delta)\, \frac{d(\xi-\delta)}{dt}$$

$$\int_o^{\xi-\delta} - \frac{\partial}{\partial z}\, \overline{\theta'w'} dz = \overline{\theta'w'}(0) - \overline{\theta'w'}(\xi-\delta)$$

$$\int_o^{\xi-\delta} - \frac{1}{\rho_o C_p} \frac{dq}{dz}\, dz = - \frac{1}{\rho_o C_p} [q(\xi-\delta) - q(0)]$$

The heat balance is therefore

$$\frac{\partial}{\partial t} \int_o^{\xi-\delta} T\, dz = T(\xi-\delta)\, \frac{d(\xi-\delta)}{dt} + \overline{\theta'w'}(0) - \overline{\theta'w'}(\xi-\delta)$$

$$- \frac{1}{\rho_o C_p} [q(\xi-\delta) - q(0)] \qquad (5.2)$$

The first right hand side (RHS) term represents the loss of heat in that fluid being entrained from the hypolimnion into the epilimnion. The other RHS terms are flux boundary conditions.

(B) Thermocline $(\xi-\delta \rightarrow \xi)$

$$\int_{\xi-\delta}^{\xi} \frac{\partial T}{\partial t}\, dz = \frac{\partial}{\partial t} \int_{\xi-\delta}^{\xi} T\, dz - T(\xi)\, \frac{d\xi}{dt} + T(\xi-\delta)\, \frac{d(\xi-\delta)}{dt}$$

(1) (2) (3)

For the purposes of the model, use is made of the observation that the thermocline is often very thin (i.e. δ and $\frac{d\delta}{dt} \rightarrow 0$). So, (1) vanishes and (2) and (3) together reduce to

$$- \Delta T\, \frac{d\xi}{dt}\ , \quad \text{where } \Delta T = T(\xi) - T(\xi-\delta)$$

next, $$\int_{\xi-\delta}^{\xi} - \frac{\partial}{\partial z}\, \overline{\theta'w'} dz = \overline{\theta'w'}(\xi-\delta) - \overline{\theta'w'}(\xi)$$

and $$\int_{\xi-\delta}^{\xi} - \frac{1}{\rho_o C_p} \frac{\partial q}{\partial z}\, dz = - \frac{1}{\rho_o C_p} [q(\xi) - q(\xi-\delta)]$$

For the type of profile q(z) shown in Figure 5.1,

$[q(\xi) - q(\xi-\delta)] \to 0$ as $\delta \to 0$, so

$$\overline{\theta'w'}(\xi) - \overline{\theta'w'}(\xi-\delta) = \Delta T \frac{d\xi}{dt} \qquad (5.3$$

This is often called the heat flux jump condition across the thermocline.

(C) Epilimnion ($\xi \to h$)

$$\int_{\xi}^{H} \frac{\partial T}{\partial t}\, dz = \frac{\partial}{\partial t} \int_{\xi}^{H} T\, dz - T(H) \frac{dH}{dt} + T(\xi) \frac{d\xi}{dt}$$

(1) (2) (3)

Now $T = T(H) = T(\xi) = T_S$ in the epilimnion so (1) becomes

$$\frac{d}{dt} (T_S H - T_S \xi),$$

Expanding via the chain rule and adding (2) and (3) gives

$$h \frac{dT_S}{dt} , \quad \text{where } h = H - \xi.$$

next, $$\int_{\xi}^{H} - \frac{\partial}{\partial z} \overline{\theta'w'} dz = \overline{\theta'w'}(\xi) - \overline{\theta'w'}(H)$$

and $$\int_{\xi}^{H} - \frac{1}{\rho_o C_p} \frac{dq}{dz} = - \frac{1}{\rho_o C_p} [q(H) - q(\xi)]$$

Combining the terms gives

$$h \frac{dT_S}{dt} = \overline{\theta'w'}(\xi) - \overline{\theta'w'}(H) - \frac{1}{\rho_o C_p} [q(H) - q(\xi)] \qquad (5.4$$

Eq. 5.3 and eq. 5.4 together describe the heat balance of the WML. Eq. 5.2, included for completeness, is not explicitly required in a WML model, although a solution to eq. 5.1 below the thermocline is required in order to evaluate ΔT over time.

5.1.2 Momentum

The form of the momentum equation for horizontal plane flow follows from eq. 2.1:

$$\frac{\partial \underset{\sim}{U}}{\partial t} = - f \underset{\sim}{\hat{k}} \times \underset{\sim}{U} - \frac{\partial}{\partial z} \overline{\underset{\sim}{u'w'}} - \frac{1}{\rho_o} \nabla p \qquad (5.5$$

Csanady (1975) gives the criterion for which internal waves in a two layer rectangular basin will not be affected substantially by rotational effects:

$$2L\ \Omega \sin\phi < \sqrt{\frac{\Delta\rho}{\rho_1}\, g\, \frac{h_1 h_2}{H}}$$

with Ω earth's angular velocity,

ϕ latitude,

h_1 & h_2 thickness of top and bottom layers,

H total depth,

$\Delta\rho$ density jump $(\rho_2 - \rho_1)$,

L basin length.

This criterion is marginally satisfied in the Wellington Reservoir, that is, the reservoir is small enough for rotational effects to be unimportant. The first RHS term will therefore be neglected and only the horizontal velocity $u = U + u'$ in the direction of the flow will be considered.

Eq. 5.5 may be integrated as follows:

(a) Thermocline $(\xi-\delta \rightarrow \xi)$

$$\overline{u'w'}(\xi) - \overline{u'w'}(\xi-\delta) = \Delta U \frac{d\xi}{dt} \qquad (5.6)$$

If flows beneath the thermocline are neglected, then the velocity difference across the thermocline $\Delta U = \Delta U_S = U_S$. The term $\overline{u'w'}(\xi-\delta)$ represents loss of momentum from the WML into the stable hypolimnion, the major mechanism being radiation of internal waves which will be discussed in the next section.

(B) Epilimnion $(\xi \rightarrow H)$

$$h \frac{dU_S}{dt} = \overline{u'w'}(\xi) - \overline{u'w'}(H) - \text{PGRAD} \qquad (5.7)$$

Discussion on the possible effects of horizontal pressure gradients in a finite length reservoir will be deferred until Section 5.3

5.1.3 Mass

A one-dimensional mass conservation equation for the configuration of Figure 5.1 is

$$\frac{\partial \rho}{\partial t} = - \frac{\partial}{\partial z} \overline{\rho' w'} + \frac{\alpha}{C_p} \frac{\partial q(z)}{\partial z} \qquad (5.8$$

where α is the thermal expansion coefficient of water. The last term represent density variations induced by internal absorption of heat from solar short-wave radiation (note that q(z) is negativ downward).

For the sake of rigour it is necessary to consider the total depth ($0 \lesssim z \lesssim H$) plus an infinitesimal conductive sublayer ($H < z \lesssim H+d$) through which heat and mass transfers occur by molecular processes; it is not stated *a priori* that turbulent fluxes are continuous across the interface.

Integrating eq. 5.8 over ($0 \lesssim z \lesssim H$) and neglecting q(0) gives

$$\frac{\partial}{\partial t} \int_o^H \rho \, dz = \rho(H) \frac{dH}{dt} - \overline{\rho' w'}(H) + \frac{\alpha}{C_p} q(H)$$

The LHS is the rate of change of total mass of a column which, intuitively, is due only to evaporation or precipitation. In the case of evaporation, fresh water is removed leaving a salt residue so that

$$\frac{\partial}{\partial t} \int_o^H \rho \, dz = - \rho(H) W (1 - \beta S_S)$$

where β is the mass coefficient for salt.

The quantity dH/dt may be independently evaluated. It is the vertical expansion or contraction of the column due to net heating or cooling, minus evaporation, so that

$$\frac{dH}{dt} = - \frac{\tilde{\alpha H}}{\rho(H)C_p} - W \qquad (5.9)$$

with $\tilde{H}$ sum of all atmospheric turbulent and radiative heat transfers at the surface.

As before, bottom transfers (z = 0) are neglected.

Combining the foregoing equations gives

$$\overline{\rho'w'}(H) = - \rho(H)\left[\frac{\alpha(\tilde{H}-q(H))}{\rho(H)C_p} + W\beta S_S\right]$$

or, expressed in terms of heat and salt components, and density ρ_o,

$$- \alpha g\overline{\theta'w'}(H) = - \frac{\alpha g}{\rho_o C_p} (\tilde{H} - q(H)) \qquad (5.10)$$

$$\beta g\ \overline{s'w'}(H) = - \beta g W S_S \qquad (5.11)$$

These are the jump conditions for heat and salt flux at the surface.

The derivation above shows that $\overline{\rho'w'}$ is not constant and continuous across the interface, but is determined, below the conductive sublayer, by the rate at which the mass of the column is falling (rising) due to thermal contraction (expansion), with an extra contribution from salt residue. The work of some previous authors, who use surface based co-ordinates, is misleading as they are obliged to consider that $\overline{\rho'w'}$ is continuous across the air-water interface.

5.1.4 Salt

Conservation of salt or any other tracer in the fluid can be written as

$$\frac{\partial S}{\partial t} = - \frac{\partial}{\partial z} \overline{s'w'} \qquad (5.12)$$

with s' salinity fluctuation. No sources or sinks are considered.

Integrating across the WML gives:

(A) Thermocline $(\xi-\delta \rightarrow \xi)$

$$\overline{s'w'}(\xi) - \overline{s'w'}(\xi-\delta) = \Delta S \frac{d\xi}{dt} \tag{5.13}$$

(B) Epilimnion $(\xi \rightarrow H)$

$$h \frac{dS_S}{dt} = \overline{s'w'}(\xi) - \overline{s'w'}(H) \tag{5.14}$$

5.1.5 Turbulent Kinetic Energy

Following Denman (1973), the equation for turbulent kinetic energy (hereafter TKE) may be written as

$$\frac{1}{2}\frac{\partial \bar{E}}{\partial t} = - \overline{u'w'} \frac{\partial U}{\partial z} - \frac{\partial}{\partial z}\left[\overline{w'\left(\frac{p'}{\rho_o} + \frac{E}{2}\right)}\right] - \frac{g}{\rho_o}\overline{\rho'w'} - \varepsilon \tag{5.15}$$

(1) (2) (3) (4) (5)

The various numbered term are defined below:

(1) time rate of change of TKE, $\frac{1}{2}\bar{E}$ in the WML, where $\bar{E} = \overline{(u'^2 + v'^2 + w'^2)}$,

(2) production of TKE due to the working of the Reynolds stress $(\overline{-u'w'})$ on the mean shear,

(3) divergence of the vertical flux of TKE induced by pressure (p' and velocity fluctuations at the upper and lower boundaries,

(4) TKE expended in working against buoyancy forces

$$\left(\frac{g}{\rho_o}\overline{\rho'w'} = - \alpha g\overline{\theta'w'} + \beta g\overline{s'w'}\right)$$

(5) rate of destruction of TKE by viscous dissipation.

Eq. 5.15 is also integrated across the WML as follows

(A) Thermocline $(\xi-\delta \rightarrow \xi)$

$$\int_{\xi-\delta}^{\xi} \frac{1}{2}\frac{\partial \bar{E}}{\partial t}\, dz = \frac{\partial}{\partial t}\int_{\xi-\delta}^{\xi} \frac{\bar{E}}{2}\, dz - \frac{1}{2}\bar{E}(\xi)\frac{d\xi}{dt} + \frac{1}{2}\bar{E}(\xi-\delta)\frac{d(\xi-\delta)}{dt}$$

(1) (2) (3)

Denman (1973) found that m = 1 gave the best results for his model which essentially follows Kraus and Turner's (1967) formulation. Larger values for m are deduced from analysis of storm deepening events, however the influence of shear deepening may invalidate these.

(b) Ball (1960) proposed that n = 1, arguing that large convective eddies would be little affected by dissipation. Other workers have provided estimates in the range $0 \leq n < 0.113$.

(c) The shear energy conversion factor s, accounting for dissipation and, to some extent, leakage via internal waves, has received little attention from researchers. A tentative estimate is s = 0.7.

5.2.5 Sherman Imberger & Corcos (1978), Fischer *et al.* (1979)

These authors have presented a generalised entrainment relation which includes all the various mechanisms proposed by KT, PRT, and ZT. Although there are some differences in approach to the problem, their results will be seen to be a special case of the analysis to follow; for this reason a separate description is not presented here.

other two, because $|dH/dt| << |d\xi/dt|$ or $|dh/dt|$ and $\bar{E}(H) < E_S$ (from Willis and Deardorff (1974)).

Expanding the first term by the chain rule gives

$$\int_{\xi}^{H} \frac{1}{2} \frac{\partial \bar{E}}{\partial t} dz = \frac{1}{2} h \frac{dE_S}{dt} - \frac{E_S}{2} \frac{d\xi}{dt} + \frac{1}{2} \bar{E}(\xi) \frac{d\xi}{dt}$$

The next integrated term is

$$\int_{\xi}^{H} \alpha g \overline{\theta' w'} dz = \frac{\alpha g h}{2} \overline{\theta' w'}(\xi) + \frac{\alpha g h}{2 \rho_o C_p} \tilde{H}_*$$

where $\tilde{H}_* = [\rho_o C_p \overline{\theta' w'}(H) + q(H) + q(\xi) - \frac{2}{h} \int_{\xi}^{H} q(z)\, dz]$

The first RHS term, after substitution of eq. 5.3, is seen to be the increase of column potential energy due to entrainment of heavier fluid through the thermocline. The second RHS term is the change of column potential energy due to the surface heat flux term $\tilde{H}_*$. The form of $\tilde{H}_*$ indicates the dependence of potential energy on the distribution of heating and cooling within the layer in particular, the form of $q(z)$ must be accurately specified.

The remaining integrated terms are

$$\int_{\xi}^{H} - \beta g \overline{s' w'} dz = - \frac{\beta g h}{2} \left(\overline{s' w'}(\xi) + \overline{s' w'}(H) \right)$$

$$\int_{\xi}^{H} - \frac{\partial}{\partial z} \left[\overline{w' \left(\frac{p'}{\rho_o} + \frac{E}{2} \right)} \right] dz = - \left[\overline{w' \left(\frac{p'}{\rho_o} + \frac{E}{2} \right)} \right]_{\xi}^{H}$$

$= K(\xi) - K(H)$ for simplicity.

$$\int_{\xi}^{H} - \overline{u' w'} \frac{\partial U}{\partial z} dz = SH(H) \text{ for simplicity.}$$

A vertically averaged WML dissipation rate may be defined as $\varepsilon_S = 1/h \int_{\xi}^{H} \varepsilon\, dz$.

Then

$$\int_{\xi}^{H} -\varepsilon \, dz = -\varepsilon_S h$$

The terms from the thermocline and epilimnion TKE balances may be added to give a total WML balance:

$$\frac{h}{2}\frac{dE_S}{dt} = \frac{E_S}{2}\frac{d\xi}{dt} + SH(\xi) + SH(H) + K(\xi-\delta) - K(H)$$

(1a) (1b) (2a) (2b) (3a) (3b)

$$+ \frac{\alpha g h}{2}\left[\overline{\theta' w'}(\xi) + \frac{\tilde{H}_*}{\rho_o C_p}\right] - \frac{\beta g h}{2}\left[\overline{s' w'}(\xi) + \overline{s' w'}(H)\right] - \varepsilon_S h \qquad (5.17)$$

(4a) (4b) (4c) (4d) (5)

Numbering of terms conforms to that of eq. 5.14. Eqs. 5.3, 5.4, 5.6, 5.7, 5.10, 5.11, 5.13, 5.14 and 5.17 form the equation set which must be solved in order to describe the behaviour of the WML.

5.2 REVIEW OF EXISTING MODELS

The above set of equations are intractable as they stand. In order to solve them it is necessary to make a number of simplifications and to parameterize some of the turbulent flux quantities in terms of mean flow quantities. In this section a review of models proposed by other authors is presented. Attention is drawn to the mixing/deepening mechanisms included or neglected and the closure hypotheses employed.

5.2.1 Kraus and Turner (1967) (KT)

These authors consider the following mechanisms from eq. 5.17:

i) mechanical energy input at the surface from wind

stirring, (terms 2b, 3b),

ii) potential energy change by entrainment plus surface heating or cooling (terms 4a, 4b).

KT also note the possible importance of dissipation but do not attempt to include a parameterization of this term. The proposed balance is therefore

$$SH(H) - K(H) + \frac{\alpha g h}{2}\left[\overline{\theta' w'}(\xi) + \frac{\tilde{H}_*}{\rho_o C_p}\right] = 0$$

Without reference to the specific forms of SH(H) and K(H) they propose that the wind working rate must be proportional to the stress times a water velocity scale,

$$SH(H) - K(H) \propto \tau\, u_* = \rho_a u_{*a}^3 \sqrt{\rho_a/\rho}\ .$$

u_* is the water friction velocity and subscript a refers to air.

5.2.2 Pollard, Rhines and Thompson (1973) (PRT)

Errors exist in the formulation of these authors' model, as pointed out by Niiler (1975). For this reason their derivation will not be discussed here. However, the model they propose can be shown to represent a balance of the following terms:

i) shear production of TKE in the entrainment zone (term 2a),

ii) potential energy increase associated with entrainment (term 4a).

i.e. $$SH(\xi) + \frac{\alpha g h}{2}\overline{\theta' w'}(\xi) = 0$$

If, as shown in Section 5.3.1,

$$SH(\xi) = \frac{C_S}{2}\Delta U_S^2 \frac{d\xi}{dt}\ ,$$

the above balance after substitution of eq. 5.3 becomes

$$\alpha g h \frac{\Delta T}{\Delta U_S^2} = C_S \tag{5.18}$$

which is these authors' Richardson No. criterion for marginal stability, with $C_S = 1$. The WML velocity ΔU_S is computed from the momentum equation 5.7. This model therefore predicts that, following the onset of wind, the layer depth will adjust to maintain the balance of eq. 5.18, so that

$$h = \frac{C_S \Delta U_S^2}{\alpha g \Delta T} \tag{5.19}$$

5.2.3 Tennekes (1973), Zeman and Tennekes (1977) (ZT)

The original work of Tennekes (1973) was corrected and expanded by Zeman and Tennekes (1977); most of the following summary refers to this latter work.

These authors attempt to solve the TKE eq. 5.15 locally at the inversion base rather than integrating eq. 5.15 and the other equations as has been done in Section 5.1. Unlike the integral formulations where terms are formally derived, their approach has necessitated a number of hypotheses and parameterizations of surface to inversion base transfers.

The flux convergence is parameterized in terms of σ_w, the average standard derivation of vertical velocity fluctuations:

$$\frac{\partial}{\partial z}\left[\overline{w'\left(\frac{p'}{\rho} + \frac{E}{2}\right)}\right] = - C_F' \frac{\sigma_w^3}{h} \tag{5.20}$$

Implicit in this is the tendency of the turbulence towards isotropy so that at all times $\bar{E} \alpha \sigma_w^2$ (recall $\bar{E} = \sigma_u^2 + \sigma_v^2 + \sigma_w^2$ where $\sigma_u^2 = \bar{u}'^2$, $\sigma_v^2 = \bar{v}'^2$, $\sigma_w^2 = \bar{w}'^2$).

It is assumed that energy is re-partitioned between the three components as fast as it is consumed through σ_w^2 by work against buoyancy.

Tennekes (1973) proposes a balance between flux convergence and entrainment potential energy at the inversion base:

$$\frac{g}{\rho}\,(\overline{\theta'w'})_i + C_F' \frac{\sigma_w^3}{h} = 0 \qquad (5.2$$

Following Deardorff (1970), ZT set σ_w proportional to the convective velocity scale

$$w_* = \left(\frac{g}{T_o}\,(\overline{\theta'w'})_o\, h\right)^{1/3}, \qquad (5.2$$

consistent with their initial assumption that the turbulence is always in equilibrium with boundary conditions (surface fluxes). Substitution of eq. 5.22 into eq. 5.21 gives

$$(\overline{\theta'w'})_i \,/\, (\overline{\theta'w'})_o = C_F' \qquad (5.2$$

This relation holds in steady-state convective conditions.

They derive a temporal term

$$\frac{1}{2}\frac{\partial E}{\partial t} = C_T \frac{\sigma_w^2}{h}\frac{dh}{dt} \qquad (5.2$$

by appealing to an independent argument. No such argument is required if the TKE equation is integrated with the use of Leibniz Rule at the inversion boundary (see eq. 5.17(1b)). For boundary layer growth in a neutral atmosphere they derive the relation

$$C_F'/C_T = 0.3u_*/\sigma_w \qquad (5.25$$

ZT attribute some (or for large ΔT, all) of the TKE flux convergence at the inversion to dissipation, identifying

internal wave radiation as the energy sink. From the integration of the TKE equation it is evident that the term $K(\xi-\delta)$ (eq. 5.17 (3a)) accounts for this sink. ZT attempt to parameterize their dissipation term but with limited success.

For the case where surface wind working is important, σ_w must be a function of both w_* and u_*. ZT hypothesise a linear combination of convective and mechanical contributions:

i.e. $(\sigma_w^2)_i \propto w_*^2 + \eta^2 u_*^2$

This hypothesis breaks down if w_* goes negative (e.g. solar heating of a reservoir) as the above relation still predicts a positive contribution of TKE from w_*^2. The correct hypothesis should specify that the flux of TKE be determined by some combination of the power per unit area available from surface wind stirring and cooling, as proposed by Sherman, Imberger and Corcos (1978):

$$(\sigma_w^3)_i \propto w_*^3 + \eta^3 u_*^3 \qquad (5.26)$$

Although ZT parameterize σ_w incorrectly, the coefficients of interest here are determined correctly. Analysis of laboratory data by ZT yields

$C_F' = 0.5 \qquad C_T = 3.55$

$\eta = 2.15$

ZT include a mechanical production term due to shear at the inversion base but the argument involves their concept of inversion base dissipation and so will not be considered here.

5.2.4 Niiler (1975), Niiler and Kraus (1977) (NK)

The reader is referred to the latter of these papers for a good up-to-date discussion of well mixed layer modelling.

NK employ integrated forms of the WML equations

but use a surface based co-ordinate system which complicates the derivation of terms like the surface buoyancy flux $g/\rho_o \overline{\rho'w'}(H)$ and the entrained fluid agitation term $1/2\ E_S\ d\xi/dt$.

Important parameterization schemes introduced by NK are summarised below:

i) the Reynolds stress at the thermocline base, $\overline{u'w'}(\xi-\delta)$ is given the form

$$\overline{u'w'}(\xi-\delta) = - C\ \Delta U_S^2 \qquad (5.27)$$

where C is a drag coefficient. The term accounts for momentum loss via internal wave radiation and acts against the build up of layer mean velocity. However, due to lack of information, no value of C is given; it is expected to be a function of hypolimnion stratification.

ii) They omit the leakage flux of TKE, $K(\xi-\delta)$, representing (in the main) the work of pressure fluctuations in the formation of internal waves in the hypolimnion.

iii) K(H), the surface flux of TKE, is taken as proportional to wind working in the atmospheric surface layer, that is, a stress times a wind velocity, so

$$- K(H) \propto u_{*a}^3$$

or in terms of the water friction velocity (where $u_* = \sqrt{\rho_a/\rho_o}\ u_{*a}$

$$- K(H) = m_1 u_*^3, \text{ where } m_1 \text{ is a constant.} \qquad (5.28)$$

iv) SH(H), the production of TKE in the surface shear layer is also taken as proportional to wind working and therefore incorporated in eq. 5.28. Kraus and Turner's (1967) formulation (stress times a water velocity scale) amounts to the same result.

The result is derived as follows. SH(H) was defined in

Section 5.1 as

$$SH(H) = \int_{\xi}^{H} - \overline{u'w'} \frac{\partial U}{\partial z} \, dz.$$

Considering a thin surface shear layer superimposed over the mean flow, with applied surface stress $\tau = \rho_o u_*^2$,

$$SH(H) = u_*^2 \int_{\xi}^{H} \frac{\partial U}{\partial z} \, dz = u_*^2[U(H) - U(\xi)]$$

The surface drift current $U(H) - U(\xi)$ is known to be proportional to u_{*_a} so

$$SH(H) \propto u_*^3$$

This may be incorporated in eq. 5.28

v) Using eq. 5.6 and their drag relation of eq. 5.27, NK evaluate the thermocline shear term

$$SH(\xi) = \lim_{\delta \to 0} \int_{\xi-\delta}^{\xi} - \overline{u'w'} \frac{\partial U}{\partial z} \, dz = \frac{1}{2} \Delta U_S^2 \frac{dh}{dt} - \frac{1}{3} C \Delta U_S^3 \qquad (5.29)$$

vi) NK indicate that dissipation is the most arbitrary link in the formulation. Dimensionally it is expected that

$$h\epsilon_S \propto \sigma_w^3 \qquad (5.30)$$

On intuitive grounds, they propose that dissipation acts to reduce the efficiency of individual TKE production mechanisms, and can therefore be accounted for by introducing efficiency coefficients or reducing the value of existing coefficients. With coefficients m, n and s, the net TKE production is

$$mu_*^3 + \frac{h}{4}[(1+n)B_o - (1-n)|B_o|] + \frac{s}{2} \Delta U_S^2 \frac{dh}{dt} \qquad (5.31)$$

In this Project, $B_o \equiv \alpha g \tilde{H}_*/\rho_o C_p - \beta g \overline{s'w'}(H)$. The peculiar form of the second term ensures that if B_o is -ve (strong solar heating) dissipation does not affect it.

Whilst this seems logical its application to a WML is questionable. Eq. 5.31 implies that, if wind stirring dominates over surface heating, only that part of wind stirring energy remaining, after depth integrated dissipation, is available to first overcome the heating potential energy deficit and then deepen the layer further. However, most of the work to increase the potential energy (to drive the negative buoyancy flux $\alpha g\overline{\theta'w'}$) is accomplished high in the layer. (For the simple case where solar penetration is absent, $\overline{\theta'w'}$ decreases linearly with depth in the well mixed model). It is reasonable to expect that the efficiency of wind working will be greater for this 'surface work', implying that m should be larger in this situation.

The internal wave radiation loss term $1/3\ C\ \Delta U_S^{\ 3}$ from eq. 5.29 is deduced to be small and is included in the shear production efficiency s.

NK assume that steady-state conditions prevail, so $dE_S/dt = 0$. They further assume that the fluid agitation flux $1/2E_S d\xi/dt$ is small compared to the entrainment working rate for most oceanic conditions and hence may be neglected. The applicability of these assumptions to the reservoir case will be discussed in the next section.

Determination of the coefficients m, n and s involves great uncertainty and is made difficult by a lack of experimental data. Limited evidence available indicates that the coefficients m and n are not constant, but are decreasing functions of the ratio of the energy consuming and producing terms. Evidence offered by NK for the possible magnitude of these terms is as follows:

(a) Laboratory experiments of Kato and Phillips (1969) gave m = 1

Denman (1973) found that m = 1 gave the best results for his model which essentially follows Kraus and Turner's (1967) formulation. Larger values for m are deduced from analysis of storm deepening events, however the influence of shear deepening may invalidate these.

(b) Ball (1960) proposed that n = 1, arguing that large convective eddies would be little affected by dissipation. Other workers have provided estimates in the range $0 \leq n < 0.113$.

(c) The shear energy conversion factor s, accounting for dissipation and, to some extent, leakage via internal waves, has received little attention from researchers. A tentative estimate is s = 0.7.

5.2.5 Sherman Imberger & Corcos (1978), Fischer *et al.* (1979)

These authors have presented a generalised entrainment relation which includes all the various mechanisms proposed by KT, PRT, and ZT. Although there are some differences in approach to the problem, their results will be seen to be a special case of the analysis to follow; for this reason a separate description is not presented here.

5.3 SELECTED PARAMETERIZATION SCHEMES

Based on the work of other researchers summarised in the previous section, plus some new hypotheses, simplifications and parameterizations of terms necessary for closure of the WML equations are presented here.

5.3.1 Individual Mechanisms

Internal Wave Effects

Too little is understood about energy and momentum transfer via internal waves in the hypolimnion to explicitly include these terms. Like NK, it must be assumed here that energy losses are to some extent accounted for by a reduction in the efficiency of entrainment work.

Consequently, the following terms are neglected:

$\overline{u'w'}(\xi-\delta)$ from eq. 5.6

and $K(\xi-\delta)$ from eq. 5.17.

Other Leakage Terms

Based on the reasonable assumption that all turbulent fluxes vanish at the thermocline base, the heat and salt fluxes

$\overline{\theta'w'}(\xi-\delta)$ from eq. 5.3

and $\overline{s'w'}(\xi-\delta)$ from eq. 5.13.

are set to zero.

Surface Wind Working

Following KT and NK, the surface TKE fluxes and the surface shear production are jointly parameterized as

$$SH(H) - K(H) = m_1 u_*^3 \qquad (5.32$$

Thermocline Shear

Niiler (1975) obtained an expression for shear production of TKE at the thermocline:

$$SH(\xi) = \frac{1}{2}\Delta U_S^2 \frac{dh}{dt} = -\frac{1}{2}\Delta U_S^2 \frac{d\xi}{dt} \tag{5.33}$$

This indicates that the mean kinetic energy lost due to entrainment of quiescent fluid becomes available to work locally to further deepen the layer. However, it is expected that a significant portion of this energy will be fed into the well mixed layer (via the term $K(\xi)$) and there be dissipated. Hence it is necessary to include an efficiency coefficient C_S analogous to NK's s.

Surface Heat and Salt Buoyancy

ZT introduced the buoyancy velocity scale defined in eq. 5.22. Combining the surface heat and salt buoyancy terms (4b) and (4d) from eq. 5.17 gives a modified buoyancy velocity scale,

$$\frac{w_*^3}{2} = \frac{gh}{2}\left[\frac{\alpha \tilde{H}_*}{\rho_o C_p} - \beta W S_S\right] \tag{5.34}$$

Dissipation

As seen in eq. 5.31, Niiler and Kraus (1977) include the effects of dissipation as a reduction of individual energy source terms, claiming that this approach is most consistent with the current understanding of dissipation processes. The approach

is limited however by a lack of information from which to determin the various efficiency coefficients. In view of this, and in orde to simplify the current model, the alternative parameterization of Mahrt and Lenschow is used:

$$\varepsilon_S h = \frac{C_E}{2} E_S^{3/2} \tag{5.35}$$

This expression is obtained from dimensional analysis. Similar forms are used by Zeman and Tennekes (1977) and Garwood (1977). Laboratory results of Willis and Deardorff (1974) support this parameterization.

Net Surface Energy Production

It is convenient to combine the buoyancy and wind drive surface production terms in the following form:

$$\frac{q_*^3}{2} = \frac{1}{2} \left[w_*^3 + 2 m_1 u_*^3 \right] . \tag{5.3}$$

5.3.2 Turbulent Kinetic Energy Convergence at the Thermocline

The vertical integral models of NK and others have neglected the energy storage terms (1a) and (1b) of eq. 5.17 in orde to close the equation set. However the formulation of ZT suggests a closure scheme whereby E_S may be explicitly retained. Eq. 5.20 expresses the TKE flux converging below the inversion in terms of the vertical component of TKE, σ_w^2, and a vertical velocity scale σ_w. This flux provides the energy for the local sinks, identified individually by ZT as entrainment work (eq. 5.21) and entrained fluid agitation (eq. 5.24).

Considering now the integrated energy balance of eq. 5.17, it is possible to hypothesise a similar energy transfer mechanism to provide closure. This is stated here in two parts:

i) The flux of TKE directly above the thermocline may be modelled by $- C_F/2\ E_S^{3/2}$ where $E_S \propto \sigma_w^2$

ii) This flux, together with any local TKE production, supplies all energy sinks at the thermocline.

From inspection of eq. 5.17 the following expression satisfies (i) and (ii) above:

$$- \frac{C_F}{2} E_S^{3/2} = \frac{\alpha g h}{2} \overline{\theta' w'}(\xi) - \frac{\beta g h}{2} \overline{s' w'}(\xi) + \frac{E_S}{2} \frac{d\xi}{dt} + SH(\xi) \quad (5.37)$$

5.3.3 Restatement of Well Mixed Layer Equations

Eq. 5.17 may be rewritten, introducing the various parameterizations and jump condition, to give

$$\frac{1}{2} h \frac{dE_S}{dt} = \frac{d\xi}{dt}\left[\frac{E_S}{2} - \frac{C_S}{2} \Delta U_S^2 + \frac{\alpha g h \Delta T}{2} - \frac{\beta g h \Delta S}{2}\right] + \frac{q_*^3}{2} - \frac{C_E}{2} E_S^{3/2} \quad (5.38)$$

Rearrangement of eq. 5.37 and eq. 5.38 yields two new equations:

$$\frac{h}{2} \frac{dE_S}{dt} = \frac{q_*^3}{2} - \frac{1}{2}(C_F + C_E) E_S^{3/2} \quad (5.39)$$

$$\frac{d\xi}{dt}\left[- \frac{E_S}{2} - \frac{\alpha g h \Delta T}{2} + \frac{\beta g h \Delta S}{2} + \frac{C_S \Delta U_S^2}{2}\right] = \frac{C_F}{2} E_S^{3/2} \quad (5.40)$$

The remaining equations are set out below, again with jump conditions for heat, salt and momentum introduced.

$$h \frac{dT_S}{dt} = \Delta T \frac{d\xi}{dt} - \frac{1}{\rho_o C_p}[H_S + H_L + Q_L + Q_S - q(\xi)] \quad (5.41)$$

$$h \frac{d\Delta U_S}{dt} = \Delta U_S \frac{d\xi}{dt} + u_*^2 - PGRAD \quad (5.42)$$

$$h \frac{dS_S}{dt} = \Delta S \frac{d\xi}{dt} + W S_S \tag{5.43}$$

$$\frac{dH}{dt} = - \frac{\alpha}{\rho_o C_p} [H_S + H_L + Q_S + Q_L] - W \tag{5.44}$$

$$h = H - \xi \tag{5.45}$$

$$\Delta T = T_S - T(\xi-\delta) \tag{5.46}$$

$$\Delta S = S_S - S(\xi-\delta) \tag{5.47}$$

Below the thermocline,

$$\frac{\partial T}{\partial t} = - \frac{1}{\rho_o C_p} \frac{\partial q(z)}{\partial z} . \tag{5.48}$$

5.3.4 Evaluation of Coefficients

To obtain a solution of the equation set 5.39 to 5.48, it is necessary first to specify the coefficients C_F, C_E, m and C_S. These must be evaluated from the results of relevant laboratory and field experiments.

The following experimental results allow determination of C_F, C_E and m, with some redundancy for checking purposes.

a) Willis and Deardorff (1974):

$$\frac{1}{2} E_S = K_{ES} w_*^2, \quad K_{ES} \simeq 0.4$$

for steady-state, free convection conditions. Steady-state, in the present context, means constant surface inputs (i.e. q_*^3 constant).

b) Willis and Deardorff (1974), Kaimal *et al.* (1976), Mahrt and Lenschow (1976):

$$\varepsilon_S h = K_E w_*^3, \quad K_E \simeq 0.4 \rightarrow 0.5$$

for steady-state, free convection conditions.

c) Willis and Deardorff (1974), Stull (1976) and others:

$$\overline{\theta' w'}(\xi) / \overline{\theta' w'}(H) = K_A, \quad K_A \simeq 0.1 \rightarrow 0.3$$

for steady-state, free convection entrainment of a strong

density jump.

d) Deardorff (1974):

$$\frac{dh}{dt} = K_W w_*, \quad K_W \simeq 0.2$$

for steady-state growth of a convective layer into a neutral environment.

e) Wu (1973), Kato and Phillips (1969):

$$\frac{dh}{dt} = K_p \frac{u_*^3}{\alpha g h \Delta T}, \quad K_p = 0.234 \text{ (Wu)}$$

$$= 2.5 \text{ (Kato and Phillips)}$$

for steady-state growth of a layer with a strong density jump. In Wu's experiment, turbulence was generated by wind shear in a wind/wave tank, with negligible internal shear. The Kato and Phillips experiments were conducted in an annular tank with surface shear. Internal shear generation of TKE was important in this case.

f) Tennekes and Lumley (1972):

$$\frac{dh}{dt} = K_U u_*, \quad K_U \simeq 0.3$$

for growth of a layer into a neutral environment with turbulence generated by surface wind shear.

Relationships between C_F, C_E, m and the various K constants are set out below in algebraic form, to allow modification of constants if new experimental data become available.

For steady-state, eq. 5.39 becomes

$$0 = q_*^3 + (C_F + C_E) E_S^{3/2}$$

so $$E_S^{3/2} = q_*^3/(C_F + C_E). \tag{5.49}$$

Then eq. 5.40 becomes

$$\frac{d\xi}{dt}[- E_S - \alpha g h \Delta T + \beta g h \Delta S + C_S \Delta U_S^2] = \frac{C_F}{(C_F+C_E)} q_*^3 \tag{5.50}$$

For steady-state convective conditions, with ΔT large, eq. 5.50 reduces to

$$- \alpha g h \Delta T \frac{d\xi}{dt} = C_F \, w_*^3 / (C_F + C_E)$$

and so from (c) above

$$C_F/(C_F + C_E) = K_A \tag{5.51}$$

or $$C_F = \frac{K_A}{(1-K_A)} C_E. \tag{5.52}$$

Note that (b) above is not independent of (c). It is easily shown from eq. 5.49 that

$$K_E = \frac{(1 - K_A)}{2} \tag{5.53}$$

Hence the choice of K_A must satisfy both criteria (c) and (b).

Comparing item (a) with eq. 5.49, where $q_*^3 = w_*^3$ in convective conditions, it may be shown that

$$C_F + C_E = (2K_{ES})^{-3/2}. \tag{5.54}$$

Simultaneous solution of eq. 5.52 and eq. 5.54 gives

$$C_E = (1-K_A) \; (2K_{ES})^{-3/2} \tag{5.55}$$

$$C_F = K_A (2K_{ES})^{-3/2}. \tag{5.56}$$

Item (d) above is now redundant information for convective conditions, allowing a check on the estimates of C_F and C_E. For the stated conditons of (d), eq. 5.50 reduces to

$$E_S \frac{dh}{dt} = \frac{C_F}{(C_F+C_E)} w_*^3 \tag{5.57}$$

and so, using eq. 5.49,

$$K_W = C_F (C_F + C_E)^{-1/3} \tag{5.58}$$

Calculated values of K_W from eq. 5.58 may be compared with the estimate in (d).

As universal coefficients, the values determined for C_F and C_E should hold for both convective and surface shear dominated conditions. Turning to the latter, an estimate of m may be obtained from (e) above as follows:

eq. 5.50 is now

(5.59)

so from (e)

(5.60)

For convenience, a new parameter C_N is defined as

(5.61)

so $q_*^3 = w_*^3 + C_N^3 u_*^3$ (5.62)

Item (f) above is now redundant, allowing a check on the value of C_N. K_U may be calculated from

(5.63)

Alternatively, C_N may be computed from an accepted value of K_U:

$$\frac{(C_F+C_E)^{1/3}}{F} \tag{5.64}$$

making (e) redundant, so

$$K_p = K_A C_N^3 \tag{5.65}$$

A comprehensive analysis of the various combinations of these coefficients was carried out, bearing in mind the experimental uncertainty of values stated in (a) to (f) above. A self-consistant set, choosen as a result of this analysis, is as follows:

$K_{ES} = 0.4, \quad K_E = 0.41, \quad K_A = 0.18$

$C_F = 0.25, \quad C_E = 1.15, \quad K_W = 0.22$

Eq. 5.60 and eq. 5.61 give (for $K_p = 0.234$)

$C_N = 1.09, \quad K_U = 0.25$

Eq. 5.64 and eq. 5.65 give

$C_N = 1.33, \quad K_p = 0.42$

These values of K_{ES}, K_E, K_A and K_W are within 10% of their expected values, giving confidence to the method of determination. K_U calculated from eq. 5.61 is somewhat lower than the expected value. Alternatively, the calculated value of K_p from eq. 5.65 is somewhat larger than Wu's estimate from (e). The latter is accepted as correct on the basis that in Wu's experiment, the wind/wave interaction would not have been fully developed in his small (2.3 m long) tank. The chosen value is much smaller than that for the Kato and Phillips experiment, as would be expecte if internal shear was dominant in their case. Model results described in Chapter 7 support the choice.

The only coefficient as yet undetermined is C_S. Experi mental evidence from which to determine C_S is sparse. Sherman, Imberger and Corcos (1978) summarise the available information, concluding that $C_S = 0.3$ is the best available estimate. From this and other papers it appears that C_S may fall between 0.2 and 0.5.

Spigel (1978) analyses the timescales of the various processes within a reservoir and provides a classification scheme for determining whether surface wind mixing or internal shear will be dominant. Diurnal mixing can be shown to fall into his regime 2

$$1 < Ri < (L/2h)(H/(H-h))^{\frac{1}{2}}$$

where $Ri = \alpha g h \Delta T / u_*^2$, H is reservoir depth and L is the length of the reservoir basin. Typically, an hour after the onset of afternoon deepening,

$$Ri \simeq 20, \quad (L/2h)(H/(H-h))^{\frac{1}{2}} \simeq 200$$

In regime 2, deepening is dominated by interfacial shear with Kelvin-Helmholtz billows present and interfacial displacements important. As afternoon deepening commences close to the surface, shear effects will rapidly dominate. In evaluating C_S then, it is reasonable to adjust the value between the above limits to correctly simulate observed deepening during the shear dominated periods. This adjustment is not an overall manipulation of results; on the contrary, the shear dominated mixing observed in the diurnal mixed layer should provide a valuable independent estimate of C_S.

The Kelvin-Helmholtz billows typical of regime 2 will lead to a smeared rather than sharp interface. Spigel and Imberger (1979) provide a formula for the stable interface thickness:

$$\delta = \frac{0.3(\Delta U_S)^2}{g\alpha\Delta T} \tag{5.66}$$

5.3.5 Horizontal Pressure Gradients

Spigel (1978) and Spigel and Imberger (1979) provide the basis for computation of the pressure gradient term in eq. 5.42. Figure 5.2, reproduced from Spigel and Imberger (1979), shows the response of a two-layered body of water to an applied surface stress. The interfacial velocity jump at the centre of the water body, ΔU, increases until time $T_i/4$, where T_i is the fundamental internal wave period given by

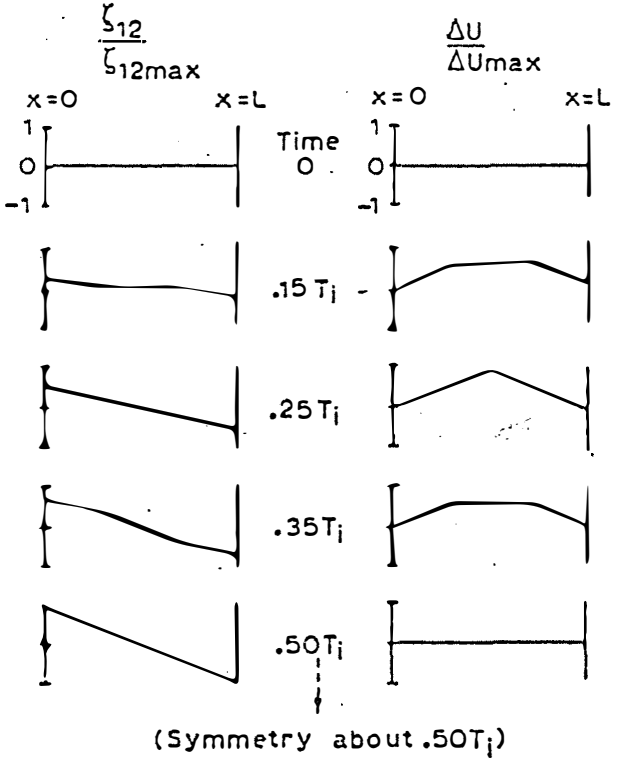

Interface shape ζ_{12} and velocity shear ΔU at five instants in time during initial half wave period.

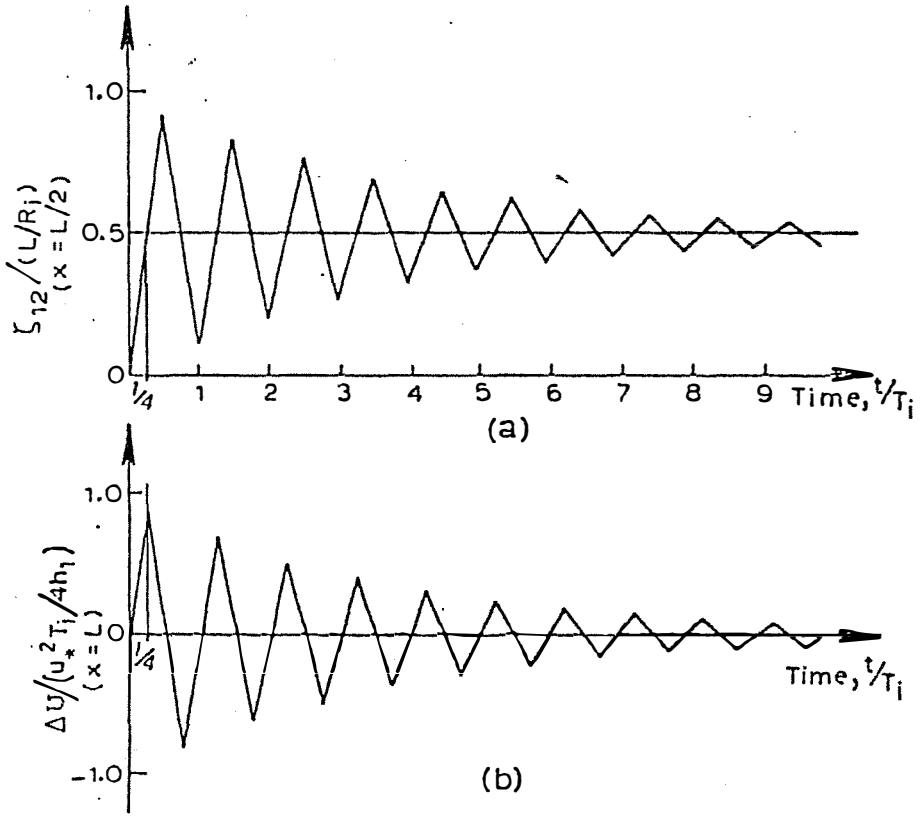

Interface displacement ζ_{12} at downwind end of basin, showing oscillatory motion about steady state set up position; (b) velocity shear ΔU at center of basin. T_i is lowest mode internal wave period.

$$T_i = 2L(\alpha g \Delta T\, h_1 h_2/H)^{-\frac{1}{2}} \simeq \frac{2L}{\sqrt{\alpha g h_1 \Delta T}} \quad (h_1 \text{ small}) \tag{5.67}$$

At this time the waves travelling toward the centre from the end walls have set up an interface slope

$$\frac{d\zeta_{12}}{dx} = \frac{u_*^2}{\alpha g h_1 \Delta T} \tag{5.68}$$

representing a balance between the applied stress and the horizontal pressure gradient. Damped oscillations with period T_i follow this initial set-up, as shown in Figure 5.2, leading to a final steady-state interface slope given by eq. 5.68, with baroclinic circulation in the top and bottom layers.

For the half wave period after time $T_i/4$, water above and below the interface will undergo negative acceleration under the influence of the pressure gradients associated with free surface tilt and interfacial tilt respectively. The net effect on ΔU_S is seen in Figure 5.2, and may be described by the term PGRAD in eq. 5.42, given by

$$\text{PGRAD} = \nabla p = \frac{2\rho_o u_*^2}{h_1} \tag{5.69}$$

The algorithm for computing PGRAD for the appropriate half wave periods is described in Chapter 6.

5.3.6 Model Response to Changing Inputs

Eq. 5.39 and eq. 5.40 together describe the response of the WML to changing inputs. If q_* suddenly increases, E_S will grow smoothly with time. Similarly the deepening response of eq. 5.40 is smoothed by the transient changes of E_S. This will introduce a time lag in deepening rate changes and also in the occurrence of layer retreat if q_* decreases suddenly.

More important then the time lag is the behaviour of the entrained fluid agitation term. If q_* suddenly decreases (e.g. the wind speed suddenly drops) this term, $E_S/2\ d\xi/dt$, decays exponentially. This response, coupled with a decay of mean velocit allows the model to proceed smoothly to a new equilibrium. An alternative scheme, equivalent to that proposed by ZT, sets $dE_S/dt =$ and computes E_S as

$$E_S = \text{constant} \times q_*^2 \qquad (5.70)$$

$E_S/2\ d\xi/dt$ now follows q_* changes instantaneously. Problems may arise in the solution if shear production is dominant so that, from the RHS of eq. 5.40, the sum

$$-\frac{\alpha g h \Delta T}{2} + \frac{\beta g h \Delta S}{2} + \frac{C_S \Delta U_S^2}{2}$$

is a small number. Here, the deepening rate $-d\xi/dt$ will be large, and $-E_S/2$ will be significant when compared with the above sum of terms. A sudden drop in $E_S/2$, as computed from eq. 5.70 for a sudden wind speed drop say, may have a serious effect on a numerical solution: it will suddenly force the solution onto the singularity of eq. 5.40. It might be argued that a numerical solution with a small enough timestep should cope with any natural wind gusts, which develop over a finite time. However, in practice, the data usually available are in the form of time averages (e.g. 10 minute, hourly), and it is most convenient to allow the model to negotiate the discontinuities of such time series by itself (i.e. without prior smoothing of the data). For such data then, q_* will exhibit sudden changes.

In summary, where WML behaviour is being modelled on a short timescale with finely resolved inputs, the formulation of model equations 5.39 to 5.48 is recommended.

5.3.7 A Model for Seasonal Simulations

For most reservoir and oceanic applications a model is required to predict seasonal behaviour of surface water rather than diurnal behaviour. Data are generally sparse and may not be resolved better than daily averages. For such a case it is justifiable to neglect the effect of transient turbulent energy storage and decay. Hence eq. 5.39 and eq. 5.40 reduce to the forms given by eq. 5.49 and eq. 5.50, rewritten here as one expression:

$$\frac{d\xi}{dt}\left[-(C_F+C_E)^{-2/3}q_*^2 - \alpha gh\Delta T + \beta gh\Delta S + C_S\Delta U_S^2\right] = \frac{C_F}{(C_F+C_E)}\,q_*^3 \qquad (5.71)$$

An entrainment relation of this form was first presented by Sherman, Imberger and Corcos (1978) and further developed by Fischer *et al.* (1979). These authors analysed the potential and kinetic energy budgets of a column of water and so derived the expression

$$\frac{dh}{dt}\left[C_T q^2 + \alpha gh\Delta T - \beta gh\Delta S - C_S\Delta U_S^2\right] = C_K q^3 \qquad (5.72)$$

where $$q^3 = \left(\frac{\alpha g h \tilde{H}}{\rho_o C_p} + \eta^3 u_*^3\right)$$

Neglecting differences in the derivation and definition of some terms, the coefficients C_K, C_T and η may be evaluated using the values of C_F, C_E and C_N from Section 5.3.4, and compared to values supplied by Fischer *et al.* (1979):

$C_K = 0.18$ (cf 0.13 from Fischer *et al.*)

$C_T = 0.8$ (cf 0.5 from Fischer *et al.*)

$\eta = 1.33$ (cf 1.2 from Fischer *et al.*)

C H A P T E R 6

A NUMERICAL MODEL OF THE DIURNAL WELL MIXED LAYER

Most of the theory developed in Chapter 5 is quite general and may be applied to both marine and atmospheric well mixed layers. It is noteworthy that some of the universal coefficients of Section 5.3 were evaluated from atmospheric field data.

The concept of a diurnal well mixed layer in a reservoi was introduced in Section 4.4. In this chapter the various algorithms required to incorporate the theory of Chapter 5 into a computer model of the diurnal cycle are described. The objectives of the modelling exercise are:

i) to predict the diurnal cycle of temperature and salinit within the bulk or seasonal WML, including both layer retreat and layer deepening, and,

ii) to investigate the roles of individual deepening mechanisms and comment on the choice of coefficients in Section 5.3

6.1 MODEL ARCHITECTURE

Figure 6.1 is a block diagram of the model showing fundamental input and output requirements. The following considerations influenced the model's architecture:

1. Simulation runs are for single days only (data were not gathered for successive days). Hence it is reasonable to be

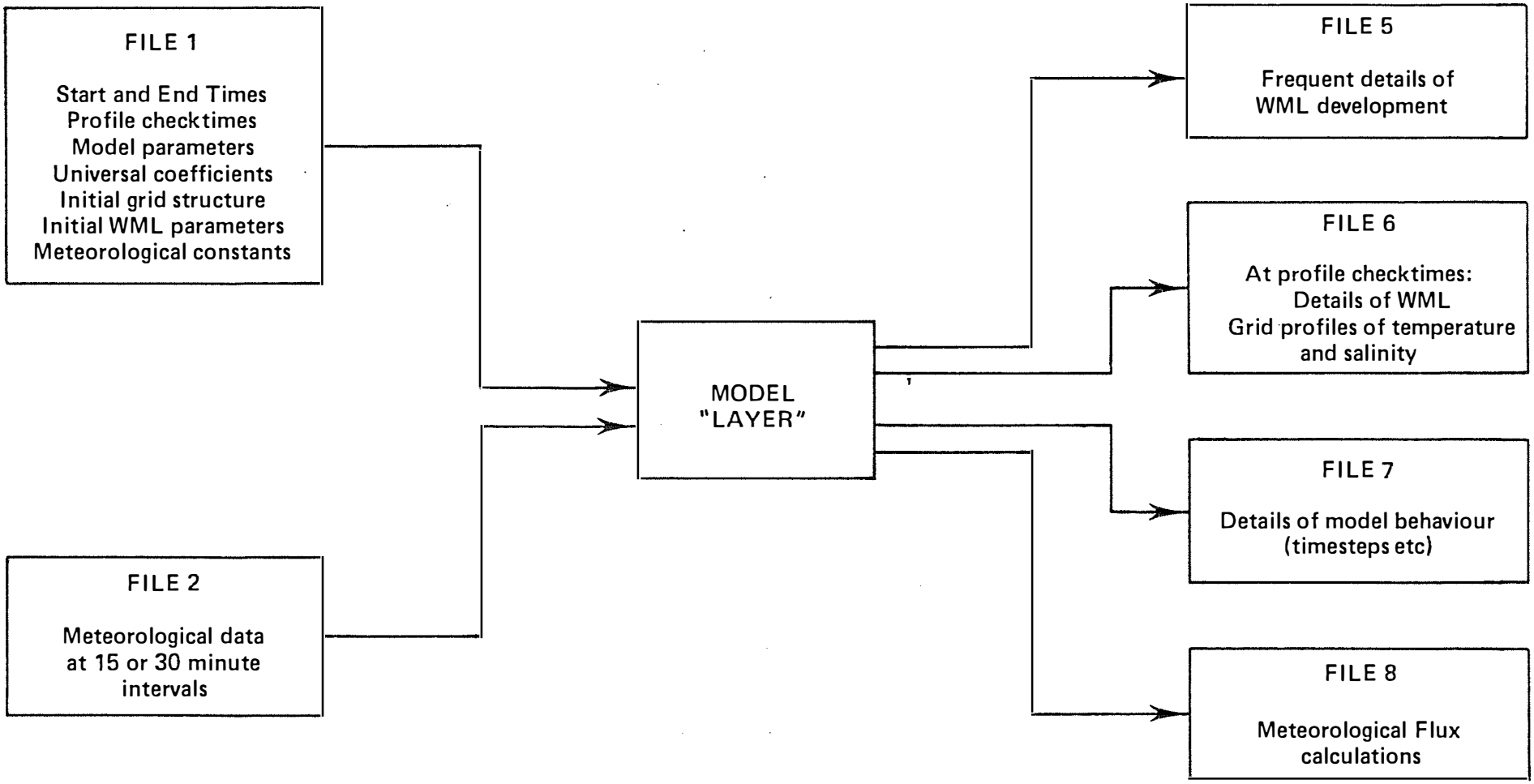

FIGURE 6.1 Model block diagram

generous with computer resources since the running costs are minimal.

2. Fluctuations of wind and surface heating were observed to produce intermittent mixing events which left skeleton step structure within the seasonal well mixed layer. For example, the effects of the previous night's mixing could be seen in the morning as a fairly sharp step near the base of the seasonal well mixed layer. This skeleton structure, containing significant density gradient, affects subsequent deepening and the model must therefore 'remember' it.

The following are the broad features of the model. Reference is made to the model flowchart (Appendix B2) and the program copy (Appendix C2).

6.1.1 Vertical Grid

To give the model memory, a vertical grid of closely and equally spaced points is used. Associated with the grid are temperature and salinity arrays, which are loaded from the initial profiles and subsequently updated as the simulation proceeds.

Superimposed over the upper part of the grid is the diurnal WML. Note that the WML depth h is not constrained to coincide with a grid point; solution of the WML equations occurs independently, except for a procedure for determining the thermocline temperature step as described in Sections 6.2.3 and 6.2.6 Grid points falling within the WML are updated to reflect WML temperature and salinity.

Required resolution is the major critierion for determining grid spacing. If WML retreat occurs, the remaining temper-

ature step is remembered as the difference between two adjacent gridpoint temperatures. If the grid spacing is large and the step was not central in the grid interval, a heat storage error is introduced. Large spacing also results in smoother gradients, giving a poor representation of steps. The surface temperature profile under strong solar heating would also be poorly represented. In view of the above and in the light of model testing, a grid spacing of between one and five centimetres is acceptable. For flexibility, grid spacing appears in the model as a variable to be specified in the input data.

6.1.2 Model Timestep

Two criteria for the model timestep must be satisfied:

i) it must be much smaller than the timescale of meteorological flux changes, and,

ii) it must be sufficiently small to ensure that not more than one gridpoint is entrained per step during WML deepening. This is to ensure that the algorithm for ΔT and ΔS determination remains valid.

The shortest timescale for fluxes is 15 minutes (see Section 3.4.3) so criterion (i) is easily met. However, the deepening rate varies greatly, being dependent on meteorological forcing and the recent history of deepening or retreat. To enhance model efficiency, the timestep is managed dynamically within the range 30 seconds to 4 minutes. Details are as follows:

i) A check is maintained on the deepening after each timestep. If it falls outside acceptable upper or lower limits (fractions of a grid interval) the

timestep is halved or doubled within the specified range.

ii) When approaching a new flux interval, or at the onset of deepening following WML retreat, the timestep is set to 30 seconds and subsequently allowed to readjust itself via (i). This minimises the integration timestep for a period where the time derivatives of eqs. 5.39 to 5.48 are likely to be large.

6.2 DESCRIPTION OF MODEL ALGORITHMS

Details of those model algorithms not fully described by the flowchart in Appendix B2 are provided below.

6.2.1 Loading Grid Arrays

Part of File 1 (see Figure 6.1) is a specified number of height/temperature/salinity records. These are read into S/R LOAD which then, by linear interpolation, assigns a temperature and salinity value to each gridpoint. These values specify the starting profile for the model.

6.2.2 Meteorological Flux Computation

S/R FLUXES initially accesses File 2 (sequential records of meteorological data) and reads records until the correct time interval is entered. In subsequent calls to S/R FLUXES, the interval is updated only if the model time has advanced past the old interval end-time.

In S/R FLUXES, the timestep-average meteorological data are determined by linear interpolation within the current interval. These data, plus the current

modelled WML temperature, are fed to S/R TURB which computes stability corrected meteorological fluxes by the method described in Section 3.5.2. Use of the model WML temperature in the computation of turbulent and long-wave radiative heat fluxes provides a feedback to the WML simulation.

Instantaneous fluxes required by the integration routine are similarly computed through ENTRY IFLUX.

6.2.3 Solar Heating Below the Well Mixed Layer

Eq. 5.48 must be solved every timestep to simulate heating by solar radiation absorption in the water below the WML. S/R SOLAR actually heats all gridpoints, but those in the resultant WML are overwritten later with the value of T_S. This process is necessary to correctly simulate the heating associated with WML retreat, should this occur.

S/R SOLAR and S/R STEP together compute the temperature and salinity gradients directly beneath the WML, by remembering the details of the most recently entrained gridpoint. This gridpoint, with pre-entrainment temperature and salinity values substituted, is heated and then used to compute the new gradients.

6.2.4 Well Mixed Layer Deepening or Retreat?

The physical insight into WML retreat afforded by eqs. 5.39 and 5.40 justifies their added complexity. It would be possible to continue solving an entrainment equation such as eq. 5.71 after q_* had become negative (e.g. for conditions of strong solar heating and light winds), giving continuous de-entrainment of water, which is not realistic.

Field observations from this project indicate that when solar heating begins to dominate, continuous mixing degenerates to sporadic mixing events and the once active thermocline region retains its position, subject only to diffusive processes. $d\xi/dt$ never becomes positive, but a new mixed layer may subsequently form within the old layer if mixing energy again becomes available at the surface.

Eq. 5.40 shows that, for entrainment to occur, there must be a positive energy level E_S within the layer. There is no such thing as negative energy; hence $d\xi/dt \leq 0$ always. A new shallow layer must therefore form whenever E_S for the existing layer decays to zero. Within the model, a check is maintained on the value of E_S, and if it is certain to decay to zero in the next timestep, layer retreat computations are initiated.

6.2.5 Layer Retreat

When E_S has decayed to zero, a new layer depth must be found such that E_S and its time derivative dE_S/dt are just held to zero. In this new layer, TKE introduced by wind stirring will just balance the buoyant damping due to solar heating. Eq. 5.39 then reduces to

$$q_*^3 = 0 \qquad (6.1)$$

where q_*^3 is a complicated function of h (or ξ) through the term $\tilde{H}_*$.

Solution of eq. (6.1) in the model is performed by the Newton-Raphson iteration method. The derivative $dq_*^3/d\xi$ necessary for this method is evaluated by ENTRY NEWSIG. The iteration is performed by S/R NEWTON. Convergence of ξ to its new value (to

within .05%) is rapid (usually less than five steps).

If the salinity flux contribution to w_*^3 is neglected, eq. 6.1 reduces to

$$h = \frac{C_N^3 u_*^3}{\alpha g \tilde{H}_* / \rho_o C_p}$$

which, from inspection, is a form of Monin-Obukhov length (see eq. 2.5). The above procedure for determining h from eq. 6.1 is consistent with the definition of the Monin-Obukhov length given in Section 2.1.1.

Having determined ξ, the equations for WML heat and salinity (5.41 and 5.43) are solved while constraining dE_S/dt, $d\xi/dt$ and dU_S/dt to zero.

The velocity jump ΔU_S at the thermocline is computed, during deepening, from eq. 5.42, which is based on the assumption that the velocity below the thermocline may be neglected. When layer retreat occurs, ΔU_S is set to zero in the model and only increases again when deepening is re-initiated. This procedure does not conserve momentum but does provide a correct description of ΔU_S. The problems of specifying momentum sinks (e.g. internal wave radiation) and changing wind directions are thus avoided. Although wind direction was not reliably measured during the field-work, it was noted that the afternoon winds responsible for deepening came from a single quadrant.

6.2.6 Integration of Well Mixed Layer Equations

S/R MESR1 is a fourth order Runge Kutta routine which computes relative accuracy of integration via a fifth step, and uses this test to govern its own timestep halving or doubling

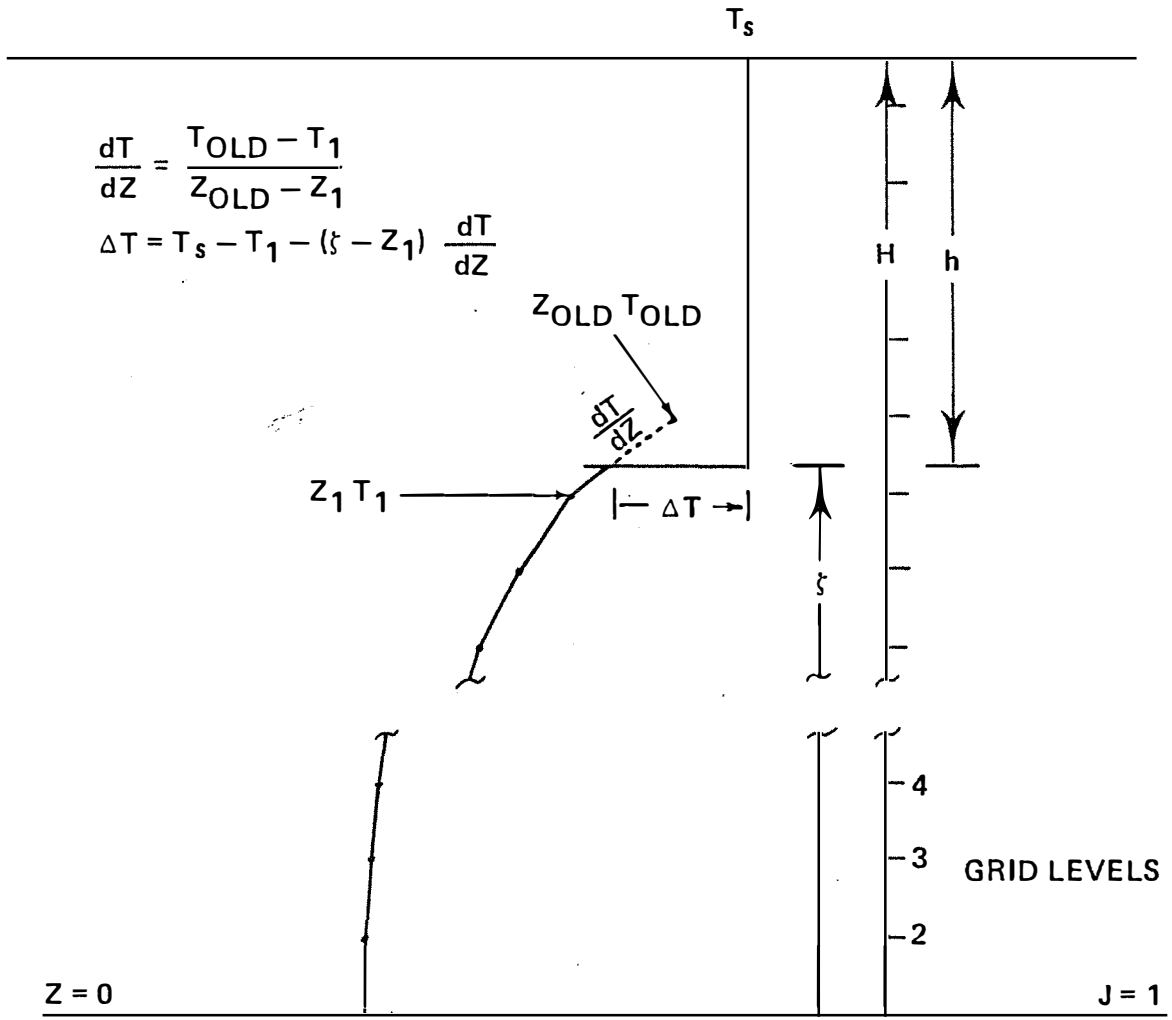
T_s
$\frac{dT}{dZ} = \frac{T_{OLD} - T_1}{Z_{OLD} - Z_1}$
$\Delta T = T_s - T_1 - (\zeta - Z_1) \frac{dT}{dZ}$
H
h
Z_{OLD} T_{OLD}
$\frac{dT}{dZ}$
Z_1 T_1
ΔT
ζ
4
3
2
GRID LEVELS
Z = 0
J = 1

procedure. This procedure is independent of the model time-step management described in the Section 6.1.2, except that the integration timestep is not allowed to exceed the model timestep. In practice the two agree except for rapidly changing conditions where the integration timestep decreases.

The WML differential equations are contained in S/R DIFF, together with other necessary expressions which are described below.

i) The temperature and salinity jumps at the bottom of the layer must be evaluated for each Runge Kutta (RK) step. ΔT and ΔS change as the layer deepens and as the water below the thermocline is heated. The scheme for computing the temperature and salinity gradients below the WML was summarised in Section 6.2.3. For increased precision, these gradients are also determined each RK step. Given the gradients and the current value of ξ, ΔT and ΔS are given by

$$\Delta T = T_S - T_1 - (\xi - z_1) \frac{dT}{dz} \qquad (6.2)$$

$$\Delta S = S_S - S_1 - (\xi - z_1) \frac{dS}{dz} \qquad (6.3)$$

T_1 and S_1 are the values at the gridpoint immediately below the WML, at height z_1. Figure 6.2 aids understanding of eq. 6.2.

ii) Instantaneous meteorological fluxes are determined each RK step, for use in the solution, by a call to ENTRY IFLUX (previously described). To facilitate interpolation in the flux interval, the RK integration range is matched to the flux interval. Each time S/R FLUXES

indexes the flux interval it also resets the RK integration range (i.e. ST = 0.0).

iii) The WML deepening equation 5.40 has a singularity discussed previously in Section 5.3.6. During deepenin with continuous determination of the fluxes, ΔT and ΔS, the RK scheme will properly manage integration if this singularity is approached. That is, $d\xi/dt$ will become large. Care is necessary, however, to ensure that deepening is initiated correctly following layer retreat (when $\Delta T = \Delta S = 0$). This is accomplished by keeping $\Delta U_S = 0$ until mixing is definitely established, that is, ξ has fallen. In practice this occurs within one or two model timesteps. It is detected in the mainline and transmitted to S/R DIFF by the variable MFLAG.

iv) As mentioned in Section 6.2.5, once ξ has been determined by iteration, the remaining WML equations (except momentum) are solved. This can be seen in S/R DIFF: when NFLAG = 0, $dE_S/dt = d\xi/dt = d\Delta U_S/dt = 0$, and dT_S/dt, dS_S/dt and dH/dt are solved normally.

6.2.7 Pressure Gradient Calculation

In varying wind conditions it is difficult to calculate a representative value of T_i from eq. 5.67 in order to determine whether the interfacial pressure gradient has been set up. An alternative procedure which was adopted is described below.

At each timestep the advected volume is updated from its value at the previous timestep:

$$V_t = V_{t-1} + h\Delta U_S \Delta t$$

Also computed is the final set-up slope from eq. 5.68 and, from this, the final advected volume

$$V_f = \frac{L^2 u_*^2}{8\alpha g h \Delta T} \quad .$$

The pressure gradient PGRAD is turned on if $V_t > V_f$ and off if $V_t < V_f$.

CHAPTER 7

RESULTS OF MODEL SIMULATIONS

The numerical model described in Chapter 6 was first developed and then refined to its final form using only the data from the field day 05 02 76. Determination of an appropriate value for C_S, as described in Section 5.3.4, was also completed using this one data set. These procedures were adopted because:

i) data from day 05 02 76 were considered to be the most reliable overall, and,

ii) data from the remaining three days then provided a realistic test for the model.

In order to provide maximum insight into the mechanics of the model, a composite set of computer plots was produced. These plots are described in Section 7.1. Section 7.2 contains an analysis of the model predictions for a full daily cycle. Section 7.3 contains an appraisal of the model's performance and a discussion of specific model deficiencies.

7.1 DESCRIPTION OF MODEL PLOTS

Two forms of model output have been plotted for analysis. These are described below.

7.1.1 Temperature Profile Plots

The measured profiles of temperature at specified times throughout the four field days were described in Section

4.4.1 and presented as computer plots in Appendix A5. Figure 6.1 shows that the model output File 6 contains modelled profiles for those times which correspond to field profiles.

The computer plots in Appendix D1 were produced, following a model run, by a program which accessed both the field profile data and File 6. Field data points are plotted as crosses while the model profile appears as a full line. The initial model profile for each day is loaded from File 1 so as to be identical to the field profile, although specification of an initial thermocline height tends to be somewhat arbitrary in mid-morning.

The temperature jump at the thermocline is plotted with its position and magnitude exact. Only one grid point in every four is plotted however, giving a depth resolution of 20 cm, equal to the finest resolution of field profiles. Note that the start and scale values on the temperature axis vary for different days.

7.1.2 Daily Cycle Plots

These plots, appearing in Appendix D2, were produced from File 5 and File 8 of Figure 6.1.

The lowermost plot on each page shows the meteorological fluxes which were computed within the model. These fluxes combine to form the net surface power term, q_*^3, plotted on a log scale in the second plot. Only values of q_*^3 above 1.0×10^{-10} are plotted; positive values below this are negligible and layer retreat precludes negative values, except for short periods immediately prior to retreat. Plotted with q_*^3, also

on a log scale starting from 1.0×10^{-7}, is the WML TKE level, E_S.

The third plot from the bottom shows the evolution of temperature, salinity and velocity differences across the thermocline. Large values of ΔT and $-\Delta S$ inhibit mixing, while ΔU_S promotes mixing at the thermocline.

The uppermost plot shows the evolution of temperature and depth of the WML. The start and scale values of axes for this plot vary from day to day.

7.2 ANALYSIS OF THE SIMULATION OF A DIURNAL CYCLE

Inspection of one of the plots of Appendix D2 will aid understanding of the mechanics of the model. The plot for day 05 02 76 is broken into convenient time intervals and discussed below.

i) 0630 to 0820

Latent cooling and surface stirring are dominant, giving a large value of q_*^3 and hence large E_S also. This period is in fact the end of the night cycle, where mixing has proceeded to a depth of 8 metres, below which there is a moderately stable temperature gradient down to the seasonal thermocline at 12 metres. (At this time of the year the seasonal thermocline is still strengthening.) With increasin solar heating and a drop in wind after 0800, q_*^3 drops rapidly to zero at 0808 and then becomes negative (not plotted). The transient response of the model is apparent at this time; E_S does not fully decay to zero until 0820. A survey of all plots shows E_S lagging q_*^3, as expected

from eq. 5.39.

ii) 0820 to 1400

At time 0820 there is a good example of layer retreat. Within one timestep (30 seconds), the WML depth h changes from 8.13 m to 3.83 m. The full plotted line representing this jump should not be considered as representing an upward movement of the thermocline. The old temperature step still remains at 8.13 m depth as seen from the 0830 model profile in Appendix D1.7(it appears somewhat diffused due to the selective plotting of gridpoints).

On three occasions before 1400, sufficient surface power q_*^3 becomes available to initiate layer deepening. As can be seen from the plot of h however, these mid-morning mixing events have little effect and serve only to distribute heat over a slightly greater depth. By 1230 the WML is only 13 cm deep and its temperature has risen dramatically. The 1230 profile shows a strong temperature gradient below the layer. Absorption of solar radiation in the surface two metres is the dominant effect. When slight mixing is initiated after 1230, a large value of ΔT inhibits its progress. At 1430, although q_*^3 goes negative for a brief period (four minutes), E_S does not completely decay.

iii) 1400 to 2310

Layer retreat does not occur again after 1400. Increasing wind speeds and latent cooling are associated with decreasing solar heating and so q_*^3 climbs to high values, providing a continuous supply of mixing energy. The importance of accurately describing short period wind

speed peaks can be seen around 1545.

The momentum of the WML (and hence ΔU_s) increases until 1815, supplying mixing energy at the thermocline. All mixing mechanisms are operative during this period, with interfacial shear dominating. At 1815 the pressure gradient described in Section 6.2.7 is set up, and by 2310 this has driven almost one complete oscillation (as shown in Figure 5.2.)

7.3 COMPARISON OF MODEL AND FIELD PROFILES

Overall, the comparison between modelled and measured temperature profiles as plotted in Appendix D1 is very good. The capability of the model to simulate the heating and mixing phases, with the transitions occurring at roughly the correct times, substantiates the form of the model equations 5.39 to 5.48 and the use of q_*^3 as the controlling parameter.

Some aspects of the model's performance are examined in detail below.

7.3.1 Model Coefficients

A value of $C_s = 0.2$ was chosen after several model runs with different values. The model response proved to be quite sensitive to this parameter. Setting $C_s = 0$ for example resulted in a 40% decrease in deepening rate during the afternoon of 05 02 76.

Table 7.1 gives all the universal coefficients and other physical constants used. Derived values applicable to the Reservoir model DYRESM are included. Also included are current values used in DYRESM (Imberger and Hebbert (1980)).

MODEL COEFFICIENT	VALUE	
C_F	0.25	
C_E	1.15	
C_N	1.33	
C_S	0.20	
DYRESM EQUIVALENTS	DERIVED VALUE	CURRENT VALUE
C_K	0.18	0.125
C_T	0.80	0.51
η	1.33	1.23
C_S	0.20	0.50
PHYSICAL CONSTANTS		
α	2.54×10^{-4} $^oC^{-1}$	
β	10^{-6} ppm^{-1}	
C_P	4180 J/kg ^oC	
ρ_o	1000 kg/m^3	
L (Latent heat)	2445 kJ/kg	

TABLE 7.1 - Model coefficients and physical constants. DYRESM equivalents are derived in Section 5.3.7. Current values of DYRESM coefficients are as specified by Imberger and Hebbert (1980).

Referring to the choice of C_N discussed in Section 5.3.4, it was found that the value obtained from eq. 5.61 caused an unrealistic delay in the onset of deepening during daytime hours. Recall that deepening commences soon after

$$q_*^3 = w_*^3 + C_N^3 u_*^3$$

becomes positive. If w_* is negative (when solar heating is strong) the value of C_N determines the wind strength necessary to initiate mixing. Mixing will occur whenever $C_N u_*^3 \geq -w_*^3$. C_N determined from eq. 5.65, however, produced very good model response to changing meteorological conditions. This value appears in Table 7.1.

7.3.2 Thermocline Thickness

The profile plots of Appendix D1 show the thermocline as having zero thickness; hence the temperature profiles include a sharp step across the thermocline, consistent with the assumptions stated in Section 5.1. In conditions of free convection where only surface cooling is important, the thermocline does become very thin (see Willis and Deardorff (1974)). In the reservoir however there is almost always some shear across the thermocline during deepening and so Kelvin-Helmholtz billows, as described in Section 5.3.4, will ensure a finite thermocline thickness.

Intuitively, it is expected that the mixing process at the thermocline is cyclic in nature. Billowing would be followed by entrainment of the diffuse region, sharpening the gradients until billowing recurs. It must be assumed for modelling purposes that the efficiency of entrainment of the

diffuse region is accounted for in the coefficient C_S, so that the model computes the correct deepening rate. Accepting this, it is possible to directly compare the model and field profiles.

An ideal procedure to aid comparison, given accurate and finely resolved field profile data, would be to 'square up' the field profiles, conserving heat and potential energy. An alternative means of aiding comparison has been adopted here. The thickness of the billowing region was calculated from eq. 5.66 for those profiles where deepening was established, prior to interface set-up. The position of this region in plotted field profiles was determined by visual inspection and is shown, on the particular plots, as the region bounded by dotted lines. The agreement between computed and observed thickness of this region is very good. Note how the billowing region becomes very thin on 05 04 76 at 0200 after mixing has encountered the seasonal thermocline. The salinity jump is also significant at this time, as shown by the daily cycle plot in Appendix D2.4.

7.3.3 Temperature Profile Representation

Accepting the thermocline step representation of the temperature profile, there remain three anomalies, common to the model profiles of all days, which require explanation:

i) The model layer retreat occurs too slowly and WML temperature is underpredicted in the mornings,

ii) Overheating of the WML occurs in early to mid-afternoon and subsequent WML deepening is impeded somewhat by the large resultant value of ΔT, and,

iii) The model underpredicts heating of the water at

medium depth below the WML in the hours around midday.

The dominant cause of both (i) and (ii) above is clearly the model's method of stability correction to meteorological fluxes. The problem was addressed in Section 3.5.2. Neglecting the precise details of the calculation procedure, the method effectively corrects the fluxes with the parameter Ri_B, where from eq. 2.43

$$Ri_B = \frac{gz}{T_V} \frac{(\Delta\theta + 0.61 T_V \Delta q)}{U^2}$$

The value of $\Delta\theta$ is evaluated by

$$\Delta\theta = T_{10} - T_S,$$

that is, the temperature at z_H is taken to be the WML temperature T_S. The correct value to use however is the temperature of the conductive sublayer at the surface, or the 'skin' temperature, which will deviate from T_S towards the air temperature. Hence, $|\Delta\theta|$ is always overestimated in the model. This leads to unrealistic enhancement of latent cooling in the morning ($\Delta\theta$ negative) and suppression of latent cooling in the early to mid-afternoon ($\Delta\theta$ positive), explaining the anomalies (i) and (ii). A similar effect on the momentum flux $\rho_o u_*^2$ enhances deepening (delays retreat) in the morning and inhibits deepening in the afternoon. Sensible heat flux is similarly affected but is small in magnitude compared with latent heat flux.

Model runs in which the stability correction was suppressed gave results which erred in the opposite sense, as expected. Having understood the problem it was decided to retain the stability correction method, as stability effects

over a medium sized reservoir are obviously important. Future work may involve modelling of the 'skin' temperature to provide the correct value for stability calculation.

In the case of (iii) above, there are two factors which may contribute to insufficient heating of gridpoints at a medium depth below the thermocline.

The form of the solar shortwave radiation attentuation profile given by eq. 3.1 may be somewhat in error. Tests of the model using different attenuation profiles indicated a marked sensitivity to the form chosen. A form which prescribes less attenuation near the surface and greater attenuation at depth would tend to correct the anomaly (iii) and also (ii). The form of eq. 3.1 will be retained, however, until more reliable field data for the Wellington Reservoir become available.

The feature of the model which is mainly responsible for (iii) (and to some extent, (ii)) however is the flux boundary condition at the base of the thermocline. In Section 5.3.1 the following are specified: $\overline{u'w'}(\xi-\delta) = \overline{\theta'w'}(\xi-\delta) = \overline{s'w'}(\xi-\delta) = 0$. In reality however, there will be leakage of these fluxes through the thermocline, especially when ΔT is small and diffuse.

Below the thermocline, residual turbulence, plus turbulence from other sources (thermocline leakage, internal wave breaking) will act to distribute the leaked heat downwards, so heating the water. The turbulence will also enhance diffusion of temperature and salinity where sharp gradients remain after WML retreat. No diffusion mechanism has been included in the model and so temperature structure below the WML retains its identity over a full daily cycle.

7.3.4 Conclusions

This Section has described various aspects of the model's performance which lead to observable differences between modelled and measured profiles. It is evident however that the model can simulate the essential mechanisms involved in the diurnal cycle on a quasi-continuous timescale (bearing in mind the smoothing of meteorological data). The results discussed in this Chapter lend strong support to the formulation of well mixed layer energetics developed in Chapter 5.

7.4 HEAT AND POTENTIAL ENERGY BUDGETS

In conclusion, an interesting observation on the sensitivity of heat and potential energy budget calculations is described below.

As stated in Section 4.1, temperature profiles were measured with, at best, an accuracy of $0.1^{o}C$, corresponding to the finest graduation on the thermometer used for calibration. If an hour by hour heat budget of the top seven metres of water is attempted, the uncertainty in the heat storage calculation associated with the above accuracy will be,

$$\Delta H = 7 \times \rho C_p \Delta T = 2930 \ kJm^{-2}$$

However, this uncertainty is of the same order of magnitude as the surface heat transfers for the period. For example, on the day 05 02 76 between 1430 and 1530 hours, the relatively large surface heat transfers were as follows:

$$H_{sensible} = -100 \ kJ \ m^{-2},$$

$$H_{latent} = 1096 \ kJ \ m^{-2},$$

$$H_{shortwave} = -2897 \ kJ \ m^{-2},$$

$H_{longwave} = 126 \text{ kJ m}^{-2}$.

Obviously on such a short timescale, no meaningful heat budget calculations are possible, as the measured temperature profiles are not sensitive enough to heat transfer. In particular it is not possible to estimate evaporation by this method.

The profiles plotted in Appendix A5 or Appendix D1 present another intriguing possibility however. Unlike the absolute temperature, the well mixed layer depth is very sensitive to the balance of surface heat transfers and its changes may be measured quite accurately. In other words, whereas heat budget calculations are impractical, it is possible to accurately estimate the potential energy increase of a water column associated with WML deepening. As confidence is gained in the values of universal coefficients (see Table 7.1), the model may be used in reverse to predict the surface heat transfers leading to an observed WML deepening pattern. Of particular interest is the steady state, free convection situation found on cold, calm nights. The deepening equation for this case (see eq. 5.51) may be rearranged to the form

$$H_S + H_L + Q_L = \frac{\rho_o C_p}{K_A} \left(\Delta T \frac{dh}{dt} \right) \qquad (7.1)$$

The longwave radiation Q_L may be calculated accurately and the product $\Delta T \, dh/dt$ may be computed from sequential measured profiles. Eq. 7.1 therefore provides a useful tool for appraising the various formulations of atmospheric turbulent heat transfer from a reservoir surface in free convection conditions.

CHAPTER 8

CONCLUSIONS

The numerical model of the diurnal cycle within the seasonal well mixed layer appears to be capable of simulating all of the important features of that cycle. A few features of lesser importance are not directly simulated, but their effects have been examined qualitatively. Important aspects of the Project in general and of the model's capability are outlined below.

The model simulates realistically the shallowing of a diurnal well mixed layer when solar heating is dominant and also the deepening of this layer when surface cooling and mixing become dominant. The success of the model lies in its formulation. Careful integration of the turbulent kinetic energy equation over the full well mixed layer depth ensures that all known contribution are included. Equations for heat, mass, momentum and salt concentration are similarly treated. The depth and temperature of the well mixed layer during strong solar heating is determined by the parameter q_*, which incorporates the effects of surface wind stirring, surface heating and cooling by all heat fluxes and, importantly, penetration of solar radiation below the surface. The parameterization schemes employed for surface energy transfers and internal shear production of energy are supported by the model's results. Also supported is the closure hypothesis which describes convergence of turbulent kinetic energy at the thermoclin leading to the final equation set of eqs. 5.39 to 5.48. Retaining

turbulent kinetic energy as a model variable results in a smooth model response to rapidly changing meteorological inputs. It also enhances interpretation of model behaviour. For example, layer retreat occurs only when the energy in the old layer has been completely consumed in overcoming the buoyancy induced by solar heating.

The model also realistically predicts the vertical temperature structure at particular times throughout a daily cycle. Predicted values of velocity and turbulent kinetic energy are also realistic, although no field measurements of these are available. The values of C_F, C_E and C_N from Table 7.1 may therefore be used with some confidence, especially considering the internal consistency of their determination. The shear production efficiency, C_S, has also been determined with some confidence as described in Section 7.3.1.

Averaged meteorological data used by the model are of high quality. As discussed in Section 7.3.3 however, using modelled or measured mean water temperature to compute a stability correction to atmospheric turbulent transfers will cause the correction to be overestimated. The correct temperature to use is that of the surface 'skin' or conductive sublayer. The problem is evidenced, in the model results, by morning over-cooling, afternoon over-heating and a time delay in the onset of either layer retreat or layer deepening. The problem should be addressed in future work.

Features of secondary importance are discussed in Chapter 7. The presence of Kelvin Helmholtz billows at the thermocline is clearly seen from field data (see Appendix D1). The model does not explicitly represent these however. Modification

of thermocline shear by reservoir end wall effects is represented i the model but has not been verified from field data. Leakage of heat, salt and momentum through the thermocline and diffusion of these below the thermocline are also evident from field data, but are not included in the model due to a lack of information on these processes.

The model equations and coefficients, now tested, may be directly incorporated into a model such as DYRESM which includes simulation of the seasonal structure. It will be profitable to continue to study the diurnal cycle, however, in order to improve some aspects of the model. Future work could involve:

i) obtaining finely resolved (e.g. 10 minute average) meteorological data over several daily cycles to allow more extensive model testing,

ii) measuring the solar radiation attenuation profile more accurately,

iii) obtaining a measure or estimate of 'skin' temperature for atmospheric stability calculation,

iv) measuring a velocity profile (if instrumentation with sufficient resolution becomes available) and so investigating the momentum budget,

v) investigating the atmospheric internal boundary layer in order to specify maximum heights for meteorological sensors,

vi) parameterizing thermocline leakage and hypolimnetic diffusion, and,

vii) improving the estimate of C_S.

REFERENCES

Badgley, F.I., Paulson, C.A. and Miyake, M. (1972) Profiles of wind, temperature and humidity over the Arabian Sea. East-West Centre Press, University of Hawaii.

Ball, F.K. (1960) Control of inversion height by surface heating. Quart. J. Roy. Meteorol. Soc., 86: 483-494.

Busch, N.E. (1973) On the mechanics of atmospheric turbulence. *In* Workshop on Micrometeorology (Ed. D.A. Haugen). American Meteorological Society.

Businger, J.A. (1973) Turbulent transfer in the atmospheric surface layer. *In* Workshop on Micrometeorology (Ed. D.A. Haugen). American Meteorological Society.

Carson, D.J. and Richards, P.J.R. (1978) Modelling surface turbulent fluxes in stable conditions. Bound.-Layer Meteorol., 14: 67-81.

Clarke, R.H., Dyer, A.J., Brook, R.R., Reid, D.G., and Troup, A.J. (1971) The Wangara experiment: boundary layer data. CSIRO Div. Meteorol. Phys., Melbourne, Australia. Tech. Paper No. 19.

Csanady, G.T. (1975) Hydrodynamics of large lakes. Ann. Review Fluid Mech., 7: 357-386.

Deardorff, J.W. (1968) Dependence of air-sea transfer coefficients on bulk stability. J. Geophys. Res., 73: 2549-2557.

Deardorff, J.W. (1970) Convective velocity and temperature scales for the unstable planetary boundary layer. J. Atmos. Sci., 27: 1211-1213.

Deardorff, J.W. (1974) Three-dimensional numerical study of the height and mean structure of a heated planetary boundary layer. Bound.-Layer Meteorol., 7: 81-106.

Denman, K.L. (1973) A time dependent model of the upper ocean. J. Phys. Oceanogr., 3: 173-184.

Dyer, A.J. (1974) A review of flux profile relationships. Bound.-Layer Meteorol., 7: 363-372.

Fischer, H.B., List, E.J., Koh, R.Y.C., Imberger, J. and Brooks, N.H. (1979) Mixing in inland and coastal waters. Academic Press: New York.

Francey, R.J. and Garratt, J.R. (1978) Eddy flux measurements over the ocean and related transfer coefficients. Bound.-Layer Meteorol., 14: 153-166.

Funk, J.P. (1959) Improved polythene-shielded net radiometer. J. Scientific Instr., 36: 267-270.

Garwood, R.W. (1977) An oceanic mixed layer model capable of simulating cyclic states. J. Phys. Oceanogr., 7: 455-468.

Hicks, B.B. (1972) Some evaluations of drag and bulk transfer coefficients over water bodies of different sizes. Bound.-Layer Meteorol., 3: 201-213.

Hicks, B.B. (1975) A procedure for the formulation of bulk transfer coefficients over water. Bound.-Layer Meteorol., 8: 515-524.

Hicks, B.B. (1976) Wind profile relationships from the 'Wangara' experiment. Quart. J. Roy. Meteorol. Soc., 102: 535-551.

Imberger, J. and Hebbert, R.H.B. (1980) Management of water quality in reservoirs. Australian Water Resources Council Technical Paper No. 49.

Irvine, W.M. and Pollack, J.B. (1968) Infrared optical properties of water and ice spheres. ICARUS, 8: 324-360.

Kaimal, J.C., Wyngaard, J.C., Haugen, D.A., Coté, O.R., Izumi, Y., Caughey, S.J., Readings, C.J. (1976) Turbulence structure in the convective boundary layer. J. Atmos. Sci., 33: 2152-2169.

Kato, H. and Phillips, O.M. (1969) On the penetration of a turbulent layer into stratified fluid. J. Fluid Mech., 37: 643-655.

Kraus, E.B. (1972) Atmosphere-ocean interaction. Clarendon Press. Oxford.

Kraus, E.B. and Turner, J.S. (1967) A one-dimensional model of the seasonal thermocline. Tellus, 19: 98-106.

Mahrt, L. and Lenschow, D.H. (1976) Growth dynamics of the convectively mixed layer. J. Atmos. Sci., 33: 41-51.

Mellor, G.L. and Durbin, P.A. (1975) The structure and dynamics of the ocean surface mixed layer. J. Phys. Oceanogr., 5: 718-728.

Monin, A.S. and Obukhov, A.M. (1954) Basic laws of turbulent mixing in the atmosphere near the ground. Jr., Akad. Nauk SSSR Geofiz. Inst., No. 24 (151): 163-187.

Monin, A.S. and Kolesnikova, V.N. (1968) The spectra of micrometeorological, synoptic and climatic oscillations of meteorological fields. Met. Issled., 16: 30-56.

Niiler, P.P. (1975) Deepening of the wind-mixed layer. J. Mar. Res., 33: 405-422.

Niiler, P.P. and Kraus, E.B. (1977) One-dimensional models of the upper ocean. *In* Modelling and Prediction of the Upper Layers of the Ocean (Ed. E.B. Kraus). Permagon Press, N.Y.

Paulson, C.A. (1970) The mathematical representation of wind speed and temperature profiles in the unstable atmospheric surface layer. J. Appl. Meteorol., 9: 857-861.

Peterson, E.W. (1969) Modification of mean flow and turbulent energy by a change in surface roughness under conditions of neutral stability. Quart. J. Roy. Meteorol. Soc., 95: 561-575.

Pollard, R.T., Rhines, P.B. and Thompson, R.O.R.Y. (1973) The deepening of the wind-mixed layer. Geophys. Fluid Dyn., 3: 381-404.

Pond, S., Fissel, D.B. and Paulson, C.A. (1974) A note on bulk aerodynamic coefficients for sensible heat and moisture fluxes. Bound.-Layer Meteorol., 6: 333-339.

Sherman, F.S., Imberger, J. and Corcos, G.M. (1978) Turbulence and mixing in stably stratified waters. Ann. Rev. Fluid Mech., 10: 267-288.

Spencer, J.W. (1976) Perth solar tables. CSIRO Div. Building Res. Technical Paper (second series) No. 10.

Spigel, R.H. (1978) Wind mixing in lakes. Ph.D. Thesis, Univ. California, Berkeley, California.

Spigel, R.H. and Imberger, J. (1979) The classification of mixed layer dynamics in lakes of small to medium size. J. Phys. Oceanogr. (in press).

Stull, R.B. (1976) The energetics of entrainment across a density interface. J. Atmos. Sci., 33: 1260-1267.

Swinbank, W.C. (1963) Longwave radiation from clear skies. Quart. J. Roy. Meteorol. Soc., 89: 339-348.

Taylor, P.A. (1970) A model of air flow above changes in surface heat flux, temperature and roughness for neutral and unstable conditions. Bound.-Layer Meteorol., 1: 18-39.

Tennekes, H. (1973) A model for the dynamics of the inversion above a convective boundary layer. J. Atmos. Sci., 30: 558-567.

Thompson, R.O.R.Y. (1974) Predicting the characteristics of the well mixed layer. Woods Hole Oceanographic Institution Tech. Report WHOI-74-82.

TVA (1972) Heat and mass transfer between a water surface and the atmosphere. Div. Water Resources Research Laboratory Report No. 14, Tennessee Valley Authority.

Weisman, K.N. (1975) A developing boundary layer over an evaporating surface. Bound.-Layer Meteorol., 8: 437-445.

Wigley, T.M.L. (1974) *Reply to* A simple but accurate formula for the saturation vapour pressure over liquid water. (S. Tabata). J. Appl. Meteorol., 12: 608.

Willis, G.E. and Deardorff, J.W. (1974) A laboratory model of the unstable planetary boundary layer. J. Atmos. Sci., 31: 1297-1307.

Wu, J. (1973) Wind-induced turbulent entrainment across a stable density interface. J. Fluid Mech., 61: 275-287.

Wyngaard, J.C. (1973) On surface layer turbulence. *In* Workshop on Micrometeorology (Ed. D.A. Haugen). American Meteorological Society.

Zeman, O. and Tennekes, H. (1977) Parameterization of the turbulent energy budget at the top of the daytime atmospheric boundary layer. J. Atmos. Sci., 34: 111-123.

APPENDIX A: FIELD DATA

DATE 150176 SERIES 1

RUN 3 DAY 1 TIME PERIOD 830 TO 930

M.M. O/P (MV)	42.0	55.3	59.8	59.8
SPOT READINGS	44.1	56.3	59.0	62.2

	AT(C)	WT(C)	RH(%)	NR(MW/SQCM)
M.M. AVERAGES	20.6	23.7	59.8	62.4
CURRENT SPOT READ.	21.4	24.1	59.0	69.7
PREVIOUS SPOT READ.	18.6	23.5	62.0	49.5

SPEED(M/S)	E.R.ANEM(M/S)	PYR(MW/SQCM)	KIPP(MW/SQCM)
.0	1.4	88.8	

RUN 4 DAY 1 TIME PERIOD 930 TO 1030

M.M. O/P (MV)	46.2	55.9	56.5	62.5
SPOT READINGS	49.9	57.7	56.0	66.5

	AT(C)	WT(C)	RH(%)	NR(MW/SQCM)
M.M. AVERAGES	22.3	24.0	56.5	70.5
CURRENT SPOT READ.	23.7	24.6	56.0	82.7
PREVIOUS SPOT READ.	21.4	24.1	59.0	69.7

SPEED(M/S)	E.R.ANEM(M/S)	PYR(MW/SQCM)	KIPP(MW/SQCM)
.0	1.6	68.8	

RUN 5 DAY 1 TIME PERIOD 1030 TO 1130

M.M. O/P (MV)	51.9	58.2	51.1	67.6
SPOT READINGS	56.2	60.4	49.0	69.1

	AT(C)	WT(C)	RH(%)	NR(MW/SQCM)
M.M. AVERAGES	24.5	24.8	51.1	85.9
CURRENT SPOT READ.	26.2	25.6	49.0	90.5
PREVIOUS SPOT READ.	23.7	24.6	56.0	82.7

SPEED(M/S)	E.R.ANEM(M/S)	PYR(MW/SQCM)	KIPP(MW/SQCM)
.0	1.6	88.8	

RUN 6 DAY 1 TIME PERIOD 1130 TO 1333

M.M. O/P (MV)	59.7	61.7	39.2	0.0
SPOT READINGS	64.7	65.0	39.0	68.6

	AT(C)	WT(C)	RH(%)	NR(MW/SQCM)
M.M. AVERAGES	27.6	26.1	39.2	0.0
CURRENT SPOT READ.	29.5	27.3	39.0	89.3
PREVIOUS SPOT READ.	26.2	25.6	49.0	90.5

SPEED(M/S)	E.R.ANEM(M/S)	PYR(MW/SQCM)	KIPP(MW/SQCM)
.0	1.5	108.3	

RUN 7 DAY 1 TIME PERIOD 1333 TO 1430

M.M. O/P (MV)	64.3	61.8	35.6	64.7
SPOT READINGS	66.9	62.5	38.0	66.7

	AT(C)	WT(C)	RH(%)	NR(MW/SQCM)
M.M. AVERAGES	29.4	26.1	35.6	77.4
CURRENT SPOT READ.	30.4	26.4	38.0	83.6
PREVIOUS SPOT READ.	29.5	27.3	39.0	89.3

SPEED(M/S)	E.R.ANEM(M/S)	PYR(MW/SQCM)	KIPP(MW/SQCM)
.0	2.5	93.5	

RUN 8 DAY 1 TIME PERIOD 1430 TO 1530

M.M. O/P (MV)	67.4	62.2	33.3	64.6
SPOT READINGS	67.7	61.9	35.0	62.6

	AT(C)	WT(C)	RH(%)	NR(MW/SQCM)
M.M. AVERAGES	30.6	26.3	33.3	77.3
CURRENT SPOT READ.	30.7	26.2	35.0	71.2
PREVIOUS SPOT READ.	30.4	26.4	38.0	83.6

SPEED(M/S)	E.R.ANEM(M/S)	PYR(MW/SQCM)	KIPP(MW/SQCM)

RUN 9 DAY 1 TIME PERIOD 1530 TO 1645

M.M. O/P (MV)	66.5	60.3	37.3	59.0
SPOT READINGS	66.0	59.4	37.0	55.0

	AT(C)	WT(C)	RH(%)	NR(MW/SQCM)
M.M. AVERAGES	30.2	25.6	37.3	60.2
CURRENT SPOT READ.	30.0	25.2	37.0	48.3
PREVIOUS SPOT READ.	30.7	26.2	35.0	71.2

SPEED(M/S)	E.R.ANEM(M/S)	PYR(MW/SQCM)	KIPP(MW/SQCM)
.0	5.7	23.7	

RUN 10 DAY 1 TIME PERIOD 1645 TO 1730

M.M. O/P (MV)	65.1	58.5	39.7	52.5
SPOT READINGS	63.5	58.4	44.0	49.7

	AT(C)	WT(C)	RH(%)	NR(MW/SQCM)
M.M. AVERAGES	29.7	24.9	39.7	40.8
CURRENT SPOT READ.	29.1	24.9	44.0	32.3
PREVIOUS SPOT READ.	30.0	25.2	37.0	48.3

RUN 11 DAY 1 TIME PERIOD 1730 TO 20 0

M.M. O/P (MV)	59.9	57.2	48.2	40.7
SPOT READINGS	54.4	56.8	54.0	36.8

	AT(C)	WT(C)	RH(%)	NR(MW/SQCM)
M.M. AVERAGES	27.7	24.4	48.2	5.2
CURRENT SPOT READ.	25.5	24.3	54.0	-6.6
PREVIOUS SPOT READ.	29.1	24.9	44.0	32.3

SPEED(M/S)	E.R.ANEM(M/S)	PYR(MW/SQCM)	KIPP(MW/SQCM)
.0	5.9	5.9	

RUN 12 DAY 1 TIME PERIOD 20 0 TO 2225

M.M. O/P (MV)	47.4	56.6	59.8	36.2
SPOT READINGS	41.5	36.2	70.0	36.3

	AT(C)	WT(C)	RH(%)	NR(MW/SQCM)
M.M. AVERAGES	22.7	24.2	59.8	-8.5
CURRENT SPOT READ.	20.4	24.1	70.0	-8.1
PREVIOUS SPOT READ.	25.5	24.3	54.0	-6.6

SPEED(M/S)	E.R.ANEM(M/S)	PYR(MW/SQCM)	KIPP(MW/SQCM)
.0	6.2	0.0	

DATE 30276 SERIES 1

RUN 3 DAY 1 TIME PERIOD 931 TO 1030

M.M. O/P (MV)	53.4	58.8	42.5	63.1
SPOT READINGS	56.6	61.2	40.0	66.3

	AT(C)	WT(C)	RH(%)	NR(MW/SQCM)
M.M. AVERAGES	25.1	24.9	42.5	70.4
CURRENT SPOT READ.	26.4	25.9	40.0	80.2
PREVIOUS SPOT READ.	24.6	24.9	44.0	67.6

SPEED(M/S)	E.R.ANEM(M/S)	PYR(MW/SQCM)	KIPP(MW/SQCM)
1.1		60.2	

RUN 4 DAY 1 TIME PERIOD 1030 TO 1130

M.M. O/P (MV)	58.5	61.9	41.3	56.0
SPOT READINGS	61.3	63.0	43.0	68.5

	AT(C)	WT(C)	RH(%)	NR(MW/SQCM)
M.M. AVERAGES	27.1	26.1	41.3	49.3
CURRENT SPOT READ.	28.2	26.5	43.0	87.2
PREVIOUS SPOT READ.	26.4	25.9	40.0	80.2

SPEED(M/S)	E.R.ANEM(M/S)	PYR(MW/SQCM)	KIPP(MW/SQCM)

RUN 5 DAY 1 TIME PERIOD 1130 TO 1230

M.M. O/P (MV)	0.0	64.0	41.2	69.0
SPOT READINGS	66.3	65.2	29.0	70.3

	AT(C)	WT(C)	RH(%)	NR(MW/SQCM)
M.M. AVERAGES	0.0	26.9	41.2	88.7
CURRENT SPOT READ.	30.2	27.4	29.0	92.6
PREVIOUS SPOT READ.	28.2	26.5	43.0	87.2

SPEED(M/S)	E.R.ANEM(M/S)	PYR(MW/SQCM)	KIPP(MW/SQCM)
2.1	.4	0.0	

RUN 6 DAY 1 TIME PERIOD 1230 TO 1330

M.M. O/P (MV)	66.0	66.2	33.6	70.0
SPOT READINGS	71.3	68.2	23.0	69.1

	AT(C)	WT(C)	RH(%)	NR(MW/SQCM)
M.M. AVERAGES	30.1	27.7	33.6	91.6
CURRENT SPOT READ.	32.1	28.5	23.0	89.0
PREVIOUS SPOT READ.	30.2	27.4	29.0	92.6

RUN 7 DAY 1 TIME PERIOD 1330 TO 1430

M.M. O/P (MV)	73.9	69.4	26.4	68.1
SPOT READINGS	72.3	69.0	23.0	67.8

	AT(C)	WT(C)	RH(%)	NR(MW/SQCM)
M.M. AVERAGES	33.2	29.0	26.4	86.3
CURRENT SPOT READ.	32.5	28.8	23.0	85.4
PREVIOUS SPOT READ.	32.1	28.5	23.0	89.0

SPEED(M/S)	E.R.ANEM(M/S)	PYR(MW/SQCM)	KIPP(MW/SQCM)
1.2	.6	222.0	

RUN 8 DAY 1 TIME PERIOD 1430 TO 1531

M.M. O/P (MV)	75.1	68.2	22.0	54.4
SPOT READINGS	75.7	70.2	23.0	65.0

	AT(C)	WT(C)	RH(%)	NR(MW/SQCM)
M.M. AVERAGES	33.6	28.5	22.0	45.5
CURRENT SPOT READ.	33.9	29.3	23.0	77.8
PREVIOUS SPOT READ.	32.5	28.8	23.0	85.4

SPEED(M/S)	E.R.ANEM(M/S)	PYR(MW/SQCM)	KIPP(MW/SQCM)
1.4	.4	116.5	

RUN 9 DAY 1 TIME PERIOD 1531 TO 1630

M.M. O/P (MV)	72.3	68.5	32.7	29.6
SPOT READINGS	74.3	67.9	22.0	57.6

	AT(C)	WT(C)	RH(%)	NR(MW/SQCM)
M.M. AVERAGES	32.7	28.6	32.7	-29.3
CURRENT SPOT READ.	33.3	28.4	22.0	54.9
PREVIOUS SPOT READ.	33.9	29.3	23.0	77.8

SPEED(M/S)	E.R.ANEM(M/S)	PYR(MW/SQCM)	KIPP(MW/SQCM)
1.2	.4	0.0	

RUN 10 DAY 1 TIME PERIOD 1630 TO 1730

M.M. O/P (MV)	75.8	67.6	26.9	53.6
SPOT READINGS	74.9	64.9	26.0	49.4

	AT(C)	WT(C)	RH(%)	NR(MW/SQCM)
M.M. AVERAGES	33.9	28.3	26.9	42.8
CURRENT SPOT READ.	33.6	27.3	26.0	30.2
PREVIOUS SPOT READ.	33.3	28.4	22.0	54.9

SPEED(M/S)	E.R.ANEM(M/S)	PYR(MW/SQCM)	KIPP(MW/SQCM)
2.4	.4	0.0	

RUN 11 DAY 1 TIME PERIOD 1730 TO 18 5

M.M. O/P (MV)	74.8	65.8	26.2	47.2
SPOT READINGS	72.3	66.0	30.0	43.8

	AT(C)	WT(C)	RH(%)	NR(MW/SQCM)
M.M. AVERAGES	33.5	27.6	26.2	23.4
CURRENT SPOT READ.	32.5	27.7	30.0	13.0
PREVIOUS SPOT READ.	33.6	27.3	26.0	30.2

SPEED(M/S)	E.R.ANEM(M/S)	PYR(MW/SQCM)	KIPP(MW/SQCM)
3.2	.4	0.0	

RUN 12 DAY 1 TIME PERIOD 18 5 TO 1940

M.M. O/P (MV)	70.8	65.2	31.6	39.3
SPOT READINGS	66.0	63.5	36.0	37.1

	AT(C)	WT(C)	RH(%)	NR(MW/SQCM)
M.M. AVERAGES	31.9	27.4	31.6	-.5
CURRENT SPOT READ.	30.1	26.7	36.0	-7.2
PREVIOUS SPOT READ.	32.5	27.7	30.0	13.0

SPEED(M/S)	E.R.ANEM(M/S)	PYR(MW/SQCM)	KIPP(MW/SQCM)

RUN 13 DAY 1 TIME PERIOD 1940 TO 2010

M.M. O/P (MV)	65.[illegible]	63.3	33.6	35.5
SPOT READINGS	64.2	63.4	36.0	37.2

	AT(C)	WT(C)	RH(%)	NR(MW/SQCM)
M.M. AVERAGES	29.9	26.7	33.6	-12.2
CURRENT SPOT READ.	29.3	26.7	36.0	-6.9
PREVIOUS SPOT READ.	30.1	26.7	36.0	-7.2

SPEED(M/S)	E.R.ANEM(M/S)	PYR(MW/SQCM)	KIPP(MW/SQCM)
4.3	.4	0.0	

DATE 50276 SERIES 2

RUN 3 DAY 1 TIME PERIOD 7 5 TO 8 0

M.M. O/P (MV)	26.6	57.3	65.5	45.8
SPOT READINGS	29.5	57.5	60.0	50.7

	AT(C)	WT(C)	RH(%)	NR(MW/SQCM)
M.M. AVERAGES	18.1	24.3	65.5	18.5
CURRENT SPOT READ.	19.3	24.4	60.0	33.8
PREVIOUS SPOT READ.	17.3	24.4	65.0	13.0

SPEED(M/S)	E.R.ANEM(M/S)	PYR(MW/SQCM)	KIPP(MW/SQCM)
3.0	2.9	32.3	

RUN 4 DAY 1 TIME PERIOD 8 0 TO 9 0

M.M. O/P (MV)	32.0	57.7	55.3	0.0
SPOT READINGS	35.7	57.9	50.0	58.3

	AT(C)	WT(C)	RH(%)	NR(MW/SQCM)
M.M. AVERAGES	20.3	24.5	55.3	0.0
CURRENT SPOT READ.	21.9	24.6	50.0	57.0
PREVIOUS SPOT READ.	19.3	24.4	60.0	33.8

SPEED(M/S)	E.R.ANEM(M/S)	PYR(MW/SQCM)	KIPP(MW/SQCM)
2.2	2.4	44.4	

RUN 5 DAY 1 TIME PERIOD 9 0 TO 10 0

M.M. O/P (MV)	0.0	0.0	0.0	0.0
SPOT READINGS	41.5	58.6	43.0	64.4

	AT(C)	WT(C)	RH(%)	NR(MW/SQCM)
M.M. AVERAGES	0.0	0.0	0.0	0.0
CURRENT SPOT READ.	24.3	24.8	43.0	75.4
PREVIOUS SPOT READ.	21.9	24.6	50.0	57.0

SPEED(M/S)	E.R.ANEM(M/S)	PYR(MW/SQCM)	KIPP(MW/SQCM)
3.5	3.7	88.8	

RUN 6 DAY 1 TIME PERIOD 10 0 TO 11 0

M.M. O/P (MV)	44.2	59.3	41.6	59.4
SPOT READINGS	46.2	61.5	39.0	67.4

	AT(C)	WT(C)	RH(%)	NR(MW/SQCM)
M.M. AVERAGES	25.4	25.1	41.6	60.5
CURRENT SPOT READ.	26.2	25.9	39.0	84.8
PREVIOUS SPOT READ.	24.3	24.8	43.0	75.4

SPEED(M/S)	E.R.ANEM(M/S)	PYR(MW/SQCM)	KIPP(MW/SQCM)
1.6	1.6	93.7	

RUN 7 DAY 1 TIME PERIOD 11 0 TO 12 0

M.M. O/P (MV)	47.8	62.6	40.2	58.1
SPOT READINGS	50.6	64.1	35.0	69.3

	AT(C)	WT(C)	RH(%)	NR(MW/SQCM)
M.M. AVERAGES	26.9	26.3	40.2	56.9
CURRENT SPOT READ.	28.0	26.9	35.0	90.9
PREVIOUS SPOT READ.	26.2	25.9	39.0	84.8

SPEED(M/S)	E.R.ANEM(M/S)	PYR(MW/SQCM)	KIPP(MW/SQCM)
1.4	1.6	93.7	

RUN 8 DAY 1 TIME PERIOD 12 0 TO 13 0

M.M. O/P (MV)	50.5	62.9	34.6	68.4
SPOT READINGS	55.6	64.7	27.8	69.2

	AT(C)	WT(C)	RH(%)	NR(MW/SQCM)
M.M. AVERAGES	28.0	26.4	34.6	88.6
CURRENT SPOT READ.	30.0	27.1	27.8	91.4
PREVIOUS SPOT READ.	28.0	26.9	35.0	90.8

RUN 9 DAY 1 TIME PERIOD 13 0 TO 14 0

M.M. O/P (MV)	58.7	67.6	25.7	69.6
SPOT READINGS	59.8	66.3	20.2	67.0

	AT(C)	WT(C)	RH(%)	NR(MW/SQCM)
M.M. AVERAGES	31.2	28.2	25.7	92.6
CURRENT SPOT READ.	31.6	27.7	20.2	84.8
PREVIOUS SPOT READ.	30.0	27.1	27.8	91.4

SPEED(M/S)	E.R.ANEM(M/S)	PYR(MW/SQCM)	KIPP(MW/SQCM)
1.6	1.9	103.6	

RUN 10 DAY 1 TIME PERIOD 14 0 TO 1510

M.M. O/P (MV)	59.5	66.6	22.8	51.2
SPOT READINGS	58.2	64.8	29.0	62.7

	AT(C)	WT(C)	RH(%)	NR(MW/SQCM)
M.M. AVERAGES	31.5	27.8	22.8	36.8
CURRENT SPOT READ.	31.0	27.1	29.0	70.9
PREVIOUS SPOT READ.	31.6	27.7	20.2	84.8

RUN 11 DAY 1 TIME PERIOD 1510 TO 16 0

M.M. O/P (MV)	58.2	63.9	24.4	59.5
SPOT READINGS	58.0	62.4	20.0	58.1

	AT(C)	WT(C)	RH(%)	NR(MW/SQCM)
M.M. AVERAGES	31.0	26.8	24.4	61.2
CURRENT SPOT READ.	30.9	26.2	20.0	57.0
PREVIOUS SPOT READ.	31.0	27.1	29.0	70.9

SPEED(M/S)	E.R.ANEM(M/S)	PYR(MW/SQCM)	KIPP(MW/SQCM)
5.9	6.2	71.0	

RUN 12 DAY 1 TIME PERIOD 16 0 TO 17 0

M.M. O/P (MV)	56.5	61.1	23.9	54.2
SPOT READINGS	57.5	62.1	20.7	50.9

	AT(C)	WT(C)	RH(%)	NR(MW/SQCM)
M.M. AVERAGES	30.3	25.8	23.9	45.3
CURRENT SPOT READ.	30.7	26.1	20.7	35.3
PREVIOUS SPOT READ.	30.9	26.2	20.0	57.0

SPEED(M/S)	E.R.ANEM(M/S)	PYR(MW/SQCM)	KIPP(MW/SQCM)
5.2	5.5	59.2	

RUN 13 DAY 1 TIME PERIOD 17 0 TO 18 0

M.M. O/P (MV)	55.8	61.9	26.7	47.4
SPOT READINGS	53.5	61.8	29.0	42.9

	AT(C)	WT(C)	RH(%)	NR(MW/SQCM)
M.M. AVERAGES	30.1	26.0	26.7	24.5
CURRENT SPOT READ.	29.1	26.0	29.0	10.9
PREVIOUS SPOT READ.	30.7	26.1	20.7	35.3

SPEED(M/S)	E.R.ANEM(M/S)	PYR(MW/SQCM)	KIPP(MW/SQCM)
4.2	4.2	14.8	

RUN 14 DAY 1 TIME PERIOD 18 0 TO 20 0

M.M. O/P (MV)	49.3	61.9	40.7	39.4
SPOT READINGS	41.6	61.2	51.5	36.2

	AT(C)	WT(C)	RH(%)	NR(MW/SQCM)
M.M. AVERAGES	27.5	26.0	40.7	.2
CURRENT SPOT READ.	24.3	25.8	51.5	-9.4
PREVIOUS SPOT READ.	29.1	26.0	29.0	10.9

SPEED(M/S)	E.R.ANEM(M/S)	PYR(MW/SQCM)	KIPP(MW/SQCM)
2.2	2.4	0.0	

RUN 15 DAY 1 TIME PERIOD 20 0 TO 23 0

M.M. O/P (MV)	39.2	60.8	53.3	36.5
SPOT READINGS	35.3	60.3	52.0	36.0

	AT(C)	WT(C)	RH(%)	NR(MW/SQCM)
M.M. AVERAGES	23.3	25.6	53.3	-8.6
CURRENT SPOT READ.	21.7	25.4	52.0	-10.3
PREVIOUS SPOT READ.	24.3	25.8	51.5	-9.4

SPEED(M/S)	E.R.ANEM(M/S)	PYR(MW/SQCM)	KIPP(MW/SQCM)
2.9	2.8	0.0	

DATE 50476 SERIES 5

RUN 2 DAY 1 TIME PERIOD 830 TO 945

M.M. O/P (MV)	9.9	47.7	69.5	50.9
SPOT READINGS	17.9	48.4	70.0	54.5

	AT(C)	WT(C)	RH(%)	NR(MW/SQCM)
M.M. AVERAGES	14.5	21.3	69.5	33.8
CURRENT SPOT READ.	16.1	21.3	70.0	44.3
PREVIOUS SPOT READ.	14.0	21.2	71.0	21.7

SPEED(M/S)	E.R.ANEM(M/S)	PYR(MW/SQCM)	KIPP(MW/SQCM)
3.4	3.6	47.4	61.6

RUN 3 DAY 1 TIME PERIOD 945 TO 11 7

M.M. O/P (MV)	23.8	48.8	62.2	57.3
SPOT READINGS	31.0	49.4	57.0	59.2

	AT(C)	WT(C)	RH(%)	NR(MW/SQCM)
M.M. AVERAGES	17.3	21.4	62.2	53.1
CURRENT SPOT READ.	18.8	21.5	57.0	58.8
PREVIOUS SPOT READ.	16.1	21.3	70.0	44.3

SPEED(M/S)	E.R.ANEM(M/S)	PYR(MW/SQCM)	KIPP(MW/SQCM)
4.2	4.3	65.0	75.5

RUN 4 DAY 1 TIME PERIOD 11 7 TO 1235

M.M. O/P (MV)	34.5	47.4	55.6	58.4
SPOT READINGS	40.9	51.5	50.0	58.8

	AT(C)	WT(C)	RH(%)	NR(MW/SQCM)
M.M. AVERAGES	19.5	21.2	55.6	56.3
CURRENT SPOT READ.	20.7	21.8	50.0	57.6
PREVIOUS SPOT READ.	18.8	21.5	57.0	58.8

SPEED(M/S)	E.R.ANEM(M/S)	PYR(MW/SQCM)	KIPP(MW/SQCM)
3.9	4.0	70.6	68.1

RUN 5 DAY 1 TIME PERIOD 1235 TO 1430

M.M. O/P (MV)	45.6	48.6	48.8	54.9
SPOT READINGS	34.7	53.1	43.0	52.7

	AT(C)	WT(C)	RH(%)	NR(MW/SQCM)
M.M. AVERAGES	21.7	21.4	48.8	46.0
CURRENT SPOT READ.	19.5	22.0	43.0	39.5
PREVIOUS SPOT READ.	20.7	21.8	50.0	57.6

SPEED(M/S)	E.R.ANEM(M/S)	PYR(MW/SQCM)	KIPP(MW/SQCM)
2.4	2.5	54.1	56.6

RUN 6 DAY 1 TIME PERIOD 1430 TO 1530

M.M. O/P (MV)	50.9	0.0	43.7	0.0
SPOT READINGS	54.0	52.7	45.0	49.6

	AT(C)	WT(C)	RH(%)	NR(MW/SQCM)
M.M. AVERAGES	22.8	0.0	43.7	0.0
CURRENT SPOT READ.	23.4	21.9	45.0	30.2
PREVIOUS SPOT READ.	19.5	22.0	43.0	39.5

SPEED(M/S)	E.R.ANEM(M/S)	PYR(MW/SQCM)	KIPP(MW/SQCM)
2.5	2.7	29.6	42.7

RUN 7 DAY 1 TIME PERIOD 1530 TO 1631

M.M. O/P (MV)	54.6	51.8	43.2	45.1
SPOT READINGS	55.5	52.3	46.0	42.8

	AT(C)	WT(C)	RH(%)	NR(MW/SQCM)
M.M. AVERAGES	23.5	21.8	43.2	16.7
CURRENT SPOT READ.	23.7	21.9	46.0	9.7
PREVIOUS SPOT READ.	23.4	21.9	45.0	30.2

RUN 8 DAY 1 TIME PERIOD 1631 TO 1835

M.M. O/P (MV)	45.9	51.3	55.1	37.9
SPOT READINGS	28.5	50.2	73.0	36.4

	AT(C)	WT(C)	RH(%)	NR(MW/SQCM)
M.M. AVERAGES	21.8	21.7	55.1	-5.1
CURRENT SPOT READ.	18.2	21.6	73.0	-9.7
PREVIOUS SPOT READ.	23.7	21.9	46.0	9.7

SPEED(M/S)	E.R.ANEM(M/S)	PYR(MW/SQCM)	KIPP(MW/SQCM)
2.0	2.0	7.2	0.0

RUN 9 DAY 1 TIME PERIOD 1835 TO 20 0

M.M. O/P (MV)	24.1	49.1	71.8	36.1
SPOT READINGS	17.4	49.4	78.0	36.0

	AT(C)	WT(C)	RH(%)	NR(MW/SQCM)
M.M. AVERAGES	17.4	21.4	71.8	-10.6
CURRENT SPOT READ.	16.0	21.5	78.0	-10.9
PREVIOUS SPOT READ.	18.2	21.6	73.0	-9.7

RUN 10 DAY 1 TIME PERIOD 20 0 TO 2130

M.M. O/P (MV)	15.2	48.4	77.8	35.2
SPOT READINGS	13.2	49.1	79.0	35.8

	AT(C)	WT(C)	RH(%)	NR(MW/SQCM)
M.M. AVERAGES	15.6	21.3	77.8	-13.4
CURRENT SPOT READ.	15.2	21.4	79.0	-11.5
PREVIOUS SPOT READ.	16.0	21.5	78.0	-10.9

SPEED(M/S)	E.R.ANEM(M/S)	PYR(MW/SQCM)	KIPP(MW/SQCM)
1.6	1.6	0.0	0.0

RUN 11 DAY 1 TIME PERIOD 2130 TO 23 5

M.M. O/P (MV)	12.8	47.7	78.3	34.8
SPOT READINGS	13.9	50.0	81.0	36.2

	AT(C)	WT(C)	RH(%)	NR(MW/SQCM)
M.M. AVERAGES	15.1	21.3	78.3	-14.2
CURRENT SPOT READ.	15.3	21.6	81.0	-9.7
PREVIOUS SPOT READ.	15.2	21.4	79.0	-11.5

SPEED(M/S)	E.R.ANEM(M/S)	PYR(MW/SQCM)	KIPP(MW/SQCM)
3.0	2.6	0.0	0.0

RUN 12 DAY 1 TIME PERIOD 23 5 TO 125

M.M. O/P (MV)	0.0	0.0	0.0	0.0
SPOT READINGS	18.2	47.7	62.0	35.4

	AT(C)	WT(C)	RH(%)	NR(MW/SQCM)
M.M. AVERAGES	0.0	0.0	0.0	0.0
CURRENT SPOT READ.	16.2	21.3	62.0	-12.1
PREVIOUS SPOT READ.	15.3	21.6	81.0	-9.7

SPEED(M/S)	E.R.ANEM(M/S)	PYR(MW/SQCM)	KIPP(MW/SQCM)
3.6	3.5	0.0	0.0

RUN 13 DAY 2 TIME PERIOD 125 TO 3 0

M.M. O/P (MV)	0.0	0.0	0.0	0.0
SPOT READINGS	10.9	47.6	76.0	35.7

	AT(C)	WT(C)	RH(%)	NR(MW/SQCM)
M.M. AVERAGES	0.0	0.0	0.0	0.0
CURRENT SPOT READ.	14.7	21.2	76.0	-11.2
PREVIOUS SPOT READ.	16.2	21.3	62.0	-12.1

SPEED(M/S)	E.R.ANEM(M/S)	PYR(MW/SQCM)	KIPP(MW/SQCM)
2.6	2.5	0.0	0.0

Time	Speed (m/s)	A.Temp (°C)	W.Temp (°C)	R.H. (%)	N.Rad (mW/sq cm)
150176					
32					
8 0	1.50	18.00	23.40	63.00	36.00
830	1.50	19.30	23.50	61.50	49.50
9 0	1.50	20.60	23.70	61.00	60.00
930	1.50	21.50	23.85	58.30	69.50
10 0	1.50	22.50	24.05	57.00	76.50
1030	1.50	23.60	24.35	54.50	82.50
11 0	1.50	24.70	24.75	51.30	87.00
1130	1.50	25.70	25.50	46.00	90.50
12 0	1.50	26.70	26.05	41.00	92.00
1230	1.50	27.50	26.20	39.00	93.00
13 0	1.50	28.30	26.25	38.00	92.00
1330	1.50	29.00	26.30	36.60	89.00
14 0	3.30	29.80	26.32	35.50	86.50
1430	2.20	30.40	26.33	34.90	83.50
15 0	2.30	30.70	26.30	34.50	77.00
1530	3.90	30.50	26.24	35.00	71.00
1545	6.00	30.40	26.00	36.00	67.00
16 0	6.00	30.25	25.80	36.50	63.00
1630	6.00	30.00	25.36	38.20	52.00
17 0	4.80	29.75	24.95	39.80	42.00
1730	5.70	29.40	24.66	42.40	32.00
18 0	5.75	28.80	24.52	45.00	20.00
1830	5.84	28.20	24.41	47.50	8.00
19 0	5.90	27.50	24.35	50.00	-2.50
1930	5.99	26.40	24.31	52.20	-6.00
20 0	6.10	25.50	24.28	54.40	-7.50
2030	6.14	24.40	24.26	56.60	-8.00
21 0	6.20	23.30	24.24	59.00	-8.50
2130	6.26	22.20	24.30	61.50	-8.50
22 0	6.35	21.20	24.18	63.50	-8.50
2230	6.30	20.10	24.14	65.30	-8.50
23 0	6.24	19.10	24.00	67.50	-8.50

Time	Speed (m/s)	A.Temp (°C)	W.Temp (°C)	R.H. (%)	N.Rad (mW/sq cm)
030276					
25					
9 0	.80	24.00	24.40	44.00	53.00
930	.80	24.70	24.90	42.50	67.00
10 0	1.10	25.10	25.35	42.50	75.00
1030	1.50	26.20	25.90	42.50	81.00
11 0	1.80	27.10	26.10	42.00	20.00
1130	2.10	28.20	26.50	41.50	87.00
12 0	2.10	29.30	26.85	40.80	91.00
1230	2.10	30.30	27.30	38.80	93.00
13 0	1.65	31.30	27.65	34.00	91.00
1330	1.30	32.40	28.50	29.50	90.00
14 0	1.10	33.30	29.20	26.00	85.00
1430	1.20	34.00	28.80	23.00	85.00
15 0	1.50	33.60	28.00	20.00	10.00
1530	1.30	33.00	26.80	30.00	78.00
16 0	1.20	32.30	28.80	35.00	63.00
1630	1.60	33.30	28.35	30.00	56.00
17 0	2.40	34.20	28.00	27.00	44.00
1730	3.00	33.90	27.80	26.00	31.00
18 0	4.00	32.90	27.60	29.00	17.00
1815	5.00	32.60	27.50	30.05	9.00
1830	5.00	32.30	27.40	31.50	3.00
19 0	5.00	31.60	27.20	32.00	-2.00
1930	5.00	31.00	27.00	32.60	-4.50
20 0	4.30	30.10	26.80	33.00	-6.00
2030	3.60	29.20	26.60	34.00	-6.00

Time	Speed (m/s)	A.Temp (°C)	W.Temp (°C)	R.H. (%)	N.Rad (mW/sq cm)
050276					
41					
630	2.30	16.80	24.30	70.00	0.00
7 0	2.80	17.30	24.30	68.00	11.00
730	3.00	18.40	24.30	64.50	23.00
8 0	3.20	19.40	24.35	60.00	35.00
830	1.80	20.80	24.40	55.00	47.00
9 0	2.20	22.00	24.50	50.00	58.00
915	4.50	22.65	24.53	48.50	63.00
930	3.50	23.30	24.58	46.50	67.00
10 0	3.40	24.40	24.75	43.50	76.00
1030	1.10	25.40	25.00	41.50	82.00
11 0	1.10	26.30	25.50	40.50	86.00
1130	1.40	27.20	26.10	40.00	89.00
12 0	1.70	28.10	26.70	38.50	91.00
1230	.90	29.20	26.90	35.50	92.00
13 0	.90	30.20	27.70	29.50	91.50
1330	.90	31.20	28.10	25.50	89.50
1345	3.30	31.55	28.30	24.50	88.00
14 0	1.60	31.70	28.40	23.00	86.00
1430	1.30	31.60	28.50	22.50	80.00
1445	4.00	31.50	28.10	22.50	76.50
15 0	3.30	31.30	27.60	22.50	73.50
1515	3.30	31.2	27.20	23.00	70.00
1530	5.50	31.05	26.85	23.50	65.00
1545	8.00	31.00	26.50	24.00	60.50
16 0	6.65	30.90	26.30	24.00	57.00
1630	5.20	30.80	25.90	24.00	48.00
17 0	4.70	30.70	26.00	25.00	36.00
1730	4.20	30.20	26.00	27.00	24.00
18 0	3.70	29.40	26.00	31.00	12.00
1830	3.35	28.60	26.00	37.00	2.00
1845	2.20	28.00	26.00	39.00	-1.50
19 0	2.00	27.40	26.00	42.00	-3.00
1930	1.65	26.30	26.00	46.00	-7.00
20 0	1.30	25.40	25.85	50.00	-9.00
2030	1.80	24.60	25.75	51.50	-9.00
21 0	2.35	24.00	25.68	53.00	-9.00
2130	2.90	23.30	25.60	54.00	-9.00
22 0	3.30	22.70	25.50	54.50	-9.00
2230	3.70	22.20	25.45	54.50	-9.00
23 0	3.70	21.70	25.35	55.00	-9.00
2330	3.50	21.20	25.25	55.00	-9.00

Time	Speed (m/s)	A.Temp (°C)	W.Temp (°C)	R.H. (%)	N.Rad (mW/sq cm)
050476					
37					
830	3.60	13.80	21.20	71.50	22.00
9 0	3.30	14.40	21.25	70.00	32.50
930	3.30	15.20	21.28	68.50	41.00
10 0	4.30	16.50	21.35	65.50	48.50
1030	4.30	17.60	21.40	61.70	53.20
11 0	4.10	18.50	21.45	59.50	57.00
1130	4.00	19.20	21.53	57.00	59.00
12 0	3.90	19.70	21.60	55.00	59.50
1230	3.15	20.30	21.67	53.00	57.60
13 0	2.40	20.90	21.72	51.00	53.00
1330	2.30	21.55	21.77	49.20	46.00
14 0	2.20	22.00	21.80	47.50	42.30
1430	2.70	22.30	21.83	45.60	39.20
15 0	2.50	22.80	21.85	43.60	35.00
1530	2.30	23.20	21.85	42.60	30.00
16 0	2.20	23.70	21.83	42.60	20.00
1630	2.10	23.70	21.80	46.00	7.00
17 0	2.05	23.30	21.75	50.00	-3.00
1730	2.00	22.50	21.73	55.00	-6.00
18 0	1.95	20.80	21.67	59.50	-8.00
1830	1.90	19.30	21.62	63.50	-9.30
19 0	1.90	17.90	21.53	68.00	-10.00
1930	1.90	16.90	21.45	73.00	-10.20
20 0	1.90	16.10	21.40	78.00	-10.20
2030	1.50	15.70	21.35	78.00	-10.60
21 0	1.60	15.40	21.30	78.00	-11.20
2130	1.60	15.30	21.28	78.00	-11.00
22 0	3.00	15.25	21.27	78.30	-11.00
2230	3.30	15.25	21.25	78.50	-11.00
23 0	3.60	15.25	21.24	78.70	-11.00
2330	3.60	15.20	21.22	78.90	-11.00
24 0	3.60	15.10	21.21	79.00	-11.00
030	3.60	15.05	21.20	79.00	-11.00
1 0	3.60	15.00	21.20	79.00	-11.00
130	3.60	15.00	21.20	79.00	-11.00
2 0	2.30	14.95	21.18	79.00	-11.00
230	2.30	14.93	21.18	79.00	-11.00

DATE 150176 SERIES 1

RUN 1 DAY 1 TIME 810

	SOLN A	SOLN B
SALINITY	379.	529.
CONDUCTIVITY ≤ 25C	734.2	925.5

SALINITY = .784*COND 25 + -196.6

BUCKET TEMP .04C PROBE THERMISTOR 12.79C

RUN 2 DAY 1 TIME 900

	SOLN A	SOLN B
SALINITY	379.	529.
CONDUCTIVITY ≤ 25C	756.8	1028.0

SALINITY = .553*COND 25 + -39.5

BUCKET TEMP 23.54C PROBE THERMISTOR 17.80C

RUN 3 DAY 1 TIME 1000

	SOLN A	SOLN B
SALINITY	379.	529.
CONDUCTIVITY ≤ 25C	826.3	1077.3

SALINITY = .597*COND 25 + -114.7

BUCKET TEMP 24.44C PROBE THERMISTOR 24.28C

RUN 4 DAY 1 TIME 1100

	SOLN A	SOLN B
SALINITY	379.	529.
CONDUCTIVITY ≤ 25C	825.5	1073.8

SALINITY = .604*COND 25 + -119.7

BUCKET TEMP 25.44C PROBE THERMISTOR 25.19C

RUN 5 DAY 1 TIME 1210

	SOLN A	SOLN B
SALINITY	379.	529.
CONDUCTIVITY ≤ 25C	822.5	1075.7

SALINITY = .593*COND 25 + -108.4

RUN 6 DAY 1 TIME 1400

	SOLN A	SOLN B
SALINITY	379.	529.
CONDUCTIVITY ≤ 25C	841.6	1097.4

SALINITY = .586*COND 25 + -114.4

BUCKET TEMP 27.44C PROBE THERMISTOR 27.36C

RUN 7 DAY 1 TIME 1500

	SOLN A	SOLN B
SALINITY	379.	529.
CONDUCTIVITY ≤ 25C	827.6	1080.1

SALINITY = .594*COND 25 + -112.6

BUCKET TEMP 26.64C PROBE THERMISTOR 26.47C

RUN 8 DAY 1 TIME 1600

	SOLN A	SOLN B
SALINITY	379.	529.
CONDUCTIVITY ≤ 25C	831.2	1086.3

SALINITY = .588*COND 25 + -109.9

BUCKET TEMP 25.64C PROBE THERMISTOR 25.50C

RUN 9 DAY 1 TIME 1700

	SOLN A	SOLN B
SALINITY	379.	529.
CONDUCTIVITY ≤ 25C	816.9	1078.4

SALINITY = .574*COND 25 + -89.5

BUCKET TEMP 24.94C PROBE THERMISTOR 24.94C

RUN 10 DAY 1 TIME 1800

	SOLN A	SOLN B
SALINITY	379.	529.
CONDUCTIVITY ≤ 25C	817.9	1070.7

SALINITY = .593*COND 25 + -106.4

RUN 11 DAY 1 TIME 2030

	SOLN A	SOLN B
SALINITY	379.	529.
CONDUCTIVITY ≤ 25C	815.3	1068.2

SALINITY = .593*COND 25 + -104.4

BUCKET TEMP 24.04C PROBE THERMISTOR 23.93C

RUN 12 DAY 1 TIME 2230

	SOLN A	SOLN B
SALINITY	379.	529.
CONDUCTIVITY ≤ 25C	808.1	1055.6

SALINITY = .606*COND 25 + -110.8

BUCKET TEMP 23.74C PROBE THERMISTOR 23.58C

DATE 30276 SERIES 1

RUN 1 DAY 1 TIME 910

	SOLN A	SOLN B
SALINITY	402.	500.
CONDUCTIVITY ≤ 25C	774.2	952.3

SALINITY = .550*COND 25 + -23.8

BUCKET TEMP 24.65C PROBE THERMISTOR 24.61C

RUN 2 DAY 1 TIME 955

	SOLN A	SOLN B
SALINITY	402.	500.
CONDUCTIVITY ≤ 25C	775.0	951.7

SALINITY = .555*COND 25 + -27.8

BUCKET TEMP 25.35C PROBE THERMISTOR 25.29C

RUN 3 DAY 1 TIME 1105

	SOLN A	SOLN B
SALINITY	402.	500.
CONDUCTIVITY ≤ 25C	774.7	959.3

SALINITY = .531*COND 25 + -9.3

BUCKET TEMP 26.05C PROBE THERMISTOR 25.99C

RUN 4 DAY 1 TIME 1200

	SOLN A	SOLN B
SALINITY	402.	500.
CONDUCTIVITY ≤ 25C	771.4	937.4

SALINITY = .590*COND 25 + -53.4

BUCKET TEMP 26.95C PROBE THERMISTOR 26.90C

RUN 5 DAY 1 TIME 1300

	SOLN A	SOLN B
SALINITY	402.	500.
CONDUCTIVITY ≤ 25C	0.0	1038.7

SALINITY = .094*COND 25 + 402.0

BUCKET TEMP 27.65C PROBE THERMISTOR 24.30C

RUN 6 DAY 1 TIME 1405

	SOLN A	SOLN B
SALINITY	402.	500.
CONDUCTIVITY ≤ 25C	775.4	951.8

SALINITY = .556*COND 25 + -28.8

BUCKET TEMP 28.05C PROBE THERMISTOR 28.00C

RUN 7 DAY 1 TIME 1500

	SOLN A	SOLN B
SALINITY	402.	500.
CONDUCTIVITY ≤ 25C	772.0	948.9

SALINITY = .554*COND 25 + -25.7

BUCKET TEMP 27.35C PROBE THERMISTOR 27.31C

RUN 8 DAY 1 TIME 1600

	SOLN A	SOLN B
SALINITY	402.	500.
CONDUCTIVITY ≤ 25C	774.5	951.9

SALINITY = .553*COND 25 + -25.9

BUCKET TEMP 28.75C PROBE THERMISTOR 28.87C

RUN 9 DAY 1 TIME 1700

	SOLN A	SOLN B
SALINITY	402.	500.
CONDUCTIVITY ≤ 25C	765.5	946.0

SALINITY = .543*COND 25 + -13.7

BUCKET TEMP 26.90C PROBE THERMISTOR 26.99C

RUN 10 DAY 1 TIME 1800

	SOLN A	SOLN B
SALINITY	402.	500.
CONDUCTIVITY ≤ 25C	770.9	942.9

SALINITY = .569*COND 25 + -37.0

BUCKET TEMP 27.45C PROBE THERMISTOR 27.47C

RUN 12 DAY 1 TIME 2000

	SOLN A	SOLN B
SALINITY	402.	500.
CONDUCTIVITY ≤ 25C	772.4	946.3

SALINITY = .563*COND 25 + -33.2

BUCKET TEMP 26.35C PROBE THERMISTOR 26.35C

DATE 50276 SERIES 2

RUN 1 DAY 1 TIME 630

	SOLN A	SOLN B
SALINITY	402.	500.
CONDUCTIVITY ≤ 25C	773.4	949.7

SALINITY = .555*COND 25 + -27.9

BUCKET TEMP 23.85C PROBE THERMISTOR 23.83C

RUN 2 DAY 1 TIME 730

	SOLN A	SOLN B
SALINITY	402.	500.
CONDUCTIVITY ≤ 25C	776.6	953.4

SALINITY = .555*COND 25 + -28.7

BUCKET TEMP 23.90C PROBE THERMISTOR 23.83C

RUN 3 DAY 1 TIME 830

	SOLN A	SOLN B
SALINITY	402.	500.
CONDUCTIVITY ≤ 25C	778.0	952.8

SALINITY = .560*COND 25 + -34.0

BUCKET TEMP 24.70C PROBE THERMISTOR 24.60C

RUN 4 DAY 1 TIME 930

	SOLN A	SOLN B
SALINITY	402.	500.
CONDUCTIVITY ≤ 25C	776.0	953.4

SALINITY = .553*COND 25 + -26.8

BUCKET TEMP 24.80C PROBE THERMISTOR 24.64C

RUN 5 DAY 1 TIME 1030

	SOLN A	SOLN B
SALINITY	402.	500.
CONDUCTIVITY ≤ 25C	778.7	953.8

SALINITY = .560*COND 25 + -33.8

RUN 6 DAY 1 TIME 1130

	SOLN A	SCLN B
SALINITY	402.	500.
CONDUCTIVITY ≤ 25C	786.6	961.4

SALINITY = .561*COND 25 + -39.0

BUCKET TEMP 26.00C PROBE THERMISTOR 26.22C

RUN 7 DAY 1 TIME 1230

	SOLN A	SOLN B
SALINITY	402.	500.
CONDUCTIVITY ≤ 25C	786.9	957.4

SALINITY = .575*COND 25 + -50.1

BUCKET TEMP 26.80C PROBE THERMISTOR 26.78C

RUN 8 DAY 1 TIME 1326

	SOLN A	SOLN B
SALINITY	402.	500.
CONDUCTIVITY ≤ 25C	781.6	955.9

SALINITY = .562*COND 25 + -37.4

BUCKET TEMP 27.80C PROBE THERMISTOR 27.76C

RUN 9 DAY 1 TIME 1430

	SOLN A	SOLN B
SALINITY	402.	500.
CONDUCTIVITY ≤ 25C	776.3	953.5

SALINITY = .553*COND 25 + -27.2

BUCKET TEMP 28.60C PROBE THERMISTOR 28.56C

RUN 10 DAY 1 TIME 1530

	SOLN A	SOLN B
SALINITY	402.	500.
CONDUCTIVITY ≤ 25C	776.7	951.7

SALINITY = .560*COND 25 + -32.9

RUN 11 DAY 1 TIME 1630

	SOLN A	SOLN B
SALINITY	402.	500.
CONDUCTIVITY ≤ 25C	779.3	952.7

SALINITY = .565*COND 25 + -38.3

BUCKET TEMP 25.95C PROBE THERMISTOR 25.95C

RUN 12 DAY 1 TIME 1730

	SOLN A	SOLN B
SALINITY	402.	500.
CONDUCTIVITY ≤ 25C	778.5	953.2

SALINITY = .561*COND 25 + -34.5

BUCKET TEMP 25.95C PROBE THERMISTOR 25.88C

RUN 14 DAY 1 TIME 2010

	SOLN A	SOLN B
SALINITY	402.	500.
CONDUCTIVITY ≤ 25C	773.5	952.5

SALINITY = .547*COND 25 + -21.4

BUCKET TEMP 25.70C PROBE THERMISTOR 25.55C

RUN 15 DAY 1 TIME 2310

	SOLN A	SOLN B
SALINITY	402.	500.
CONDUCTIVITY ≤ 25C	776.7	956.4

SALINITY = .545*COND 25 + -21.6

BUCKET TEMP 25.10C PROBE THERMISTOR 24.94C

DATE 50476 SERIES 5

RUN 1 DAY 1 TIME 930

	SOLN A	SOLN B
SALINITY	402.	500.
CONDUCTIVITY ≤ 25C	759.3	936.0

SALINITY = .555*COND 25 + -19.3

BUCKET TEMP 21.15C PROBE THERMISTOR 21.01C

RUN 2 DAY 1 TIME 1030

	SOLN A	SOLN B
SALINITY	402.	500.
CONDUCTIVITY ≤ 25C	759.7	933.2

SALINITY = .565*COND 25 + -27.0

BUCKET TEMP 21.15C PROBE THERMISTOR 21.08C

RUN 4 DAY 1 TIME 1400

	SOLN A	SOLN B
SALINITY	402.	500.
CONDUCTIVITY ≤ 25C	765.9	939.5

SALINITY = .565*COND 25 + -30.4

BUCKET TEMP 21.60C PROBE THERMISTOR 21.79C

RUN 6 DAY 1 TIME 1500

	SOLN A	SOLN B
SALINITY	402.	500.
CONDUCTIVITY ≤ 25C	765.1	937.3

SALINITY = .569*COND 25 + -33.4

BUCKET TEMP 21.70C PROBE THERMISTOR 21.82C

RUN 7 DAY 1 TIME 1600

	SOLN A	SOLN B
SALINITY	402.	500.
CONDUCTIVITY ≤ 25C	764.1	937.4

SALINITY = .565*COND 25 + -30.0

BUCKET TEMP 21.65C PROBE THERMISTOR 21.81C

RUN 8 DAY 1 TIME 1845

	SOLN A	SOLN B
SALINITY	402.	500.
CONDUCTIVITY ≤ 25C	764.8	940.3

SALINITY = .558*COND 25 + -25.0

BUCKET TEMP 21.30C PROBE THERMISTOR 21.35C

RUN 9 DAY 1 TIME 2030

	SOLN A	SOLN B
SALINITY	402.	500.
CONDUCTIVITY ≤ 25C	764.8	940.3

SALINITY = .558*COND 25 + -25.0

BUCKET TEMP 21.00C PROBE THERMISTOR 21.06C

RUN 10 DAY 1 TIME 2200

	SOLN A	SOLN B
SALINITY	402.	500.
CONDUCTIVITY ≤ 25C	764.8	940.3

SALINITY = .558*COND 25 + -25.0

BUCKET TEMP 21.00C PROBE THERMISTOR 21.16C

RUN 11 DAY 1 TIME 2350

	SOLN A	SOLN B
SALINITY	402.	500.
CONDUCTIVITY ≤ 25C	764.8	940.3

SALINITY = .558*COND 25 + -25.0

BUCKET TEMP 20.85C PROBE THERMISTOR 21.05C

RUN 12 DAY 2 TIME 200

	SOLN A	SOLN B
SALINITY	402.	500.
CONDUCTIVITY ≤ 25C	764.8	940.3

SALINITY = .558*COND 25 + -25.0

BUCKET TEMP 20.50C PROBE THERMISTOR 20.67C

15 01 76 SALINITY AND TEMPERATURE STRUCTURE

TIME 810

DEPTH	TEMPERATURE	SALINITY
0.0	23.13	426.9
.2	23.15	425.9
.4	23.15	424.3
.6	23.14	422.7
.8	23.14	421.9
1.0	23.14	421.2
1.4	23.14	420.3
1.8	23.13	419.6
2.0	23.13	418.8
2.5	23.11	417.4
3.0	23.09	416.8
3.5	23.09	416.0
4.0	23.05	415.7
4.5	22.73	413.4
5.0	22.69	412.2
6.0	22.57	411.8
7.0	22.40	410.3
8.0	22.24	408.8
9.0	22.00	408.2
10.0	21.59	410.1
11.0	19.37	445.8
12.0	16.76	524.5

TIME 900

DEPTH	TEMPERATURE	SALINITY
0.0	23.38	452.0
.2	23.33	451.9
.4	23.30	451.7
.6	23.28	451.3
.8	23.26	450.3
1.0	23.24	449.9
1.4	23.21	448.6
1.8	23.18	447.1
2.0	23.16	446.2
2.5	23.14	445.2
3.0	23.13	443.7
3.5	23.09	442.4
4.0	22.98	441.1
4.5	22.90	439.0
5.0	22.76	437.6
6.0	22.69	436.5
7.0	22.56	434.9
8.0	22.39	434.3
9.0	22.18	434.0
10.0	21.97	432.6

TIME 1000

DEPTH	TEMPERATURE	SALINITY
0.0	24.06	454.2
.2	24.02	454.6
.4	23.65	454.7
.6	23.51	454.2
.8	23.42	454.5
1.0	23.38	454.3
1.4	23.28	454.0
1.8	23.26	454.3
2.0	23.23	453.9
2.5	23.18	453.8
3.0	23.15	454.0
3.5	23.09	454.1
4.0	23.01	453.0
4.5	22.89	452.4
5.0	22.81	451.9
6.0	22.72	451.0
7.0	22.58	450.5
8.0	22.40	450.4
9.0	22.23	448.3
10.0	22.10	447.2
11.0	21.26	452.6
12.0	19.49	478.6

TIME 1100

DEPTH	TEMPERATURE	SALINITY
0.0	24.60	452.7
.2	24.55	452.6
.4	24.32	454.9
.6	23.98	453.3
.8	23.72	454.0
1.0	23.60	453.4
1.4	23.47	454.1
1.8	23.32	452.5
2.0	23.26	453.0
2.5	23.21	453.0
3.0	23.16	452.8
3.5	23.09	452.9
4.0	22.97	452.2
4.5	22.90	451.7
5.0	22.77	451.1
6.0	22.71	450.4
7.0	22.61	449.5
8.0	22.42	449.0
9.0	22.27	447.9
10.0	21.93	448.8

TIME 1210

DEPTH	TEMPERATURE	SALINITY
0.0	26.16	459.4
.2	25.14	458.0
.4	24.35	459.6
.6	23.98	459.1
.8	23.78	457.9
1.0	23.68	457.2
1.4	23.51	457.0
1.8	23.35	456.8
2.0	23.30	457.3
2.5	23.26	457.1
3.0	23.22	457.4
3.5	23.13	456.5
4.0	23.03	456.3
4.5	23.01	455.8
5.0	22.88	456.5
6.0	22.75	454.1
7.0	22.71	453.9
8.0	22.46	452.1
9.0	22.40	450.2
10.0	22.10	450.7
11.0	21.59	453.9
12.0	19.66	476.9

TIME 1400

DEPTH	TEMPERATURE	SALINITY
0.0	26.01	448.2
.2	25.73	449.7
.4	24.79	452.3
.6	24.48	448.7
.8	24.26	446.7
1.0	24.15	445.9
1.4	23.78	446.5
1.8	23.63	445.6
2.0	23.57	445.6
2.5	23.48	445.9
3.0	23.40	445.5
3.5	23.36	445.3
4.0	23.29	444.7
4.5	23.11	444.7
5.0	23.09	443.1
6.0	22.84	442.5
7.0	22.77	442.0
8.0	22.60	440.6
9.0	22.46	439.5
10.0	22.15	442.0

TIME 1500

0.0	26.07	450.4
.2	26.04	449.5
.4	25.88	449.3
.6	25.34	450.8
.8	24.55	448.3
1.0	24.27	446.7
1.4	23.98	446.5
1.8	23.73	447.1
2.0	23.68	447.0
2.5	23.55	447.1
3.0	23.47	446.7
3.5	23.38	448.1
4.0	23.32	448.7
4.5	23.20	448.7
5.0	23.10	448.5
6.0	22.87	447.0
7.0	22.80	446.5
8.0	22.56	445.8
9.0	22.44	444.5
10.0	22.17	444.0
11.0	21.68	446.4
12.0	19.43	477.2

TIME 1600

0.0	25.27	445.7
.2	25.27	445.7
.4	25.26	445.2
.6	25.19	445.9
.8	25.09	445.1
1.0	25.09	445.7
1.4	24.32	444.1
1.8	23.92	444.3
2.0	23.84	443.9
2.5	23.69	444.1
3.0	23.60	443.6
3.5	23.44	444.2
4.0	23.34	443.3
4.5	23.22	443.3
5.0	23.13	442.9
6.0	22.94	442.3
7.0	22.81	441.7
8.0	22.60	440.8
9.0	22.44	439.8
10.0	22.22	439.5
11.0	21.76	441.0
12.0	19.72	472.3

TIME 1700

0.0	24.73	447.5
.2	24.73	447.5
.4	24.73	447.5
.6	24.72	447.5
.8	24.71	447.7
1.0	24.70	447.7
1.4	24.67	448.0
1.8	24.56	447.9
2.0	24.31	447.3
2.5	23.89	447.7
3.0	23.53	447.5
3.5	23.39	447.1
4.0	23.31	447.2
4.5	23.26	446.5
5.0	23.21	445.8
6.0	22.89	445.9
7.0	22.82	444.7
8.0	22.60	444.4
9.0	22.44	442.9
10.0	22.17	443.1
11.0	21.57	447.0
12.0	19.66	473.8

TIME 1800

0.0	24.39	447.7
.2	24.38	447.9
.4	24.38	447.8
.6	24.34	447.6
.8	24.34	447.6
1.0	24.35	447.5
1.4	24.24	448.6
1.8	24.20	447.7
2.0	24.23	447.4
2.5	23.97	447.5
3.0	23.73	447.4
3.5	23.40	446.3
4.0	23.25	446.5
4.5	23.17	446.1
5.0	23.04	446.1
6.0	22.84	445.7
7.0	22.81	445.3
8.0	22.61	444.8
9.0	22.43	444.0
10.0	22.10	444.2
11.0	21.59	447.3
12.0	19.22	485.3

TIME 2030

0.0	23.92	447.7
.2	23.94	447.5
.4	23.94	447.5
.6	23.94	448.1
.8	23.94	447.5
1.0	23.94	447.5
1.4	23.94	447.5
1.8	23.92	447.7
2.0	23.94	448.1
2.5	23.90	447.8
3.0	23.88	447.4
3.5	23.86	447.1
4.0	23.78	446.6
4.5	23.63	447.4
5.0	23.27	446.6
6.0	23.05	445.1
7.0	22.78	445.3
8.0	22.53	444.5
9.0	22.25	444.3
10.0	21.96	444.6
11.0	20.85	455.7
12.0	18.80	496.1

TIME 2230

0.0	23.74	450.9
.2	23.77	450.6
.4	23.80	451.0
.6	23.80	451.0
.8	23.80	451.0
1.0	23.79	451.1
1.4	23.79	450.9
1.8	23.80	451.0
2.0	23.79	451.1
2.5	23.78	451.1
3.0	23.79	451.1
3.5	23.76	450.7
4.0	23.65	450.6
4.5	23.55	450.3
5.0	23.14	450.6
6.0	22.72	449.1
7.0	22.51	448.7
8.0	22.36	448.3
9.0	22.04	448.3
10.0	21.86	448.7
11.0	21.35	453.2
12.0	17.90	524.7

03 02 76 SALINITY AND TEMPERATURE STRUCTURE

DEPTH	TEMPERATURE	SALINITY
TIME 910		
0.0	24.49	455.8
.2	24.49	458.0
.4	24.49	457.9
.6	24.48	459.8
.8	24.47	460.9
1.0	24.47	461.0
1.5	24.40	462.2
2.0	24.34	462.8
2.5	24.32	463.5
3.0	24.30	463.8
3.5	24.29	464.4
4.0	24.22	464.5
4.5	24.20	464.2
5.0	24.09	464.1
6.0	23.89	463.4
7.0	23.72	463.3
8.0	23.67	462.8
9.0	23.41	463.1
10.0	23.31	463.5
11.0	22.55	472.5
12.0	21.62	488.2
13.0	19.70	562.0
14.0	17.00	637.6
15.0	16.11	658.5
TIME 955		
0.0	25.20	468.8
.2	24.90	469.0
.4	24.82	469.2
.6	24.73	469.0
.8	24.66	469.7
1.0	24.62	469.6
1.5	24.52	470.0
2.0	24.45	469.6
2.5	24.38	469.7
3.0	24.37	469.2
3.5	24.34	469.5
4.0	24.27	469.7
4.5	24.23	469.6
5.0	24.16	469.1
6.0	23.96	468.3
7.0	23.77	467.4
8.0	23.53	467.0
9.0	23.40	466.6
10.0	23.22	467.8
11.0	22.79	472.4
12.0	22.17	480.1
13.0	18.94	574.8
TIME 1105		
0.0	26.02	468.3
.2	25.94	469.0
.4	25.75	468.7
.6	25.23	468.5
.8	25.08	468.3
1.0	24.99	468.6
1.5	24.66	469.1
2.0	24.49	468.6
2.5	24.43	468.7
3.0	24.39	468.5
3.5	24.33	468.5
4.0	24.32	468.1
4.5	24.28	467.9
5.0	24.24	467.8
6.0	24.00	460.4
7.0	23.70	444.6
8.0	23.56	426.4
9.0	23.46	465.1
10.0	23.38	457.6
11.0	22.98	462.6
12.0	21.89	479.3
13.0	18.76	573.6
14.0		
15.0		
TIME 1200		
0.0	26.75	477.7
.2	26.59	477.6
.4	26.28	477.9
.6	25.67	477.3
.8	25.38	476.3
1.0	25.21	476.3
1.5	24.85	476.6
2.0	24.59	475.8
2.5	24.54	475.7
3.0	24.46	476.6
3.5	24.42	475.8
4.0	24.38	475.6
4.5	24.34	474.8
5.0	24.30	475.3
6.0	24.09	473.9
7.0	23.79	473.5
8.0	23.70	472.7
9.0	23.51	471.7
10.0	23.39	471.9
11.0	22.98	476.3
12.0	22.17	486.5
13.0	18.98	590.3
TIME 1300		
0.0	27.50	486.9
.2	26.92	487.0
.4	26.03	488.0
.6	25.52	487.3
.8	25.41	486.7
1.0	25.20	486.9
1.5	24.77	486.8
2.0	24.57	487.0
2.5	24.54	486.9
3.0	24.53	486.8
3.5	24.51	486.8
4.0	24.46	486.8
4.5	24.43	486.8
5.0	24.38	486.7
6.0	24.25	486.8
7.0	23.83	486.6
8.0	23.76	486.4
9.0	23.58	486.5
10.0	23.29	486.4
11.0	22.81	487.2
12.0	21.28	491.3
13.0	19.26	502.2
14.0		
15.0		
TIME 1405		
0.0	28.01	469.6
.2	27.71	471.3
.4	26.46	468.4
.6	25.89	469.6
.8	25.63	469.4
1.0	25.38	469.2
1.5	25.02	469.9
2.0	24.66	469.7
2.5	24.64	469.3
3.0	24.65	469.2
3.5	24.53	472.7
4.0	24.49	472.4
4.5	24.46	472.2
5.0	24.43	468.0
6.0	24.20	469.8
7.0	23.90	467.7
8.0	23.67	467.8
9.0	23.53	466.9
10.0	23.34	467.7
11.0	23.13	470.4
12.0	21.60	499.4
13.0		

TIME 1500

0.0	27.68	472.2
.2	27.37	473.2
.4	26.92	473.2
.6	26.61	472.4
.8	26.17	474.6
1.0	25.48	473.1
1.5	24.95	472.9
2.0	24.72	473.5
2.5	24.71	473.0
3.0	24.67	473.4
3.5	24.55	473.5
4.0	24.51	473.4
4.5	24.47	473.3
5.0	24.43	473.1
6.0	24.16	471.9
7.0	23.97	470.9
8.0	23.68	470.5
9.0	23.57	470.5
10.0	23.43	470.2
11.0	22.91	476.7
12.0	21.72	494.9
13.0		
14.0		
15.0		

TIME 1600

0.0	29.20	465.9
.2	28.75	464.9
.4	26.92	467.8
.6	26.09	465.6
.8	25.30	470.6
1.0	25.16	468.1
1.5	24.86	468.2
2.0	24.78	467.4
2.5	24.78	467.4
3.0	24.72	466.3
3.5	24.69	466.7
4.0	24.53	466.6
4.5	24.48	465.9
5.0	24.47	466.1
6.0	24.28	464.6
7.0	23.97	464.3
8.0	23.72	463.4
9.0	23.59	463.0
10.0	23.42	464.1
11.0	22.84	470.1
12.0	21.68	489.5
13.0		
14.0		
15.0		

TIME 1700

0.0	27.55	473.0
.2	26.40	472.8
.4	26.05	472.4
.6	25.75	472.1
.8	25.49	471.9
1.0	25.41	472.1
1.5	25.29	471.7
2.0	25.15	471.9
2.5	25.08	472.6
3.0	24.81	472.6
3.5	24.77	471.8
4.0	24.67	471.2
4.5	24.51	471.1
5.0	24.50	470.7
6.0	24.37	470.8
7.0	24.11	470.1
8.0	23.82	468.5
9.0	23.71	467.3
10.0	23.54	467.3
11.0	22.99	472.8
12.0	21.60	495.5
13.0		
14.0		
15.0		

TIME 1800

0.0	27.36	472.0
.2	27.42	471.5
.4	27.42	472.0
.6	27.38	472.4
.8	27.16	472.9
1.0	26.37	470.7
1.5	25.82	471.7
2.0	25.33	471.1
2.5	25.06	472.1
3.0	24.85	471.4
3.5	24.76	471.8
4.0	24.63	471.4
4.5	24.48	471.1
5.0	24.47	470.7
6.0	24.18	470.2
7.0	23.89	468.6
8.0	23.69	468.3
9.0	23.58	468.2
10.0	23.46	467.8
11.0	23.03	474.1
12.0	22.00	490.1
13.0		
14.0		
15.0		

TIME 2000

0.0	26.31	471.4
.2	26.34	471.1
.4	26.37	470.8
.6	26.36	470.9
.8	26.33	471.7
1.0	26.29	471.6
1.5	25.69	472.6
2.0	25.25	470.3
2.5	24.97	469.7
3.0	24.83	470.6
3.5	24.73	470.4
4.0	24.65	470.2
4.5	24.44	469.9
5.0	24.40	469.8
6.0	24.17	469.3
7.0	23.93	467.1
8.0	23.73	468.1
9.0	23.53	467.2
10.0	23.42	467.2
11.0	22.63	477.3
12.0	21.62	493.1
13.0		
14.0		
15.0		

05 02 76 SALINITY AND TEMPERATURE STRUCTURE

DEPTH	TEMPERATURE	SALINITY
TIME 630		
0.0	24.30	468.8
.2	24.33	469.0
.4	24.33	469.0
.6	24.34	468.9
.8	24.34	469.0
1.0	24.34	469.0
1.5	24.35	468.9
2.0	24.35	468.9
2.5	24.35	468.9
3.0	24.34	468.9
3.5	24.34	468.9
4.0	24.33	469.0
4.5	24.34	469.0
5.0	24.33	468.4
6.0	24.32	469.2
7.0	24.32	468.6
8.0	24.07	467.7
9.0	23.53	466.9
10.0	23.31	466.9
11.0	22.89	471.8
12.0	19.00	566.5
TIME 730		
0.0	24.31	466.7
.2	24.33	466.5
.4	24.32	466.6
.6	24.33	466.5
.8	24.33	466.5
1.0	24.33	466.5
1.5	24.33	467.0
2.0	24.32	466.6
2.5	24.35	466.9
3.0	24.35	466.3
3.5	24.35	466.3
4.0	24.34	466.4
4.5	24.34	466.4
5.0	24.34	466.4
6.0	24.33	466.5
7.0	24.30	466.3
8.0	24.22	465.9
9.0	23.52	463.9
10.0	23.33	464.1
11.0	22.83	470.4
12.0	20.83	497.7
TIME 830		
0.0	24.41	470.1
.2	24.43	470.0
.4	24.44	469.9
.6	24.43	470.0
.8	24.42	470.1
1.0	24.43	470.0
1.5	24.41	470.2
2.0	24.40	470.3
2.5	24.40	470.3
3.0	24.39	469.8
3.5	24.39	469.8
4.0	24.39	469.9
4.5	24.37	470.0
5.0	24.37	469.5
6.0	24.34	469.7
7.0	24.33	469.3
8.0	24.13	469.0
9.0	23.59	468.9
10.0	23.36	467.2
11.0	22.77	472.8
12.0	21.93	487.9
TIME 930		
0.0	24.57	468.7
.2	24.58	469.1
.4	24.57	469.8
.6	24.56	469.3
.8	24.56	469.3
1.0	24.56	469.3
1.5	24.53	469.6
2.0	24.52	469.1
2.5	24.45	469.8
3.0	24.45	469.4
3.5	24.41	469.7
4.0	24.41	469.2
4.5	24.39	469.4
5.0	24.37	469.6
6.0	24.35	469.2
7.0	24.34	468.8
8.0	23.91	467.4
9.0	23.71	467.8
10.0	23.44	466.6
11.0	22.75	473.7
12.0	21.54	493.2
TIME 1030		
0.0	24.86	470.7
.2	24.83	471.0
.4	24.81	471.2
.6	24.81	471.3
.8	24.76	471.1
1.0	24.74	471.3
1.5	24.70	471.2
2.0	24.68	470.8
2.5	24.63	470.8
3.0	24.53	471.2
3.5	24.49	471.1
4.0	24.49	471.1
4.5	24.47	470.8
5.0	24.45	470.4
6.0	24.41	470.7
7.0	24.38	470.5
8.0	24.05	469.3
9.0	23.88	467.7
10.0	23.53	468.4
11.0	22.76	474.2
12.0	21.68	492.5
TIME 1130		
0.0	26.10	468.5
.2	25.53	469.2
.4	25.60	465.7
.6	25.14	469.1
.8	25.05	469.0
1.0	24.98	469.1
1.5	24.84	468.9
2.0	24.80	468.1
2.5	24.79	468.3
3.0	24.74	468.2
3.5	24.62	467.7
4.0	24.58	467.6
4.5	24.57	467.7
5.0	24.52	467.6
6.0	24.45	467.2
7.0	24.39	466.1
8.0	24.08	465.3
9.0	23.86	464.1
10.0	23.56	464.3
11.0	23.10	466.9
12.0	21.79	486.4

TIME 1230

0.0	26.72	470.9
.2	26.51	470.3
.4	25.49	471.1
.6	25.32	470.6
.8	25.17	470.4
1.0	25.07	470.3
1.5	24.91	469.7
2.0	24.88	469.4
2.5	24.79	469.2
3.0	24.73	469.3
3.5	24.69	469.1
4.0	24.65	468.9
4.5	24.61	468.7
5.0	24.57	468.6
6.0	24.51	468.0
7.0	24.32	467.1
8.0	24.01	467.5
9.0	23.92	465.5
10.0	23.67	464.6
11.0	23.02	469.2
12.0	22.29	478.4

TIME 1326

0.0	28.10	472.4
.2	26.76	470.9
.4	25.80	470.6
.6	25.55	470.3
.8	25.38	469.7
1.0	25.24	470.0
1.5	25.02	469.5
2.0	24.96	468.9
2.5	24.90	469.0
3.0	24.81	469.3
3.5	24.75	468.8
4.0	24.71	468.7
4.5	24.67	468.5
5.0	24.64	468.3
6.0	24.52	467.8
7.0	24.38	468.1
8.0	24.23	467.4
9.0	23.97	466.6
10.0	23.69	464.8
11.0	22.48	477.1
12.0	21.68	494.3

TIME 1430

0.0	28.44	472.5
.2	26.67	469.8
.4	26.09	469.0
.6	25.80	469.1
.8	25.46	469.7
1.0	25.30	469.1
1.5	25.05	469.3
2.0	24.95	469.3
2.5	24.88	468.8
3.0	24.87	468.9
3.5	24.82	468.9
4.0	24.75	469.0
4.5	24.70	468.9
5.0	24.67	468.2
6.0	24.53	467.9
7.0	24.41	467.4
8.0	24.26	467.2
9.0	23.97	465.7
10.0	23.56	465.2
11.0	22.56	475.0
12.0	21.62	491.7

TIME 1530

0.0	26.87	470.2
.2	26.85	469.8
.4	26.84	470.4
.6	26.82	470.6
.8	26.61	469.4
1.0	26.20	470.1
1.5	25.18	469.2
2.0	25.07	469.8
2.5	25.03	469.0
3.0	24.96	469.2
3.5	24.92	469.0
4.0	24.80	469.1
4.5	24.68	469.2
5.0	24.63	469.1
6.0	24.54	468.4
7.0	24.41	467.9
8.0	24.37	467.8
9.0	23.83	465.3
10.0	23.63	466.2
11.0	22.81	470.6
12.0	20.92	500.6

TIME 1630

0.0	25.88	468.1
.2	25.88	468.7
.4	25.86	468.8
.6	25.84	468.5
.8	25.86	468.9
1.0	25.78	469.1
1.5	25.74	468.9
2.0	25.56	468.5
2.5	25.47	468.2
3.0	25.19	467.7
3.5	24.83	468.0
4.0	24.74	467.7
4.5	24.70	468.7
5.0	24.67	468.4
6.0	24.63	467.8
7.0	24.50	467.3
8.0	24.41	467.2
9.0	23.74	466.0
10.0	23.58	465.2
11.0	22.76	471.6
12.0	21.53	492.3

TIME 1730

0.0	25.88	468.6
.2	25.90	468.9
.4	25.89	469.6
.6	25.89	469.6
.8	25.88	469.1
1.0	25.88	469.7
1.5	25.89	469.6
2.0	25.85	469.4
2.5	25.70	468.7
3.0	25.59	467.6
3.5	25.47	466.3
4.0	24.84	469.0
4.5	24.70	467.5
5.0	24.68	467.7
6.0	24.62	467.2
7.0	24.50	467.4
8.0	24.43	466.9
9.0	23.86	465.3
10.0	23.55	465.6
11.0	22.53	475.1
12.0	21.45	492.4

TIME 2010

0.0	25.69	468.8
.2	25.70	468.8
.4	25.70	469.3
.6	25.70	469.3
.8	25.70	468.8
1.0	25.70	468.8
1.5	25.66	468.6
2.0	25.58	469.4
2.5	25.43	468.7
3.0	25.33	468.6
3.5	25.27	468.1
4.0	25.26	467.6
4.5	25.03	469.3
5.0	24.70	468.2
6.0	24.57	467.8
7.0	24.44	466.9
8.0	24.38	466.9
9.0	24.09	465.9
10.0	23.49	466.3
11.0	22.54	473.8
12.0	21.04	502.3

TIME 2310

0.0	25.31	468.9
.2	25.33	469.2
.4	25.38	468.8
.6	25.36	469.0
.8	25.36	468.4
1.0	25.34	468.6
1.5	25.35	468.5
2.0	25.38	468.3
2.5	25.36	468.4
3.0	25.25	469.5
3.5	25.16	468.2
4.0	25.15	467.8
4.5	25.11	468.1
5.0	24.61	468.1
6.0	24.45	467.6
7.0	24.35	467.4
8.0	23.85	465.7
9.0	23.28	468.1
10.0	23.09	467.7
11.0	22.92	468.9
12.0	20.94	502.0

05 04 76 SALINITY AND TEMPERATURE STRUCTURE

TIME 930

DEPTH	TEMPERATURE	SALINITY
0.0	21.03	514.8
.1	21.04	502.9
.15	21.05	502.8
.2	21.05	502.8
.4	21.05	502.8
.6	21.05	502.9
.8	21.05	503.0
1.0	21.05	502.8
1.5	21.05	502.9
2.0	21.04	503.0
2.5	21.04	502.5
3.0	21.03	502.6
3.5	21.03	502.4
4.0	21.03	501.8
4.5	21.03	502.1
5.0	21.03	502.0
6.0	21.02	501.8
7.0	21.03	501.0
8.0	21.02	500.9
9.0	21.02	500.6
10.0	21.01	500.5
11.0	21.01	501.1
12.0	20.90	507.1
12.3		
12.5		
12.7		
13.0	17.65	666.3

TIME 1030

DEPTH	TEMPERATURE	SALINITY
0.0	21.16	503.3
.1	21.18	503.7
.15	21.18	503.6
.2	21.18	503.6
.4	21.18	503.5
.6	21.17	503.5
.8	21.17	503.5
1.0	21.17	503.7
1.5	21.17	503.7
2.0	21.16	503.6
2.5	21.16	503.6
3.0	21.12	503.6
3.5	21.11	503.4
4.0	21.11	503.4
4.5	21.11	503.1
5.0	21.10	502.6
6.0	21.10	502.1
7.0	21.09	502.1
8.0	21.08	501.8
9.0	21.06	501.2
10.0	21.05	500.1
11.0	21.03	500.6
12.0	20.87	512.9
12.3		
12.5		
12.7		
13.0	17.97	6833.1

TIME 1400

DEPTH	TEMPERATURE	SALINITY
0.0	21.75	497.8
.1	21.76	497.9
.15	21.76	498.0
.2	21.75	498.2
.4	21.73	498.2
.6	21.73	498.0
.8	21.68	498.4
1.0	21.66	497.7
1.5	21.61	497.5
2.0	21.56	497.4
2.5	21.48	497.6
3.0	21.45	497.4
3.5	21.43	497.6
4.0	21.39	497.9
4.5	21.36	497.7
5.0	21.32	497.0
6.0	21.27	497.0
7.0	21.22	497.0
8.0	21.22	496.7
9.0	21.20	496.6
10.0	21.17	496.5
11.0	21.08	499.2
12.0	20.78	512.7
12.3		
12.5		
12.7		
13.0	19.26	629.6

TIME 1500

DEPTH	TEMPERATURE	SALINITY
0.0	21.76	499.4
.1	21.77	499.7
.15	21.77	499.5
.2	21.76	499.4
.4	21.77	499.4
.6	21.77	499.1
.8	21.74	498.7
1.0	21.68	499.1
1.5	21.64	499.0
2.0	21.57	498.4
2.5	21.44	498.8
3.0	21.41	498.8
3.5	21.34	498.9
4.0	21.27	498.0
4.5	21.26	498.4
5.0	21.26	498.2
6.0	21.21	498.1
7.0	21.17	498.0
8.0	21.16	497.7
9.0	21.15	497.5
10.0	21.13	497.4
11.0	21.06	500.6
12.0	20.84	503.4
12.3		
12.5		
12.7		
13.0	18.74	617.2

TIME 1600

DEPTH	TEMPERATURE	SALINITY
0.0	21.76	499.3
.1	21.76	499.5
.15	21.77	499.6
.2	21.78	499.5
.4	21.76	499.4
.6	21.78	499.3
.8	21.78	499.1
1.0	21.76	499.4
1.5	21.66	499.0
2.0	21.57	498.5
2.5	21.52	498.7
3.0	21.38	498.8
3.5	21.28	498.4
4.0	21.30	498.2
4.5	21.27	498.1
5.0	21.24	497.7
6.0	21.22	497.2
7.0	21.20	497.2
8.0	21.21	497.1
9.0	21.19	497.1
10.0	21.14	496.3
11.0	21.10	496.8
12.0	21.06	499.1
12.3		
12.5		
12.7		
13.0	19.23	629.7

TIME 1845

DEPTH	TEMPERATURE	SALINITY
0.0	21.38	500.1
.1	21.39	499.8
.15	21.39	500.2
.2	21.40	499.6
.4	21.41	499.6
.6	21.44	499.0
.8	21.44	499.2
1.0	21.41	499.4
1.5	21.44	499.3
2.0	21.44	499.3
2.5	21.43	499.2
3.0	21.47	498.7
3.5	21.45	498.6
4.0	21.35	499.0
4.5	21.28	498.9
5.0	21.28	499.2
6.0	21.24	498.2
7.0	21.19	498.8
8.0	21.16	498.8
9.0	21.15	497.8
10.0	21.11	497.4
11.0	20.99	498.9
12.0	20.76	506.1
12.3		
12.5		
12.7		
13.0		

TIME 2030

0.0	21.34	497.1
.1	21.36	497.0
.15	21.37	497.4
.2	21.38	497.1
.4	21.39	497.0
.6	21.39	497.0
.8	21.39	497.0
1.0	21.39	497.0
1.5	21.39	496.9
2.0	21.38	496.9
2.5	21.38	496.6
3.0	21.39	496.4
3.5	21.40	496.4
4.0	21.40	496.5
4.5	21.41	496.1
5.0	21.40	496.1
6.0	21.27	495.6
7.0	21.25	494.9
8.0	21.22	494.5
9.0	21.18	495.0
10.0	21.13	495.6
11.0	21.00	496.4
12.0	20.86	498.5
12.3		
12.5		
12.7		
13.0	18.16	653.0

TIME 2200

0.0	21.28	498.0
.1	21.29	498.2
.15	21.27	498.5
.2	21.32	497.9
.4	21.32	497.6
.6	21.34	497.5
.8	21.32	497.5
1.0	21.32	497.7
1.5	21.32	497.6
2.0	21.33	497.5
2.5	21.33	497.3
3.0	21.35	497.0
3.5	21.34	497.1
4.0	21.33	497.0
4.5	21.32	496.9
5.0	21.32	496.7
6.0	21.29	496.5
7.0	21.26	498.4
8.0	21.24	496.2
9.0	21.23	495.5
10.0	21.11	496.3
11.0	21.05	496.6
12.0	20.93	499.0
12.3	20.21	530.1
12.5	19.93	541.6
[illegible]	[illegible]	[illegible]

TIME 2350

0.0	21.22	498.0
.1	21.26	497.6
.15	21.27	497.5
.2	21.29	497.3
.4	21.30	497.2
.6	21.29	497.3
.8	21.30	497.2
1.0	21.29	497.3
1.5	21.29	497.2
2.0	21.30	497.2
2.5	21.30	497.1
3.0	21.30	497.1
3.5	21.31	497.1
4.0	21.32	497.0
4.5	21.30	497.2
5.0	21.31	496.5
6.0	21.28	496.7
7.0	21.26	496.4
8.0	21.24	496.0
9.0	21.23	496.1
10.0	21.14	497.2
11.0	21.10	497.0
12.0	21.05	497.5
12.3	20.18	542.9
12.5		
12.7	19.83	554.2
13.0	18.04	658.7

TIME 200

0.0	21.15	500.7
.1	21.18	500.3
.15	21.21	500.6
.2	21.20	500.7
.4	21.22	500.5
.6	21.23	500.4
.8	21.24	500.3
1.0	21.23	500.3
1.5	21.22	500.5
2.0	21.23	500.4
2.5	21.23	500.4
3.0	21.23	499.8
3.5	21.22	499.9
4.0	21.23	499.8
4.5	21.23	499.7
5.0	21.24	499.7
6.0	21.23	499.1
7.0	21.27	498.8
8.0	21.26	498.3
9.0	21.24	497.8
10.0	21.15	498.3
11.0	21.14	498.4
12.0	21.09	499.5
12.3	20.64	507.

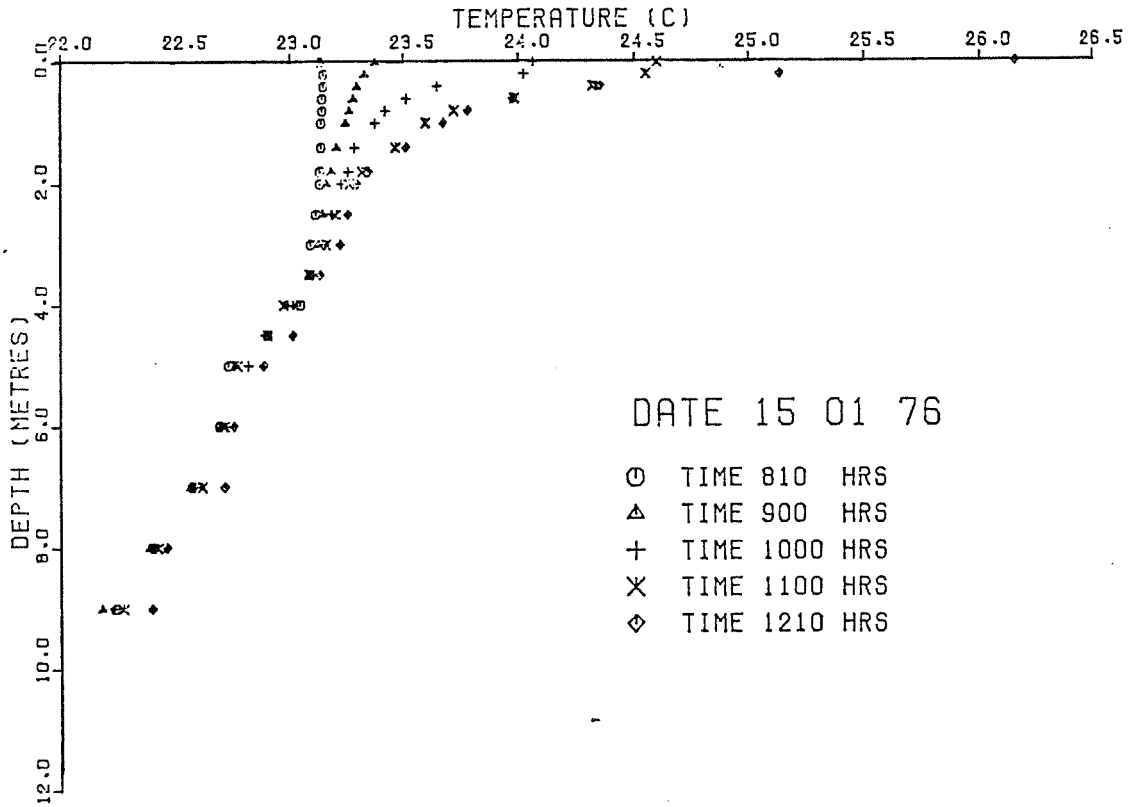

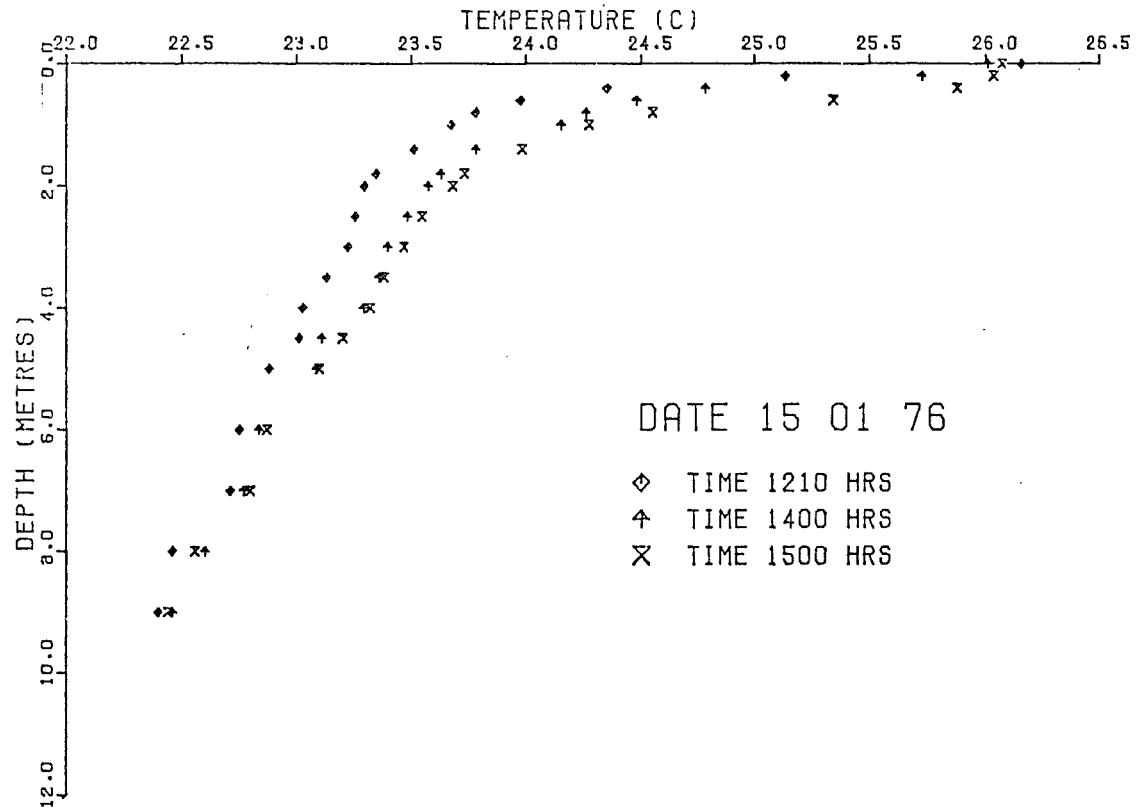

A5 Computer Plots of Measured Temperature Profiles.

Date and times for each symbol are as printed on the plots. The last profile of each plot appears on the next plot for comparison.

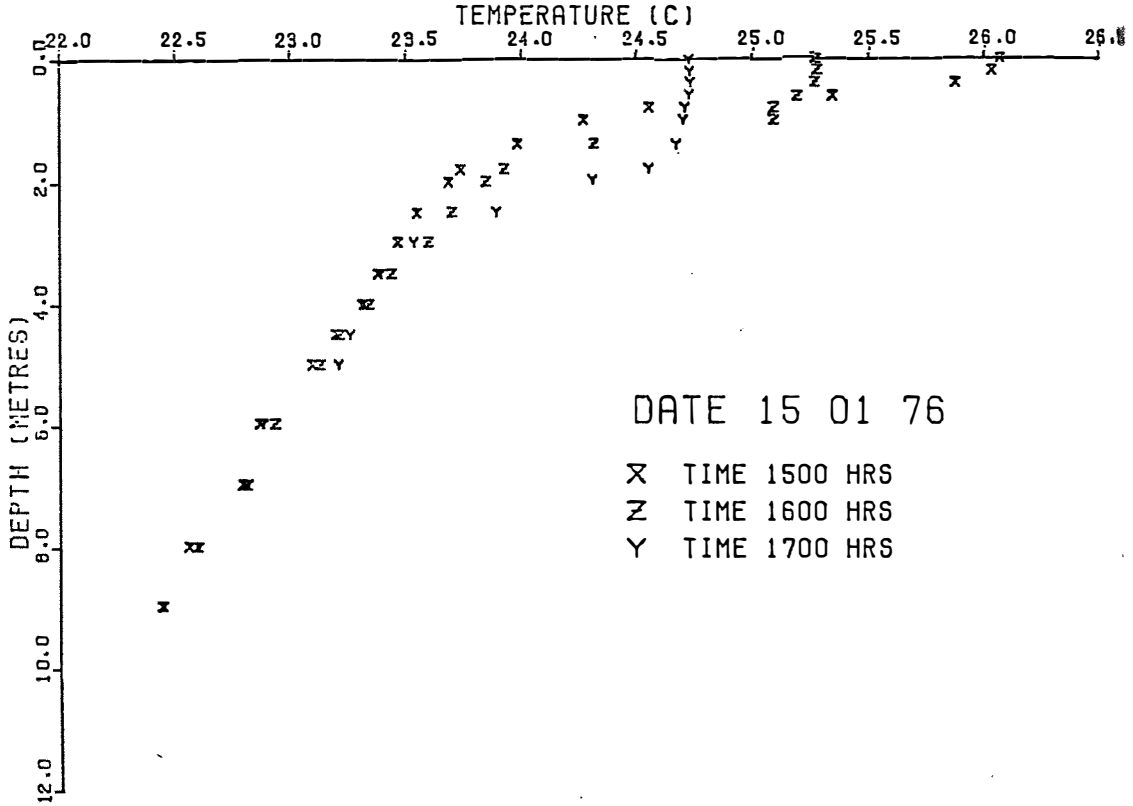
TEMPERATURE (C)
22.0
22.5
23.0
23.5
24.0
24.5
25.0
25.5
26.0
0.0
2.0
4.0
6.0
8.0
10.0
12.0
DEPTH (METRES)
DATE 15 01 76
X TIME 1500 HRS
Z TIME 1600 HRS
Y TIME 1700 HRS

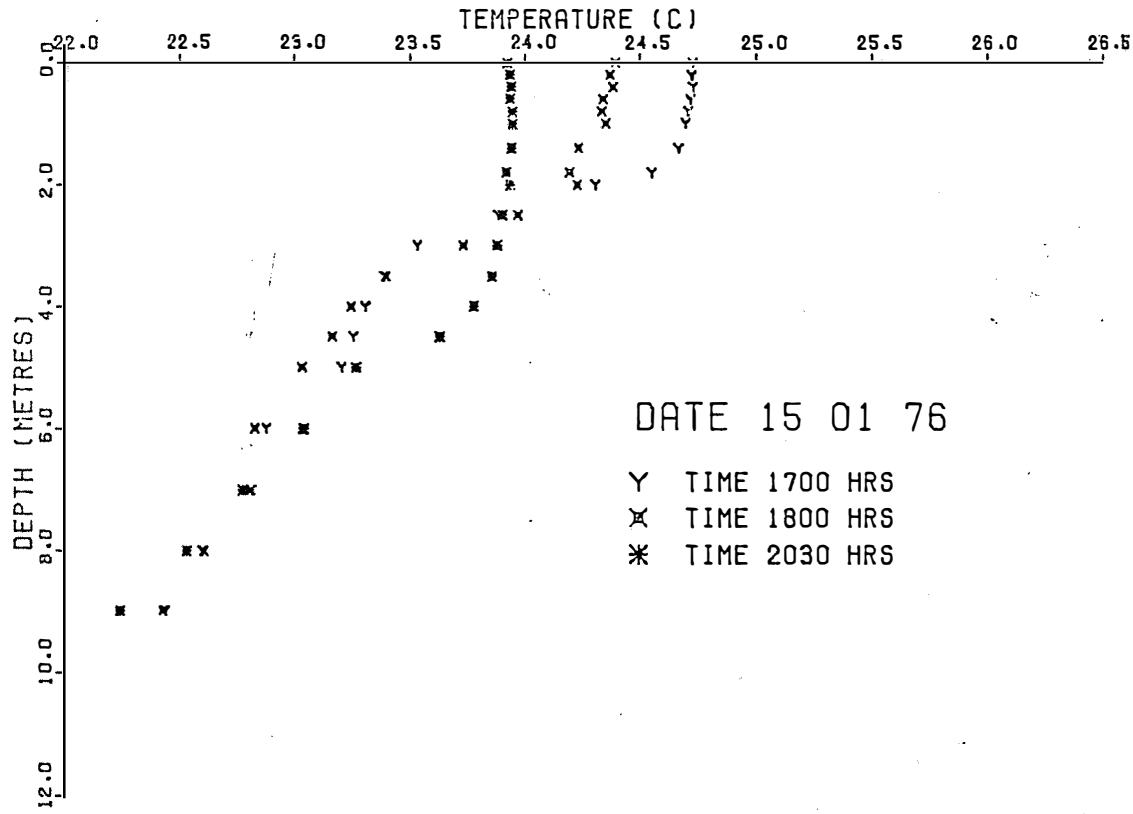
TEMPERATURE (C)
22.0
22.5
23.0
23.5
24.0
24.5
25.0
25.5
26.0
0.0
2.0
4.0
6.0
8.0
10.0
12.0
DEPTH (METRES)
DATE 15 01 76
Y TIME 1700 HRS
TIME 1800 HRS
TIME 2030 HRS

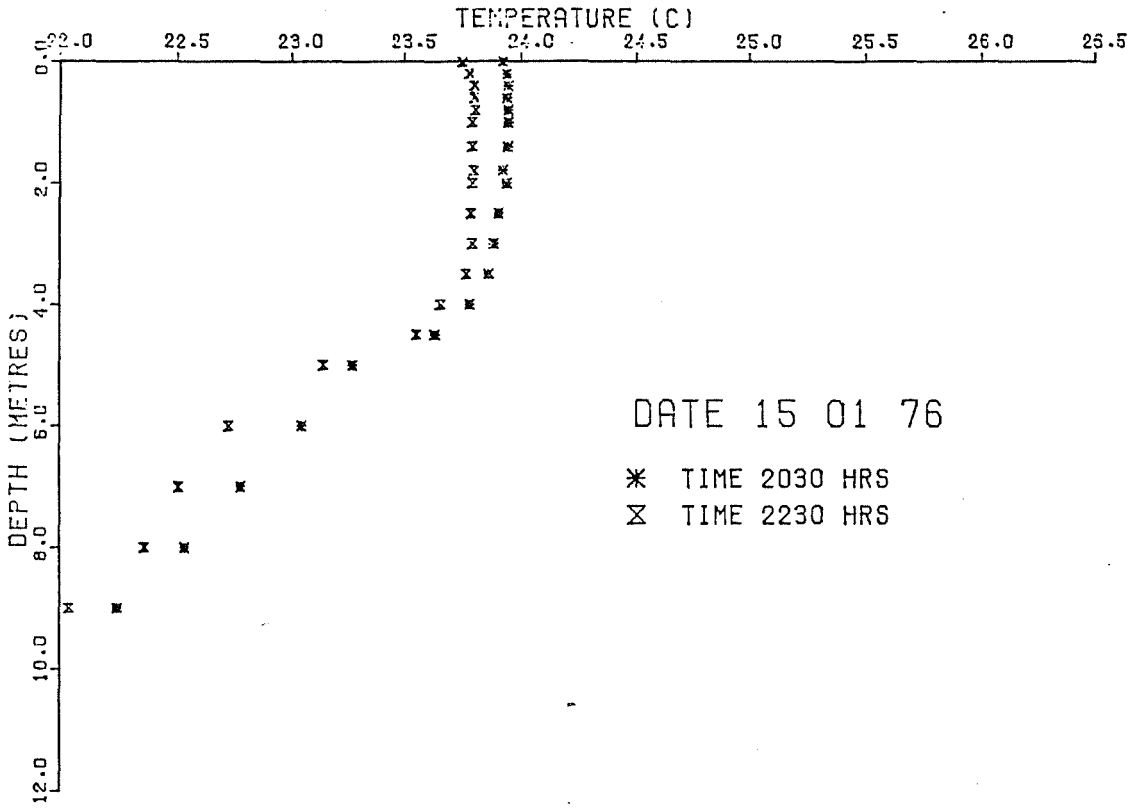
TEMPERATURE (C)
22.0
22.5
23.0
23.5
24.0
24.5
25.0
25.5
26.0
26.5
DEPTH (METRES)
0.0
2.0
4.0
6.0
8.0
10.0
12.0
DATE 15 01 76
TIME 2030 HRS
TIME 2230 HRS

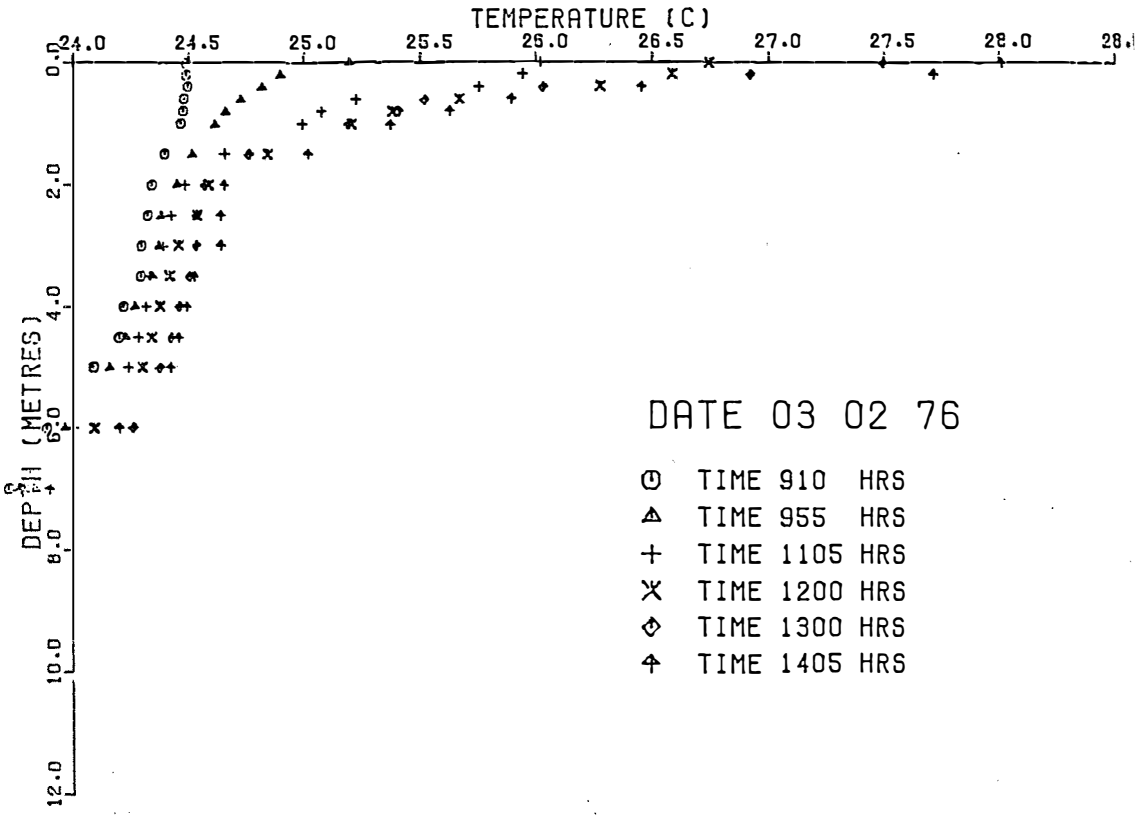
TEMPERATURE (C)
24.0
24.5
25.0
25.5
26.0
26.5
27.0
27.5
28.0
0.0
2.0
4.0
6.0
8.0
10.0
12.0
DEPTH (METRES)
DATE 03 02 76
TIME 910 HRS
TIME 955 HRS
TIME 1105 HRS
TIME 1200 HRS
TIME 1300 HRS
TIME 1405 HRS

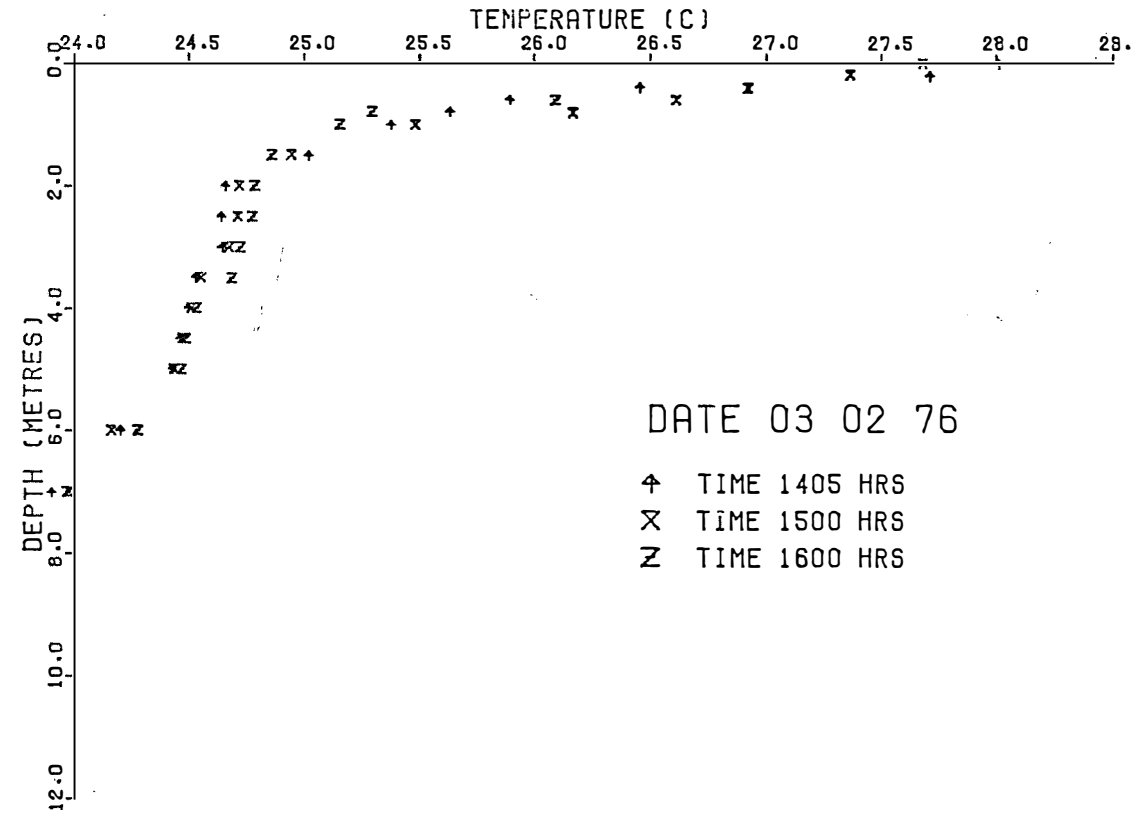
TEMPERATURE (C)
24.0
24.5
25.0
25.5
26.0
26.5
27.0
27.5
28.0
0.0
2.0
4.0
6.0
8.0
10.0
12.0
DEPTH (METRES)
DATE 03 02 76
TIME 1405 HRS
TIME 1500 HRS
TIME 1600 HRS

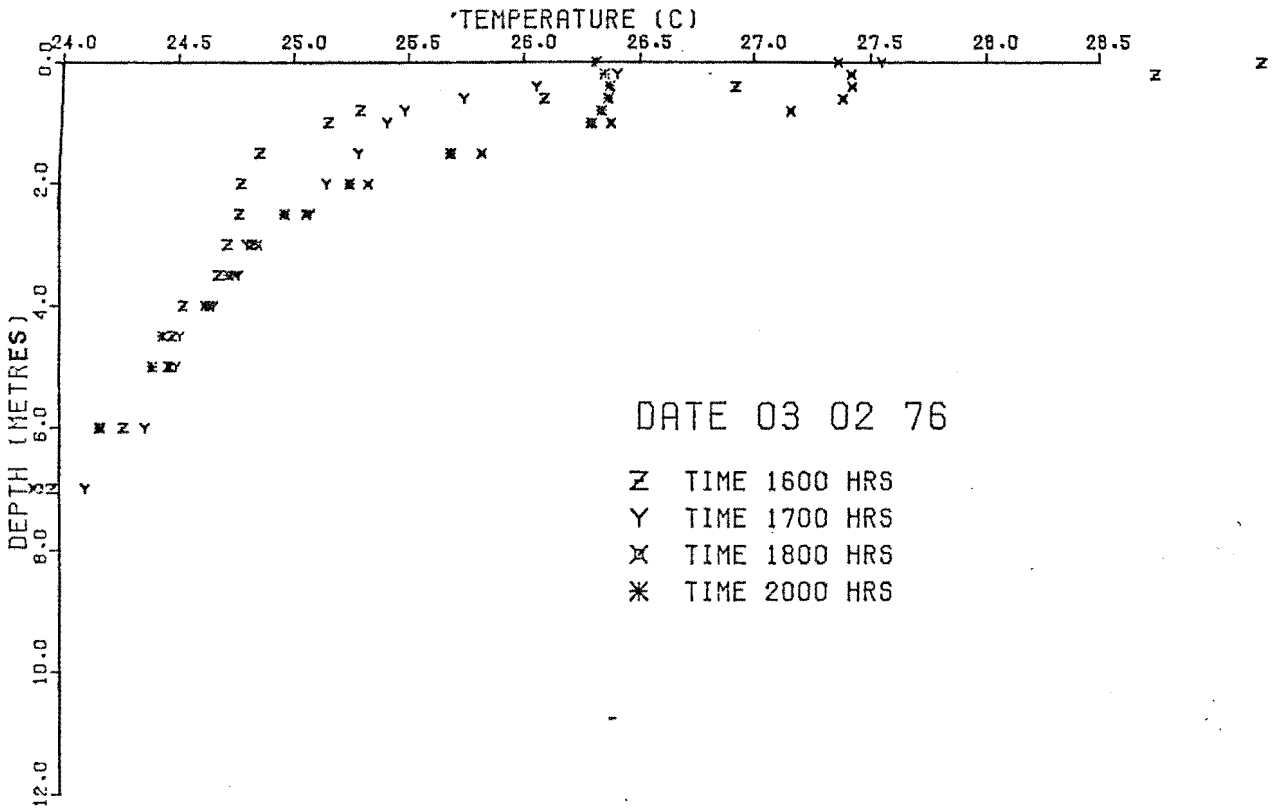
TEMPERATURE (C)
24.0
24.5
25.0
25.5
26.0
26.5
27.0
27.5
28.0
28.5
DEPTH (METRES)
0.0
2.0
4.0
6.0
8.0
10.0
12.0
DATE 03 02 76
Z TIME 1600 HRS
Y TIME 1700 HRS
X TIME 1800 HRS
* TIME 2000 HRS

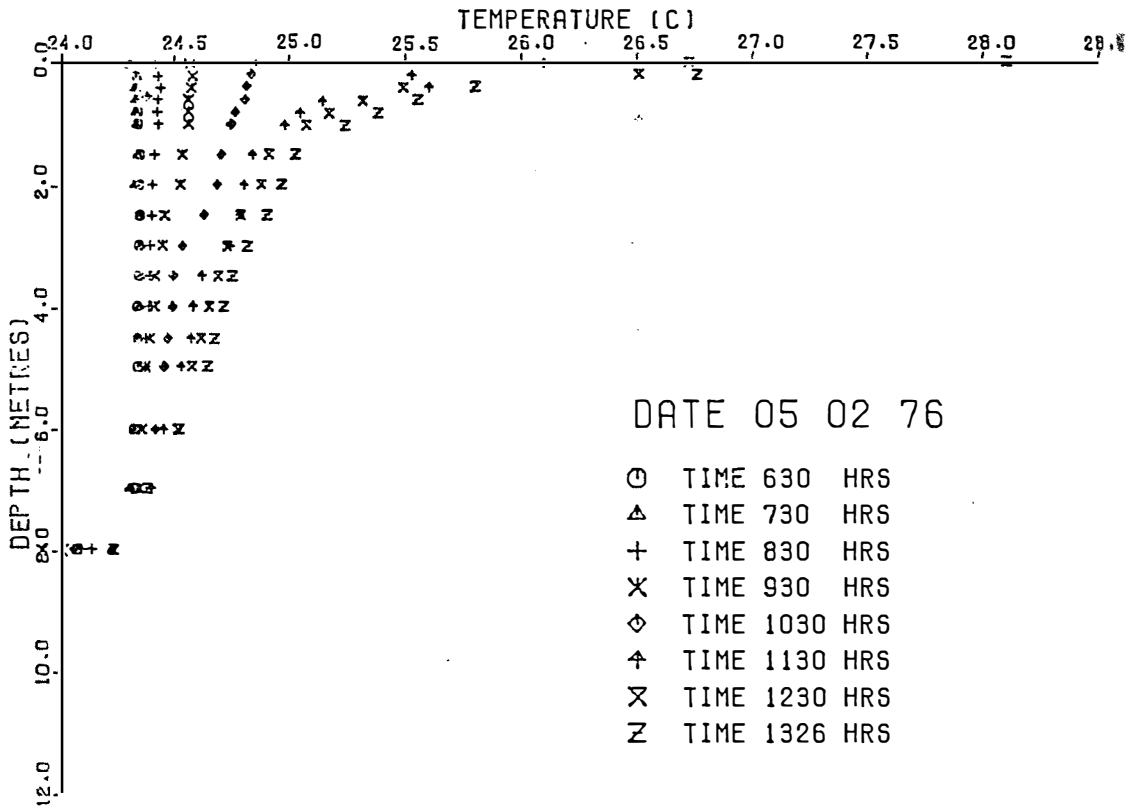
TEMPERATURE (C)
24.0
24.5
25.0
25.5
26.0
26.5
27.0
27.5
28.0
0.0
2.0
4.0
6.0
8.0
10.0
12.0
DEPTH (METRES)
DATE 05 02 76
TIME 630 HRS
TIME 730 HRS
TIME 830 HRS
TIME 930 HRS
TIME 1030 HRS
TIME 1130 HRS
TIME 1230 HRS
TIME 1326 HRS

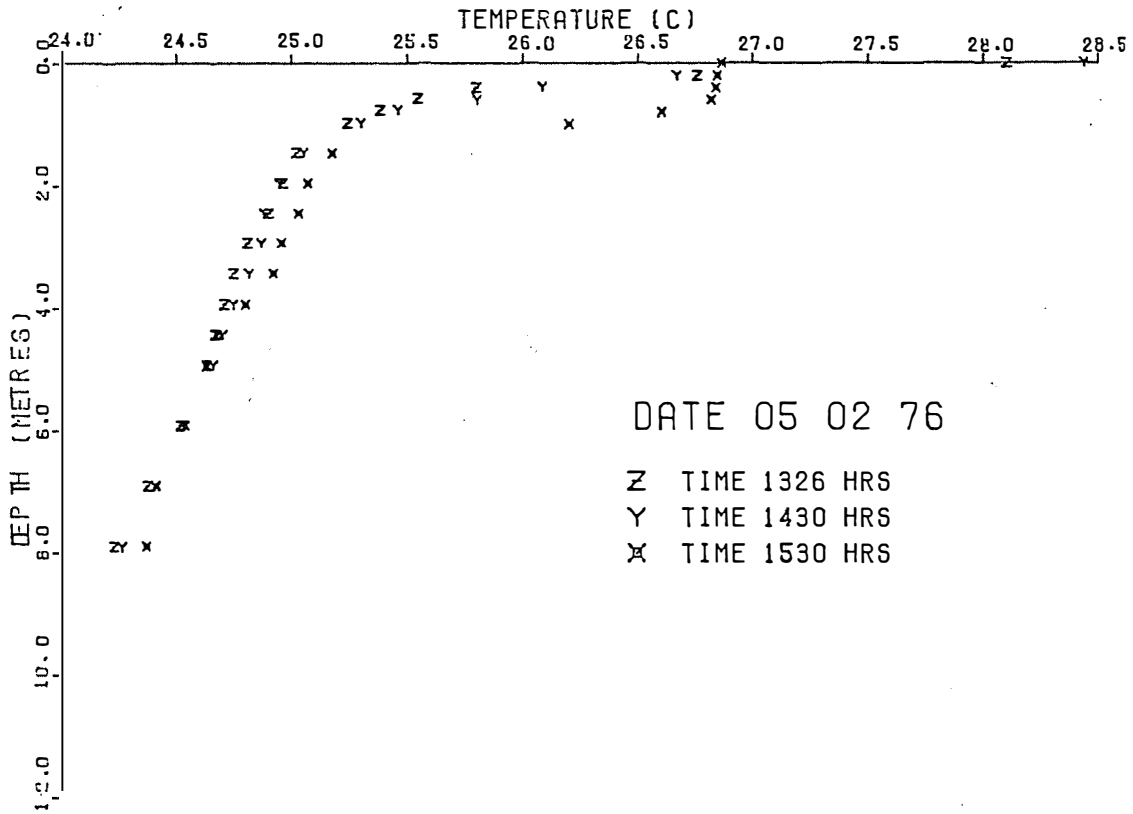
TEMPERATURE (C)
24.0
24.5
25.0
25.5
26.0
26.5
27.0
27.5
28.0
28.5
0.0
2.0
4.0
6.0
8.0
10.0
12.0
DEPTH (METRES)
DATE 05 02 76
TIME 1326 HRS
TIME 1430 HRS
TIME 1530 HRS

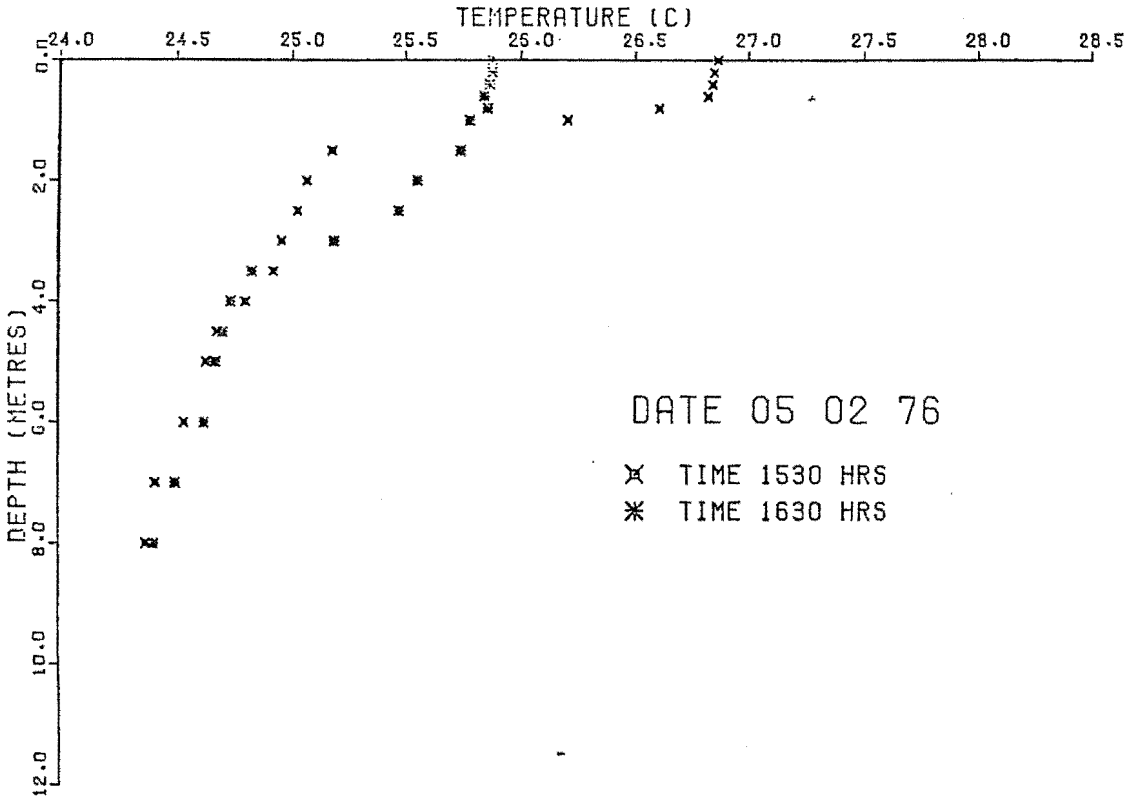
TEMPERATURE (C)
24.0
24.5
25.0
25.5
26.0
26.5
27.0
27.5
28.0
28.5
DEPTH (METRES)
0.0
2.0
4.0
6.0
8.0
10.0
12.0
DATE 05 02 76
TIME 1530 HRS
TIME 1630 HRS

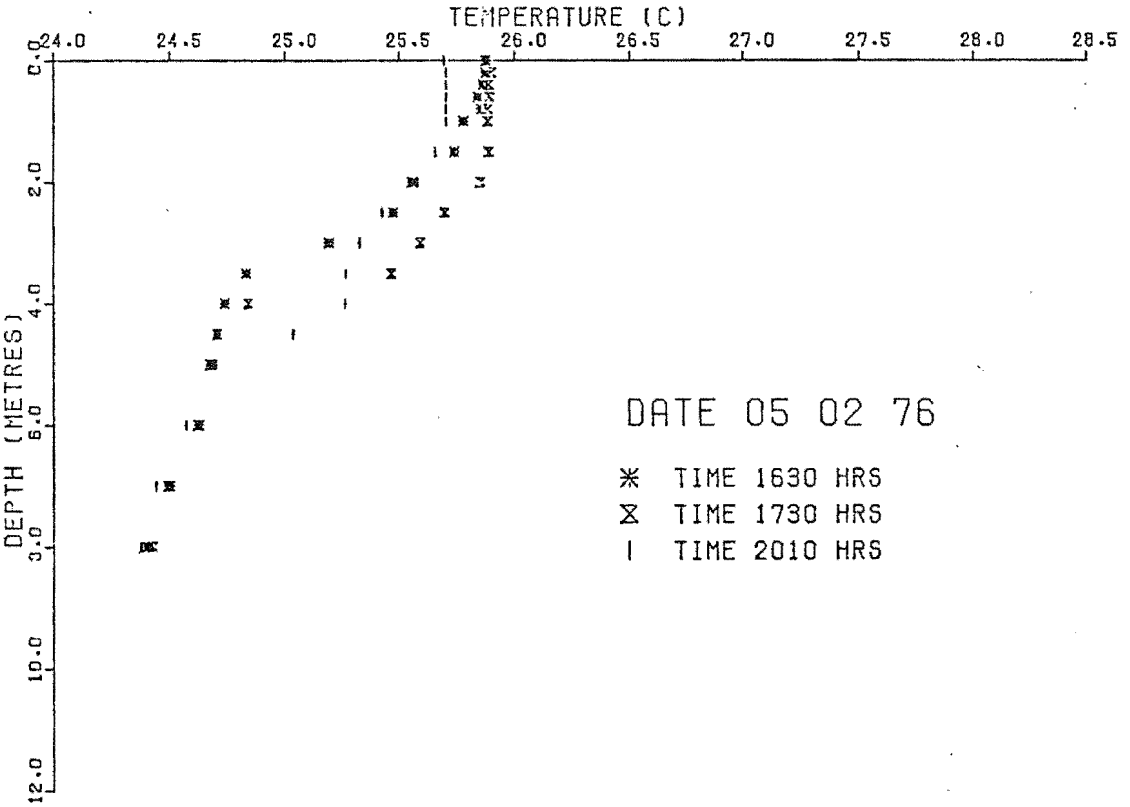
TEMPERATURE (C)
24.0
24.5
25.0
25.5
26.0
26.5
27.0
27.5
28.0
28.5
DEPTH (METRES)
0.0
2.0
4.0
6.0
8.0
10.0
12.0
DATE 05 02 76
TIME 1630 HRS
TIME 1730 HRS
TIME 2010 HRS

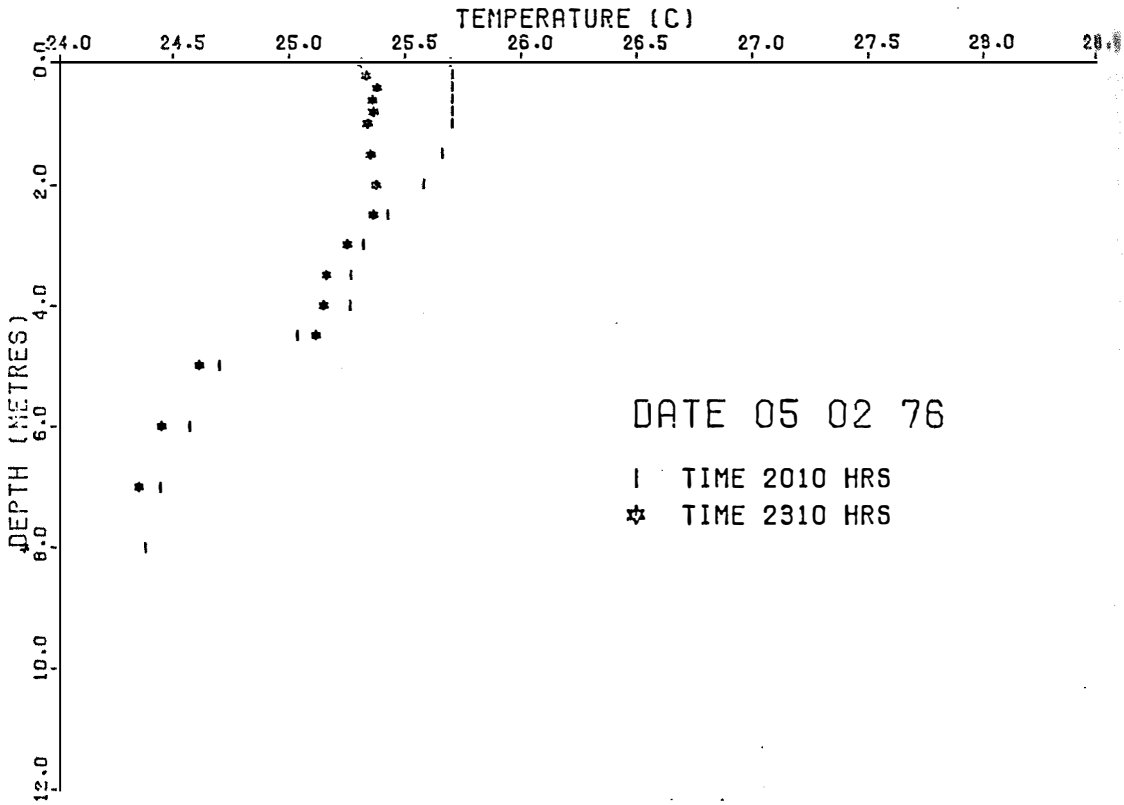
TEMPERATURE (C)
24.0
24.5
25.0
25.5
26.0
26.5
27.0
27.5
28.0
0.0
2.0
4.0
6.0
8.0
10.0
12.0
DEPTH (METRES)
DATE 05 02 76
TIME 2010 HRS
TIME 2310 HRS

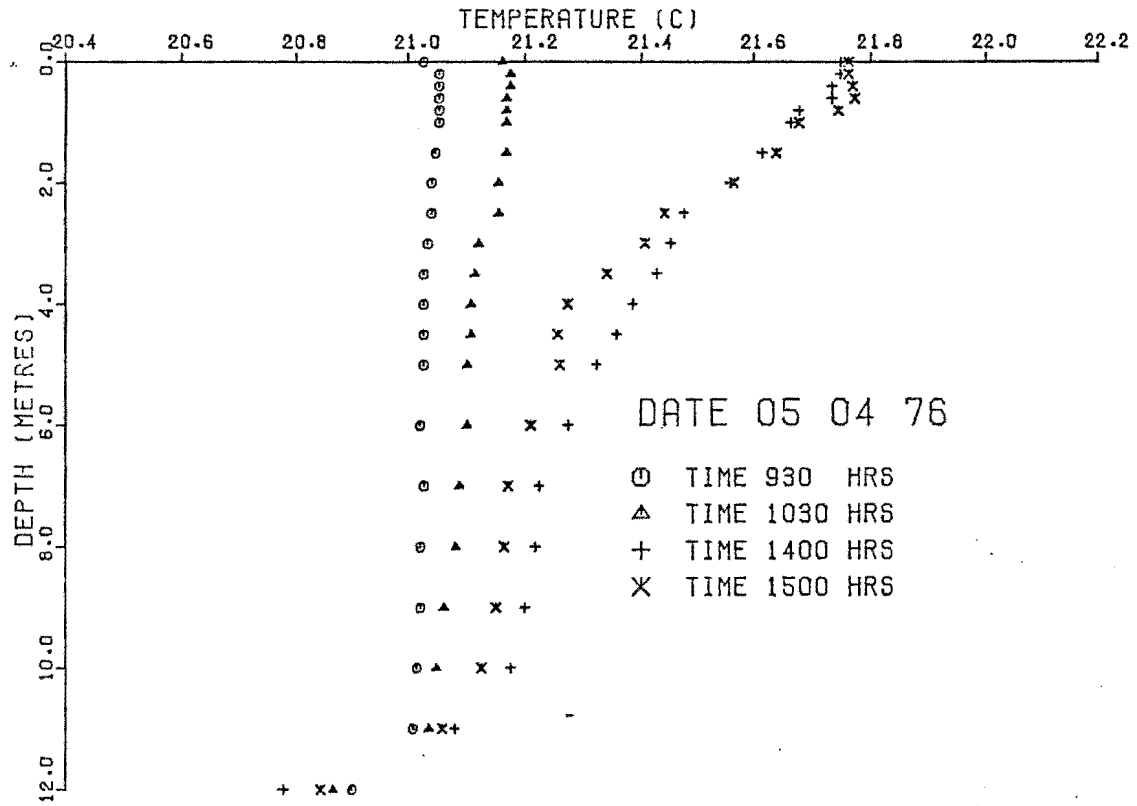
TEMPERATURE (C)
20.4
20.6
20.8
21.0
21.2
21.4
21.6
21.8
22.0
22.2
DEPTH (METRES)
0.0
2.0
4.0
6.0
8.0
10.0
12.0
DATE 05 04 76
TIME 930 HRS
TIME 1030 HRS
TIME 1400 HRS
TIME 1500 HRS

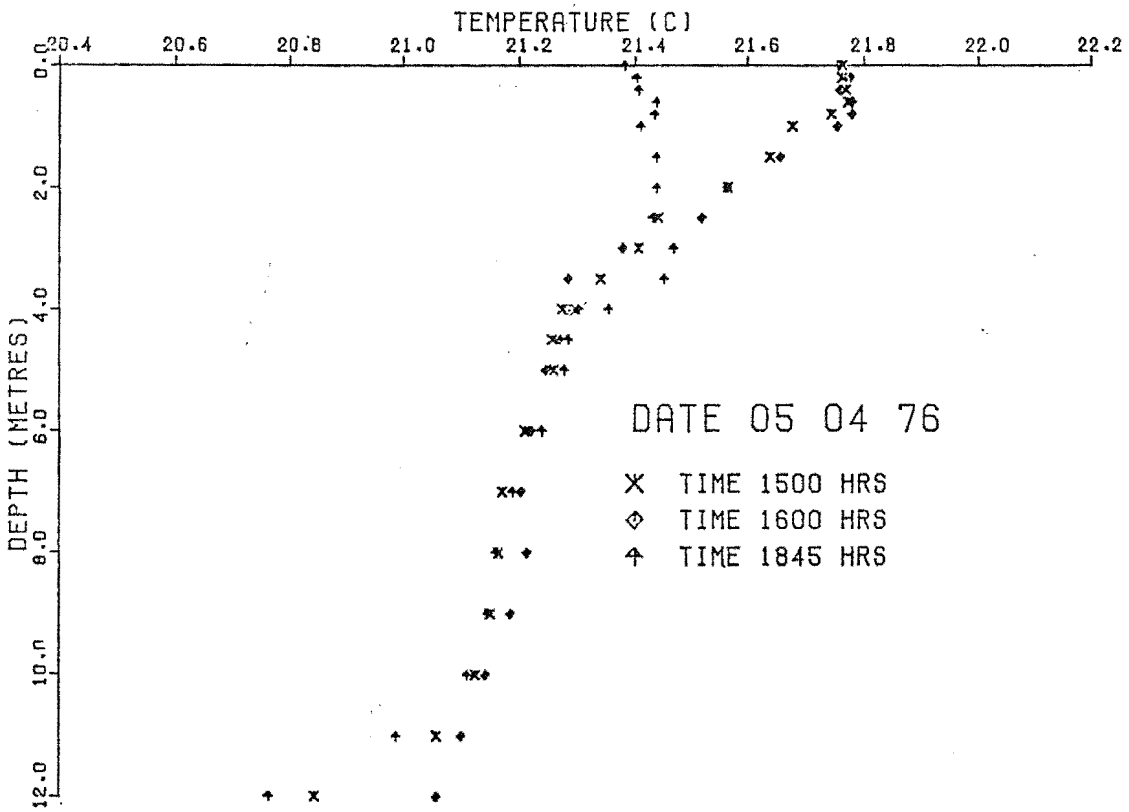
TEMPERATURE (C)
20.4
20.6
20.8
21.0
21.2
21.4
21.6
21.8
22.0
22.2
DEPTH (METRES)
0.0
2.0
4.0
6.0
8.0
10.0
12.0
DATE 05 04 76
TIME 1500 HRS
TIME 1600 HRS
TIME 1845 HRS

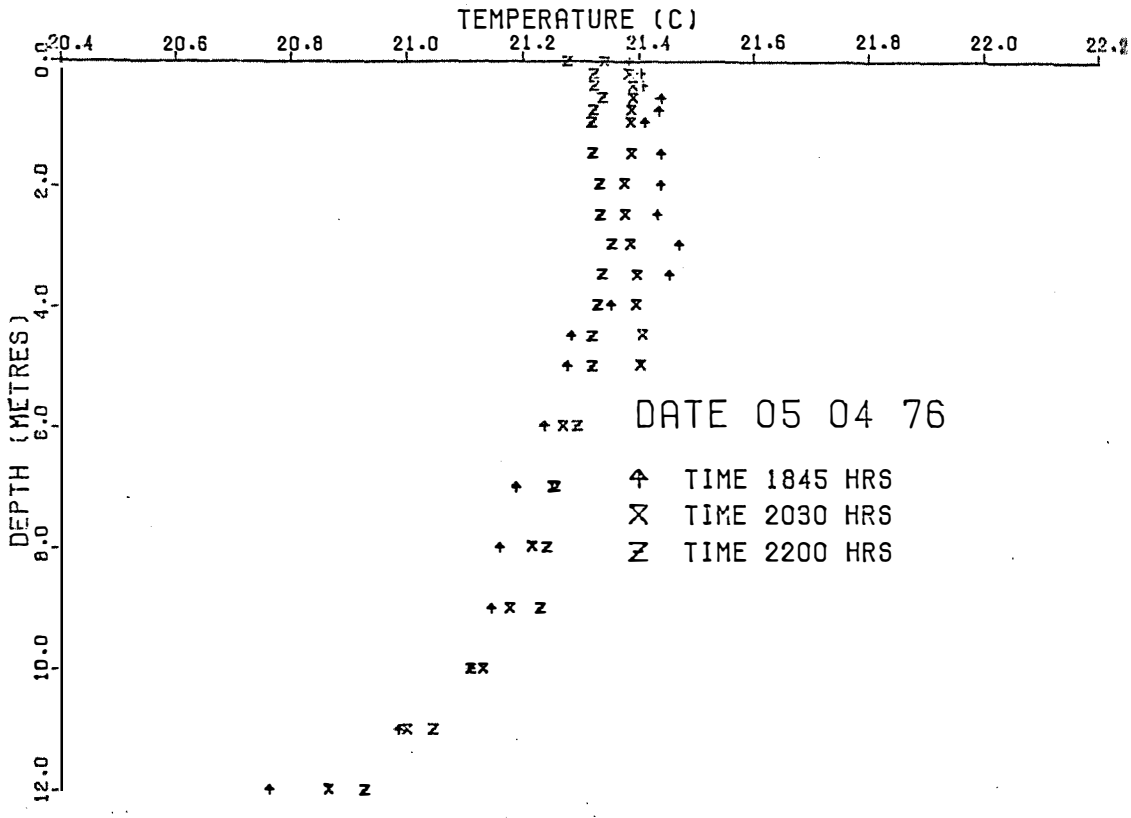
TEMPERATURE (C)
20.4
20.6
20.8
21.0
21.2
21.4
21.6
21.8
22.0
22.2
DEPTH (METRES)
0.0
2.0
4.0
6.0
8.0
10.0
12.0
DATE 05 04 76
TIME 1845 HRS
TIME 2030 HRS
TIME 2200 HRS

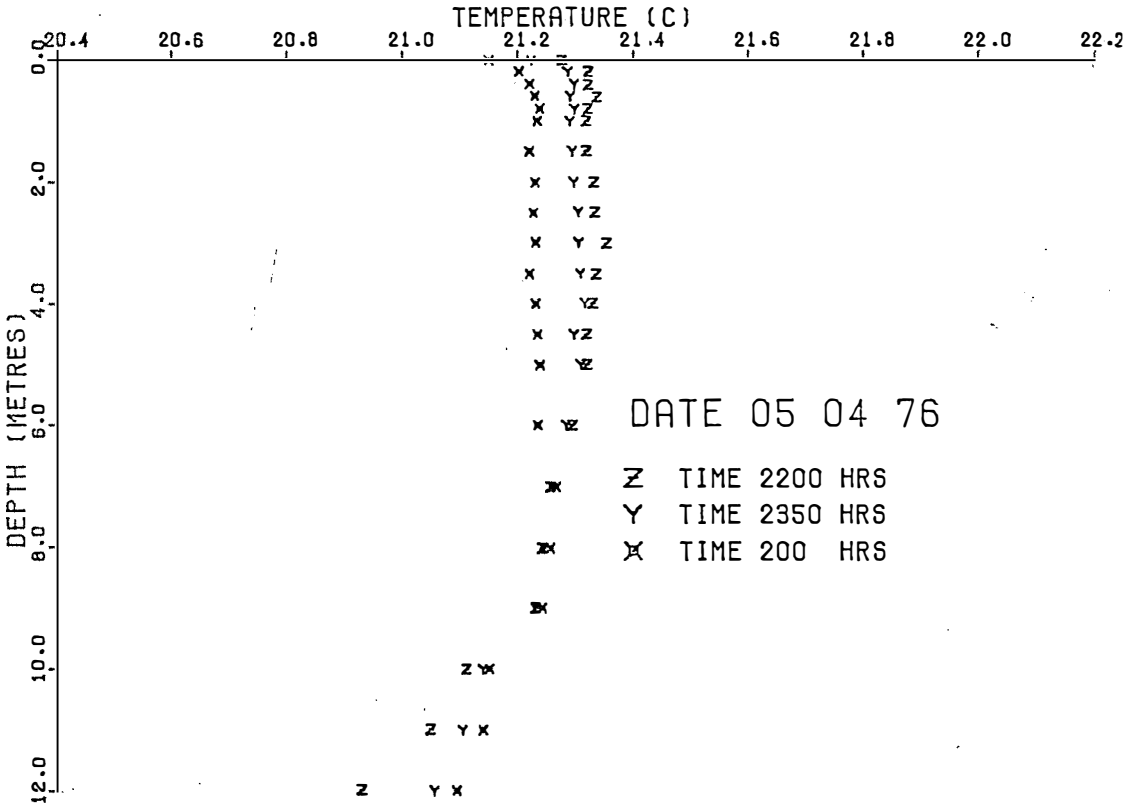
TEMPERATURE (C)
20.4
20.6
20.8
21.0
21.2
21.4
21.6
21.8
22.0
22.2
DEPTH (METRES)
0.0
2.0
4.0
6.0
8.0
10.0
12.0
DATE 05 04 76
TIME 2200 HRS
TIME 2350 HRS
TIME 200 HRS

APPENDIX B: PROGRAM FLOWCHARTS

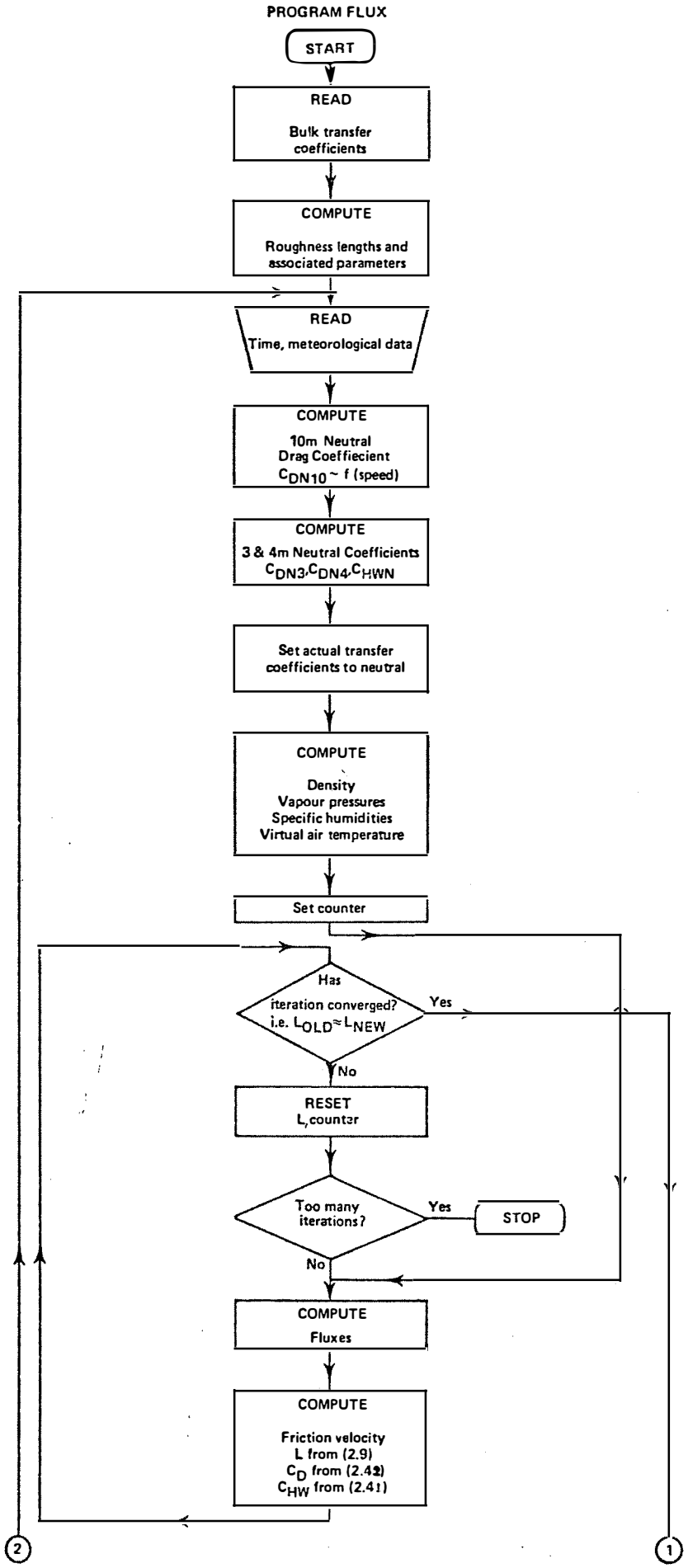

B1 Flowchart for Program FLUX

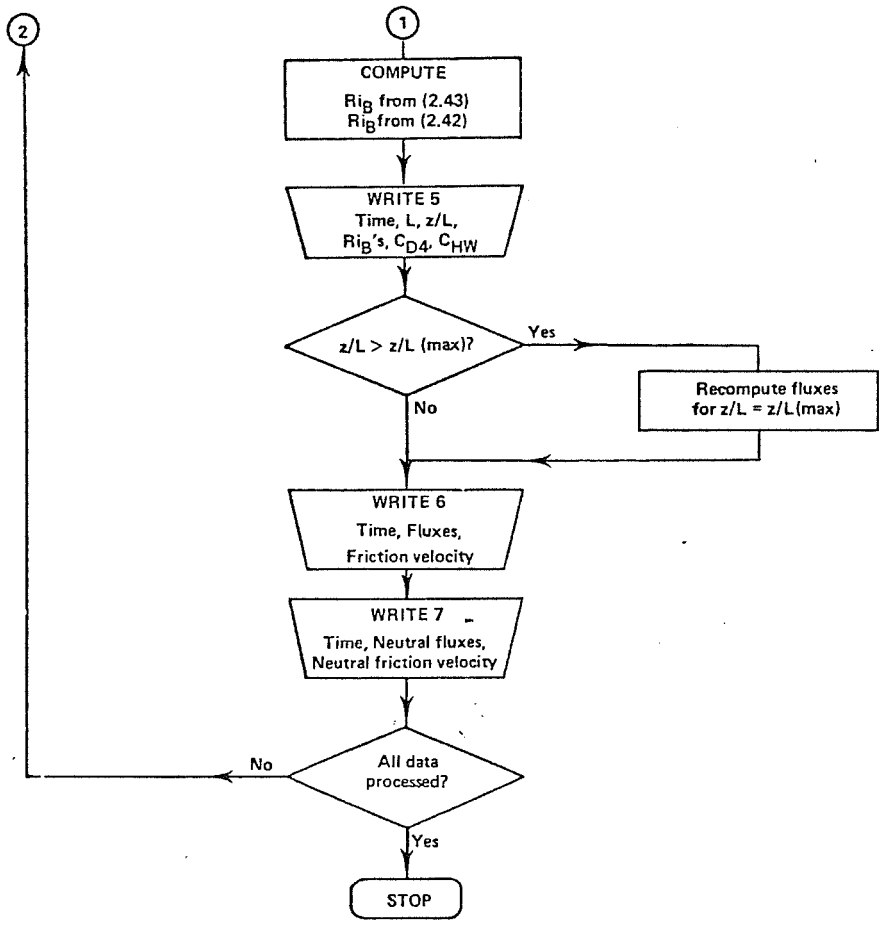
2
1
COMPUTE
Ri_B from (2.43)
Ri_B from (2.42)
WRITE 5
Time, L, z/L,
Ri_B's, C_{D4}, C_{HW}
z/L > z/L (max)?
Yes
No
Recompute fluxes
for z/L = z/L(max)
WRITE 6
Time, Fluxes,
Friction velocity
WRITE 7
Time, Neutral fluxes,
Neutral friction velocity
All data
processed?
No
Yes
STOP

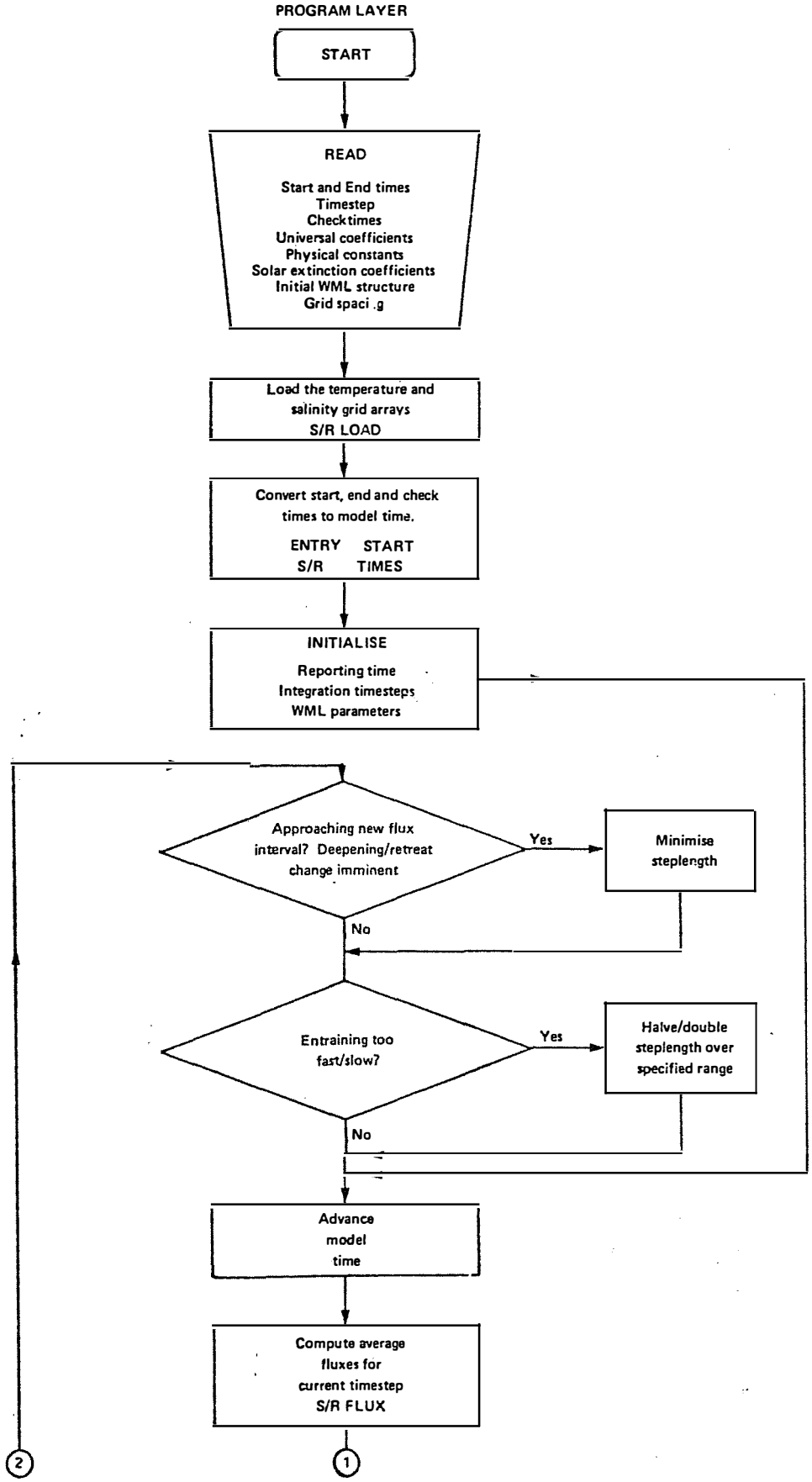

B2 Flowchart for the Model LAYER

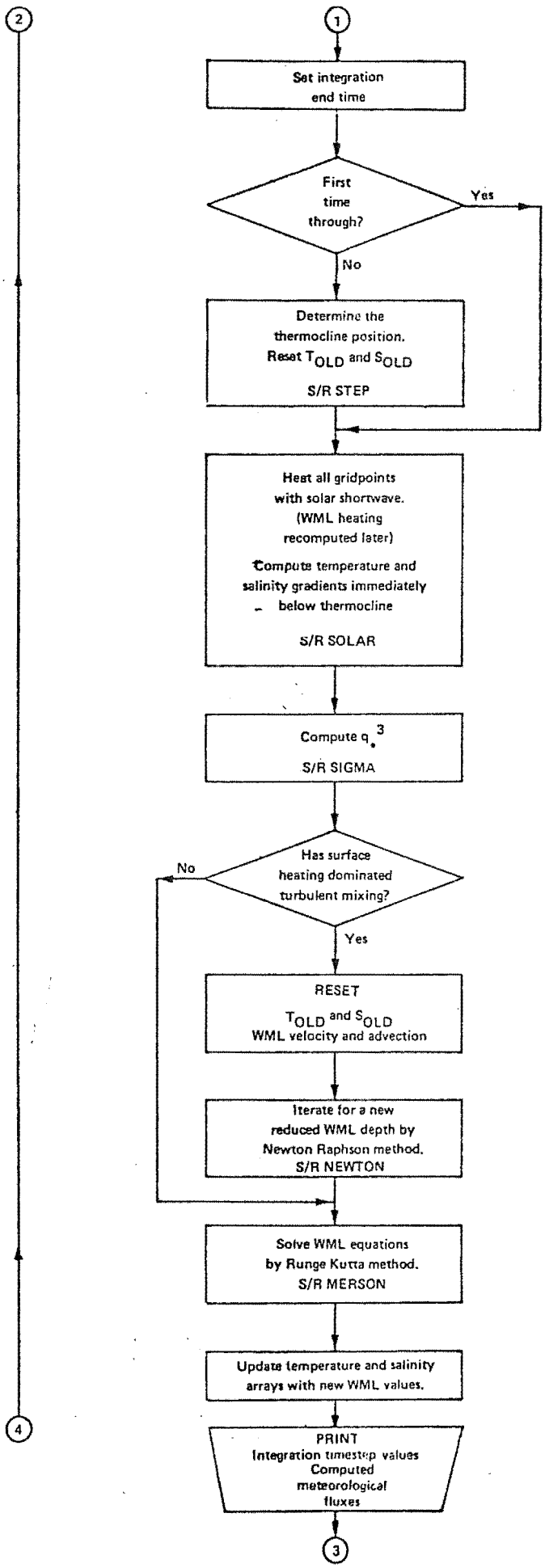
2
1
Set integration end time
First time through?
Yes
No
Determine the thermocline position. Reset T_{OLD} and S_{OLD}
S/R STEP
Heat all gridpoints with solar shortwave. (WML heating recomputed later)
Compute temperature and salinity gradients immediately below thermocline
S/R SOLAR
Compute q_*^3
S/R SIGMA
Has surface heating dominated turbulent mixing?
No
Yes
RESET
T_{OLD} and S_{OLD}
WML velocity and advection
Iterate for a new reduced WML depth by Newton Raphson method.
S/R NEWTON
Solve WML equations by Runge Kutta method.
S/R MERSON
Update temperature and salinity arrays with new WML values.
PRINT
Integration timestep values
Computed meteorological fluxes
4
3

B2.2

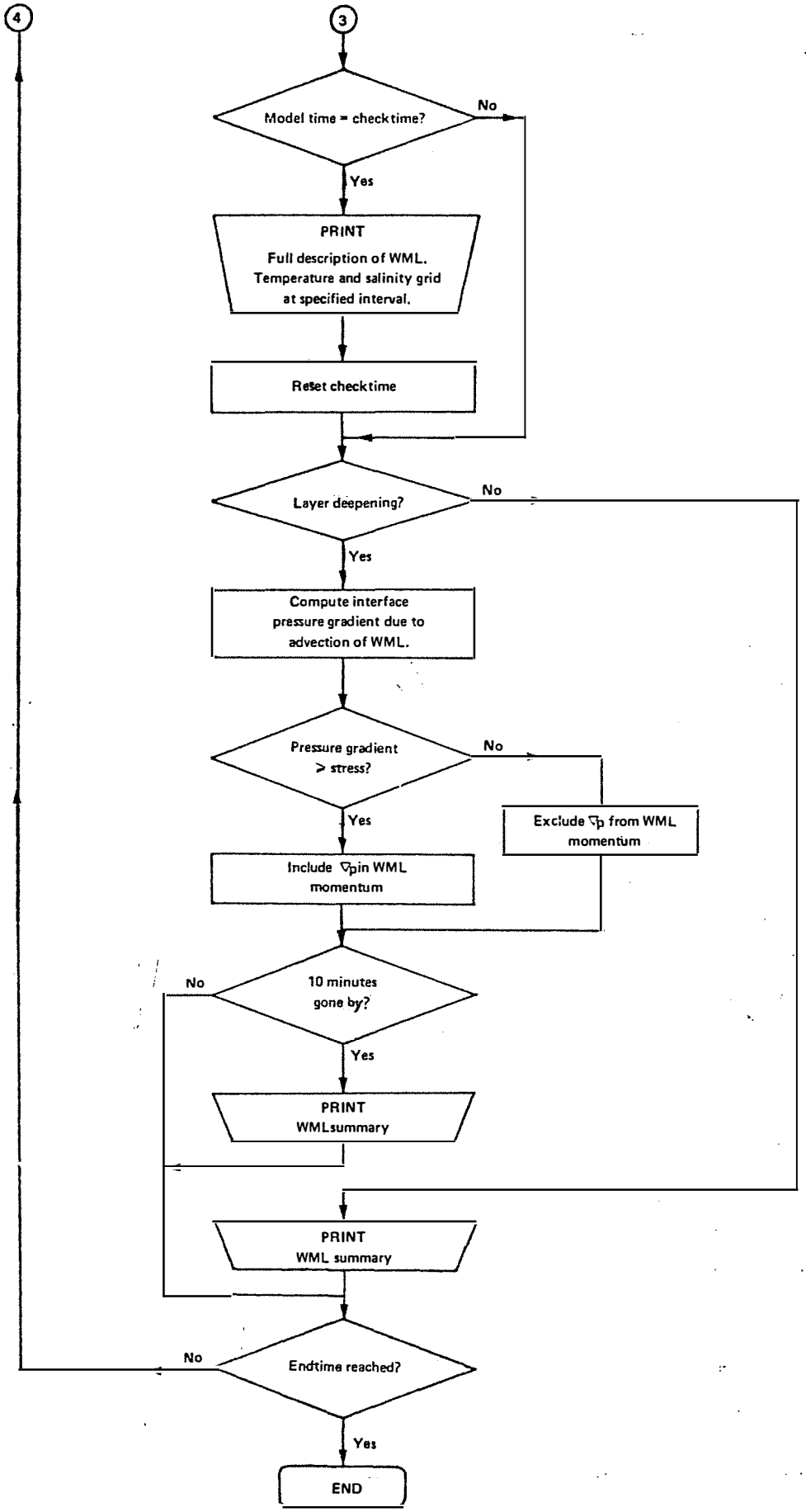
4
3
Model time = checktime?
No
Yes
PRINT
Full description of WML.
Temperature and salinity grid
at specified interval.
Reset checktime
Layer deepening?
No
Yes
Compute interface
pressure gradient due to
advection of WML.
Pressure gradient
> stress?
No
Yes
Exclude ∇p from WML
momentum
Include ∇p in WML
momentum
No
10 minutes
gone by?
Yes
PRINT
WMLsummary
PRINT
WML summary
No
Endtime reached?
Yes
END

B2.3

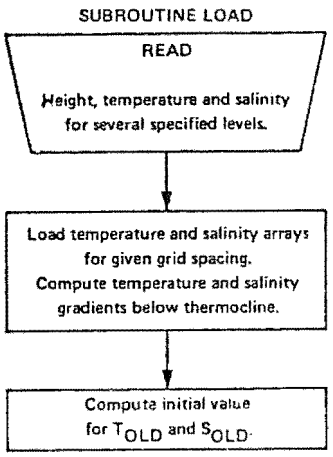
SUBROUTINE LOAD
READ
Height, temperature and salinity for several specified levels.
Load temperature and salinity arrays for given grid spacing. Compute temperature and salinity gradients below thermocline.
Compute initial value for T_{OLD} and S_{OLD}

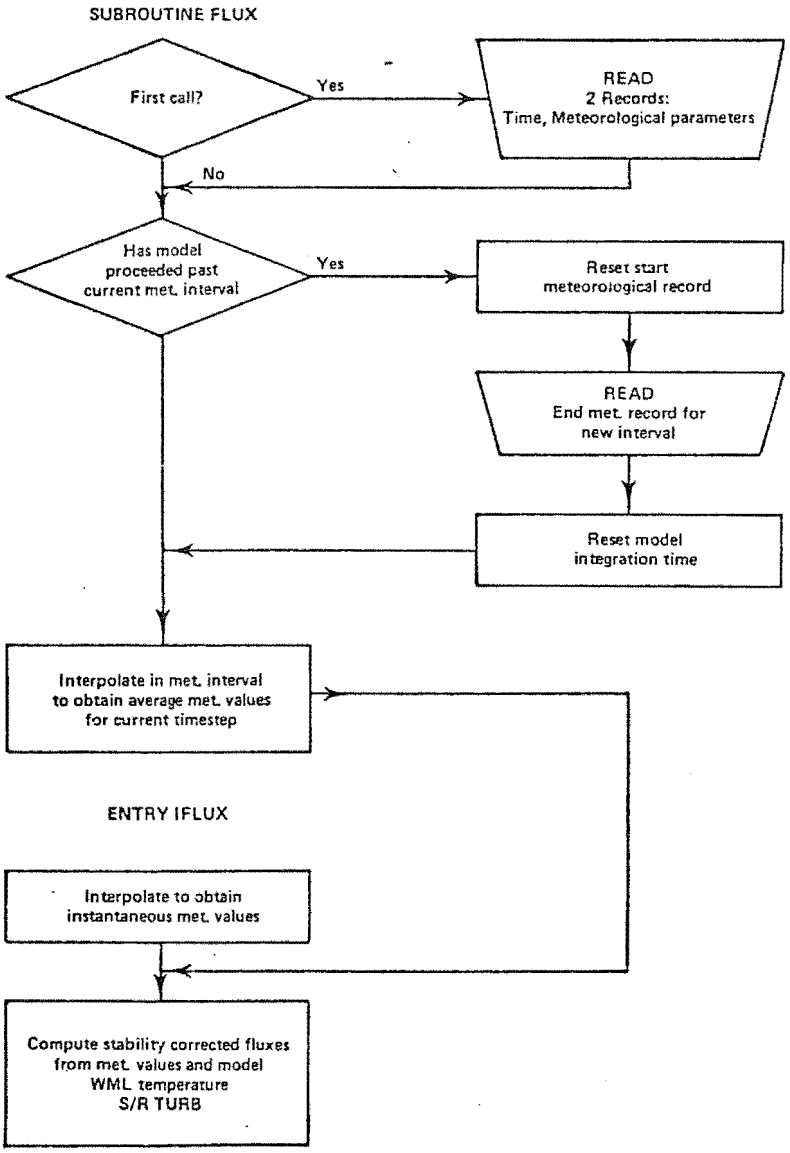
SUBROUTINE FLUX
First call?
Yes
READ
2 Records:
Time, Meteorological parameters
No
Has model proceeded past current met. interval
Yes
Reset start meteorological record
READ
End met. record for new interval
Reset model integration time
Interpolate in met. interval to obtain average met. values for current timestep
ENTRY IFLUX
Interpolate to obtain instantaneous met. values
Compute stability corrected fluxes from met. values and model WML temperature
S/R TURB

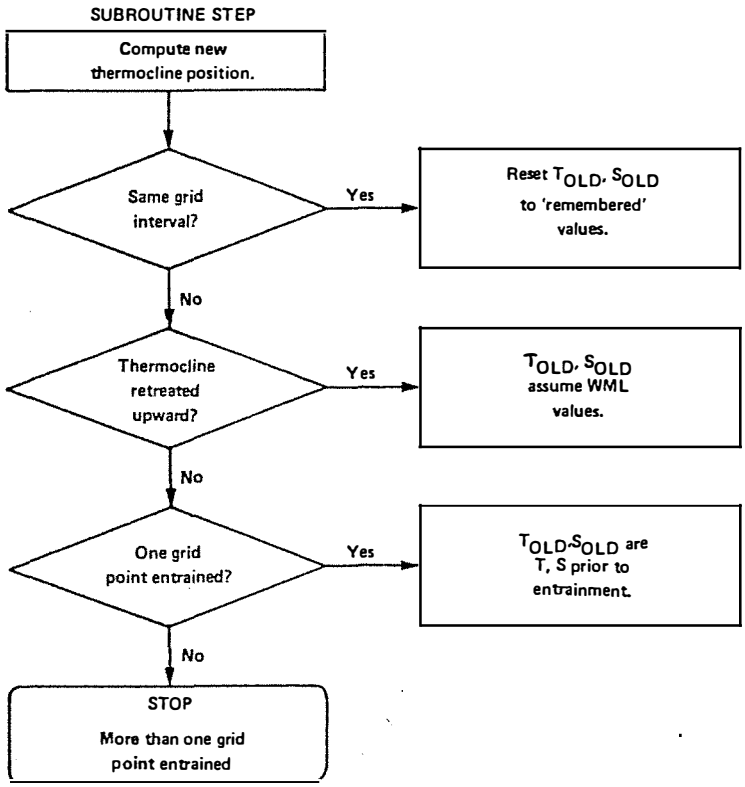
SUBROUTINE STEP
Compute new thermocline position.
Same grid interval?
Yes
Reset T_{OLD}, S_{OLD} to 'remembered' values.
No
Thermocline retreated upward?
Yes
T_{OLD}, S_{OLD} assume WML values.
No
One grid point entrained?
Yes
T_{OLD},S_{OLD} are T, S prior to entrainment.
No
STOP
More than one grid point entrained

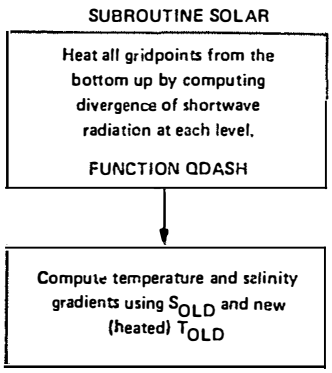
SUBROUTINE SOLAR
Heat all gridpoints from the bottom up by computing divergence of shortwave radiation at each level.
FUNCTION QDASH
Compute temperature and salinity gradients using S_{OLD} and new (heated) T_{OLD}

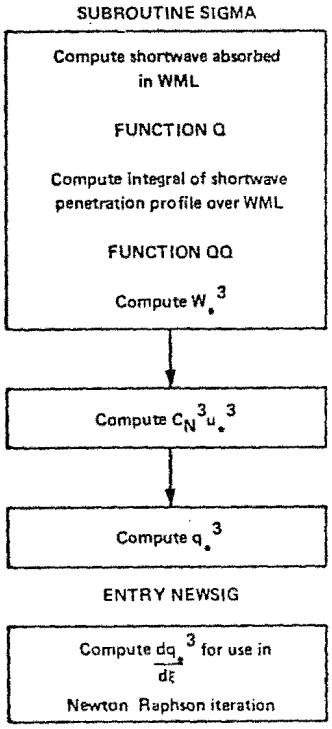
SUBROUTINE SIGMA
Compute shortwave absorbed in WML
FUNCTION Q
Compute integral of shortwave penetration profile over WML
FUNCTION QQ
Compute W_*^3
Compute $C_N^3 u_*^3$
Compute q_*^3
ENTRY NEWSIG
Compute $\frac{dq_*^3}{d\xi}$ for use in Newton Raphson iteration

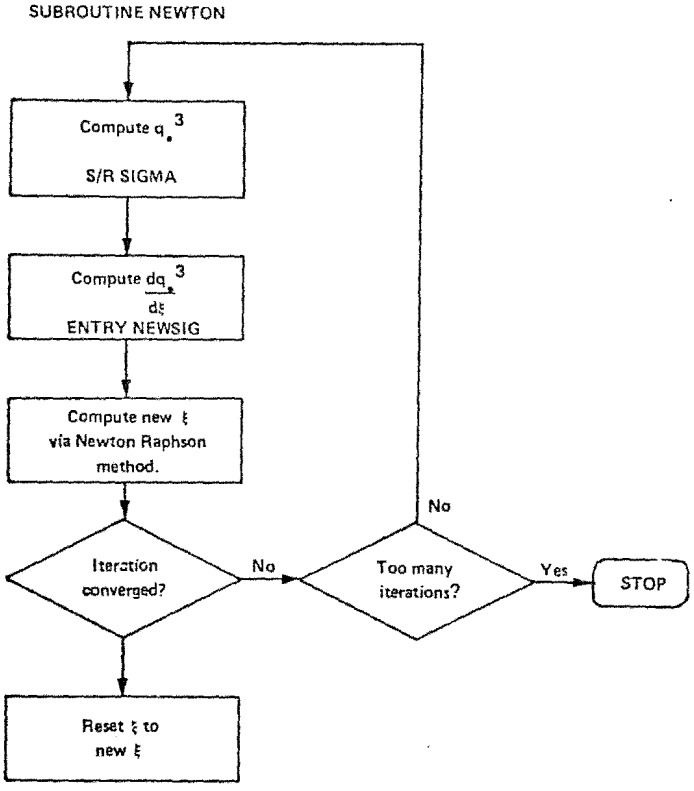
SUBROUTINE NEWTON
Compute q_*^3
S/R SIGMA
Compute $\frac{dq_*^3}{d\xi}$
ENTRY NEWSIG
Compute new ξ via Newton Raphson method.
Iteration converged?
No
Too many iterations?
Yes
STOP
No
Reset ξ to new ξ

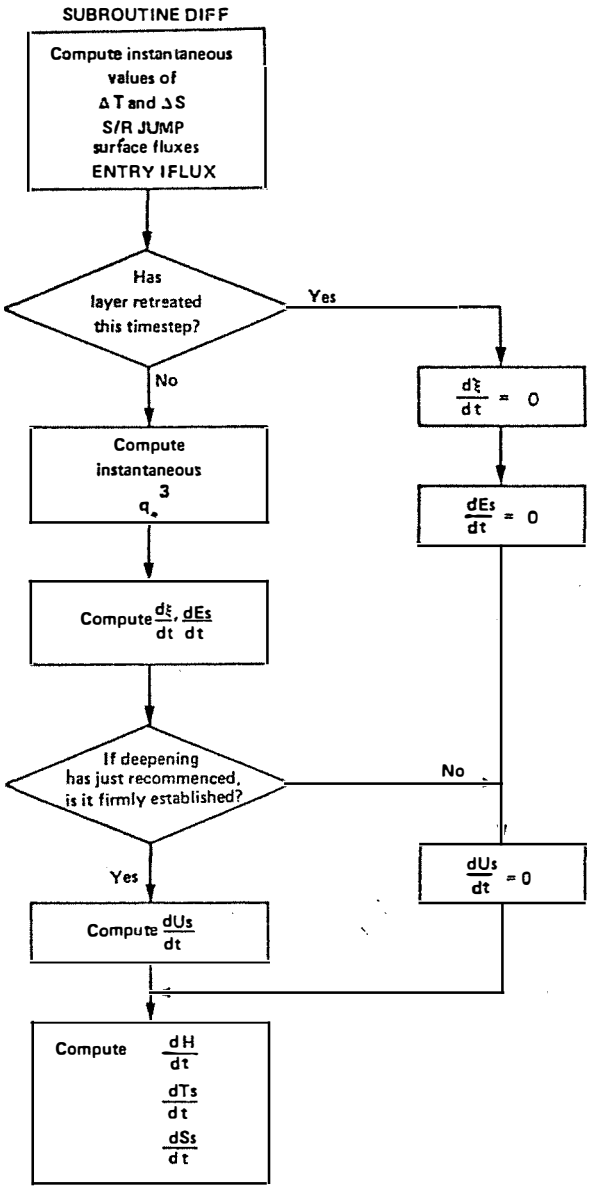
SUBROUTINE DIFF
Compute instantaneous values of ΔT and ΔS S/R JUMP surface fluxes ENTRY IFLUX
Has layer retreated this timestep?
Yes
No
dξ/dt = 0
dEs/dt = 0
Compute instantaneous q*3
Compute dξ/dt, dEs/dt
If deepening has just recommenced, is it firmly established?
No
Yes
dUs/dt = 0
Compute dUs/dt
Compute dH/dt
dTs/dt
dSs/dt

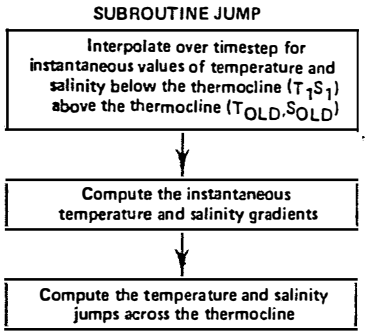
SUBROUTINE JUMP
Interpolate over timestep for instantaneous values of temperature and salinity below the thermocline (T_1S_1) above the thermocline (T_{OLD},S_{OLD})
Compute the instantaneous temperature and salinity gradients
Compute the temperature and salinity jumps across the thermocline

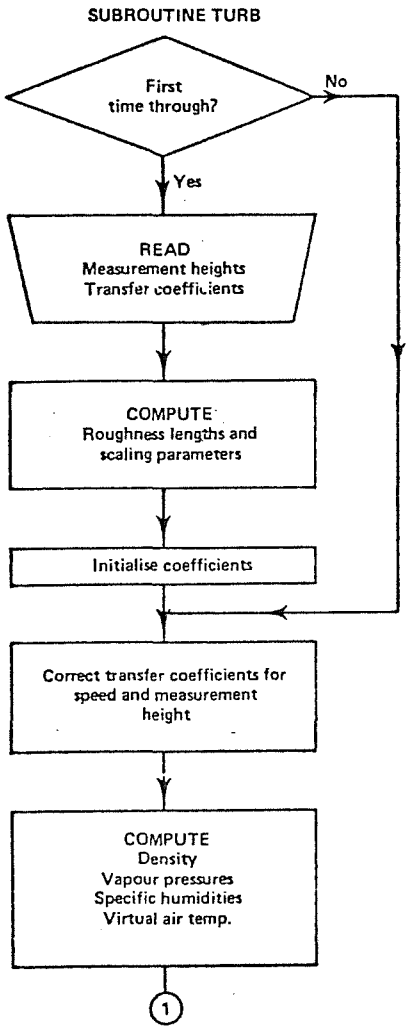
SUBROUTINE TURB
First time through?
No
Yes
READ
Measurement heights
Transfer coefficients
COMPUTE
Roughness lengths and scaling parameters
Initialise coefficients
Correct transfer coefficients for speed and measurement height
COMPUTE
Density
Vapour pressures
Specific humidities
Virtual air temp.
1

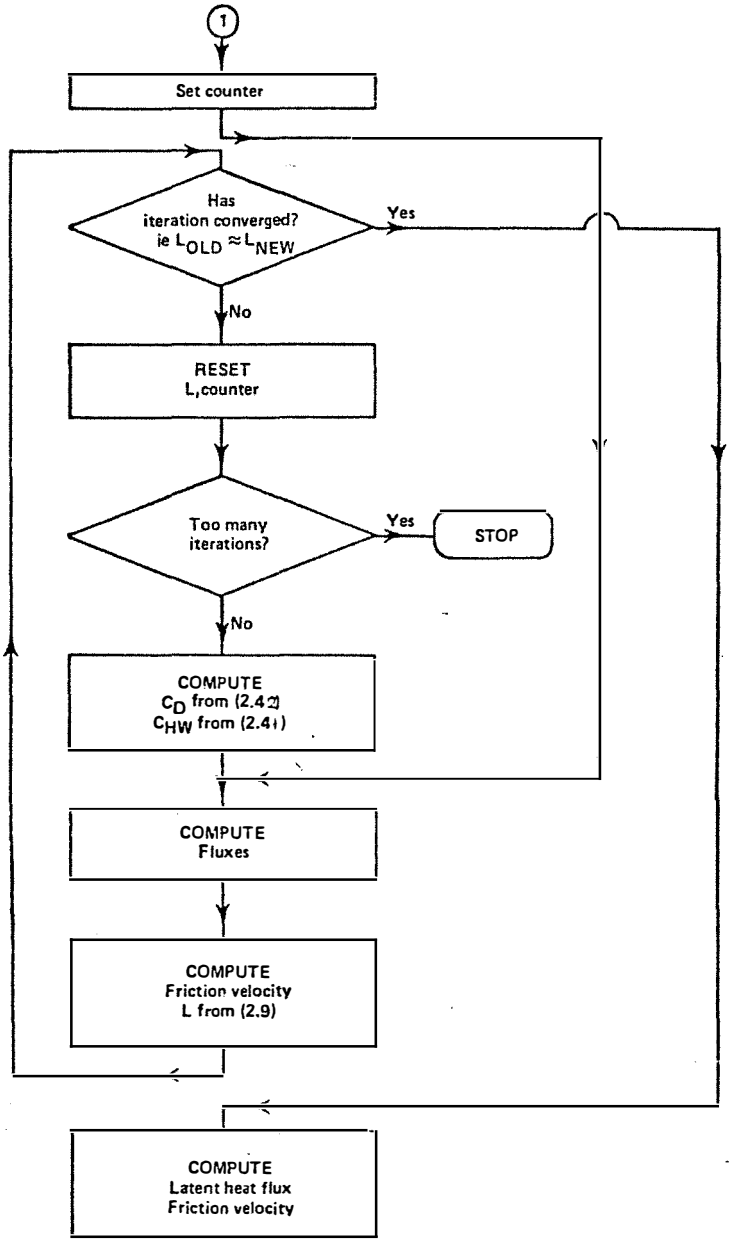
1
Set counter
Has iteration converged? ie $L_{OLD} \approx L_{NEW}$
Yes
No
RESET L, counter
Too many iterations?
Yes
STOP
No
COMPUTE C_D from (2.42) C_{HW} from (2.41)
COMPUTE Fluxes
COMPUTE Friction velocity L from (2.9)
COMPUTE Latent heat flux Friction velocity

APPENDIX C: PROGRAM LISTINGS

```
      PROGRAM FLUX(INPUT,OUTPUT,TAPE1,TAPE5,TAPE6,TAPE7)
      REAL L,K
      INTEGER HH
C
      DATA Z3,Z4/3.0,4.0/
      DATA CHWN10,HL,P,CP,G,K/0.00135,2445.,1013.25,1010.,9.81,.41/
      DATA CHW3MX,CD4MX/.00240,.00148/,ZLMAX/-0.99323/
C
      REWIND 1
      REWIND 5
      REWIND 6
      READ(1,10) IDATE
   10 FORMAT(I6)
      READ(1,10) NI
      WRITE(5,10) IDATE
      WRITE(5,10) NI
      WRITE(6,10) IDATE
      WRITE(6,10) NI
      WRITE(7,10) IDATE
      WRITE(7,10) NI
      WRITE(5,12)
   12 FORMAT(/,2X,*TIME*,10X,*L*,7X,*Z/L*,6X,*RIBC*,6X,*RIBU*,7X,
     *,*CD4*,6X,*CH43*,/)
      WRITE(6,13)
      WRITE(7,13)
   13 FORMAT(/,2X,*TIME*,5X,*STRESS*,2X,*SENSIBLE*,4X,*LATENT*,6X,
     *,*EVAP*,3X,*FR.VEL.*,/,12X,*N/M2*,2(6X,*W/M2*),6X,*MM/HR*,
     *6X,*M/S*,/)
C                 COMPUTE ROUGHNESS LENGTHS
      CDN10=0.0013
      Z0=10.0/(EXP(K/(SQRT(CDN10))))
      ZS=10.0/(EXP(K*K/(CHWN10*ALOG(10./Z0))))
      G1=ALOG(10./Z0)
      G2=ALOG(10./ZS)
      G3=ALOG(Z3/ZS)
      G5=ALOG(Z3/Z0)
      G6=ALOG(Z4/Z0)
C
      PRINT *,* Z0,ZS,G1-G6 *,Z0,ZS,G1,G2,G3,G5,G6
C
      DO 100 I=1,NI
C
      READ(1,20) HH,MM,U,AT,WT,RH
   20 FORMAT(5X,2I2,4F10.2)
C                   WIND SPEED AT 2ND LEVEL
      U3=U*G5/G6
C                   NEUTRAL 10M DRAG COEFF.
      IF(U.LE.5.) CDN10=.001
      IF(U.GT.5.) CDN10=(1.0+0.07*(U-5.))/1000.
C                   INITIALISE COEFFICIENTS
      CDN4=CDN10*(G1*G1)/(G6*G6)
      CDN3=CDN10*(G1*G1)/(G5*G5)
      CHWN=CHWN10*(G1*G2)/(G5*G3)
      CD4=CDN4
      CD3=CDN3
      CHW=CHWN
      PRINT *,* U3=*,U3,*CDN4,CDN3,CHWN *,CDN4,CDN3,CHWN
C                   ATMOSPHERIC DENSITY
      D=1.294*273./(AT+273.)
C                   PARTIAL WATER VAPOUR PRESSURE
      T1=1.-373.16/(AT+273.)
      T2=1.-373.16/(WT+273.)



      ES1=SATVP(T1)
      E1=(RH*ES1)/100.
      ES2=SATVP(T2)
C                   SPECIFIC HUMIDITY
      Q=0.662/P*E1
C                   VIRTUAL AIR TEMPERATURE
      TV=(AT+273.)*(1.+0.61*Q)
      PRINT *,* D,ES1,E1,ES2,Q,AT,TV *,D,ES1,E1,ES2,Q,AT,TV
```

C1 Program FLUX

```
C
C                   FLUX COMPUTATION/ITERATION
      ZL0=0.
      ICOUNT=1
      GO TO 30
C
   25 CONTINUE
      IF((ABS((ZL-ZL0)/ZL)).LT.0.0001) GO TO 50
      ZL0=ZL
      ICOUNT=ICOUNT+1
      IF(ICOUNT.GE.50) STOP *TOO MANY ITERATIONS*
C
   30 H=CHW*D*CP*U3*(WT-AT)
      W=CHW*D*U3*0.662/P*(ES2-E1)
      S=CD4*D*U*U
C
C                   FRICTION VELOCITY
      UX=SQRT(S/D)
      IF(ICOUNT.NE.1) GO TO 45
      HN=H
      WN=W
      SN=S
      UXN=UX
      HLFXN=WN*HL*1000.
      EWN=WN*3600.
C                   M.O.LENGTH
   45 L=-D*UX*UX*UX*TV/(K*G*(H/CP+0.61*(AT+273.)*W))
C                   RECOMPUTE TRANSFER COEFFICIENTS
      ZL=Z4/L
      P4=PSIM(ZL)
      C=SQRT(CDN4)
      CD4=CDN4/(1.+CDN4*(P4*P4-2.*K*P4/C)/(K*K))
C
      ZL=Z3/L
      P1=PSIM(ZL)
      P2=PSIHW(ZL)
      C=SQRT(CDN3)
      CHW=CHWN/(1.+CHWN*(P1*P2-K*P2/C-K*P1*C/CHWN)/(K*K))
C
      GO TO 25
C
C                   COMPUTE BULK RICHARDSON NO.S AT LEVEL Z3
   50 RIB1=ZL*(K*C/CHWN-P2)/((K/C-P1)*(K/C-P1))
      U3=U*(G5-P1)/(G6-P4)
      PRINT *,*  CORRECTED U3= *,U3,*    W= *,W
      PRINT 99,HH,MM,ICOUNT
   99 FORMAT(/,5X,2I2,*   NO. OF ITERATIONS =*,I3,///)
      RIB2=G*Z3/TV*(AT-WT+0.61*TV*(0.662/P*(E1-ES2)))/U3*U3)
C
C
      WRITE(5,110) HH,MM,L,ZL,RIB1,RIB2,CD4,CHW
  110 FORMAT(2X,2I2,2X,6F10.5)
      IF(ZL.GT.ZLMAX) GO TO 115
      H=CHW3MX*D*CP*U3*(WT-AT)



      W=CHW3MX*D*U3*0.662/P*(ES2-E1)
      S=CD4MX*D*U*U
  115 CONTINUE
      HLFX=W*HL*1000.
      EW=W*3600.
      UX=SQRT(S/D)
      WRITE(6,120) HH,MM,S,H,HLFX,EW,UX
  120 FORMAT(2X,2I2,2X,F10.5,2F10.2,2F10.5)
      WRITE(7,120) HH,MM,SN,HN,HLFXN,EWN,UXN
C
C
  100 CONTINUE
C
      ENDFILE 5
      ENDFILE 6
      END
```

```
      FUNCTION SATVP(T)
C           COMPLTES SATURATION VAPOUR PRESSURE IN MB
      SATVP=1013.25*EXP(T*(13.3185+T*(-1.9760+T*(-0.6445-1.299*T))))
      RETURN
      END
C
C
C
      FUNCTION PSIM(ZL)
      REAL K
      DATA K,A,PI/0.41,5.0,3.1415927/
C
C
      IF(ZL.LT.0.) GO TO 10
      IF(ZL.GT.0.) GO TO 20
C
      PSIM=0.
      GO TO 30
C
   10 X=(1.-16.*ZL)**0.25
      PSIM=2.*ALOG((1.+X)/2.)+ALOG((1.+X*X)/2.)-2.*ATAN(X)+PI/2.
      GO TO 30
C
   20 IF(ZL.GT.0.5) GO TO 21
      PSIM=-A*ZL
      GO TO 25
   21 IF(ZL.GT.10.) GO TO 22
      PSIM=0.5/(ZL*ZL)-4.25/ZL-7.0*ALOG(ZL)-0.852
      GO TO 25
   22 PSIM=ALOG(ZL)-0.76*ZL-12.093
   25 CONTINUE
C
   30 RETURN
      END
C
C
C
      FUNCTION PSIHW(ZL)
      REAL K
      DATA K,A,PI/0.41,5.0,3.1415927/
C
C
      IF(ZL.LT.0.) GO TO 10
      IF(ZL.GT.0.) GO TO 20
C
      PSIHW=0.
      GO TO 30
C
   10 X=(1.-16.*ZL)**0.25
      PSIHW=2.*ALOG((1.+X*X)/2.)
      GO TO 30
C
   20 IF(ZL.GT.0.5) GO TO 21
      PSIM=-A*ZL
      GO TO 25
   21 IF(ZL.GT.10.) GO TO 22
      PSIM=0.5/(ZL*ZL)-4.25/ZL-7.0*ALOG(ZL)-0.852
      GO TO 25
   22 PSIM=ALOG(ZL)-0.76*ZL-12.093
   25 PSIHW=PSIM
C
   30 RETURN
      END
```

```
      PROGRAM LAYER(INPUT,OUTPUT,TAPE1=64,TAPE2=64,TAPE5=64,TAPE6,TAPE7 000100
     *,TAPE8)                                                           000110
C                                                                       000120
C                                                                       000130
C   MODEL OF THE EPILIMNION MIXING IN A MEDIUM SIZE RESERVOIR.          000140
C                                                                       000150
C                                                                       000160
      EXTERNAL DIFF                                                     000170
      LOGICAL OK,PRESS                                                  000180
      REAL INT                                                          000190
      INTEGER DDD0,HH0,DDD1,HH1,CD(20),CH(20),CM(20)                    000200
      COMMON/WML/ZH,ZL,TS,US,SS,ES,H,TT,TTOLD,JOLD,TOLD,SOLD,T1,S1,Z1   000210
      COMMON/STRUCT/T(2000),S(2000)                                     000220
      COMMON/FLUX/A(6),INT,BRB(5)                                       000230
      COMMON/PARAM/C1,C2,C3,C4,C5,AL,B,CP,D,A1,B1,A2,B2,A3,B3           000240
      COMMON/UNMIX/NFLAG,MFLAG,PGRAD                                    000250
      COMMON/JUMP/ST,SECEND,GRID                                        000260
      COMMON/COUNT/ICOUNT,ADVECT,WW,TIME                                000270
C                                                                       000280
      DATA ICOUNT,NFLAG,N/1,0,1/,MFLAG/0/,LFLAG/0/                      000290
      DATA IBOMB,PRESS/0,.FALSE./,PGRAD/0.0/                            000300
      DATA ST,MODT/0.,0./                                               000310
C                                                                       000320
      REWIND 1                                                          000330
      REWIND 2                                                          000340
      REWIND 5                                                          000350
      REWIND 6                                                          000360
      REWIND 7                                                          000370
      REWIND 8                                                          000380
C                                                                       000390
C        ENTER DATES AND TIMES                                          000400
C                                                                       000410
      READ(1,5) DDD0,HH0,MM0,DDD1,HH1,MM1,DELT,NCHECK                   000420
    5 FORMAT(2(2X,I5,1X,2I2),3X,F5.2,I5)                                000430
      READ(1,10) (CD(J),CH(J),CM(J),J=1,NCHECK)                         000440
   10 FORMAT(I5,1X,2I2)                                                 000450
C                                                                       000460
      CALL START(DDD0,HH0,MM0)                                          000470
      CTIME=TIMES(CD(1),CH(1),CM(1))                                    000480
      ETIME=TIMES(DDD1,HH1,MM1)                                         000490
C                                                                       000500
C        ENTER INITIAL WML PARAMETERS PLUS OTHER CONSTANTS              000510
C                                                                       000520
      READ(1,15) TS,SS,ES,US,ZH,ZL,NPTS,GRID,IINT                       000530
   15 FORMAT(2F6.3,F8.8,3F8.3,I2,F8.3,I5)                               000540
      READ(1,20) C1,C2,C3,C4,C5,AL,B,CP,D                               000550
   20 FORMAT(9F8.4)                                                     000560
      READ(1,25) A1,B1,A2,B2,A3,B3                                      000570
   25 FORMAT(6F10.4)                                                    000580
C                                                                       000590
C       LOAD THE TEMPERATURE AND SALINITY GRIDS                         000600
      CALL LOAD(NPTS,GRID)                                              000610
C                                                                       000620
C        INITIALISE PARAMETERS                                          000630
      TIME=TIMES(DDD0,HH0,MM0)                                          000640
      ITIME=TIME/IINT-1                                                 000650
      SECINT=DELT/8.0                                                   000660
      TSTEP=DELT/8.0                                                    000670
      INT=TSTEP/60.0                                                    000680
      SINT=DELT*0.00005                                                 000690
      ZLOLD=ZL                                                          000700
      H=ZH-ZL                                                           000710


      ADVECT=0.0                                                        000720
C                                                                       000730
C                                                                       000740
C   START OF LOOP                                                       000750
  100 CONTINUE                                                          000760
      IF(ICOUNT.EQ.1) GO TO 101                                         000770
C                                                                       000780
C         CHECK COMPATIBILTY OF DEEPENING RATE,INTEGRATION RANGE &      000790
C           GRID SPACING.  HALVE OR DOUBLE INTEGRATION RANGE.           000800
      IF(LFLAG.EQ.1) GO TO 121                                          000810
      IF(((TNEXT-TIME)*60.).LT.DELT) GO TO 122                          000820
      IF(WW.LE.0.0.AND.MFLAG.EQ.0) GO TO 122                            000830
      GO TO 104                                                         000840
  121 LFLAG=0                                                           000850
  122 TSTEP=DELT*0.125                                                  000860
      GO TO 103                                                         000870
  104 IF(TSTEP.GT.(0.95*DELT)) GO TO 102                                000880
      IF((ZLOLD-ZL).GT.(0.2*GRID)) GO TO 102                            000890
      TSTEP=TSTEP+TSTEP                                                 000900
      GO TO 103                                                         000910
  102 IF(TSTEP.LT.(0.15*DELT)) GO TO 103                                000920
      IF((ZLOLD-ZL).GT.(0.8*GRID)) TSTEP=TSTEP*0.5                      000930
  103 INT=TSTEP/60.0                                                    000940
      IF(SECINT.GT.TSTEP) SECINT=TSTEP                                  000950
      ZLOLD=ZL                                                          000960
  101 TIME=TIME+INT                                                     000970
```

C2 Program LAYER

```
C                                                                       000C80
C       COMPUTE INSTANTANEOUS METEOROLICAL FLUXES                       000C90
      CALL FLUXES(ICOUNT,TIME,MODT,ST,TNEAT)                            001000
      SECEND=ST+TSTEP                                                   001010
C       RESET ENTRAINED GRID POINT VALUES                               001020
      IF(ICOUNT.NE.1) CALL STEP(GRID)                                   001030
C                                                                       001040
C       SOLAR SHORTWAVE HEATING OF ALL GRIDPOINTS                       001050
      CALL SOLAR(TSTEP,GRID)                                            001060
C                                                                       001070
C       COMPUTE SIGMA (ENTRAINMENT POWER PARAMETER)                     001080
      CALL SIGMA(WW)                                                    001090
C       IS THE LEVEL OF TKE STILL  +VE+                                 001100
      IF(WW.GT.0.0) GO TO 40                                            001110
      IF(ES.LT.1.0E-10) GO TO 39                                        001120
      ES32=SQRT(ES*ES*ES)                                               001130
      DECAY=-((WW-(C2+C3)*ES32)/H)*TSTEP                                001140
      IF(DECAY.LT.(0.5*ES)) GO TO 40                                    001150
      PRINT 38,TIME,ES,DECAY                                            001160
   38 FORMAT(/,5X,'TIME ',F10.1,'   ES',E12.3,'  DECAY',E12.3)          001170
C                                                                       001180
C       TKE HAS DECAYED TO ZERO ; ITERATE A NEW H.                      001190
   39 T(JOLD+1)=TS                                                      001200
      S(JOLD+1)=SS                                                      001210
      US=0.0                                                            001220
      ES=0.0                                                            001230
      ADVECT=0.0                                                        001240
      CALL NEWTON                                                       001250
      NFLAG=1                                                           001260
      IF(H.GT.0.05) GO TO 40                                            001270
      H=0.05                                                            001280
      ZL=ZH-H                                                           001290
C                                                                       001300
C                                                                       001310
C   SOLVE WML EQUATIONS BY RUNGE KUTTA METHOD                           001320
C                                                                       001330
```

```
   40 CALL MERS1(ST,SECEND,6,0.0001,SECINT,SINT,0,OK,DIFF)              001340
      IF(OK) GO TO 128                                                  001350
      PRINT 127,TIME                                                    001360
  127 FORMAT(//,5X,'TIMESTEP DIVISION LIMIT REACHED AT ',F10.1,//)      001370
      PRINT *,'     ST=',ST,'    SECEND=',SECEND                        001380
      STOP                                                              001390
C                                                                       001400
  128 IF(ZL.LE.GRID) STOP'MIXED TO BOTTOM OF LAYER'                     001410
      WRITE(7,976) TIME,WW,ES,SECINT,SECEND                             001420
  976 FORMAT(5X,F12.1,2E12.3,2F15.0)                                    001430
C       UPDATE GRID VALUES                                              001440
      H=ZH-ZL                                                           001450
      J1=ZL/GRID                                                        001460
      J1=J1+2                                                           001470
      JJ=ZH/GRID                                                        001480
      JJ=JJ+1                                                           001490
      DO 130 J=J1,JJ                                                    001500
      T(J)=TS                                                           001510
  130 S(J)=SS                                                           001520
C                                                                       001530
      IF(NFLAG.NE.1) GO TO 133                                          001540
      TJUMP=0.0                                                         001550
      SJUMP=0.0                                                         001560
      GO TO 134                                                         001570
  133 CALL JUMP(SECEND,TJUMP,SJUMP)                                     001580
C   PRINTOUT FULL GRID STRUCTURE AT TIMES SPECIFIED                     001590
C                                                                       001600
  134 IF((TIME-CTIME).LE.(-0.49*TINT)) GO TO 200                        001610
      WRITE(6,137) CD(N),CH(N),CM(N),TIME                               001620
  137 FORMAT(1H1,///,5X,'MODEL PROFILE FOR DAY ',I4,1X,2I2,3X,          001630
     1'MODEL TIME',F8.1,' MINS.')                                       001640
      WRITE(6,138) ZH,ZL,H,TS,SS,ES,US                                  001650
  138 FORMAT(/,5X,'ZH=',F6.3,3X,'ZL=',F6.3,3X,'H=',F6.3,3X,'TS=',F5.2,3X,C01660
     1,'SS=',F6.2,3X,'ES=',E10.3,3X,'US=',F6.4)                         001670
      WRITE(6,139) TJUMP,SJUMP                                          001680
  139 FORMAT(/,5X,'TJUMP=',F6.2,3X,'SJUMP=',F6.2,//,4X,                 001690
     1'HEIGHT',5X,'TEMPERATURE',6X,'SALINITY')                          001700
      Z=0.0                                                             001710
      DO 160 K=1,JJ,4                                                   001720
      WRITE(6,150) Z,T(K),S(K)                                          001730
  150 FORMAT(4X,F6.3,10X,F5.2,9X,F6.2)                                  001740
  160 Z=Z+4.0*GRID                                                      001750
      N=N+1                                                             001760
      IF(N.GT.NCHECK) GO TO 500                                         001770
      CTIME=TIMES(CD(N),CH(N),CM(N))                                    001780
```

```
C                                                                       001790
C       COMPUTE THERMOCLINE TILT OVER 2KM IF LAYER IS DEEPENING         001800
  200 IF(NFLAG.EQ.1) GO TO 250                                          001810
      ADVECT=ADVECT*.005*TSTEP                                          001820
      TILT=ADVECT*0.002                                                 001830
C       DIMENSIONLESS DENSITY JUMP                                      001840
      DELRHO=AL*TJUMP                                                   001850
C       PRESS GRADIENT/RHO0  OVER 1KM HALF                              001860
      DPDX=9.81*DELRHO*TILT/1000.                                       001870
C       COMPARE STRESS AND PRESS GRADIENT                               001880
      IF((A(6)*A(6)).GT.DPDX) GO TO 215                                 001890
      IF(PRESS) 235,210                                                 001900
  210 PGRAD=2.*DPDX                                                     001910
      LFLAG=1                                                           001920
      PRESS=.TRUE.                                                      001930
      PRINT *,#     PRESSURE GRADIENT ON AT #,TIME                      001940
      GO TO 235                                                         001950


  215 IF(PRESS) 220,235                                                 001960
  220 PRESS=.FALSE.                                                     001970
      PGRAD=0.                                                          001980
      PRINT *,#     PRESSURE GRADIENT OFF AT #,TIME                     001990
  235 CONTINUE                                                          002000
C                                                                       002010
C   PRINT A SUMMARY WHEN LAYER DEEPENS                                  002020
C                                                                       002030
      WRITE(5,240) TIME,ZH,ZL,H,TS,SS,US,ES,WW,TJUMP,SJUMP,PGRAD        002040
  240 FORMAT(1X,7F9.3,2E12.3,2F9.2,E12.3)                               002050
      GO TO 300                                                         002060
C                                                                       002070
C   PRINT A SUMMARY WHENEVER LAYER RETREATS                             002080
C                                                                       002090
  250 WRITE(5,255) TIME,ZH,ZL,H,TS,SS,US,ES,WW,TJUMP,SJUMP              002100
  255 FORMAT(1X,7F9.3,2E12.3,2F9.2)                                     002110
C                                                                       002120
  300 CONTINUE                                                          002130
C                                                                       002140
C   PRINT FLUXES                                                        002150
      FL3=A(3)*3600000                                                  002160
      FL6=A(6)/0.0343                                                   002170
      WRITE(8,270) TIME,A(1),A(2),FL3,A(4),A(5),FL6                     002180
  270 FORMAT(3F10.1,F10.5,2F10.1,F10.5)                                 002190
C   RESET MODEL PARAMETERS AND CHECK TIME                               002200
C                                                                       002210
      IF(NFLAG.EQ.1.AND.NFLAG.EQ.0) GO TO 350                           002220
      GO TO 380                                                         002230
  350 LFLAG=1                                                           002240
      IF(ZLOLD.GT.ZL) GO TO 380                                         002250
      GO TO 390                                                         002260
  380 NFLAG=NFLAG                                                       002270
  390 NFLAG=0                                                           002280
      IF((ETIME-TIME).LT.INT) GO TO 500                                 002290
      ICOUNT=ICOUNT+1                                                   002300
      GO TO 100                                                         002310
C                                                                       002320
C                                                                       002330
C   THATS IT FOLKS!                                                     002340
C                                                                       002350
  500 ENDFILE 5                                                         002360
      ENDFILE 6                                                         002370
      ENDFILE 7                                                         002380
      ENDFILE 8                                                         002390
      PRINT 510,ICOUNT                                                  002400
  510 FORMAT(//,5X,#FINAL ICOUNT= #,I8)                                 002410
C                                                                       002420
      END                                                               002430
```

```
      SUBROUTINE DIFF(TIME,YDOT)                                        002A00
C                                                                       002A05
C   SUBROUTINE CONTAINING THE D.E.'S FOR SOLUTION                       002A10
C                                                                       002A15
      DIMENSION YDOT(6)                                                 002A20
      COMMON/WML/DUMMY(6),H,TT1,TTOLD,JOLD,TOLD,SOLD,T1,S1,ZI          002A25
      COMMON/DES/ZH,ZL,TS,US,SS,ES                                      002A30
      COMMON/PARAM/CN,CF,CE,CS,CL,AL,B,CP,O                             002A35
      COMMON/FLUX/A(6)                                                  002A40
      COMMON/UNMIX/NFLAG,MFLAG,PGRAD                                    002A45
      COMMON/COUNT/I,ADVECT,WW,RTIME                                    002A50
C                                                                       002A55
      DATA CC1/0.333333333/,G/9.81/                                     002A60
C                                                                       002A65
      H=ZH-ZL                                                           002A70
C         COMPUTE INSTANTANEOUS FLUXES                                  002A75
      CALL IFLUX(I,DUM1,TIME,DUM2,DUM3)                                 002A80
C                                                                       002A85
C       HAS LAYER RETREATED                                             002A90
      IF(NFLAG.NE.1) GO TO 50                                           002A95
   19 YDOT(2)=0.0                                                       002B00
      UE=0.0                                                            002B05
      YDOT(4)=0.0                                                       002B10
      US=0.0                                                            002B15
      YDOT(6)=0.0                                                       002B20
      ES=0.0                                                            002B25
      GO TO 20                                                          002B30
C                                                                       002B35
C   COMPUTE TEMP & SAL JUMPS AT BOTTOM OF WML                           002B40
   50 CALL JUMP(TIME,TJUMP,SJUMP)                                       002B45
C        COMPUTE SURFACE INPUT POWER                                    002B50
      CALL SIGMA(WW)                                                    002B55
C                                                                       002B60
C             TKE FLUX                                                  002B65
      IF(ES.GT.0.0.OR.WW.GT.0.0) GO TO 45                               002B70
      NFLAG=1                                                           002B75
      PRINT *,*    ENERGY DECAYED AT TIME  *,RTIME                      002B80
      ADVECT=0.0                                                        002B85
      GO TO 19                                                          002B90
   45 ES32=SQRT(ES*ES*ES)                                               002B95
C  COMPUTE THE DERIVATIVES                                              002C00
C                                                                       002C05
   30 YDOT(2)=CF*ES32/(CS*US*US+B*G*H*SJUMP-AL*G*H*TJUMP-ES)            002C10
      UE=YDOT(2)                                                        002C15
   31 YDOT(6)=(WW-(CF+CE)*ES32)/H                                       002C20
   32 CONTINUE                                                          002C25
C                                                                       002C30
C         IS MIXING ESTABLISHED WELL ENOUGH TO INCLUDE SHEAR            002C35
      IF(MFLAG.EQ.1) GO TO 15                                           002C40
      YDOT(4)=(A(6)*A(6)+US*US)/H-PGRAD                                 002C45
      GO TO 20                                                          002C50
   15 YDOT(4)=0.0                                                       002C55
   20 YDOT(1)=-A(3)                                                     002C60
      YDOT(3)=(TJUMP*UE-1.0/(D*CP)*(A(1)+A(2)+A(5)+A(4)*                002C65
     1(1.-Q(ZL,ZH))))/H                                                 002C70
      YDOT(5)=(SJUMP*UE+A(3)*SS)/H                                      002C75
C                                                                       002C80
      RETURN                                                            002C85
      END                                                               002C90
```

```
      SUBROUTINE LOAD(NPTS,GRID)                                        003030
C                                                                       003040
C     SUBROUTINE TO LOAD ALL GRID POINT VALUES (TEMP & SAL) FROM SPECIFIED003050
C       INITIAL STRUCTURE.                                              003060
C                                                                       003070
      DIMENSION HT(20),TEMP(20),SAL(20)                                 003080
      COMMON/WML/ZH,ZL,TS,US,SS,ES,H,TT1,TTOLD,JOLD,TOLD,SOLD,T1,S1,Z1  003090
      COMMON/STRUCT/T(2000),S(2000)                                     003100
C                                                                       003110
C        READ THE SPECIFIED INITIAL STRUCTURE                           003120
      READ(1,10) (HT(K),TEMP(K),SAL(K),K=1,NPTS)                        003130
   10 FORMAT(F5.2,2F10.1)                                               003140
      IF(EOF(1)) 11,12                                                  003150
   11 STOP #EOF IN INITIAL STRUCTURE FILE#                              003160
   12 IF(HT(1).NE.0.0) STOP #INITIAL STRUCTURE SPECIFIED INCORRECT#     003170
C                                                                       003180
C        LOAD THE GRID                                                  003190
C                                                                       003200
      Z=0.0                                                             003210
      J=1                                                               003220
      K=1                                                               003230
      ZHH=ZH+0.01*GRID                                                  003240
      GO TO 27                                                          003250
C                                                                       003260
   20 IF(Z.LE.(HT(K+1)+0.01*GRID)) GO TO 30                             003270
      K=K+1                                                             003280
      IF(Z.GE.ZL) GO TO 20                                              003290
   27 TDASH=(TEMP(K+1)-TEMP(K))/(HT(K+1)-HT(K))                         003300
      SDASH=(SAL(K+1)-SAL(K))/(HT(K+1)-HT(K))                           003310
      GO TO 20                                                          003320
C                                                                       003330
   30 T(J)=TEMP(K)+(Z-HT(K))/(HT(K+1)-HT(K))*(TEMP(K+1)-TEMP(K))        003340
      S(J)=SAL(K)+(Z-HT(K))/(HT(K+1)-HT(K))*(SAL(K+1)-SAL(K))           003350
      J=J+1                                                             003360
      Z=Z+GRID                                                          003370
      IF(K.EQ.NPTS) STOP #TOO MANY POINTS LOADED#                       003380
      IF(Z.GT.ZHH) GO TO 50                                             003390
      GO TO 20                                                          003400
C                                                                       003410
   50 K=K+1                                                             003420
      J=J-1                                                             003430
      PRINT 60,J,K                                                      003440
   60 FORMAT(/,5X,I4,# GRID POINTS LOADED FROM #,I4,# LEVELS#)          003450
C                                                                       003460
C        RESET WML BASE TEMP & SAL                                      003470
      J=ZL/GRID                                                         003480
      J=J+1                                                             003490
      T(J+1)=T(J)+TDASH*GRID                                            003500
      S(J+1)=S(J)+SDASH*GRID                                            003510
      JOLD=J                                                            003520
C                                                                       003530
      RETURN                                                            003540
      END                                                               003550
```

```
      SUBROUTINE FLUXES(I,T,TM,<T,TNEXT)                                003560
C                                                                       003570
C   SUBROUTINE TO COMPUTE METEOROLOGICAL FLUXES BY LINEAR INTERPOLATION 003580
C     BETWEEN KNOWN VALUES.                                             003590
C                                                                       003600
      DIMENSION F(2,6),FT(2)                                            003610
      INTEGER FD,FH,FM                                                  003620
      COMMON/FLUX/A(6),TINT,B(5)                                        003630
      COMMON/WHL/ZH,ZL,TS                                               003640
C                                                                       003650
C        FIRST TIME THROUGH, READ IN KNOWN FLUXES.                      003660
C                                                                       003670
      IF(I.NE.1) GO TO 10                                               003680
      DO 6 K=1,2                                                        003690
      READ(2,5) FD,FH,FM,(F(K,J),J=1,5)                                 003700
    5 FORMAT(I5,1X,2I2,5F10.2)                                          003710
      IF(EOF(2)) 3,4                                                    003720
    3 STOP *EMPTY FLUX FILE*                                            003730
    4 FT(K)=TIMES(FD,FH,FM)                                             003740
    6 CONTINUE                                                          003750
      TNEXT=FT(2)                                                       003760
C                                                                       003770
      IF(T.GE.FT(1)) GO TO 10                                           003780
      PRINT 7,T,FT(1)                                                   003790
    7 FORMAT(/,5X,*MODEL TIME*,F10.1,* PRECEEDS FIRST FLUX RECORD AT*,  003800
     1F10.1,* MINUTES*)                                                 003810
      STOP                                                              003820
C                                                                       003830
C      INTERPOLATE FOR FLUXES WITHIN THE CORRECT INTERVAL               003840
C                                                                       003850
   10 IF(T.LT.(FT(2)+0.001)) GO TO 30                                   003860
      FT(1)=FT(2)                                                       003870
      DO 15 J=1,6                                                       003880
   15 F(1,J)=F(2,J)                                                     003890
      READ(2,5) FD,FH,FM,(F(2,J),J=1,5)                                 003900
      IF(EOF(2)) 16,17                                                  003910
   16 STOP *INSUFFICIENT RECORDS IN FLUX FILE*                          003920
   17 FT(2)=TIMES(FD,FH,FM)                                             003930
      TNEXT=FT(2)                                                       003940
      ST=0.0                                                            003950
      GO TO 10                                                          003960
C                                                                       003970
   30 IF(I.EQ.1) ST=((T-TINT)-FT(1))*60.                                003980
      DO 40 J=1,5                                                       003990
   40 B(J)=F(1,J)+((T-TINT/2.)-FT(1))/(FT(2)-FT(1))*(F(2,J)-F(1,J))     004000
C  WHERE B1=SPEED,B2=A.TEMP,B3=G.H.,B4=L.W.IN,B5=S.W.IN                 004010
      GO TO 200                                                         004020
C                                                                       004030
      ENTRY IFLUX                                                       004040
      DO 50 J=1,5                                                       004050
   50 B(J)=F(1,J)+(TM/60.)/(FT(2)-FT(1))*(F(2,J)-F(1,J))                004060
  200 CALL TURB(I)                                                      004070
   60 A(3)=A(3)/(1000.)                                                 004080
      A(6)=A(6)*0.0343                                                  004090
      QLO=5.669E-8*0.96*(TS+273.)**4                                    004100
      A(5)=QLO+B(4)                                                     004110
      A(4)=B(5)                                                         004120
C                                                                       004130
      RETURN                                                            004140
      END                                                               004150
```

```
      SUBROUTINE STEP(GRID)                                              004160
C                                                                        004170
C   SUBROUTINE TO RESET WML BASE TEMP & SAL VALUES TO FACILITATE         004180
C     COMPUTATION OF GRADIENTS BELOW THE WML                             004190
C                                                                        004200
      COMMON/STRUCT/T(2000),S(2000)                                      004210
      COMMON/WML/ZH,ZL,TS,US,SS,ES,H,TT1,TTOLD,JOLD,TOLD,SOLD,T1,S1,Z1   004220
C                                                                        004230
      J=ZL/GRID                                                          004240
      J=J+1                                                              004250
      IF(J.EQ.JOLD) GO TO 10                                             004260
      IF(J.GT.JOLD) GO TO 30                                             004270
      IF(J.EQ.(JOLD-1)) GO TO 50                                         004280
      STOP #ENTRAINED MORE THAN 1 GRIDPOINT#                             004290
C                                                                        004300
   10 T(J+1)=TOLD                                                        004310
      S(J+1)=SOLD                                                        004320
      RETURN                                                             004330
C                                                                        004340
   30 JOLD=J                                                             004350
      RETURN                                                             004360
C                                                                        004370
   50 JOLD=J                                                             004380
      T(J+1)=T1                                                          004390
      S(J+1)=S1                                                          004400
      RETURN                                                             004410
      END                                                                004420


      SUBROUTINE SOLAR(TINT,GRID)                                        004430
C                                                                        004440
C   SUBROUTINE TO INPUT HEAT TO ALL GRIDPOINTS FROM SOLAR SHORTWAVE      004450
C     RADIATION ABSORPTION                                               004460
C                                                                        004470
      COMMON/FLUX/A(6)                                                   004480
      COMMON/WML/ZH,ZL,TS,US,SS,ES,H,TT1,TTOLD,JOLD,TOLD,SOLD,T1,S1,Z1   004490
      COMMON/STRUCT/T(2000),S(2000)                                      004500
      COMMON/PARAM/C1,C2,C3,C4,C5,AL,B,CP,D,A1,B1,A2,B2,A3,B3            004510
C                                                                        004520
      TT1=T(JOLD)                                                        004530
      TTOLD=T(JOLD+1)                                                    004540
C                                                                        004550
C       HEAT ALL GRIDPOINTS FROM THE BOTTOM UP                           004560
C                                                                        004570
      JJ=ZH/GRID                                                         004580
      JJ=JJ+1                                                            004590
      DO 20 J=1,JJ                                                       004600
      Z=(J-1)*GRID                                                       004610
      T(J)=T(J)-TINT*A(4)*QDASH(Z,ZH)/(D*CP)                             004620
   20 CONTINUE                                                           004630
C                                                                        004640
      T1=T(JOLD)                                                         004650
      TOLD=T(JOLD+1)                                                     004660
      S1=S(JOLD)                                                         004670
      SOLD=S(JOLD+1)                                                     004680
      Z1=(JOLD-1)*GRID                                                   004690
C                                                                        004700
      RETURN                                                             004710
      END                                                                004720


      SUBROUTINE SIGMA(WW)                                               004730
C                                                                        004740
C        SUBROUTINE TO COMPUTE THE SURFACE INPUT POWER                   004750
C                                                                        004760
      COMMON/FLUX/A(6)                                                   004770
      COMMON/PARAM/C1,C2,C3,C4,C5,AL,B,CP,D,A1,B1,A2,B2,A3,B3            004780
      COMMON/WML/ZH,ZL,TS,US,SS,ES,H,TT1,TTOLD,JOLD,TOLD,SOLD,T1,S1,Z1   004790
C                                                                        004800
      H9=(A(1)+A(2)+A(5))+A(4)*(1.0+Q(ZL,ZH)-QQ(ZH,ZL))                  004810
      W9=(9.81*AL*H)/(D*CP)*H9-(9.81*B*H)*A(3)*SS                        004820
      WW=(W9+(C1*A(6))**3)                                               004830
C                                                                        004840
      RETURN                                                             004850
      ENTRY NEWSIG                                                       004860
C                                                                        004870
C   THIS SECTION COMPUTES THE DERIVATIVE OF SIGMA USING THE PREVIOUSLY   004880
C     STORED VALUE OF H9.                                                004890
C                                                                        004900
      WW=AL*9.81/(D*CP)*(-H9-A(4)*(-QDASH(ZL,ZH)*H+QQ(ZH,ZL)-2.0*        004910
     1Q(ZL,ZH)))+B*9.81*A(3)*SS                                          004920
C                                                                        004930
      RETURN                                                             004940
      END                                                                004950
```

```
      SUBROUTINE NEWTON                                                 004860
C                                                                       004870
C  SUBROUTINE TO ITERATE A NEW SOLUTION FOR ZL SUCH THAT SIGMA = 0.     004880
C    USES A NEWTON RAPHSON PROCEDURE.                                   004890
C                                                                       004900
      COMMON/WML/ZH,ZL,TS,US,SS,ES,H,TT1,TTOLD,JOLD,TOLD,SOLD,T1,S1,Z1  005010
C                                                                       005020
      DATA ACC/0.0005/                                                  005030
C                                                                       005040
      I=1                                                               005050
   10 CALL SIGMA(FZL)                                                   005060
      CALL NEWSIG(DFZL)                                                 005070
      ZLNEW=ZL-FZL/DFZL                                                 005080
      IF(ABS((ZLNEW-ZL)/ZL).LE.ACC) GO TO 20                            005090
      I=I+1                                                             005100
      IF(I.GE.50) STOP *TOO MANY ITERATIONS*                            005110
      ZL=ZLNEW                                                          005120
      H=ZH-ZL                                                           005130
      GO TO 10                                                          005140
C                                                                       005150
   20 ZL=ZLNEW                                                          005160
      H=ZH-ZL                                                           005170
      RETURN                                                            005180
      END                                                               005190


      FUNCTION TIMES(D,H,M)                                             005200
C                                                                       005210
C  FUNCTION TO CALCULATE MODEL TIME (MINUTES AFTER START).              005220
C                                                                       005230
      INTEGER D,H                                                       005240
C                                                                       005250
      TIMES=M+60*(H+24*D)-ST                                            005260
C                                                                       005270
      RETURN                                                            005280
C                                                                       005290
      ENTRY START                                                       005300
C                                                                       005310
      ST=M+60*(H+24*D)                                                  005320
      TIMES=ST                                                          005330
C                                                                       005340
      RETURN                                                            005350
      END                                                               005360


      FUNCTION Q(Z,ZH)                                                  005370
C                                                                       005380
C  FUNCTION FOR FRACTION OF SHORTWAVE PENETRATIING TO Z.                005390
C                                                                       005400
      COMMON/PARAM/C1,C2,C3,C4,C5,AL,B,CP,D,A1,B1,A2,B2,A3,B3           005410
C                                                                       005420
      X=Z-ZH                                                            005430
      Q=A1*PEX(B1,X)+A2*PEX(B2,X)+A3*PEX(B3,X)                          005440
      RETURN                                                            005450
      END                                                               005460
      FUNCTION QDASH(Z,ZH)                                              005470
C                                                                       005480
C  CALCULATES DQ/DZ FOR HEAT ABSORPTION CALCULATION                     005490
C                                                                       005500
      COMMON/PARAM/C1,C2,C3,C4,C5,AL,B,CP,D,A1,B1,A2,B2,A3,B3           005510
C                                                                       005520
      X=Z-ZH                                                            005530
      QDASH=A1*B1*PEX(B1,X)+A2*B2*PEX(B2,X)+A3*B3*PEX(B3,X)             005540
      RETURN                                                            005550
      END                                                               005560
      FUNCTION QQ(ZH,ZL)                                                005570
C                                                                       005580
C  FUNCTION INCORPORATES THE INTEGRAL OF SHORTWAVE OVER THE WML.        005590
C                                                                       005600
      COMMON/PARAM/C1,C2,C3,C4,C5,AL,B,CP,D,A1,B1,A2,B2,A3,B3           005610
C                                                                       005620
      X=ZL-ZH                                                           005630
      QQ=-2.0/X*(A1/B1*(1.-PEX(B1,X))+A2/B2*(1.-PEX(B2,X))+             005640
     1A3/B3*(1.-PEX(B3,X)))                                             005650
      RETURN                                                            005660
      END                                                               005670


      FUNCTION PEX(B,X)                                                 005680
C                                                                       005690
C  COMPUTES EXPONENT IF ARGUEMENT NOT TOO SMALL                         005700
      Y=B*X                                                             005710
      IF(Y.GT.-25.) GO TO 10                                            005720
      PEX=0.0                                                           005730
      RETURN                                                            005740
   10 PEX=EXP(Y)                                                        005750
      RETURN                                                            005760
      END                                                               005770
```

```
      SUBROUTINE MERS1(X,XEND,N,ACC,H,HMIN,JTEST,OK,DIFF)                005780
C                                                                        005790
C     CERN LIBRARY NO D 208.                                             005800
C                                                                        005810
C     REVISED VERSION JULY 1971.                                         005820
C                                                                        005830
C     THIS VERSION OF MERSON IS A MODIFICATION OF THE PROGRAM RECEIVED    005840
C     FROM KJELLER COMPUTER INSTALLATION NORWAY.THE MAIN DIFFERENCE       005850
C     BEEING A CHANGE OF THE TEST FOR STEPLENGTH HALVING.                005860
C                                                                        005870
C                                                                        005880
C     PURPOSE = STEP BY STEP INTEGRATION OF A SYSTEM OF FIRST ORDER      005890
C               DIFFERENTIAL EQUATIONS                                   005900
C                                                                        005910
C                 DYK(X)/DX=FK(X,Y1(X),Y2(X),.....,YN(X)) , K=1(1)N      005920
C                                                                        005930
C                 WITH AUTOMATIC ERROR CONTROL USING THE METHOD DUE TO   005940
C                 MERSON.                                                005950
C                                                                        005960
C     PARAMETERS                                                         005970
C                                                                        005980
C     X       = START VALUE FOR THE DOMAIN OF INTEGRATION (INPUT POINT).005990
C     XEND    = END VALUE FOR THE DOMAIN OF INTEGRATION (OUTPUT POINT).  006000
C     Y       = ARRAY CONTAINING THE DEPENDENT VARIABLES.WHEN ENTERING   006010
C               THE ROUTINE THE FUNCTION VALUES YK(X),K=1(1)N AND WHEN   006020
C               RETURNING TO THE CALLING PROGRAM THE COMPUTED FUNCTION   006030
C               VALUES YK(XEND),K=1(1)N.                                 006040
C     N       = THE NUMBER OF DIFFERENTIAL EQUATION,EQUAL OR LESS 100.   006050
C     ACC     = PRESCRIBED RELATIVE ACCURACY (TO BE OBTAINED FOR ALL     006060
C               FUNCTION VALUES IN THE ARRAY Y).                         006070
C     H       = INITIAL STEPLENGTH.                                      006080
C     HMIN    = ABSOLUTE VALUE OF MINIMUM STEPLENGTH WANTED.             006090
C     JTEST   = TEST PARAMETER RELATED TO THE STEPLENGTH IN THE FOLLOW-  006100
C               ING WAY.                                                 006110
C               JTEST = 0 , IF DURING THE CALCULATION WE GET             006120
C                           ABS(H).LT.HMIN (BY REPEATED HALVING OF THE   006130
C                           STEPLENGTH),THEN AN ERROR MESSAGE IS PRINT-  006140
C                           ED,OK SET EQUAL TO .FALSE. FOLLOWED BY RE-   006150
C                           TURN TO THE CALLING PROGRAM.                 006160
C               JTEST = 1 , CHECKING AS FOR JTEST=0,BUT THE CALCULATION  006170
C                           WILL CONTINUE WITH THE FIXED STEPLENGTH HMIN  006180
C***** THE FOLLOWING LINE INSERTED R.J.WRIGHT 26/02/74 TO ALLOW COMPILAT  006190
      LOGICAL OK                                                         006200
C     OK      = A LOGICAL VARIABLE WHICH IS SET EQUAL TO .TRUE. WHEN EN- 006210
C               TERING THE ROUTINE.THE VALUE LATER IS DEPENCING OF JTEST 006220
C               IN THE FOLLOWING WAY                                     006230
C               JTEST = 1 , OK = .TRUE. ALWAYS.                          006240
C               JTEST = 0 , OK = .FALSE. IF THE STEPLENGTH BECOMES TOO   006250
C               SMALL (SEE DESCRIPTION FOR JTEST).                       006260
C     DIFF    = USER SUPPLIED SUBROUTINE FOR THE CALCULATION OF THE      006270
C               RIGHT HAND SIDES OF THE SYSTEM OF DIFFERENTIAL EQUATIONS 006280
C               (I.E.THE FIRST ORDER DERIVATIVES).CALLING SEQUENCE       006290
C                                                                        006300
C                 CALL DIFF(X,W,F) , WHERE                               006310
C                 X = THE CURRENT VALUE OF THE ARGUMENT                  006320
C                 W = AN ARRAY WITH THE ELEMENTS WK(X),K=1(1)N I.E. THE  006330
C                     FUNTION VALUES FOR WHICH THE DERIVATIVES ARE TO BE 006340
C                     COMPUTED.                                          006350
C                 F = AN ARRAY WITH THE ELEMENTS FK(X),K=1(1)N (WE HAVE  006360
C                     FK(X)=FK(X,W1(X),W2(X),....,WN(X))) TO BE COMPUTED 006370
C                     BY  DIFF AND RETURNED TO MERSON.                   006380
C                 THE CHOSEN NAME FOR DIFF MUST APPEAR IN AN EXTERNAL    006390
C                 STATEMENT IN THE PROGRAM CALLING MERSON.               006400
C                                                                        006410
C     THE ARRAYS IN THE COMMON BLOCK BELOW ARE ONLY USED INTERNALLY IN   006420
C     MERSON (AND DIFF) AND ARE TO FREE DISPOSAL OUTSIDE MERSON.         006430
C     THE MAXIMUM NUMBER OF EQUATIONS WHICH  MAY BE INTEGRATED ARE 100.  006440
C     THIS NUMBER MAY BE CHANGED BY CHANGING THE DIMENSION IN THE        006450
C     COMMON BLOCK BELOW ACCORDINGLY.                                    006460
C                                                                        006470
      DIMENSION YZ(6),A(6),B(6),F(6)                                     006480
C                                                                        006490
      COMMON/WML/ Y(6)                                                   006500
      COMMON/DES/ W(6)                                                   006510
C                                                                        006520
C     RZERO IS A NUMBER WITH A MAGNITUDE OF ORDER EQUAL TO THE NOISE     006530
C     LEVEL OF THE MACHINE I.E. IN THE RANGE OF THE ROUNDING OFF ERRORS. 006540
C                                                                        006550
      DATA RZERO / 1.E-13 /                                              006560
C                                                                        006570
C     CHECK NUMBER OF EQUATIONS,EQUAL OR LESS THAN 100.                  006580
C                                                                        006590
      IF (N.GT.100) GO TO 86                                             006600
C                                                                        006610
      OK=.TRUE.                                                          006620
C                                                                        006630
C     STORE INTERNALLY PARAMETERS IN LIST
```

```
C
      NN=N                                                              006***
      DO 1 K=1,NN                                                       006***
    1 W(K)=Y(K)                                                         006***
      Z=X                                                               006***
      ZEND=XEND                                                         006***
      BCC=ACC                                                           006***
      ZMIN=HMIN                                                         006***
      ITEST=JTEST                                                       006***
      S   =H                                                            006***
      ISWH=0                                                            006***
C                                                                       006***
    2 HSV=S                                                             006***
      IF(HSV.GT.RZERO)GO TO 4                                           006***
      PRINT 3                                                           006***
    3 FORMAT(* ***** SUBROUTINE MERSON - STEPLENGTH LESS THAN MACHINE RO006***
     1UNDING ERROR LEVEL ******)                                        006***
      STOP                                                              006***
    4 COF = ZEND - Z                                                    006***
      IF (ABS(S).LT.ABS(COF)) GO TO 8                                   006***
      S=COF                                                             006***
      IF (ABS(COF/HSV).LT.RZERO) GO TO 50                               006***
      ISWH=1                                                            006***
C                                                                       006***
C     IF ISWH=1 THEN  S IS EQUAL TO MAXIMUM POSSIBLE STEPLENGTH         006***
C     WITHIN THE REMAINING PART OF THE DOMAIN OF INTEGRATION.           006***
C                                                                       006***
    8 DO 10 K=1,NN                                                      006***
   10 YZ(K)=W(K)                                                        006***
   12 HT=.33333333333333*S                                              006***
C                                                                       006***
      CALL DIFF(Z,F)                                                    006***
C                                                                       006***
      Z=Z+HT                                                            006***
      DO 20 K=1,NN                                                      006***
      A(K)=HT*F(K)                                                      006***
   20 W(K)=A(K)+YZ(K)                                                   007***
C                                                                       007***
      CALL DIFF(Z,F)                                                    007***
C                                                                       007***
      DO 22 K=1,NN                                                      007***
      A(K)=.5*A(K)                                                      007***
   22 W(K)=.5*HT*F(K)+A(K)+YZ(K)                                        007***
C                                                                       007***
      CALL DIFF(Z,F)                                                    007***
C                                                                       007***
      Z=Z+.5*HT                                                         007***
      DO 24 K=1,NN                                                      007***
      B(K)=4.5*HT*F(K)                                                  007***
   24 W(K)=.25*B(K)+.75*A(K)+YZ(K)                                      007***
C                                                                       007***
      CALL DIFF(Z,F)                                                    007***
C                                                                       007***
      Z=Z+.5*S                                                          007***
      DO 26 K=1,NN                                                      007***
      A(K)=2.*HT*F(K)+A(K)                                              007***
   26 W(K)=3.*A(K)-B(K)+YZ(K)                                           007***
C                                                                       007***
      CALL DIFF(Z,F)                                                    007***
C                                                                       007***
      DO 28 K=1,NN                                                      007***
      B(K)=-.5*HT*F(K)-B(K)+2.*A(K)                                     007***
      W(K)=W(K)-B(K)                                                    007***
      A(K)=ABS(S.*BCC*W(K))                                             007***
      B(K)=ABS(B(K))                                                    007***
      IF (ABS(W(K)).LE.RZERO) GO TO 28                                  007***
      IF(B(K).GT.A(K)) GO TO 60                                         007***
   28 CONTINUE                                                          007***
C                                                                       007***
C     REQUIRED ACCURACY OBTAINED FOR ALL COMPUTED FUNCTION VALUES.      007***
C                                                                       007***
      IF (ISWH.EQ.1) GO TO 50                                           007***
C                                                                       007***
C     TEST IF STEPLENGTH DOUBLING IS POSSIBLE.                          007***
C                                                                       007***
   40 DO 42 K=1,NN                                                      007***
      IF(B(K).GT. .03125*A(K)) GO TO 2                                  007***
   42 CONTINUE                                                          007***
      S=S+S                                                             007***
      GO TO 2                                                           007***
C                                                                       007***
C     CALCULATION FINISHED.REPLACE INPUT FUNCTION VALUES WITH THE FUNC- 007***
C     TION VALUES COMPUTED FOR THE OUTPUT POINT XEND.REPLACE INPUT STEP-007***
C     LENGTH H WITH NEW COMPUTED STEPLENGTH.                            007***
C                                                                       007***
   50 H=HSV                                                             007***
      X=Z                                                               007***
      DO 52 K=1,NN                                                      007***
   52 Y(K)=W(K)                                                         007***
C                                                                       007***
```

```
      RETURN                                                            007E40
C                                                                       007E50
C     REQUIRED ACCURACY NOT OBTAINED.                                   007E60
C                                                                       007E70
C                                                                       007E80
   60 COF=.5*S                                                          007E90
      IF (ABS(COF).GE.ZMIN) GO TO 80                                    007F00
      IF (ITEST.EQ.0) GO TO 84                                          007F10
C                                                                       007F20
C     JTEST=1, CONTINUE WITH CONSTANT STEPLENGTH EQUAL HMIN.            007F30
C                                                                       007F40
      S=ZMIN                                                            007F50
      IF (HSV.LT.0.) S=-S                                               007F60
      IF (ISWH.EQ.1) GO TO 50                                           007F70
      GO TO 2                                                           007F80
C                                                                       007F90
C     DO CALCULATIONS RELATED TO HALVING OF STEPLENGTH.                 007G00
C                                                                       007G10
   80 DO 82 K=1,NN                                                      007G20
   82 W(K)=YZ(K)                                                        007G30
      Z=Z-S                                                             007G40
      S=COF                                                             007G50
      ISWH=0                                                            007G60
      GO TO 2                                                           007G70
C                                                                       007G80
C     JTEST=0 AND ABS(S).LT.HMIN, PRINT ERROR MESSAGE, SET OK=.FALSE. AND 007G90
C     RETURN TO CALLING PROGRAM.                                        007H00
C                                                                       007H10
   84 PRINT 88 , ITEST , S , ZMIN , Z                                   007H20
      OK=.FALSE.                                                        007H30
      GO TO 50                                                          007H40
C                                                                       007H50
   86 PRINT 90 , N                                                      007H60
      STOP                                                              007H70
C                                                                       007H80
   88 FORMAT(//,5X,31H*** SUBROUTINE MERSON ERROR ***,2X,8HJTEST = ,I2, 007H90
     12X,4HH = ,E12.5,2X,7HHMIN = ,E12.5,2X,4HX = ,E12.5,//)            007I00
   90 FORMAT(//,5X,31H*** SUBROUTINE MERSON ERROR ***,4H  N=,I4,1X,55HGR007I10
     1EATER THAN THE MAXIMUM NUMBER OF EQUATIONS PERMITTED.,//)         007I20
C                                                                       007I30
      END                                                               007I40
C                                                                       007I50
C                                                                       007I60
      SUBROUTINE JUMP(TIME,TJUMP,SJUMP)                                 007I70
C                                                                       007I80
C          SUBROUTINE TO COMPUTE TEMP AND SAL JUMPS BELOW WML.          007I90
C                                                                       008J00
      COMMON/JUMP/ST,SECEND,GRID                                        008J10
      COMMON/WML/ZH,ZL,TS,US,SS,ES,H,TT1,TTOLD,JOLD,TOLD,SOLD,T1,S1,Z1  008J20
C                                                                       008J30
      TB=TT1+(T1-TT1)*(TIME-ST)/(SECEND-ST)                             008J40
      TA=TTOLD+(TOLD-TTOLD)*(TIME-ST)/(SECEND-ST)                       008J50
      TDASH=(TA-TB)/GRID                                                008J60
      TJUMP=TS-TB-TDASH*(ZL-Z1)                                         008J70
C                                                                       008J80
      SDASH=(SOLD-S1)/GRID                                              008J90
      SJUMP=SS-S1-SDASH*(ZL-Z1)                                         008K00
C                                                                       008K10
      RETURN                                                            008K20
      END                                                               008K30
C                                                                       008K40
C                                                                       008K50
```

```
      SUBROUTINE TURB(ICOUNT)                                           008760
C                                                                       008770
C           SUBROUTINE TO COMPUTE FLUXES FROM MET DATA                  008780
C                                                                       008790
      REAL L,K                                                          008800
      COMMON/FLUX/H,HLFX,W,A4,A5,UX,TINT,U,AT,RH,B4,B5                  008810
      COMMON/WML/DUM1,DUM2,WT                                           008820
      DATA HL,P,CP,G,K/2445.,1013.25,1010.,9.81,.41/                    008830
      DATA ZL0/0.0/,JOG/0/                                              008840
C                                                                       008850
      IF(ICOUNT.NE.1) GO TO 15                                          008860
      IF(JOG.EQ.1) GO TO 15                                             008870
      JOG=1                                                             008880
      READ(1,10) Z3,Z4,CHWN10,CHW3MX,CD4MX,ZLMAX                        008890
   10 FORMAT(6F10.3)                                                    008900
      IF(EOF(1)) 11,12                                                  008910
   11 STOP# EOF IN TAPE1-DETECTED IN S/R TURB#                          008920
C               COMPUTE ROUGHNESS LENGTHS                               008930
   12 CON10=0.0013                                                      008940
      Z0=10.0/(EXP(K/(SQRT(CON10))))                                    008950
      ZS=10.0/(EXP(K*K/(CHWN10*ALOG(10./Z0))))                          008960
      G1=ALOG(10./Z0)                                                   008970
      G2=ALOG(10./ZS)                                                   008980
      G3=ALOG(Z3/ZS)                                                    008990
      G5=ALOG(Z3/Z0)                                                    009000
      G6=ALOG(Z4/Z0)                                                    009010
C                  INITIALISE COEFFICIENTS                              009020
      CON10=0.001                                                       009030
      CON4=CON10*(G1*G1)/(G6*G6)                                        009040
      CON3=CON10*(G1*G1)/(G5*G5)                                        009050
      CHWN=CHWN10*(G1*G2)/(G6*G3)                                       009060
      CD4=CDN4                                                          009070
      CD3=CDN3                                                          009080
      CHW=CHWN                                                          009090
C                                                                       009100
   15 CONTINUE                                                          009110
C                                                                       009120
C                  WIND SPEED AT 2ND LEVEL                              009130
      U3=U*G5/G6                                                        009140
C                  NEUTRAL 10M DRAG COEFF.                              009150
      IF(U.LE.5.) CDN10=.001                                            009160
      IF(U.GT.5.) CDN10=(1.0+0.07*(U-5.))/1000.                         009170
      CDN4=CON10*(G1*G1)/(G6*G6)                                        009180
      CDN3=CON10*(G1*G1)/(G5*G5)                                        009190
C                  ATMOSPHERIC DENSITY                                  009200
      D=1.294*273./(AT+273.)                                            009210
C                  PARTIAL WATER VAPOUR PRESSURE                        009220
      T1=1.-373.16/(AT+273.)                                            009230
      T2=1.-373.16/(WT+273.)                                            009240
      ES1=SATVP(T1)                                                     009250
      E1=(RH*ES1)/100.                                                  009260
      ES2=SATVP(T2)                                                     009270
C                  SPECIFIC HUMIDITY                                    009280
      Q=0.662/P*E1                                                      009290
C                  VIRTUAL AIR TEMPERATURE                              009300
      TV=(AT+273.)*(1.+0.61*Q)                                          009310
C                                                                       009320
C                  FLUX COMPUTATION/ITERATION                           009330
      NCOUNT=1                                                          009340
      GO TO 30                                                          009350
C                                                                       009360
   25 CONTINUE                                                          009370


      IF((ABS((ZL-ZL0))).LT.0.02) GO TO 50                              009380
      ZL0=ZL                                                            009390
      NCOUNT=NCOUNT+1                                                   009400
      IF(NCOUNT.GE.15) STOP #TOO MANY ITERATIONS IN SR TURB#            009410
C                  RECOMPUTE TRANSFER COEFFICIENTS                      009420
      ZL=Z4/L                                                           009430
      P4=PSIM(ZL)                                                       009440
      C=SQRT(CDN4)                                                      009450
      CD4=CDN4/(1.+CON4*(P4*P4-2.*K*P4/C)/(K*K))                        009460
C                                                                       009470
      ZL=Z3/L                                                           009480
      P1=PSIM(ZL)                                                       009490
      P2=PSIHW(ZL)                                                      009500
      C=SQRT(CDN3)                                                      009510
      CHW=CHWN/(1.+CHWN*(P1*P2-K*P2/C-K*P1*C/CHWN)/(K*K))               009520
C                                                                       009530
C                                                                       009540
   30 H=CHW*D*CP*U3*(WT-AT)                                             009550
      W=CHW*D*U3*0.662/P*(ES2-E1)                                       009560
      S=CD4*D*U*U                                                       009570
```

```
C                                                                       008A80
C                     FRICTION VELOCITY                                 008B90
      UX=SQRT(S/D)                                                      009000
C                     M.O.LENGTH                                        009010
   45 L=-D*UX*UX*UX*TV/(K*G*(H/EP+0.61*(AT+273.)*W))                    009020
      ZL=Z3/L                                                           009030
      GO TO 25                                                          009040
C                                                                       009050
   50 CONTINUE                                                          009060
C                                                                       009070
      IF(ZL.GT.ZLMAX) GO TO 115                                         009080
      H=CH*RMX*D*CP*U3*(WT-AT)                                          009090
      W=CH*RMX*D*U3*0.662/P*(ESP-E1)                                    009100
      S=CD*RMX*D*U*U                                                    009110
  115 CONTINUE                                                          009120
      HLFX=W*HL*1000.                                                   009130
      UX=SQRT(S/D)                                                      009140
C                                                                       009150
      RETURN                                                            009160
      END                                                               009170
C                                                                       009180
C                                                                       009190
C                                                                       009200
      FUNCTION SATVP(T)                                                 009210
C           COMPUTES SATURATION VAPOUR PRESSURE IN MB                   009220
      SATVP=1013.25*EXP(T*(13.3185+T*(-1.4760+T*(-0.6445-1.299*T))))    009230
      RETURN                                                            009240
      END                                                               009250
C                                                                       009260
C                                                                       009270
C                                                                       009280
      FUNCTION PSIM(ZL)                                                 009290
      REAL K                                                            009300
      DATA K,A,PI/0.41,5.0,3.14159/                                     009310
C                                                                       009320
C                                                                       009330
      IF(ZL.LT.0.) GO TO 10                                             009340
      IF(ZL.GT.0.) GO TO 20                                             009350
C                                                                       009360
      PSIM=0.                                                           009370
      GO TO 30                                                          009380
C                                                                       009390
```

```
   10 X=(1.-16.*ZL)**0.25                                               009400
      PSIM=2.*ALOG((1.+X)/2.)+ALOG((1.+X*X)/2.)-2.*ATAN(X)+PI/2.        009410
      GO TO 30                                                          009420
C                                                                       009430
   20 IF(ZL.GT.0.5) GO TO 21                                            009440
      PSIM=-A*ZL                                                        009450
      GO TO 25                                                          009460
   21 IF(ZL.GT.10.) GO TO 22                                            009470
      PSIM=0.5/(ZL*ZL)-4.25/ZL-7.0*ALOG(ZL)-0.852                       009480
      GO TO 25                                                          009490
   22 PSIM=ALOG(ZL)-0.76*ZL-12.093                                      009500
   25 CONTINUE                                                          009510
C                                                                       009520
   30 RETURN                                                            009530
      END                                                               009540
C                                                                       009550
C                                                                       009560
C                                                                       009570
      FUNCTION PSIHW(ZL)                                                009580
      REAL K                                                            009590
      DATA K,A,PI/0.41,5.0,3.14159/                                     009600
C                                                                       009610
C                                                                       009620
      IF(ZL.LT.0.) GO TO 10                                             009630
      IF(ZL.GT.0.) GO TO 20                                             009640
C                                                                       009650
      PSIHW=0.                                                          009660
      GO TO 30                                                          009670
C                                                                       009680
   10 X=(1.-16.*ZL)**0.25                                               009690
      PSIHW=2.*ALOG((1.+X*X)/2.)                                        009700
      GO TO 30                                                          009710
C                                                                       009720
   20 IF(ZL.GT.0.5) GO TO 21                                            009730
      PSIM=-A*ZL                                                        009740
      GO TO 25                                                          009750
   21 IF(ZL.GT.10.) GO TO 22                                            009760
      PSIM=0.5/(ZL*ZL)-4.25/ZL-7.0*ALOG(ZL)-0.852                       009770
      GO TO 25                                                          009780
   22 PSIM=ALOG(ZL)-0.76*ZL-12.093                                      009790
   25 PSIHW=PSIM                                                        009800
C                                                                       009810
   30 RETURN                                                            009820
      END                                                               009830
```

APPENDIX D: MODEL RESULTS

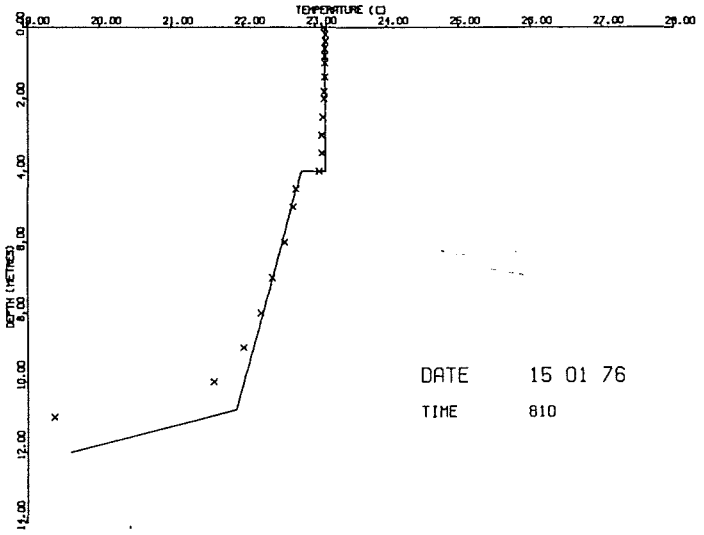

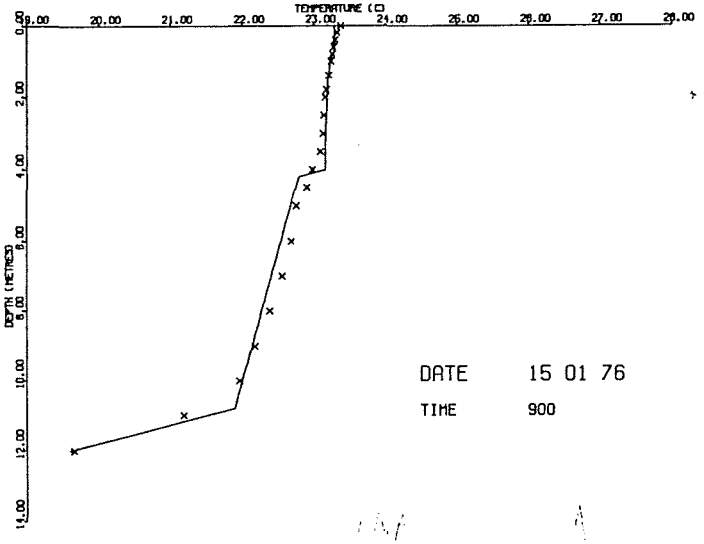

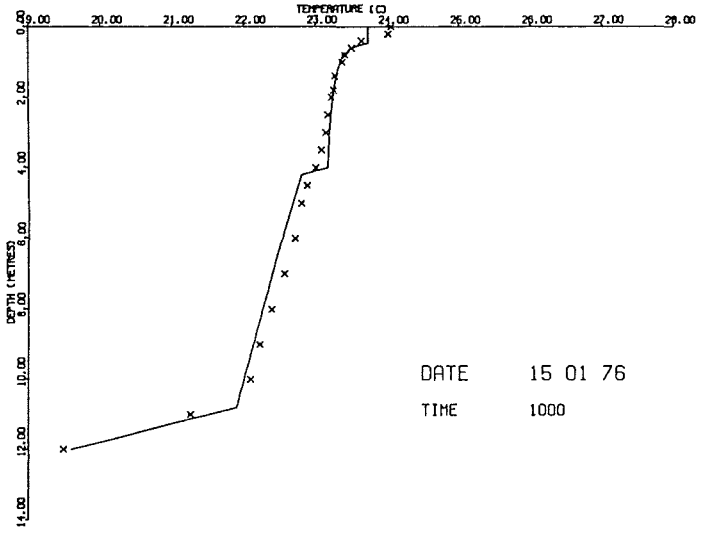

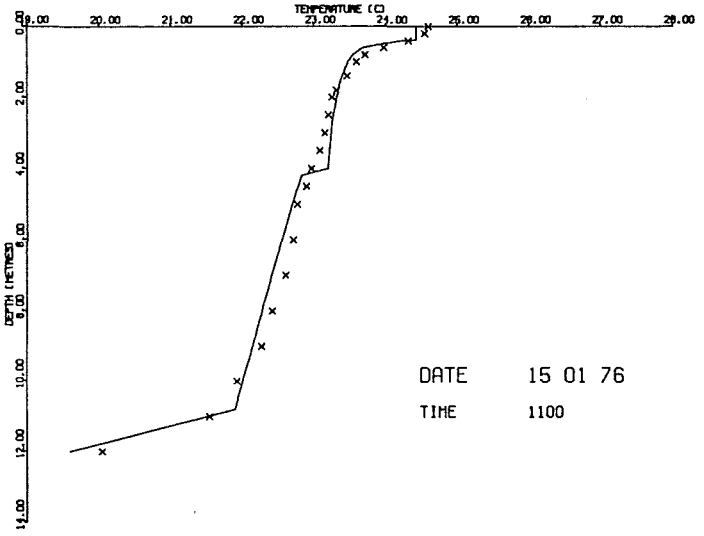

D1 Measured and Modelled Temperature Profiles

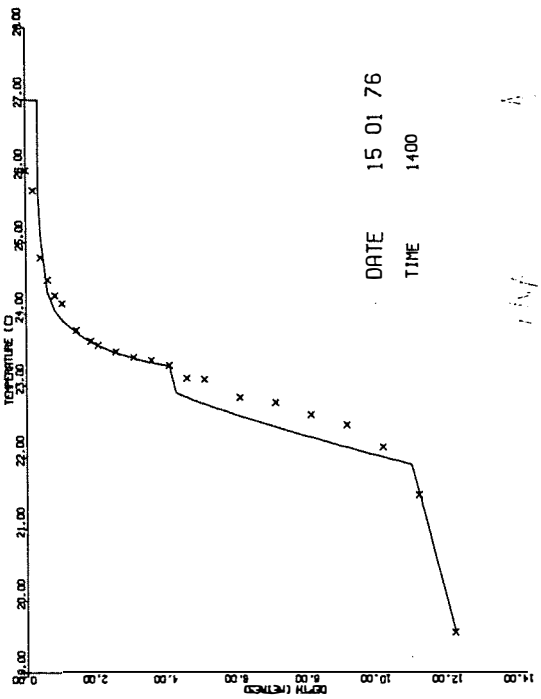
DATE 15 01 76
TIME 1400
TEMPERATURE (C)
DEPTH (METRES)

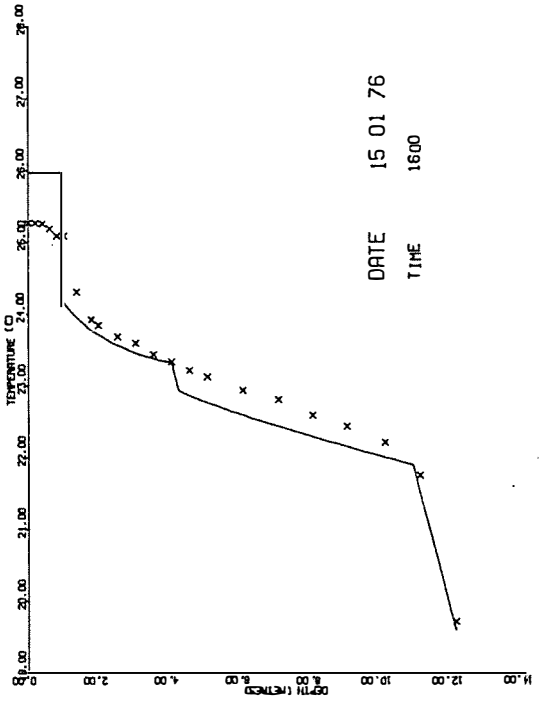
DATE 15 01 76
TIME 1600
TEMPERATURE (C)
DEPTH (METRES)

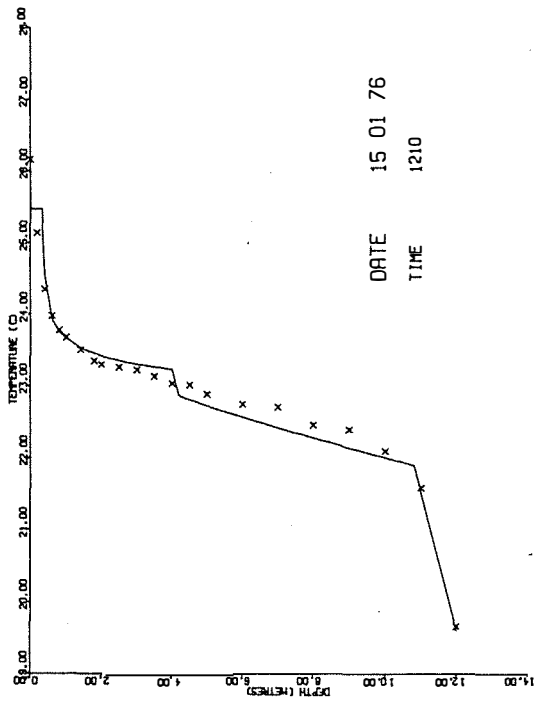
DATE 15 01 76
TIME 1210
TEMPERATURE (C)
DEPTH (METRES)

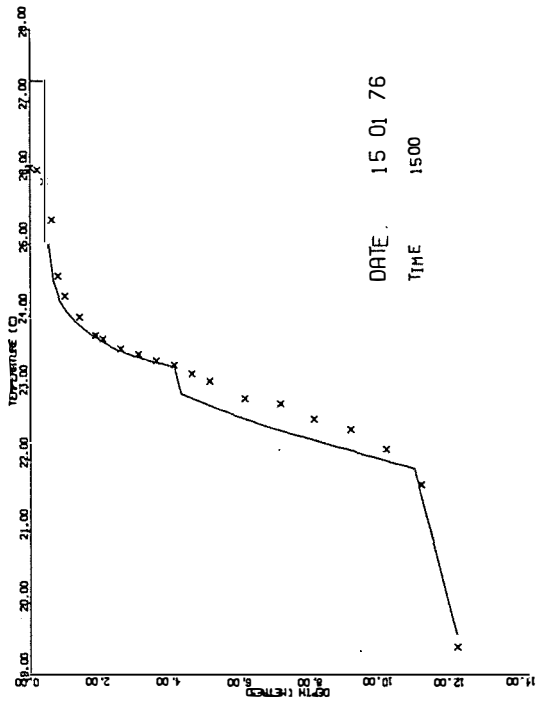
DATE 15 01 76
TIME 1500
TEMPERATURE (C)
DEPTH (METRES)

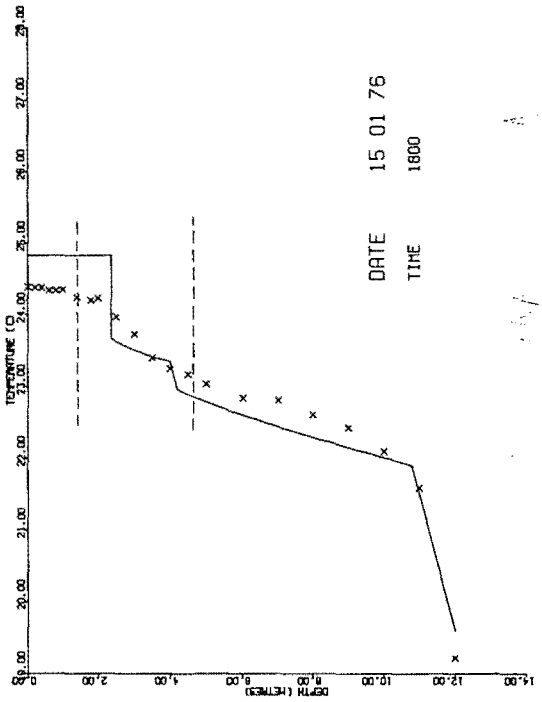
DATE 15 01 76
TIME 1800
TEMPERATURE (C)
DEPTH (METRES)

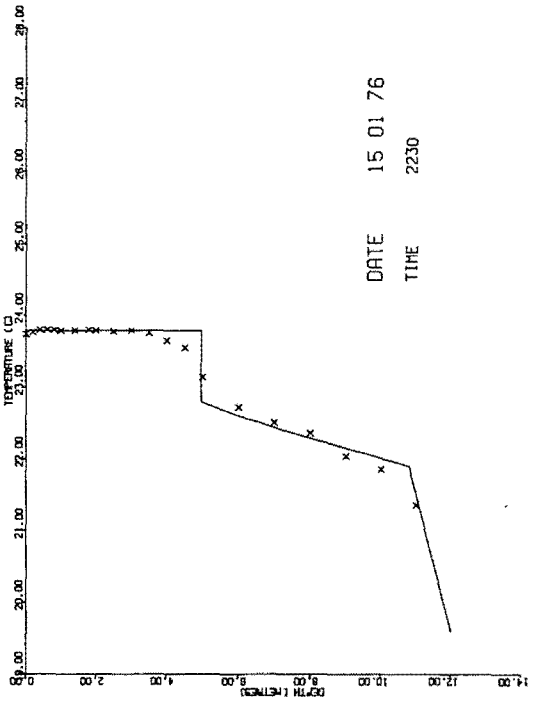
DATE 15 01 76
TIME 2230
TEMPERATURE (C)
DEPTH (METRES)

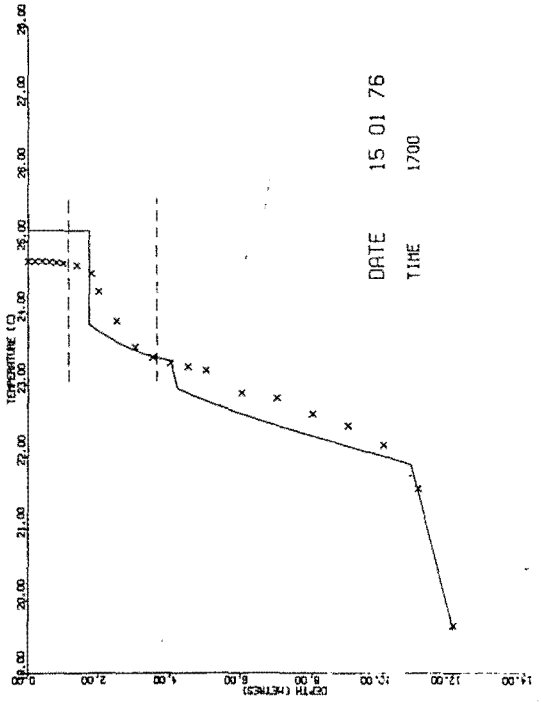
DATE 15 01 76
TIME 1700
TEMPERATURE (C)
DEPTH (METRES)

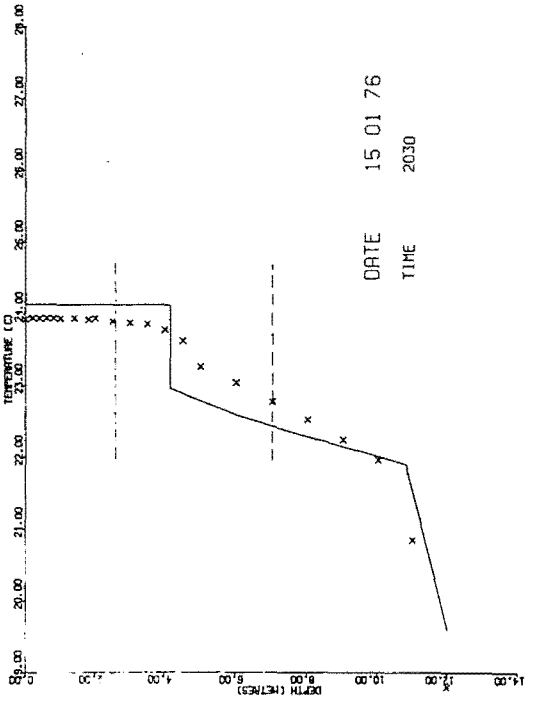
DATE 15 01 76
TIME 2030
TEMPERATURE (C)
DEPTH (METRES)

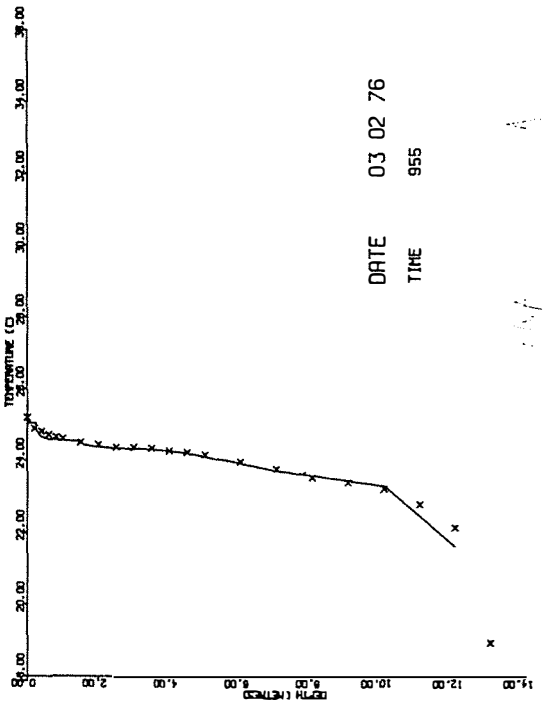
DATE 03 02 76
TIME 955

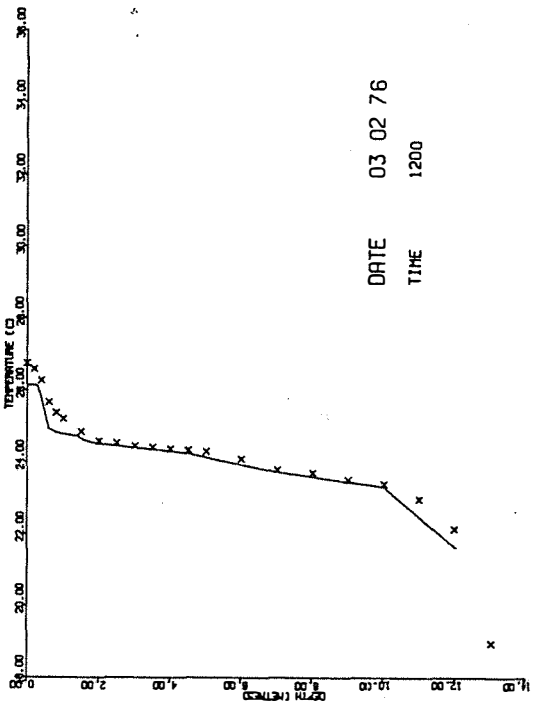
DATE 03 02 76
TIME 1200

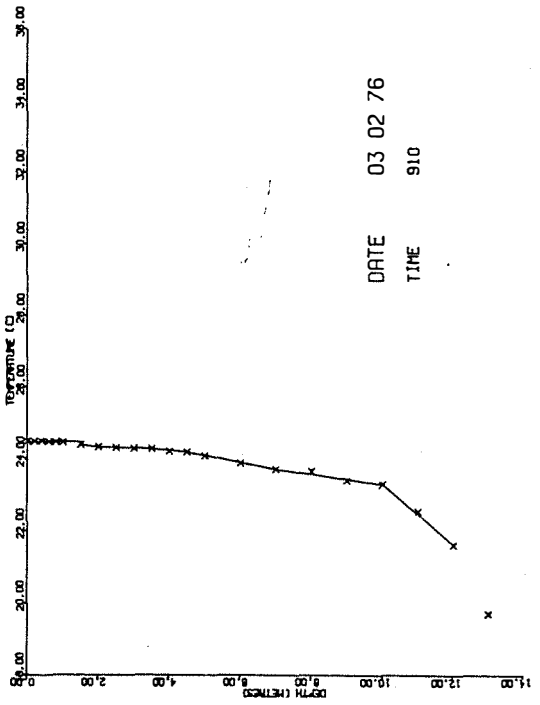
DATE 03 02 76
TIME 910

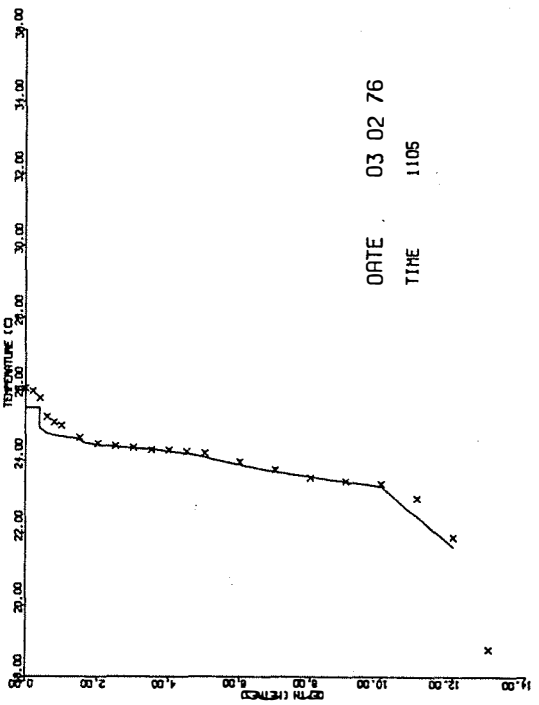
DATE 03 02 76
TIME 1105

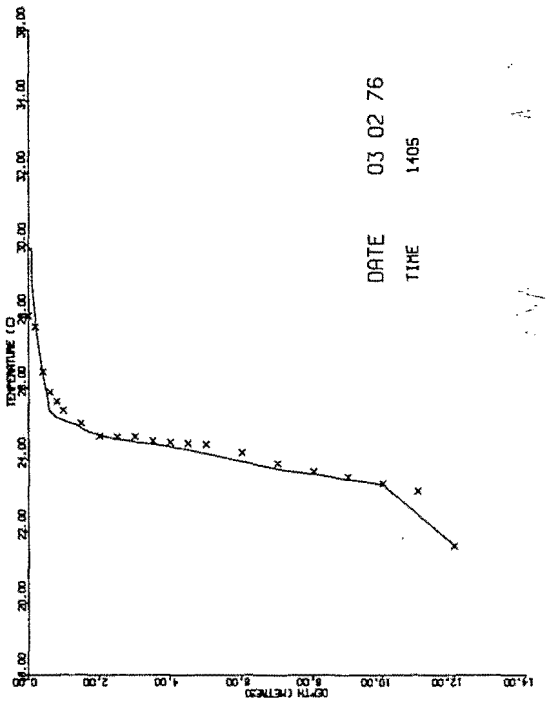
DATE 03 02 76
TIME 1405
TEMPERATURE (C)
DEPTH (METRES)

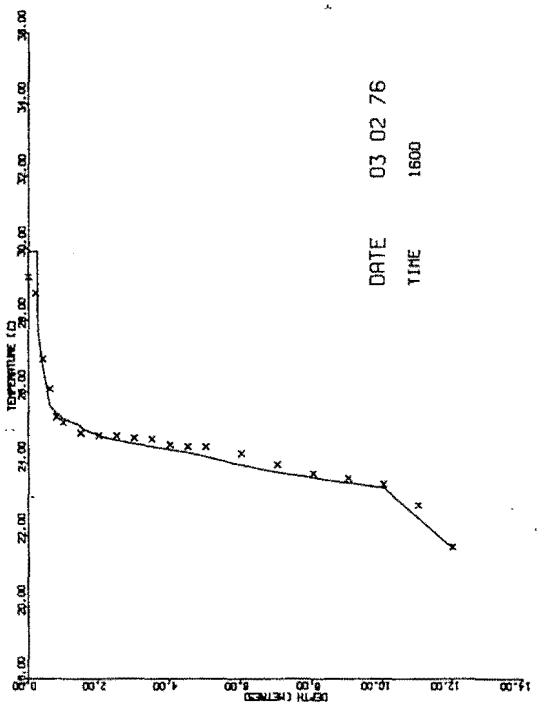
DATE 03 02 76
TIME 1600
TEMPERATURE (C)
DEPTH (METRES)

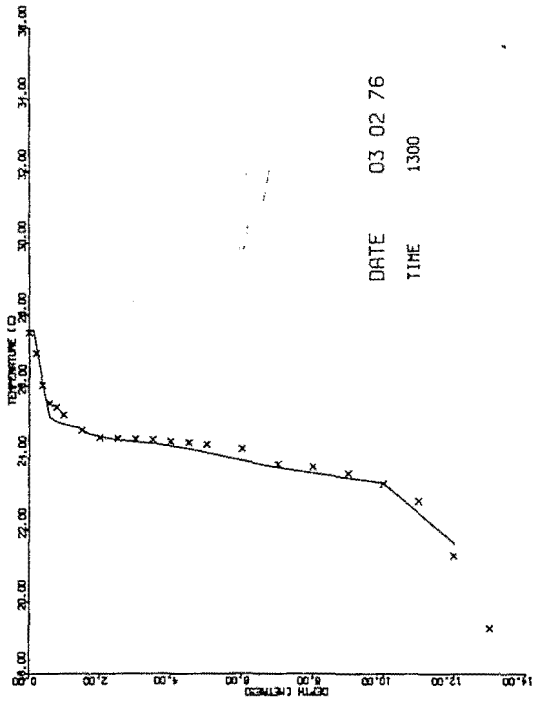
DATE 03 02 76
TIME 1300
TEMPERATURE (C)
DEPTH (METRES)

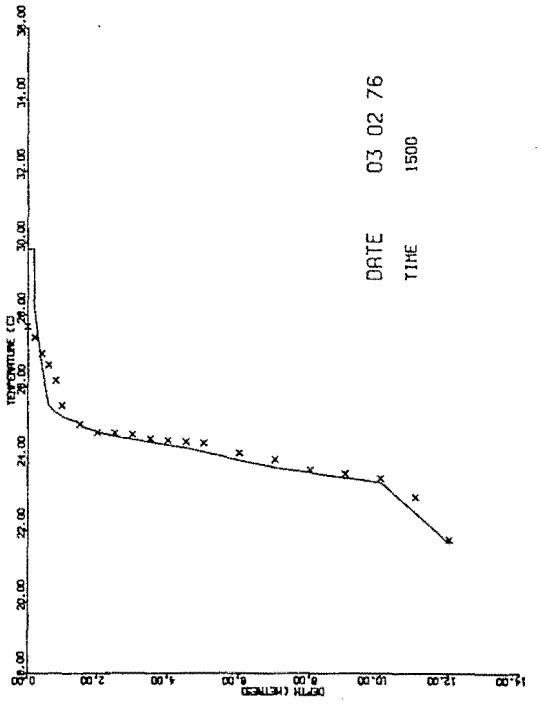
DATE 03 02 76
TIME 1500
TEMPERATURE (C)
DEPTH (METRES)

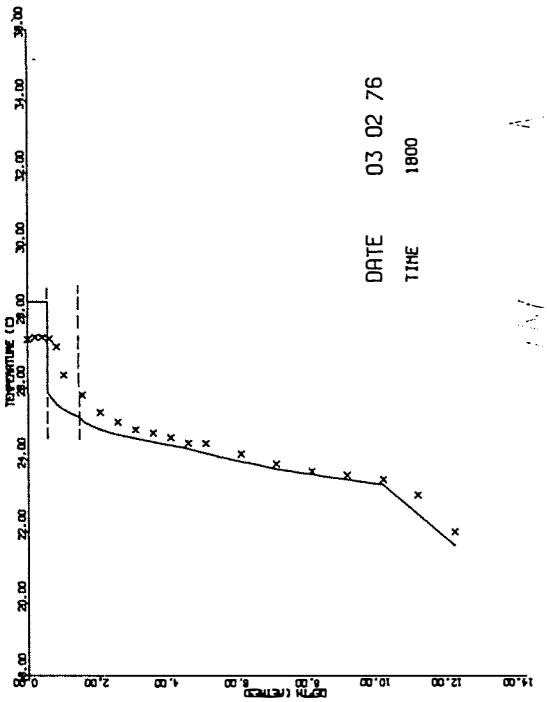
DATE 03 02 76
TIME 1800

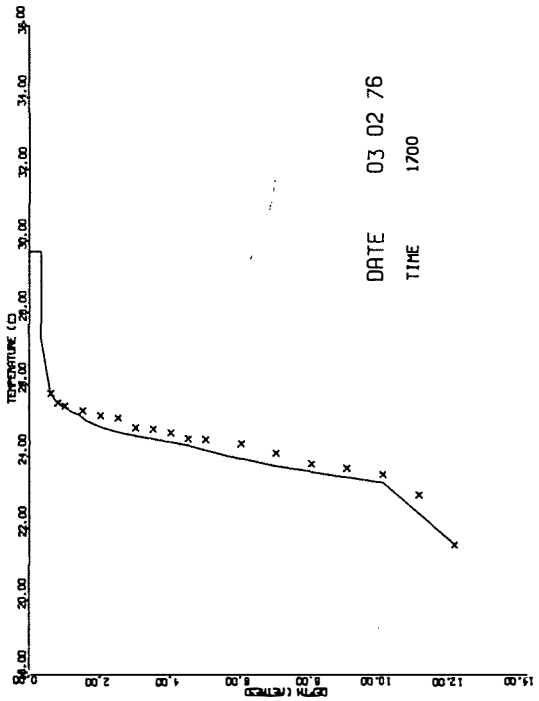
DATE 03 02 76
TIME 1700

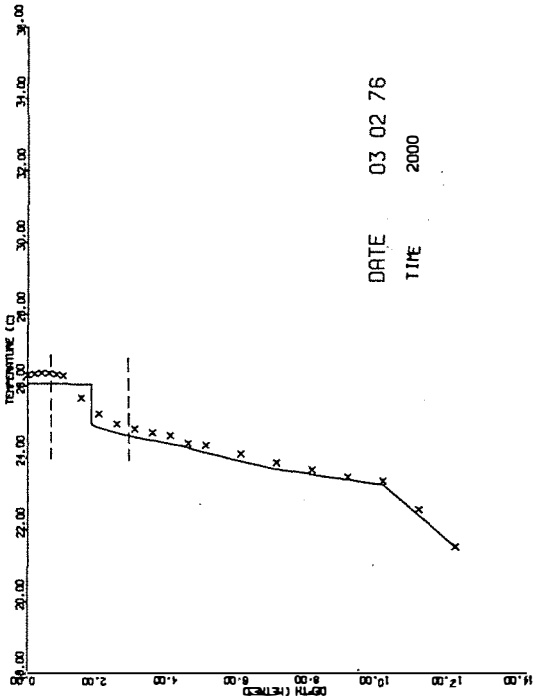
DATE 03 02 76
TIME 2000

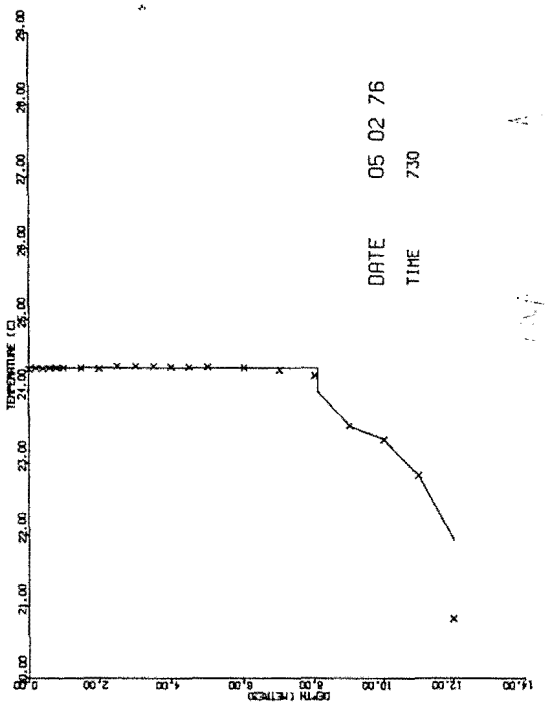
DATE 05 02 76
TIME 730
TEMPERATURE (C)
DEPTH (METRES)

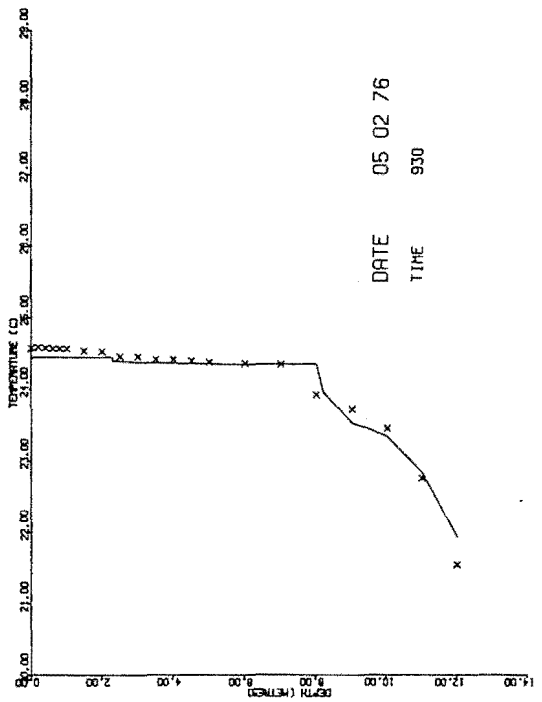
DATE 05 02 76
TIME 930
TEMPERATURE (C)
DEPTH (METRES)

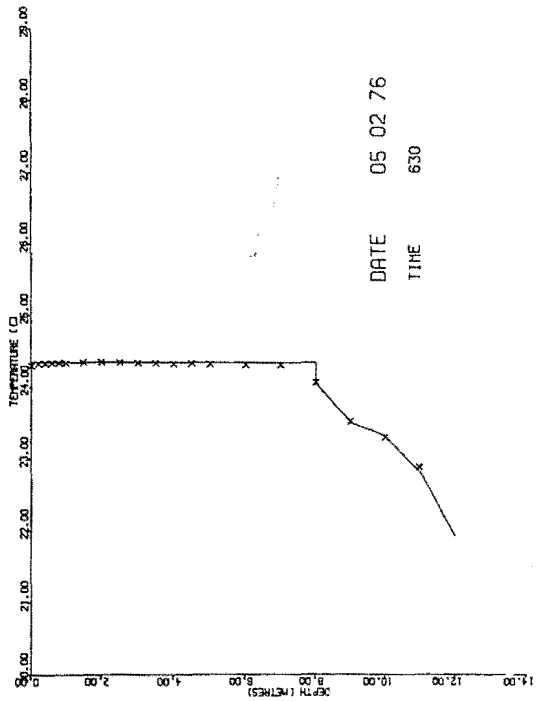
DATE 05 02 76
TIME 630
TEMPERATURE (C)
DEPTH (METRES)

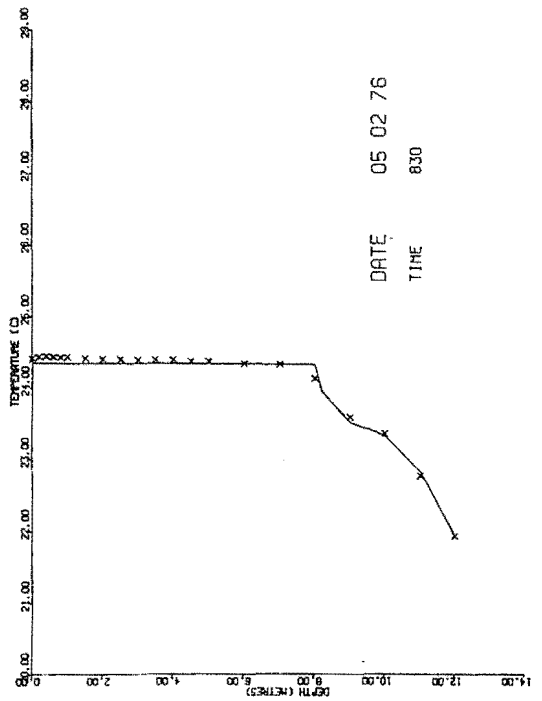
DATE 05 02 76
TIME 830
TEMPERATURE (C)
DEPTH (METRES)

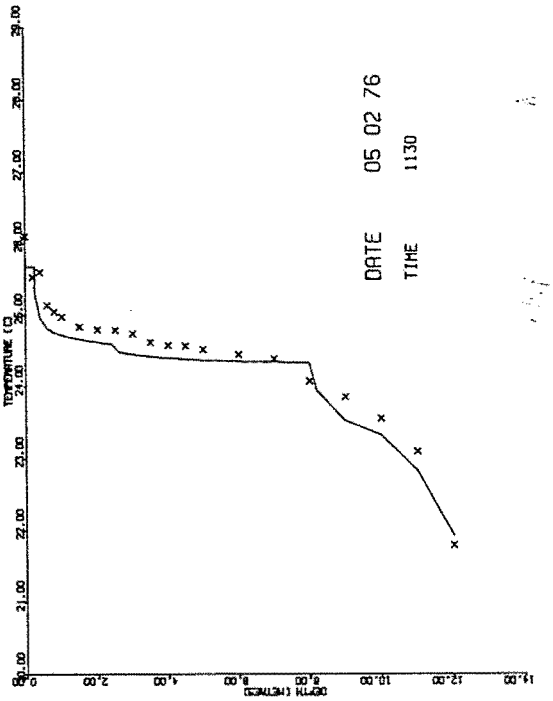
DATE 05 02 76
TIME 1130
TEMPERATURE (C)
DEPTH (METRES)

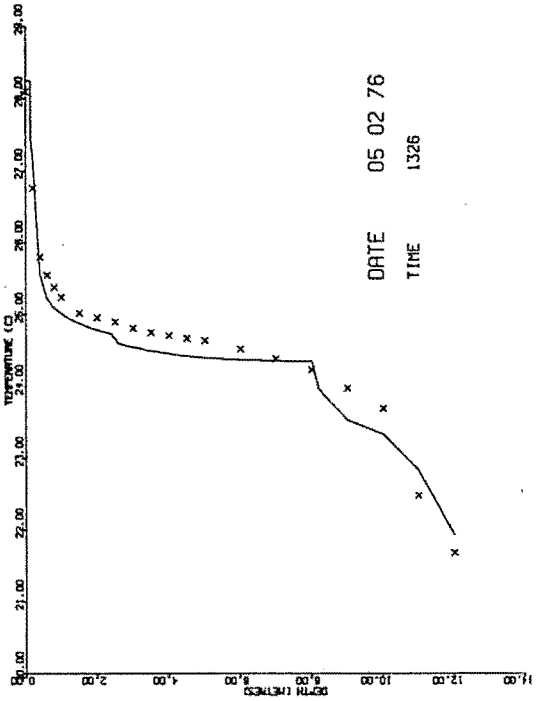
DATE 05 02 76
TIME 1326
TEMPERATURE (C)
DEPTH (METRES)

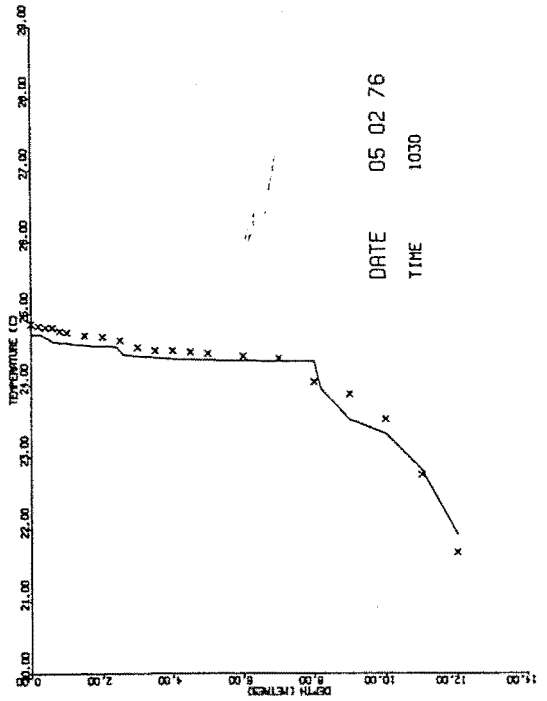
DATE 05 02 76
TIME 1030
TEMPERATURE (C)
DEPTH (METRES)

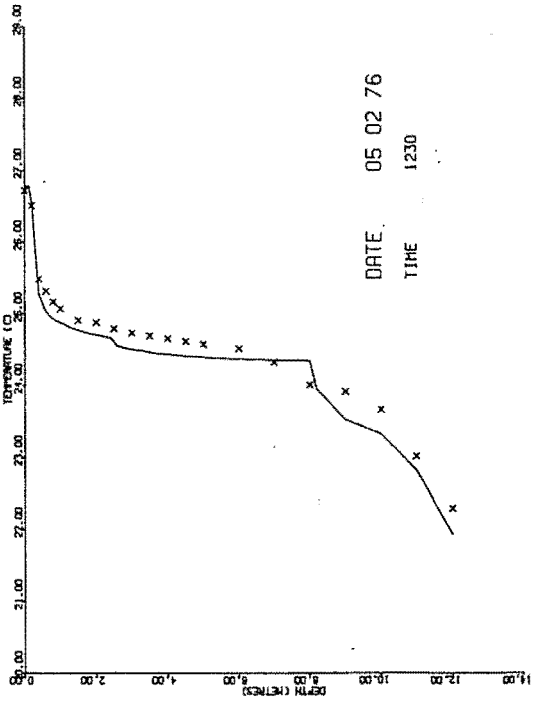
DATE 05 02 76
TIME 1230
TEMPERATURE (C)
DEPTH (METRES)

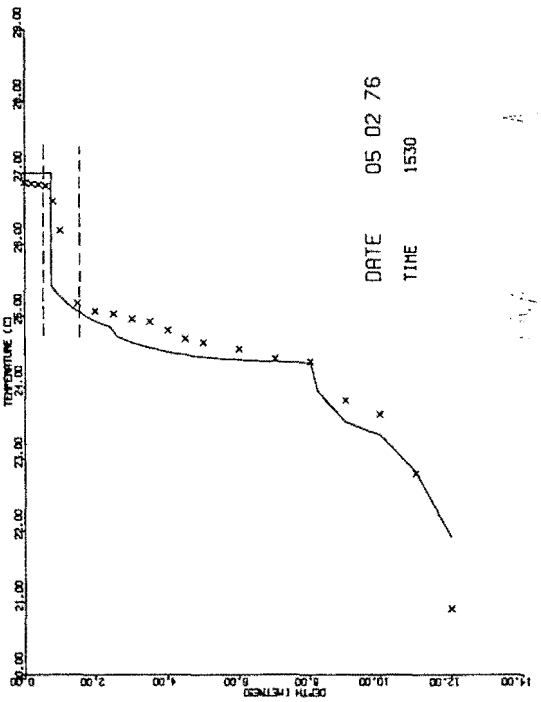
DATE 05 02 76
TIME 1530
TEMPERATURE (C)
DEPTH (METRES)

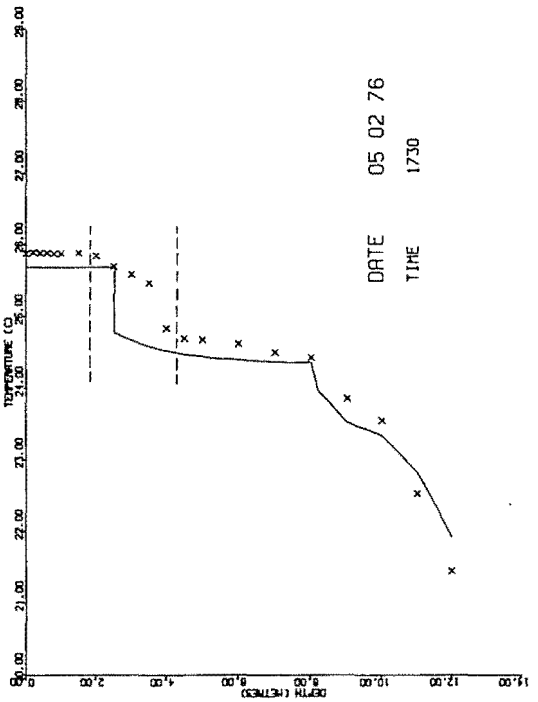
DATE 05 02 76
TIME 1730
TEMPERATURE (C)
DEPTH (METRES)

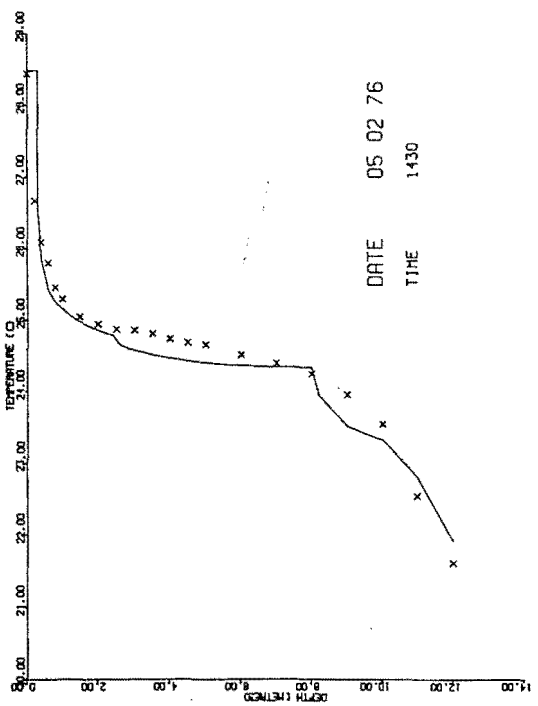
DATE 05 02 76
TIME 1430
TEMPERATURE (C)
DEPTH (METRES)

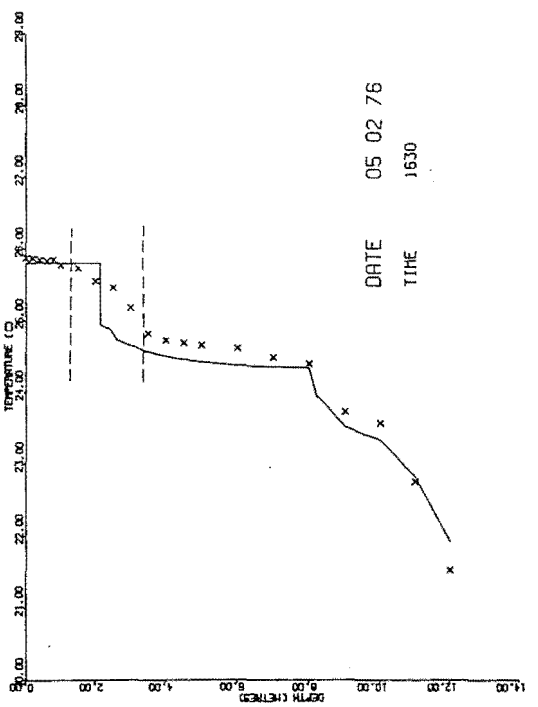
DATE 05 02 76
TIME 1630
TEMPERATURE (C)
DEPTH (METRES)

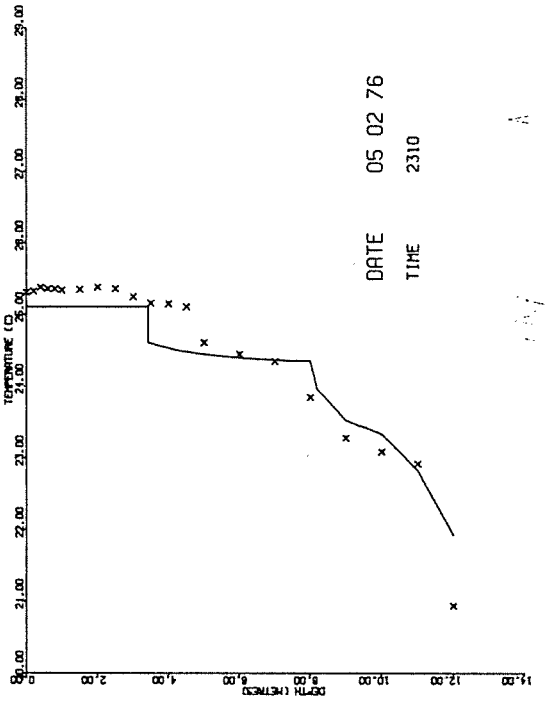
DATE 05 02 76
TIME 2310
TEMPERATURE (C)
DEPTH (METRES)

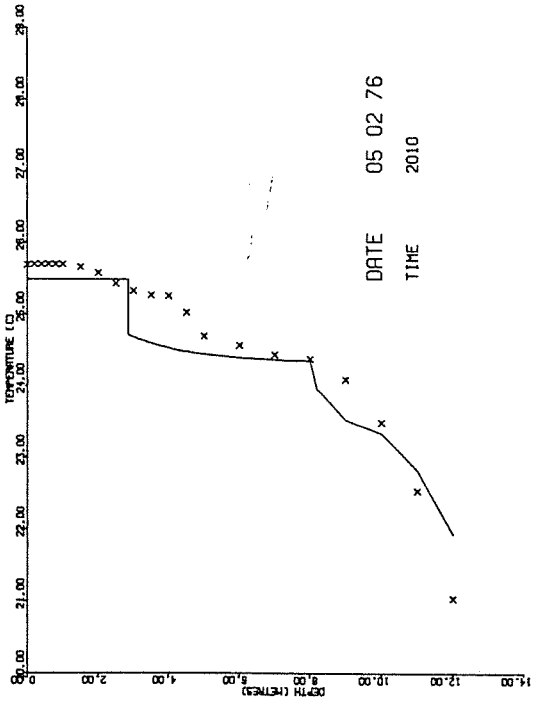
DATE 05 02 76
TIME 2010
TEMPERATURE (C)
DEPTH (METRES)

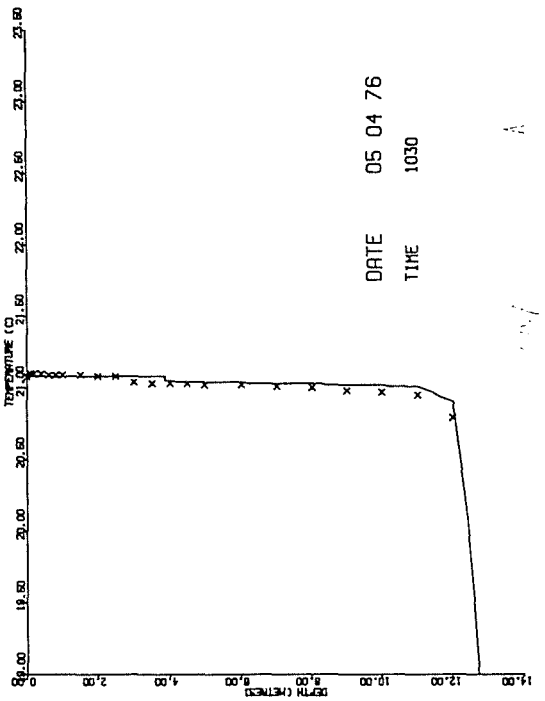
DATE 05 04 76
TIME 1030
TEMPERATURE (C)
DEPTH (METRES)

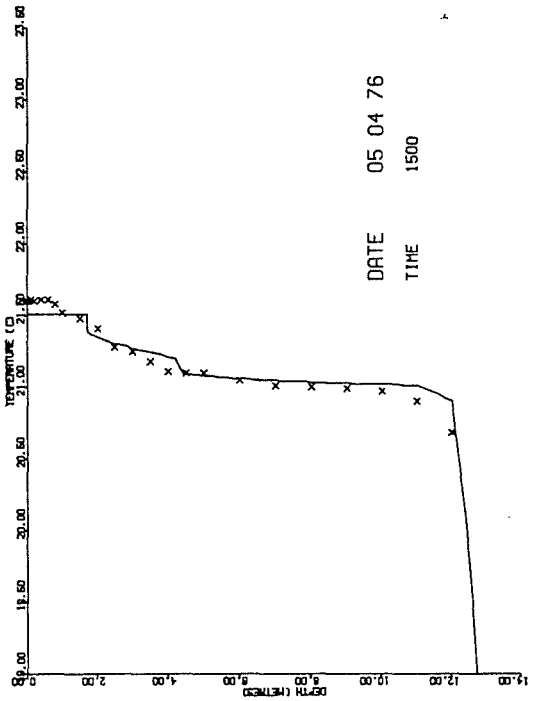
DATE 05 04 76
TIME 1500
TEMPERATURE (C)
DEPTH (METRES)

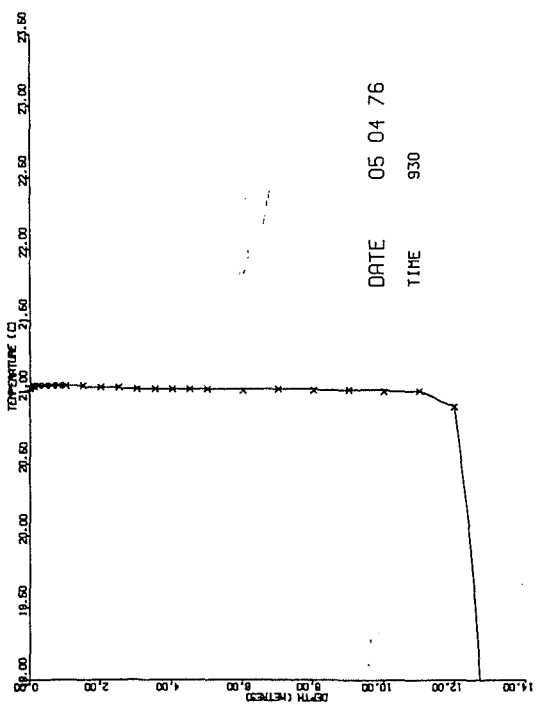
DATE 05 04 76
TIME 930
TEMPERATURE (C)
DEPTH (METRES)

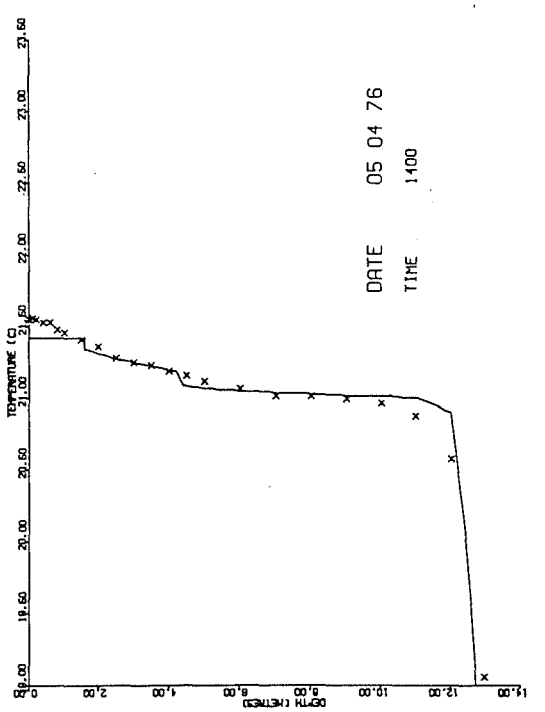
DATE 05 04 76
TIME 1400
TEMPERATURE (C)
DEPTH (METRES)

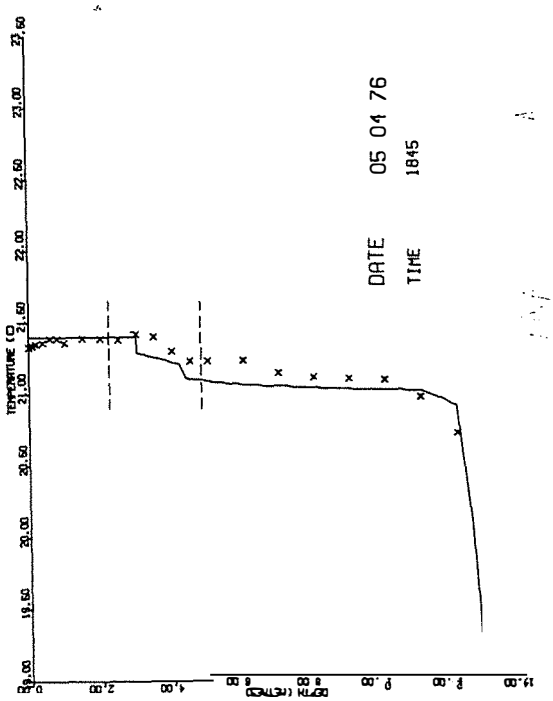
DATE 05 04 76
TIME 1845

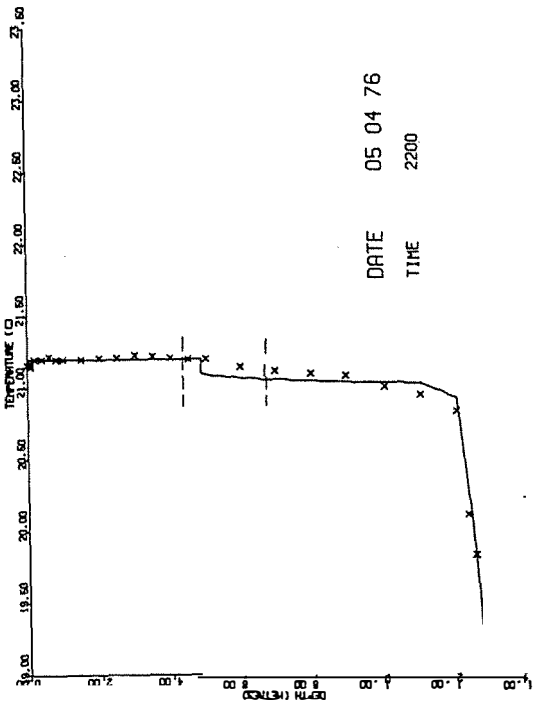
DATE 05 04 76
TIME 2200

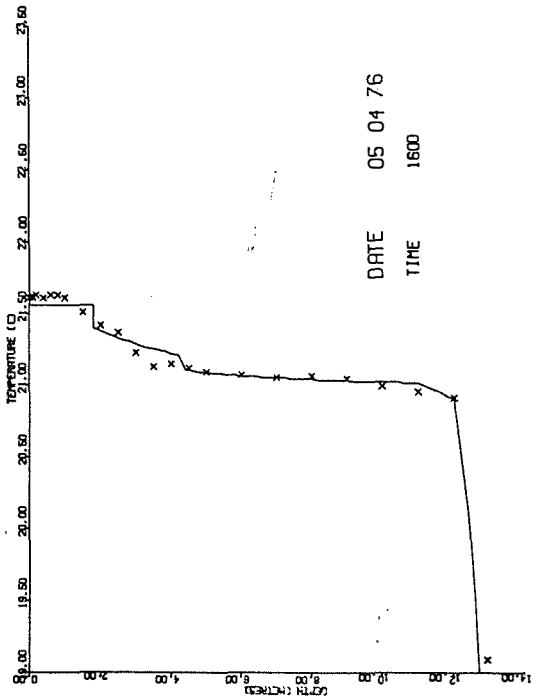
DATE 05 04 76
TIME 1600

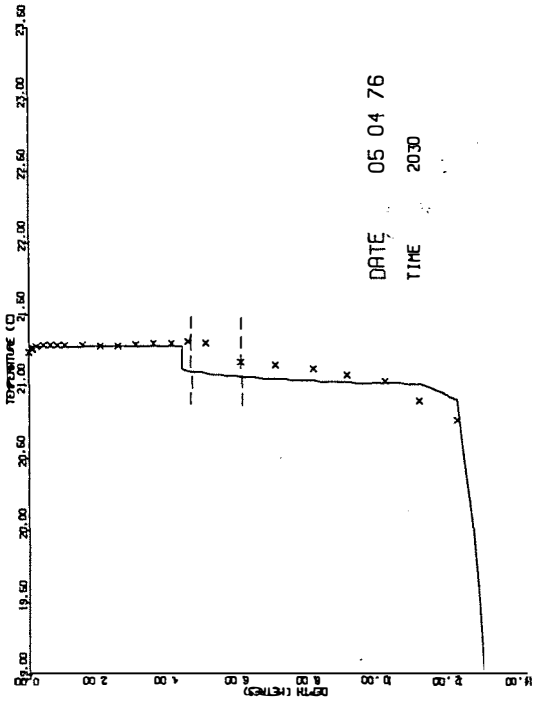
DATE 05 04 76
TIME 2030

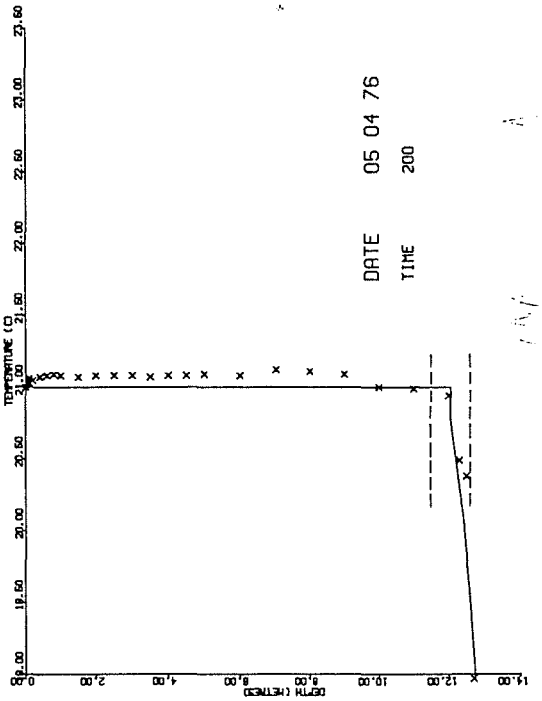
DATE 05 04 76
TIME 2000
TEMPERATURE (C)
DEPTH (METRES)

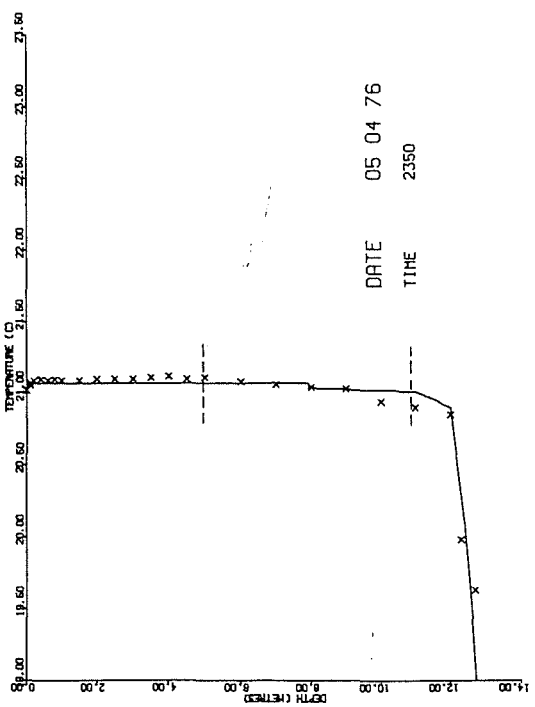
DATE 05 04 76
TIME 2350
TEMPERATURE (C)
DEPTH (METRES)

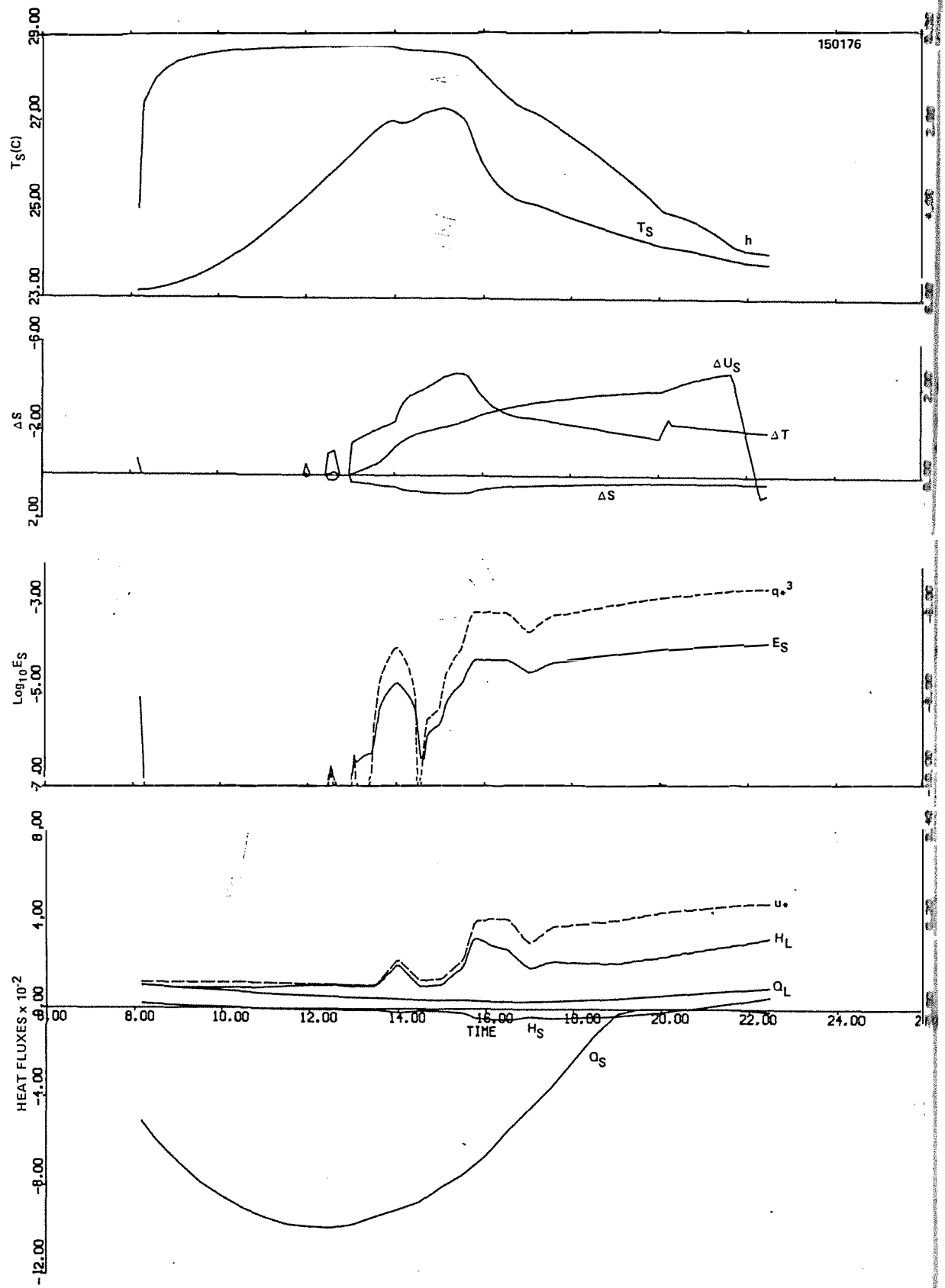

D2 Diurnal Cycle Plots

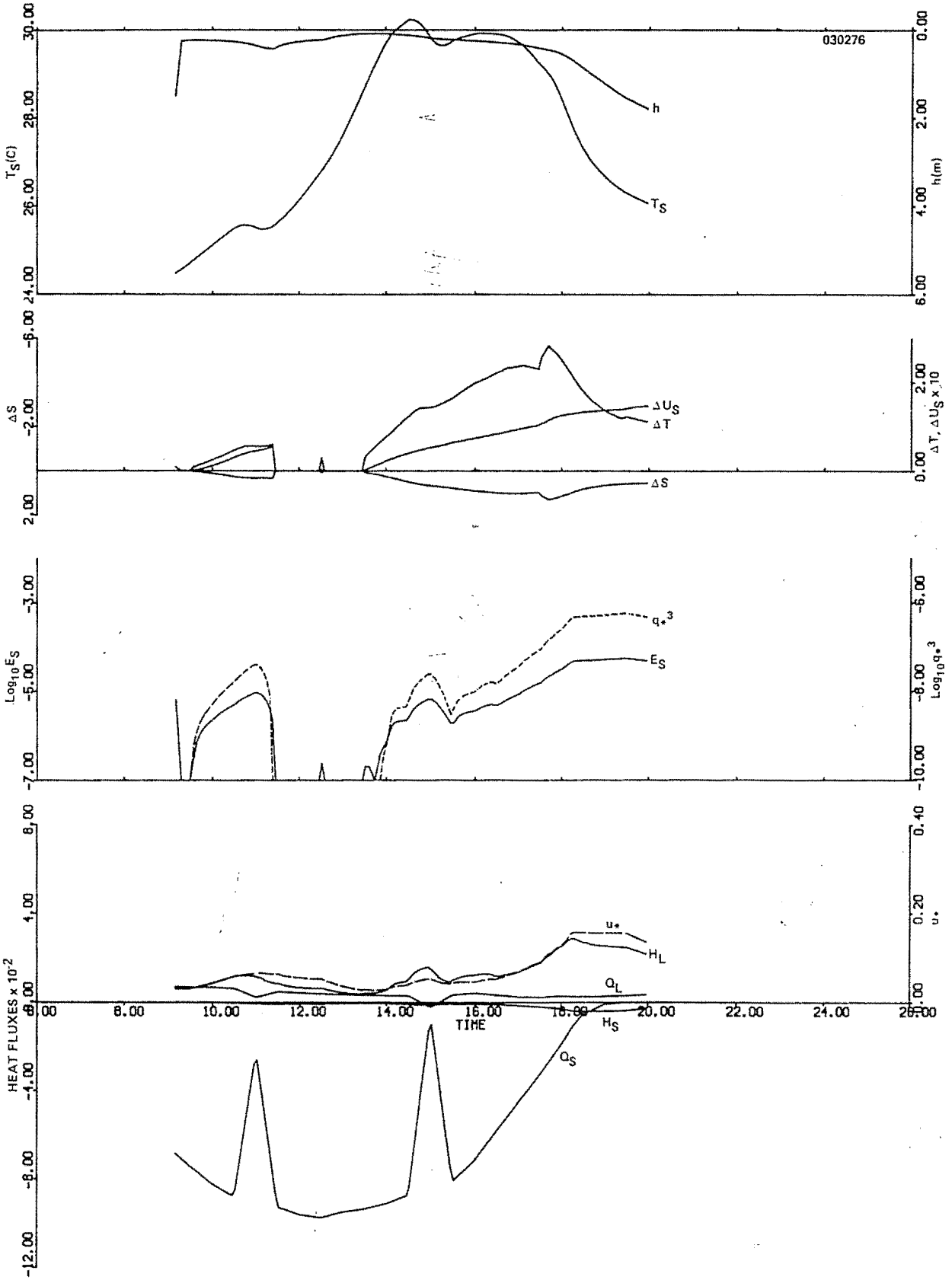
030276
T_S(C)
h(m)
h
T_S
ΔS
ΔT, ΔU_S x 10
ΔU_S
ΔT
ΔS
$Log_{10}E_S$
$Log_{10}q_*^3$
q_*^3
E_S
HEAT FLUXES x 10^{-2}
u_*
H_L
Q_L
H_S
Q_S
TIME
8.00
10.00
12.00
14.00
16.00
18.00
20.00
22.00
24.00

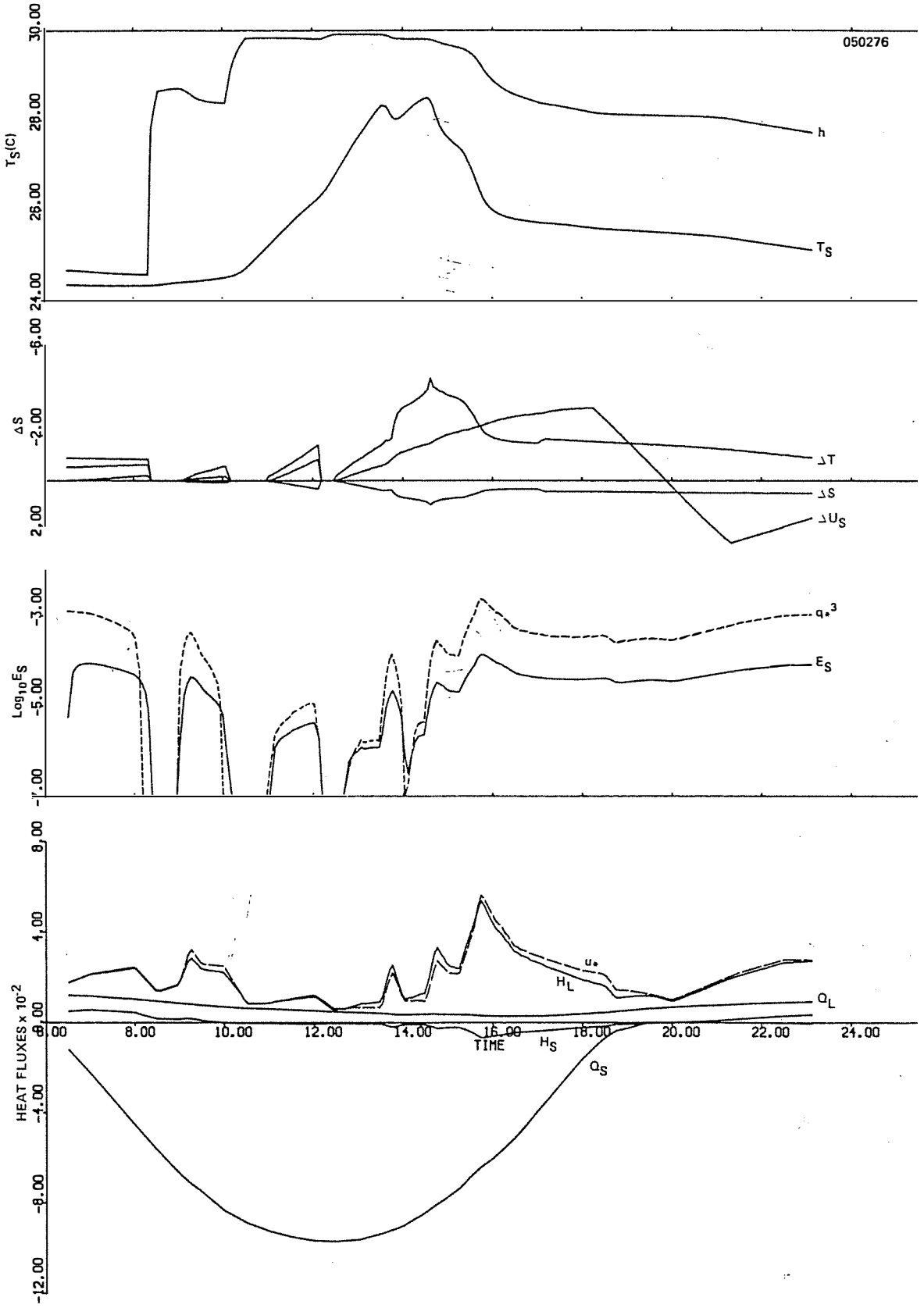
050276
T_S(C)
30.00
28.00
26.00
24.00
h
T_S
ΔS
-6.00
-2.00
2.00
ΔT
ΔS
ΔU_S
$Log_{10} E_S$
-3.00
-5.00
-7.00
q_*^3
E_S
HEAT FLUXES x 10^{-2}
8.00
4.00
0.00
-4.00
-8.00
-12.00
u_*
H_L
Q_L
6.00
8.00
10.00
12.00
14.00
16.00
18.00
20.00
22.00
24.00
TIME
H_S
Q_S

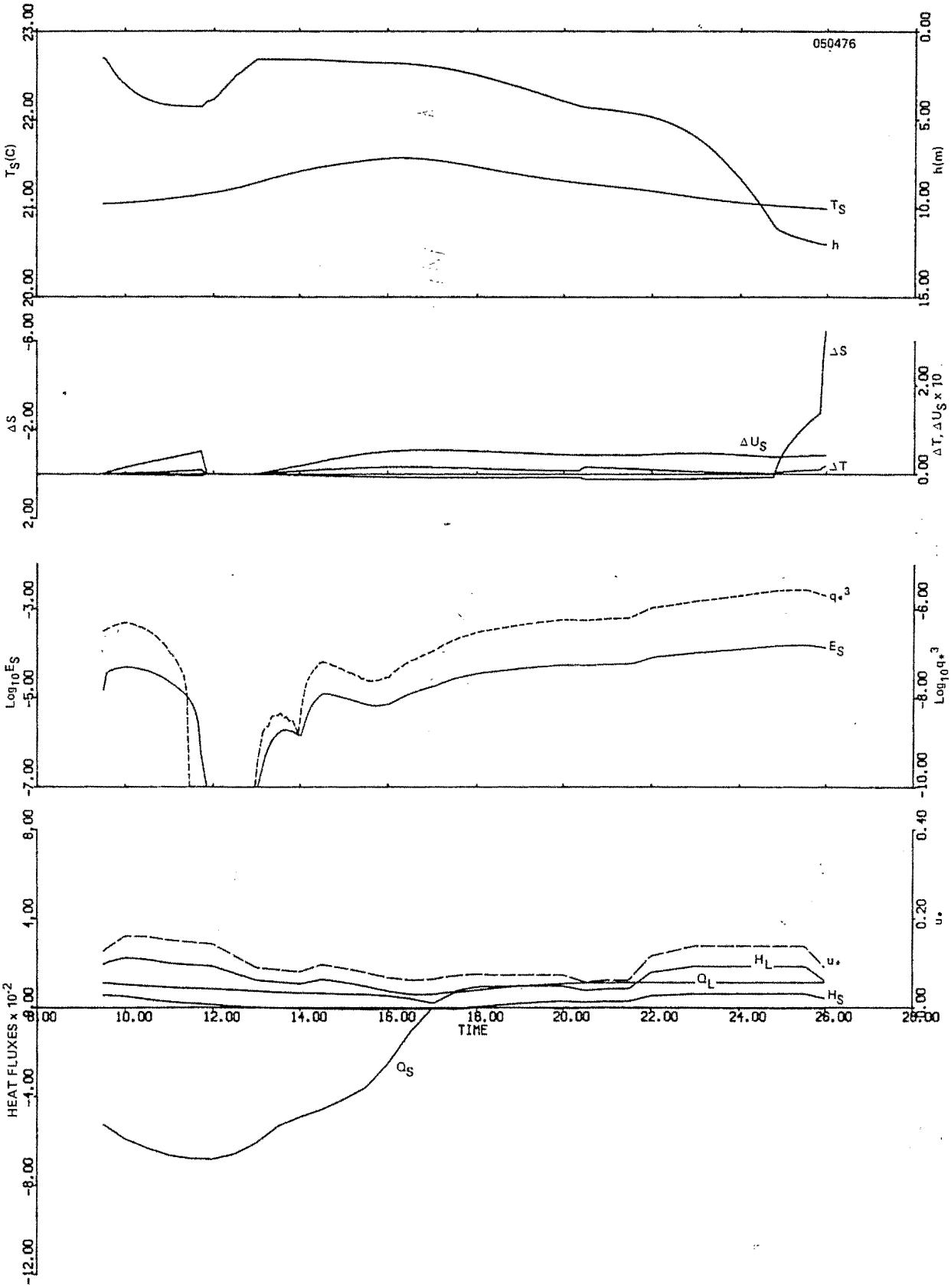
050476
T_S(C)
h(m)
T_S
h
ΔS
ΔU_S
ΔT
ΔT, $\Delta U_S \times 10$
$\text{Log}_{10} E_S$
$\text{Log}_{10} q_*^3$
q_*^3
E_S
HEAT FLUXES $\times 10^{-2}$
u_*
H_L
Q_L
H_S
Q_S
TIME

D2.4